



Chair of Waste Processing Technology and Waste Management

Doctoral Thesis

Potential of Sensor-Based Sorting in
Enhanced Landfill Mining under
Consideration of the Effects of
Defilements

Bastian Küppers, M.Sc.

December 2019



EIDESSTATTLICHE ERKLÄRUNG

Ich erkläre an Eides statt, dass ich diese Arbeit selbständig verfasst, andere als die angegebenen Quellen und Hilfsmittel nicht benutzt, und mich auch sonst keiner unerlaubten Hilfsmittel bedient habe.

Ich erkläre, dass ich die Richtlinien des Senats der Montanuniversität Leoben zu "Gute wissenschaftliche Praxis" gelesen, verstanden und befolgt habe.

Weiters erkläre ich, dass die elektronische und gedruckte Version der eingereichten wissenschaftlichen Abschlussarbeit formal und inhaltlich identisch sind.

Datum 20.12.2019

Unterschrift Verfasser/in
Bastian Küppers
Matrikelnummer: 1633378

Danksagung

Danke.

Kurzfassung

Potential der sensorgestützten Sortierung im Enhanced Landfill Mining unter Berücksichtigung der Auswirkungen von Verschmutzungen

In bislang durchgeführten Landfill-Mining-Projekten wurden vorwiegend rudimentäre Prozessketten mit geringen spezifischen Aufbereitungskosten, aber auch mit geringwertigen Outputfraktionen verwendet. Das Konzept des „Enhanced Landfill Mining“ dagegen ist darauf ausgelegt, durch komplexere Prozessketten, inkl. sensorgestützter Sortierung, ein höheres Ausbringen und höherwertige Outputfraktionen zu erzeugen. Die primäre Herausforderung beim Einsatz von sensorgestützten Sortierern stellt der hohe Grad an Verunreinigungen dar, der die Funktionsfähigkeit der verwendeten Sensorik beeinträchtigen kann.

In dieser Dissertation wurden zwei Fallstudien, die Deponien Halbenrain (Österreich) und Mont-Saint-Guibert (Belgien) betreffend, durchgeführt. Das Schwergut aus der Windsichtung bzw. die 3D-Fraktion der ballistischen Separation wurden dabei als geeignete Materialströme für den Einsatz sensorgestützter Nahinfrarot-Sortierer identifiziert. Vor der Sortierung von Materialien aus diesen Fraktionen, wurden zunächst grundlegende Untersuchungen an Referenzmaterialien durchgeführt. Zum einen wurden die Einflüsse von Oberflächenrauheit und –wasser auf die Nahinfrarot-Sortierung untersucht. Es wurde gezeigt, dass angeraute Oberflächen eine verbesserte Klassifizierung von Materialien zulassen, während Oberflächenfeuchtigkeit systematische Veränderungen im stoffspezifischen Spektrum hervorruft. Durch entsprechende Anpassungen der Sortieralgorithmen gelang es, eine Fehlklassifizierung von Materialien trotz Oberflächenfeuchtigkeit zu vermeiden. Zum anderen wurde gezeigt, dass der Einfluss von Oxidschichten auf die Röntgenfluoreszenzsortierung gering ist. Zusätzlich wurden die Einflüsse von Inputzusammensetzung und Durchsatz auf die Sortiereffizienz quantifiziert. Die Ergebnisse zeigen, dass der mechanische Aufrag neben der Erkennung einen erheblichen Einflussfaktor auf die Sortierleistung darstellt.

Die gewonnenen Erkenntnisse wurden anschließend für die Sortierung des gewonnenen Windsichter-Schwerguts aus der Deponie Halbenrain bzw. der Schwergut- und 3D-Fraktionen aus der Deponie Mont-Saint-Guibert verwendet. Dabei wurden heizwertreiche und inerte Fraktionen sensorgestützt voneinander getrennt. Außerdem wurde die Umsetzbarkeit einer Separierung verschiedener Kunststoffsorten mittels Nahinfrarotsortierung aus LFM Fraktionen belegt (Wertstoffausbringen verschiedener Kunststoffe >90 Gew.-%).

Die Erkenntnisse aus den Sortierversuchen wurden verwendet um auf Basis der Materialzusammensetzung verschiedener Landfill-Mining-Projekte das Potential der sensorgestützten Sortierung zu bewerten. Die Ergebnisse zeigen, dass das mögliche Ausbringen durch den Einsatz sensorgestützter Sortierer um bis zu 36 Gew.-% auf etwa 51 Gew.-% gesteigert werden kann. Durch großtechnische Versuchen muss die Langzeitstabilität dieser Technologien im Enhanced Landfill Mining nachgewiesen werden.

Abstract

Potential of Sensor-Based Sorting in Enhanced Landfill Mining under Consideration of the Effects of Defilements

In the past, landfill mining has been conducted with simple processing technology to keep specific processing costs down, yielding low value output fractions. The concept of enhanced landfill mining focuses on the production of high-quality output fractions, targeting improved economic efficiency. Sensor-based sorting machinery can contribute to this by material-specific separation of exploitable fractions. As a result, the production of marketable products is increased, reducing the share of landfill space that is occupied by these materials. The main challenge of implementing sensor-based sorting in enhanced landfill mining is the high degree of impurities, adhesions and contaminations in landfill material. This can inhibit the functioning of sensor-based sorting technology.

To study the most relevant impurities for sensor-based sorting, the material streams that show potential for such sorting technologies in mechanical processing of landfill material were identified: heavy fractions from air-classification and 3D-fractions from ballistic separation. Since near-infrared technology was found to be suitable for this sorting task, the most decisive factors that affect the selected spectral information and are therefore essential to make sorting decisions, were studied in detail: surface roughness and humidity. Increased surface roughness proved to enhance particle classification, while water absorbs near-infrared radiation and alters the material-specific spectral fingerprint of near-infrared active materials. This effect can be counteracted by adjustments in the sorting algorithm. Furthermore, first tests on the effect of thick oxide layers on x-ray fluorescence-based sorting were conducted and indicated technological feasibility for the application to landfill mining. For a comprehensive assessment of this technology further in-depth experiments are necessary.

In addition, the effects of input composition and throughput rate on sorting performance were quantified to gain a more comprehensive understanding of their relevance for sensor-based sorting stages and to determine potential for their improvement. By implementing the knowledge gained in these studies, the separation of combustibles and inert materials and the differentiation of various plastic types were carried out successfully. For example, the yields of polyethylene, polypropylene and polyvinylchloride were higher than 90 wt%. If successfully applied to enhanced landfill mining, sensor-based sorting technology could enable the recovery of 36 wt% of landfilled material in addition to approximately 15 wt% that could be unlocked with conventional mechanical processing technology. The long-term stability of sensor-based sorting machinery in enhanced landfill mining has to be proven in large-scale tests.

Publikationen

In der Folge sind die im Zuge der vorliegenden Dissertation erstellten Publikationen aufgelistet.

Konferenzbeiträge

Küppers B, García López C, Höllen D, Pomberger R, Clausen A, Pretz T (2017) Das „EU Training Network for Resource Recovery through Enhanced Landfill Mining“ (NEW-MINE). In: 7. Wissenschaftskongress Abfall- und Ressourcenwirtschaft

García López C, **Küppers B**, Höllen D, Clausen A, Pretz T (2017) Landfilled Materials Composition at the Landfill Site in Halbenrain (Austria). In: 5th International Conference on Sustainable Solid Waste Management – Athen

Pomberger R, **Küppers B** (2017) Entwicklungen in der sensorgestützten Sortiertechnik. In Österreichische Abfallwirtschaftstagung 2017

Küppers B, Muras A, Höllen D, Rothschedl R (2018) Landfill Mining of a Mixed Municipal Solid Waste and Commercial Waste Landfill: Application of Existing Processing Technology - Opportunities and Limitations. In: 4th International Symposium On Enhanced Landfill Mining

Vollprecht D, **Küppers B**, Pomberger R, Machiels L, Bernardo E, Krook J (2018) Das „EU Training Network for Resource Recovery Through Enhanced Landfill Mining (NEW-MINE). In: Recy & DepoTech Band 14

Hernández Parrodi JC, García López C, Raulf K, Pretz T, **Küppers B**, Vollprecht D, Pomberger R (2018) Characterization of Fine fractions from Landfill Mining – A Case Study of a Landfill Site in Belgium. In: Recy & DepoTech Band 14

Küppers B, Möllnitz S (2018) Versuchsstand für sensorgestützte Erkennung und Sortierung. In: 8. Wissenschaftskongress „Abfall- und Ressourcenwirtschaft“

Küppers B, Vollprecht D, Pomberger R (2018) Einfluss von Verschmutzungen auf die sensorgestützte Sortierung. In: Recy & DepoTech Band 14

Küppers B (2019) Möglichkeiten einer sensorgestützten Sortierung von Kunststoffabfällen – Der Einfluss von Verunreinigungen. In: ÖWAV Seminar Wertstoff Kunststoff, Kunststoffrecycling – Quoten und Herausforderungen

Küppers B, Vollprecht D, Pomberger R (2019) Einsatz sensorgestützter Sortierverfahren im Landfill Mining. In: Berliner Konferenz Mineralische Nebenprodukte und Abfälle: Aschen, Schlacken, Stäube, Baurestmassen. Band 6

Küppers B, Schlögl S, Friedrich K, Lederle L, Pichler C, Freil J, Pomberger R, Vollprecht D (2020) Correlations between Input Composition, Throughput Rate and Sorting Efficiency. In: Sensor-Based Sorting & Control (submitted)

Beiträge in Fachzeitschriften

García López C, **Küppers B**, Clausen A, Pretz T (2018) LANDFILL MINING: A CASE STUDY REGARDING SAMPLING, PROCESSING AND CHARACTERIZATION OF EXCAVATED WASTE FROM AN AUSTRIAN LANDFILL. In: Detritus

García López C, Ni A, Hernández Parrodi JC, **Küppers B**, Raulf K, Pretz T (2019) CHARACTERIZATION OF LANDFILL MINING MATERIAL AFTER BALLISTIC SEPARATION TO EVALUATE MATERIAL AND ENERGY RECOVERY POTENTIAL. Detritus

Küppers B, Schloegl S, Oreski G, Pomberger R, Vollprecht D (2019) Influence of surface roughness and surface moisture of plastics on sensor-based sorting in the near infrared range. In: Waste Management & Research

Küppers B, Chen X, Seidler I, Friedrich K, Raulf K, Pretz T, Feil A, Pomberger R, Vollprecht D (2019) INFLUENCES AND CONSEQUENCES OF MECHANICAL DELABELLING ON PET RECYCLING. In: Detritus

Pfandl K, **Küppers B**, Scheiber S, Stockinger G, Holzer J, Pomberger R, Antrekowitsch H, Vollprecht D (2019) X-ray fluorescence sorting of non-ferrous metal fractions from municipal solid waste incineration bottom ash processing depending on particle surface properties. Waste Management & Research

Vollprecht D, Bobe C, Stiegler R, Van De Vijver E, Wolfsberger T, **Küppers B**, Scholger R (accepted) Relating magnetic properties of municipal solid waste constituents to iron content – Implications for enhanced landfill mining. In: Detritus

Hernández Parrodi JC, García López C, **Küppers B**, Raulf K, Vollprecht D, Pretz T, Pomberger R (accepted) CASE STUDY ON ENHANCED LANDFILL MINING AT MONT-SAINT-GUIBERT LANDFILL IN BELGIUM: CHARACTERIZATION AND POTENTIAL OF FINE FRACTIONS. In: Detritus

Küppers B, Seidler I, Koinig G, Pomberger R, Vollprecht D (accepted) Influence of Throughput Rate and Input Composition on Sensor-Based Sorting Efficiency. Accepted by Detritus

Küppers B, Hernández Parrodi JC, García López C, Pomberger R, Vollprecht, D (accepted) Potential of Sensor-Based Sorting in Enhanced Landfill Mining. Accepted by Detritus

Table of Contents

	Page
1 INTRODUCTION.....	2
1.1 Problem Formulation.....	3
1.2 Scope of Investigations.....	4
1.2.1 Research Paper 1.....	5
1.2.2 Research Paper 2.....	5
1.2.3 Research Paper 3.....	6
1.2.4 Research Paper 4.....	6
1.2.5 Research Paper 5.....	6
1.2.6 Research Paper 6.....	7
1.2.7 Research Paper 7.....	7
2 PUBLICATION 1.....	8
3 PUBLICATION 2.....	26
4 PUBLICATION 3.....	46
5 PUBLICATION 4.....	55
6 PUBLICATION 5.....	64
7 PUBLICATION 6.....	76
8 PUBLICATION 7.....	93
9 SUMMARY.....	101
10 DISCUSSION.....	112
11 OUTLOOK AND FUTURE RESEARCH.....	117
12 REFERENCES.....	118
13 LIST OF ABBREVIATIONS.....	121

1 INTRODUCTION

Landfill mining (LFM) can be described as the extraction of materials that have been disposed of in a landfill (Krook et al., 2012). According to estimations 150,000 to 500,000 landfills exist in Europe, posing environmental and social potential for mining (Jones et al., 2013). The possibility of avoiding future gaseous and aqueous emissions from landfills by thermal or mechanical-biological treatment of excavated waste is considered as the main driver for LFM. Most often the economical profitability is questionable since revenues can only be created by the sale of metals which constitute merely a few wt% of the landfilled materials (Krook and Baas, 2013). As a result of the economic inefficiency of mining a landfill, simple and cheap processing technology is usually applied to conduct LFM, yielding in turn relatively few amounts of recyclables of low value (Krook and Baas, 2013). Furthermore, landfills are characterized by a high heterogeneity, especially when containing municipal solid waste, which additionally complicates the consistent processing of landfill material (Crowley et al., 2003).

In recent years, the concept of enhanced landfill mining (ELFM) has gained more attention as an improved practice of LFM. In ELFM, the benefit of producing marketable high-quality output fractions for material recycling and energetic use by applying innovative technologies is emphasized. With this enhanced concept, the economics of mining a landfill shall be positively impacted (Jones et al., 2013). Such output fractions comprise soil, metals, glass/ceramics and stones for material recovery and plastics, paper/cardboard, wood and textile for energetic use, e.g., in conventional waste-to-energy facilities with state-of-the-art technology (Danthurebandara et al., 2015; Quaghebeur et al., 2013a; Rotheut and Quicker, 2017). If more pre-treatment is conducted (cleaning, drying, cutting, sorting, etc.), technologies as gasification, pyrolysis, hydrogenation and recycling could also be implemented (Zhou et al., 2014).

Since the economic feasibility of ELFM is dependent on the quality and quantity of the output fractions, it is essential to choose processing technologies suitable for the production of such outputs (Danthurebandara et al., 2015). E.g., for the production of a compost product, material-specific separation of stone, glass, metals and plastics is needed (Masi et al., 2014). If solid recovered fuels are generated, the chlorine content must be limited due to its corrosive impact (Kaartinen et al., 2013). For such sorting tasks, simple processing technologies as screening or ballistic separation alone are not sufficient. However, the application of sensor-based sorting (SBS) machinery poses a suitable option for separating specific material fractions that potentially generate more high quality output fractions.

1.1 Problem Formulation

Applications for sensor technology, e.g. in form of SBS machinery, exist in the mining industry (Lessard et al., 2014; Wotruba et al., 2014), food industry (Alaya et al., 2019; Cubero et al., 2011) and in the recycling sector (Gundupalli et al., 2017; Serranti et al., 2012).

Near-infrared (NIR) spectroscopy has proven to be useful for distinguishing and separating plastic types (Gundupalli et al., 2017), wood (Tsuchikawa and Kobori, 2015), and minerals, whereby a sufficiently coarse grain size of at least 5 mm must be ensured with state-of-the-art technology (Wotruba et al., 2014). Accordingly, in the TönsLM project, NIR sorting technology is considered in ELFM scenarios for the production of plastic fractions for material recycling and the production of combustible fractions that could be further cleaned by separation of polyvinylchloride (PVC) (Breitenstein et al., 2016). Based on these findings, the theoretical suitability of NIR sorters for ELFM is given. However, no sorting experiments with state-of-the-art NIR sorting technology have been applied to landfill material yet.

X-ray fluorescence (XRF) sorting machinery presents another technology that enables the sorting of material flows based on material specific characteristics (Gundupalli et al., 2017). While this technology is not applicable to the separation of most plastic types, it is especially suitable for the distinction of various metal alloys (Gaustad et al., 2012; Gundupalli et al., 2017). Accordingly, for ELFM of landfills rich in metals, XRF sorting machinery provides an opportunity to reclaim various metal fractions as marketable output fractions, e.g., from municipal solid waste bottom ash. Therefore, the theoretical suitability of SBS technology for ELFM is given although it has never been tested in this context.

The implementation of SBS technology, e.g. NIR- or XRF-based sorters, in ELFM bears two main issues. First, the economic feasibility of SBS technology in ELFM is questionable but out of the scope of this thesis: A discrepancy between the high price of the sorting machine and the relatively low value of the marketable output fractions exists. Second, the technical feasibility of such machinery in the field of ELFM has not yet been investigated, which is the object of this thesis. Even though SBS technology has been implemented in several industries for sorting tasks, the field of ELFM bears particular challenges for implementing SBS. The share of contaminants, e.g., in form of surface defilements as rust, adhesive fines, water, surface roughness and organics, in landfill material is significant. This can be a particular hurdle for implementing SBS technologies with low penetration depths as NIR and XRF (Gundupalli et al., 2017). Therefore, the studies presented in this thesis assess the suitability of specific sensor technologies for ELFM.

1.2 Scope of Investigations

This doctoral thesis investigates the potential of SBS technology in ELFM and is subdivided into three subject areas that build on each other (compare Figure 1).

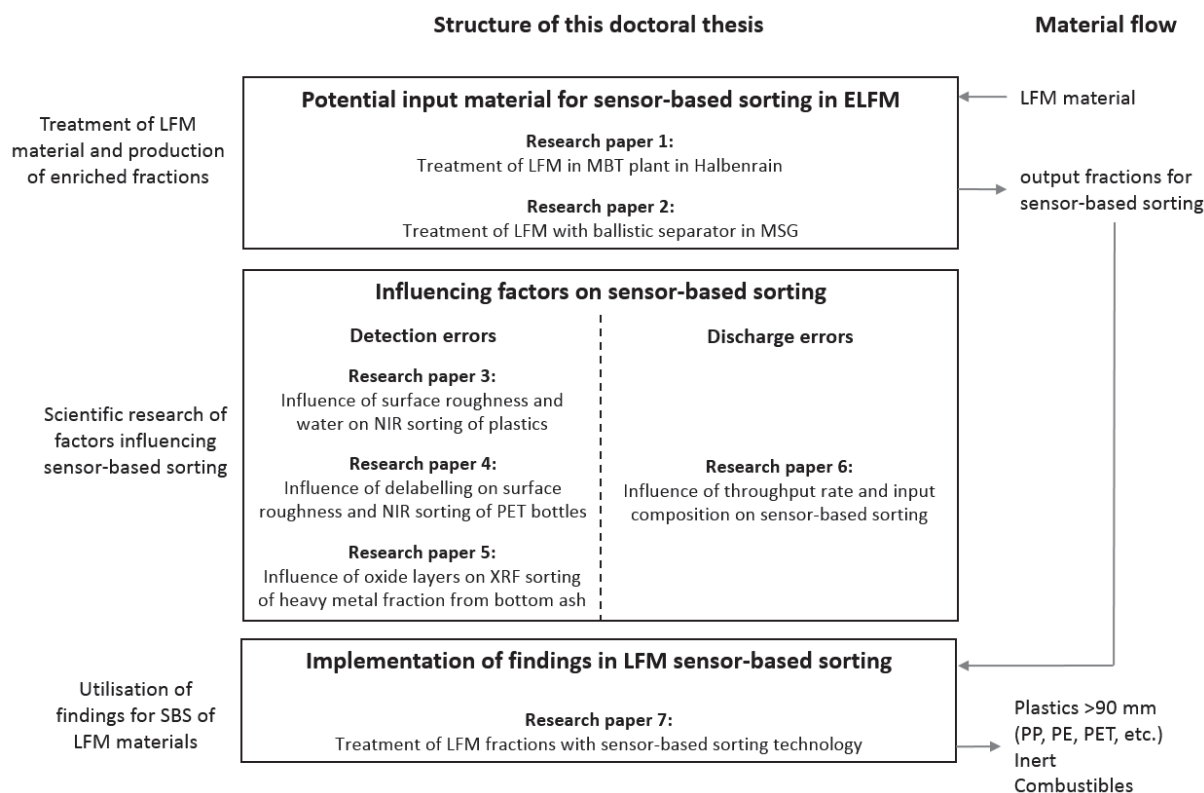


Figure 1: Concept of this doctoral thesis, divided into three subject areas (black boxes), MSG: Mont-Saint-Guibert.

In the first subject area, the material flows and sorting tasks that are relevant to the choice of SBS technology in an ELFM process are ascertained. This task is performed in publication 1 and publication 2. They reveal that material fractions from mechanical processing of ELFM materials contain potentially recyclable material, which could be gained via SBS. In addition, defilements and impurities, possibly impairing the sorting process in these fractions, were determined.

Based on this information, the predominant factors influencing SBS performance were selected for the second subject area, which pertains comprehensive investigations of the most relevant factors influencing SBS performance. The conducted studies fall into two sections: studies on detection errors resulting in the misclassification of materials and on discharge errors, which lead back to mechanical errors and/or overlapping particles. The first section consists of the publications 3, 4 and 5, dealing with the influence of water, surface roughness and labels on NIR-based classification of plastics and the effect of oxide layers on XRF-based sorting of metals. The second section includes publication 6 whose results allow conclusions on the influences of throughput rate and input composition on SBS, independent of the accuracy of the sensor technology installed in a sorting machine.

In the third subject area, the knowledge obtained from the first and second subject area is evaluated and applied to sorting trials with landfill material (publication 7). The results from these trials give insight into the expected sensor performance when implemented in ELFM processes. The findings concerning the influences of throughput rate and input composition on the sorting performance allow an improved modelling of SBS stages in various industry sectors such as mining, recycling and the food industry. By implementing the gained knowledge, the technical feasibility of SBS technology in ELFM was determined.

A research question was formulated based on each scientific elaboration and the emerging findings. The following subchapters present the scope of each paper and its specific research question.

1.2.1 Research Paper 1

In 2016, a landfill mining project was conducted on the landfill site of FCC Environment in Halbenrain, Austria. The landfill material, excavated within this project, was processed in the mechanical biological treatment (MBT) plant on site. Accordingly, the material was first dried biologically in rotting tunnels followed by mechanical processing in form of shredding, multiple screening stages, manual sorting of specific coarse fractions, ferrous and non-ferrous metal separation and air classification. Samples were taken at various sampling points along the process chain to analyse the input material and assess the MBT plant utilization for LFM by investigating the generated output fractions. The analyses comprised sieving analysis, distinguishing and quantifying material classes via hand sorting, determining water, ash and heavy metal contents and analysing the calorific value.

Research question:

Which output fractions of a mechanical-biological treatment plant, used for the processing of landfill material, show potential for sensor-based sorting?

1.2.2 Research Paper 2

In 2017, a second landfill mining project was conducted on a landfill site in MSG, Belgium. Within this project on an area of approx. 2150 m², a geophysical exploration was conducted. Subsequently, the cover layer (clay) was removed, enabling the excavation of 130 m³ of landfilled municipal solid waste as well as construction and demolition waste in four batches. Each batch was treated with a ballistic separator in a two-stage process (screen cuts: 200 mm and 90 mm) without any pre-treatment, resulting in five output fractions: 3D >200 mm, 2D >200 mm, 3D 200-90 mm, 2D 200-90 mm, <90 mm. Samples from all output fractions were taken based on the German Directives LAGA PN 78 and LAGA PN 98. The samples were dried and screened to analyse the grain size fractions via manual sorting. The calorific values and ash contents of the 2D fractions were additionally analysed.

Research question:

What output fractions of a simplified LFM treatment process show potential for sensor-based sorting?

1.2.3 Research Paper 3

The influences of surface roughness and water on NIR sorting of plastics were investigated, using an experimental setup for SBS and plastic reference materials. The spectral changes of various types of polyethylene, polyethylene terephthalate, polypropylene, polyvinylchloride and thermoplastic polyurethane due to water contamination and enhanced surface roughness were studied. Besides, the relevance of spectral changes for the classification and yield of plastic particles when sorted via compressed air shocks on a chute sorter was determined. The influences of surface roughness and water on the spectral information of plastics was investigated within the raw spectrum detected by the NIR sensor. This investigation achieved comprehensive understanding of changes in the normalized and smoothed first derivative, most commonly used for NIR-based SBS. To determine the influence of both factors on the classification of each object pixel, a sorting recipe was created specifically for the conducted trials.

Research question:

What effects do increased surface roughness and water have in principle on sensor-based sorting with NIR technology?

1.2.4 Research Paper 4

In pilot scale tests, the influences of labels and surface roughness on polyethylene terephthalate (PET) sorting were investigated. A sample of PET bottles, with fully attached labels from a public collection system, were used as the input material for delabelling trials with the “STADLER label remover”. The input material was fed to the delabeller at a throughput rate of approx. 4 t/h. The PET bottles in the output of each delabeller trial were sorted into three categories according to the share of the label that was successfully separated from each bottle: >98 %, 98-90 % and <90 %. In addition, a screening analysis of each fraction was conducted. Samples from the input and output material were taken and analysed with NIR sensor technology to assess the influences of the labels and the surface roughness generated via delabelling on PET recognition.

Research question:

Can the observed effects of increased surface roughness be transferred from laboratory testing to real waste fractions?

1.2.5 Research Paper 5

By sampling the heavy non-ferrous (NF) metals fraction <50 mm, about 2 t of input material were obtained for experiments from the Brantner Wet Slag process, which treats municipal solid waste incineration (MSWI) bottom ashes. This sample was screened into five grain size fractions: 0-6.3 mm, 6.3-10 mm, 10-16 mm, 16-20 mm and 20-50 mm. The ferrous (Fe) metals were separated from each fraction by using a drum magnet with traversing operation. NF metals were separated by eddy-current separation. NF metals from the fractions 6.3-10 mm, 10-16 mm and 16-20 mm were used for XRF sorting trials. To investigate the influence of

surface treatment on XRF sorting, the NF metals from each grain size fraction were divided into three samples for varying processing steps: no treatment, dry surface treatment and wet surface treatment. The surface treatment was conducted with a concrete mixer. Each sample was fed to the XRF chute sorter after the respective processing step to separate precious metals, zinc, copper, brass and stainless steel from each other via air shocks. The resulting product fractions from the grain size range 16-20 mm were examined in melting tests and chemical analyses.

Research question:

What influence do oxide layers and (wet mechanical) surface treatment have on XRF-based sorting of heavy metal fractions from bottom ash?

1.2.6 Research Paper 6

In total, 160 sorting trials were conducted on a pilot scale SBS machine with 1,000 red and white plastic chips. For each test series, eight overall, a distinct mixture of red and white particles (95 %/5 %, 90 %/10 %, 85 %/15 %, 80 %/20 %, 70 %/30 %, 60 %/40 %, 50 %/50 %, 20 %/80 %) was created and sorted 20 times at varying throughput rates/occupation densities. A sorting recipe ensured the correct recognition of all particles. Therefore, only mechanical errors and overlapping particles remain as factors that influence the performance of the sorting machine. The sorting efficiency for each trial was validated by manual sorting of the output fractions. The assessment of the sorting performance is carried out on the basis of three evaluation criteria: recovery (directly linked to product quantity), yield and product purity.

Research question:

How do input composition and throughput rate of a material stream influence the performance of a sensor-based sorting machine?

1.2.7 Research Paper 7

NIR-SBS technology was applied to assess the distinguishability and sortability of samples of output fractions taken from the two above-mentioned LFM case studies. The heavy fraction from the air classification step of a MBT plant, which was used for the processing of LFM material, was used to investigate the potential of NIR sorting technology for separating specific polymer types. Various particle size fractions of the fines product from a ballistic separator, tested for the processing of landfill material without any further pre-treatment, were used in sorting trials to assess the potential of NIR-SBS technology for the separation of combustibles and inert material. The sorting trials consisted of two phases. First, the raw spectra of the constituents of each sample were used to generate a sorting recipe for the distinction of the material classes. Second, sorting trials were conducted with all samples.

Research question:

Is the application of sensor-based sorting technology in ELFM technically feasible?

2 PUBLICATION 1

Landfill Mining: A Case Study regarding Sampling, Processing and Characterization of Excavated Waste from an Austrian Landfill

García López C, Küppers B, Clausen A, Pretz T (2018) LANDFILL MINING: A CASE STUDY REGARDING SAMPLING, PROCESSING AND CHARACTERIZATION OF EXCAVATED WASTE FROM AN AUSTRIAN LANDFILL. *Detritus* 02:29-45. Doi: 10.31025/2611-4135/2018.13664

Annotation on my own contribution to publication 1:

Cristina García López and I jointly carried out the sampling, processing and characterization of the excavated waste in consultation with Adele Clausen and Thomas Pretz. This included the development of a sampling plan, sampling, screening analysis, ferrous and non-ferrous separation, and manual sorting. Furthermore, I provided support and guidance for the evaluation and assessment of the obtained data. All co-authors reviewed the publication.

LANDFILL MINING: A CASE STUDY REGARDING SAMPLING, PROCESSING AND CHARACTERIZATION OF EXCAVATED WASTE FROM AN AUSTRIAN LANDFILL

Cristina García López ^{1,*}, Bastian Küppers ², Adele Clausen ¹ and Thomas Pretz ¹

¹ Department of Processing and Recycling, RWTH Aachen University, Aachen, 52062, Germany

² Chair of Waste Processing Technology and Waste Management, Montanuniversität Leoben, Leoben, 8700, Austria

Article Info:

Received:
17 January 2018
Revised:
14 May 2018
Accepted:
24 June 2018
Available online:
30 June 2018

Keywords:

Landfilled waste
Mechanical biological treatment
Enhanced landfill mining
Landfill directive
Recycling
New mine

ABSTRACT


The following case study belongs to the New-Mine project and the objective of the project is to develop a new "Enhanced Landfill Mining" (ELFM) scenario for a combined resource-recovery and remediation strategy. This strategy could reduce future remediation costs and reclaim valuable land while simultaneously unlocking valuable resources. In the past, insufficiently reliable data about the composition of landfills, overestimation of the quality of excavated material and poor product marketing of the possible recyclables have resulted in a bad reputation for landfill-mining projects. The ongoing research in the NEW-MINE project shall show that there are possibilities to create valuable outputs from landfills with enhanced treatment processes, such as a better distribution of the different mechanical processes. To create mechanical routes to recover valuable materials from old landfills, it is important to characterize the material, creating a basis for the research. The objective of this case study, executed from November 2016 until June 2017 at the landfill site in Halbenrain (Austria), is to study the efficiency of different sorting technologies with old landfill material. The excavated material was transported and used as feedstock in a configured state-of-the-art mechanical-biological treatment (MBT) plant located next to the landfill. During the mechanical processing, metals and high-calorific fractions were sorted out from the input flow. As a result of the mechanical processing, approx. 3% of the ferrous metals were recovered, approx. 20% of potential RDF (pRDF) was separated and could have been energetically recovered, and approx. 74% belonged to the finer fraction (< 40 mm). Each sample from the sampling campaign was sieved to obtain the particle size distribution. Via manual sorting, the material was classified into plastics, wood, paper, textile, inerts, Fe metal, NF metals, glass/ceramic and residuals. In addition, the moisture (wt%), the ash content (wt%), the calorific value (MJ/kg) and the concentration of heavy metals (%) of the finer fraction (<40 mm) were analysed. The aim of this study is to assess the possibilities of different mechanical processes with landfill mining (LFM) material and to gain information about the characterization of five material flows derived from the mechanical treatment, together with the mass balance of the MBT. Although every landfill has its own characteristics, the results obtained from this case study can help to understand the general potential, contribute to develop methodologies for characterization of old landfill material and identify problematic fields that require further research.

1. INTRODUCTION

As the world population increases, the generation of municipal solid waste (MSW) is increasing, and landfills continue to be filled with recyclables that could be used otherwise as raw materials or for energy recovery. The situation is even more critical if we look back in time. Before the European Directive 1999/31/CE was implemented and defined different categories of waste, MSW could

have been mixed and buried without treatment/sorting according to local legislation. Moreover, insufficient disposal charges for landfilling did not prevent the negative impacts of landfills, either.

In the 1970s, there was a period of rapidly increasing raw material prices and rising concern about finite natural resources. Several studies forecasted serious shortages by the end of the century. Recycling of household waste was considered a partial solution to the problem. There

 * Corresponding author:
Cristina García López
email: garcialopez@ifa.rwth-aachen.de

was also increasing awareness regarding the negative impact of simple dumping without appropriate barrier systems or pretreatment prior to landfilling. Since then, many technological advances have been developed to produce refused-derived fuels (RDF) and to separate recyclable materials from residual MSW (Ferranti et al. 1985). However, despite the efforts in the last 40 years to improve the situation, landfilling is still the most common method of organized waste disposal in Europe, according to Eurostat.

In 2014, Europe treated 2319 mill t of MSW by six treatment operations, defined in the Waste Framework Directive 75/442/EEC: 41% disposal on land, 36% recovery (other than energy recovery - except backfilling), 10% recovery (backfilling), 7% land treatment/release into water, 5% energy recovery, and 1% incineration (Eurostat, 2014). Figure 1 shows four of six management systems for MSW in Europe by country.

Currently, Europe accumulates between 150.000 and 500.000 old landfill sites, of which approximately 10% meet the EU Landfill Directive requirements and are considered sanitary landfills. In most cases, non-sanitary landfills lack the required environmental protection technologies and will eventually demand costly remediations to avoid future problems (NEW-MINE, 2016). Due to the existence of those non-sanitary and sanitary landfills, possible valuable resources are being lost and concurrently the environment and human health damaged. Therefore, remediation strategies for existing landfills are fundamental in the direction to preserve resources, environment and human health. A further argument to recover the valuable resources is the crisis that concerns the economic situation and the energetic matrix, which is mainly based on fossil fuels and water energy, where prices for energy and secondary resources are increasing steadily.

The composition inside a landfill generally depends on different parameters, such as waste regulations and legislation, differences in the waste management systems,

recycling systems, standard of living and the society and culture of the setting (Quaghebeur et al., 2013). Proper investigations of each site, including the operation history, waste type dumped, dimensions of the landfill, topography and physical-chemical analyses, are necessary to make a careful feasibility analysis about the material potential inside the landfill (Salerni, 1995). Apart from considering the material potential, a critical factor to take in consideration before starting an ELFM project is the quality of the materials to recover and the market price, which varies over time and region.

The present work belongs to the New-Mine project, supported by the European Commission since September 2016, in collaboration with another landfill mining project of FCC at the landfill site of Halbenrain (Austria). The scope of the project is to transform a large fraction of old excavated LFM into higher-added-value products. The project is designed to combine a remediation strategy with the recovery of resources, as seen in Figure 2.

The purpose of this study is to provide foundational knowledge of the composition and characteristics of excavated material from a specific MSW and Industrial landfill, which is important for the sizing of mechanical sorting. Moreover, this paper aims to assess the possibilities of different mechanical processes with landfill mining (LFM) material and to gain information about the characterization of five material flows derived from the mechanical treatment, together with the mass balance of the MBT. The novelty of this research is the biological treatment (drying stage) prior to mechanical treatment, in addition to the use of a complete MBT plant, which differs from other studies in which mobile machinery is applied.

Although every landfill has its own characteristics, the results obtained from this case study can help to understand general potentials, contribute to develop methodologies for characterization of old landfill material and identify problematic fields that require further research.

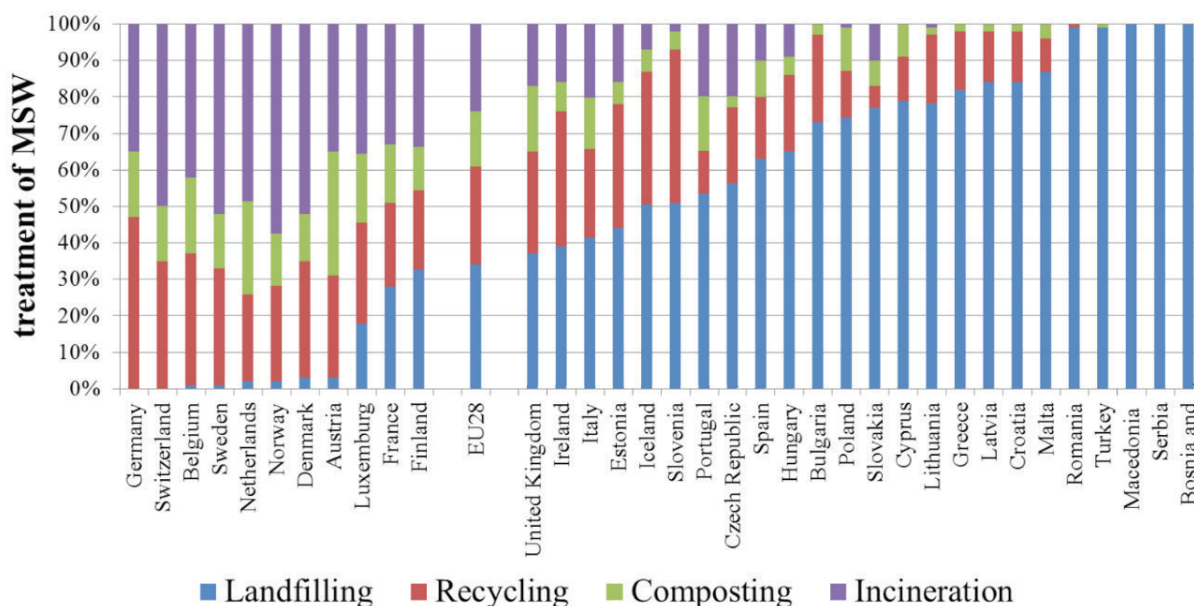


FIGURE 1: Relevance of the main MSW management systems in the EU-28 in 2012 (Source: Eurostat, 2014).

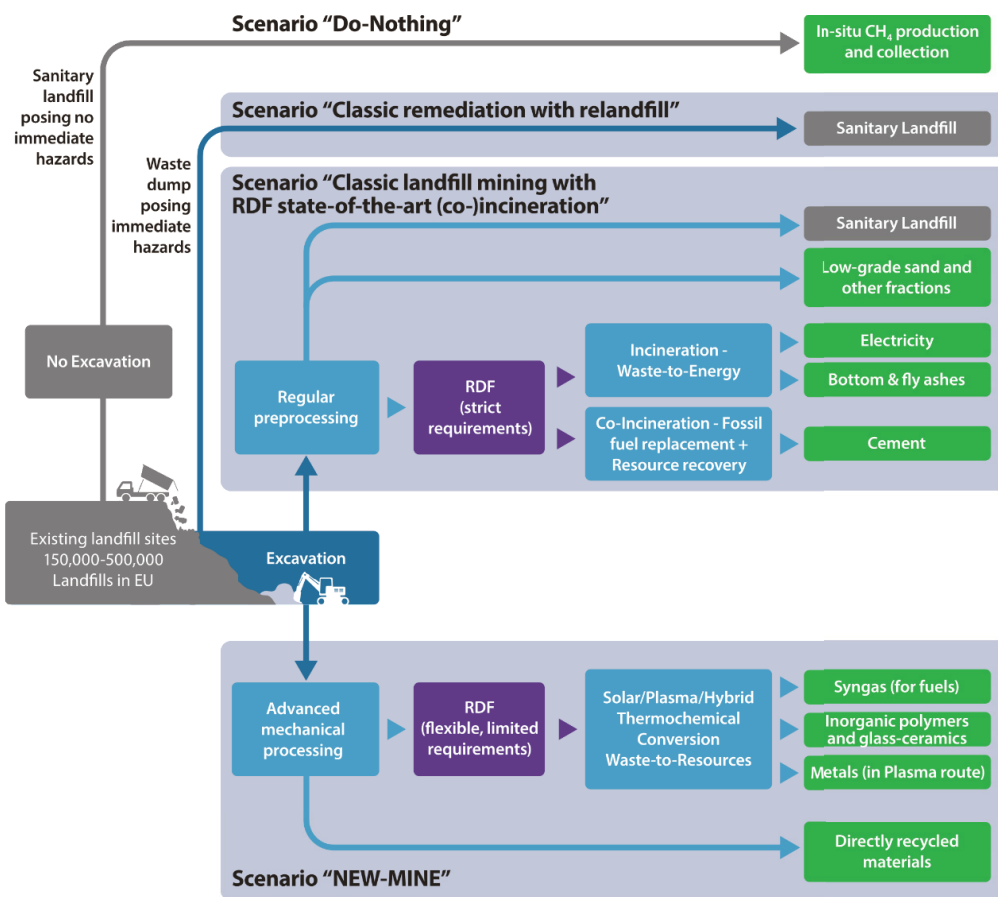


FIGURE 2: Comparison of different scenarios for the EU's landfills, Do-Nothing (only acceptable for well-monitored sanitary landfills), Classic Remediation (where the materials are excavated and re-landfilled), and Classic Landfill Mining coupled with (co)incineration, and the NEW-MINE, ELFM Scenario (Source: EURELCO www.new-mine.eu).

2. MATERIAL AND METHODS

2.1 Site description

The landfill site in Halbenrain belongs to FCC Halbenrain Waste Treatment Centre and is located 75 km south-east of Graz (Austria). The landfill was established in 1978 and received MSW and industrial waste. Currently, the examined area is in the post-closure phase, and it has an extension of 16 ha, with a total volume of 2.4 million m³ of waste. The site has developed over the years to include a waste disposal facility with leachate treatment, conversion of landfill gas into electricity, composting, sorting and mechanical-biological waste treatment.

2.2 Excavation and processing at the site

In June 2016, FCC initiated a landfill-mining project on site with the aim of recovering metals disposed between 1997 and 1999. Based on records about the landfill composition, eight areas of interest were estimated to contain a relatively high percentage of recyclable materials, being metals of great interest for ELFM. The material examined during the case study was extracted of the projected area marked in red (Figure 3), approx. 20x20x10 m, at a depth of 6 m.

The mining activity included the following steps: 1) excavation (Figure 4), 2) transportation to a Mechanical and

Biological Treatment (MBT) plant, 3) biological treatment and 4) mechanical treatment with potential Refused Derived Fuels (RDF) separation and metal recovery.

During the case study, two batches (batch 1: 220 t, batch 2: 280 t) were excavated, treated and characterized.

Normally, MBT plants stand at the beginning of an efficient waste treatment process. By using a selective treatment process, unsorted waste can be separated into different fractions, which then can undergo further treatment (e.g., potential RDF) or be used for material recovery (metals). The design of these processes must be adapted to national regulations and market situations to be successful.

After the excavation, the LFM material was sent to an already-existing and configured MBT plant on site, which is used to treat fresh household waste. As a first step of the MBT process, the material was dried by aerobic activity (rotting boxes for 3-4 weeks). During this treatment, a loss of water of approx. 10 wt% and a possible organic matter reduction were achieved. Once the material was stabilized, it was sent to the full-scale mechanical process.

The semi-dry material was fed to a single shaft shredder that reduced the particle size of the material to 250 mm. The shredder also transformed the input material to a uniform size and eliminated overlengths that could interfere with the successive process. Afterwards, an overbelt magnet separated the large pieces of ferrous metals. After

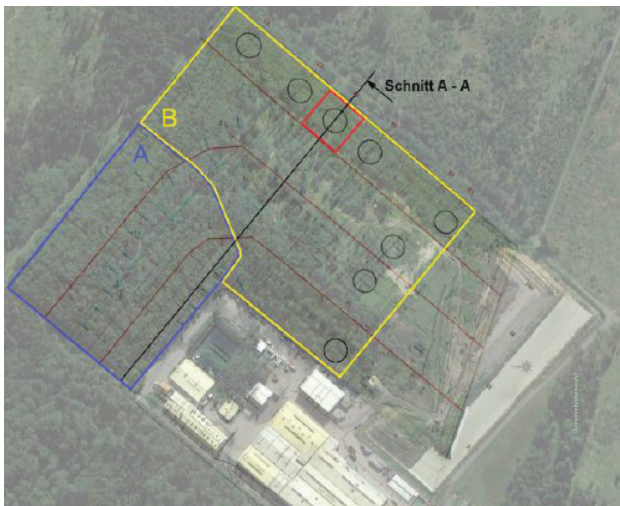


FIGURE 3: Overview of landfill site Halbenrain; "A" filled 1979-1990; "B" filled after 1990; black circles mark especially interesting areas with higher amount of metals; projected area marked in red.

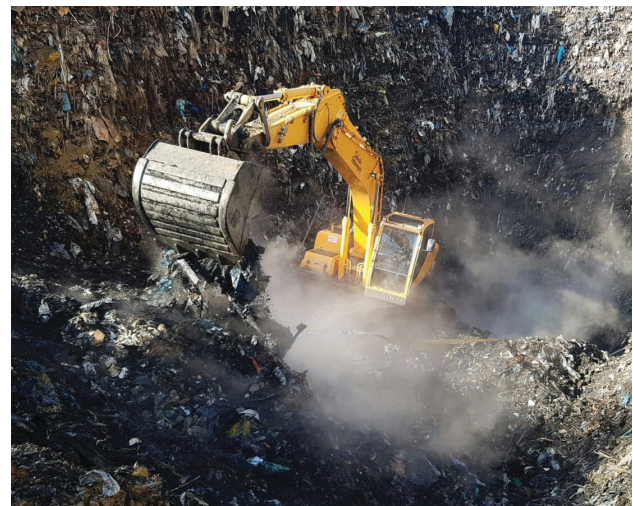


FIGURE 4: Excavation of LFM material from late 1990s at the landfill site in Halbenrain (Austria).

the magnet, the first sampling point (SP1) was established; see Figure 5.

Due to the plant design, the input material (prior the magnetic separator) was not accessible as a sampling point, and the Fe-metal concentration (wt%) sorted before the SP1 was calculated by measuring the weight of the pile after processing the batch of excavated waste. After passing the magnetic separator, the material was screened with circular vibratory screens with a mesh size of 60 mm (S1). The screen enabled the enrichment of metals and high calorific fractions – referred as potential RDF in the following – in the coarse and to concentrate the biogenic material in the underflow.

The material flows of the 250-60 mm and <60 mm fractions were further processed and characterized:

1. The overflow, 250-60 mm, was sorted with an additional overbelt magnetic separator (MS2) and screened at a diameter of 200 mm (S2). The fines from the 200-mm screen (fraction: 200-60 mm) were treated with a zig-zag windsifter to separate the light and heavy fractions of the flow. The coarse fraction, 250-200 mm, was directly balled, together with the light fraction of the windsifter.
2. The underflow, <60 mm, was stored for further treatment. The results are not reported in the present publication.

2.3 Sampling campaign

The selection of a method for representative sampling is one of the most difficult decisions regarding waste flow analysis due to the material's heterogeneity. Normally, the material composition inside the landfill is variable, depending on the digging point chosen for the excavation. The sampling campaign was designed in order to obtain reliable information about different techniques of waste segregation (Figure 6).

In this study, the material was organized by batches, and during the processing of the whole batch, several sam-

ples were taken at different times. The sampling points, labelled SPx in Figure 5, were directly conveyor belt discharges. The number (n) of the single samples in each SPx was based on the German directive LAGA PN 98 - procedures for physical, chemical and biological testing in connection with the recovery/disposal of waste. LAGA PN 98 defines that the number of samples depends on the total quantity (m³) of the material flow (see Appendix A: Tables). The mass of the sample depends on the maximum diameter, D_{max}, of the particle size (Formula 1) according to LAGA PN 78.

$$\text{Single sample in kg} = D_{\text{max}} [\text{mm}] \times 0,06 \text{ kg} \quad (1)$$

During the sampling campaign, two batches of ~230 t/batch of semi-dried landfill material were characterized.

2.4 Mass balance

The mass balance of the MBT plant in Halbenrain was calculated based on the batches that fed the MBT plant. The weight of both input and outputs were measured.

2.5 Characterization of LFM material

The outcome of the characterization helps to study the potential of landfills for raw materials. In addition, it provides data about the effect of MBT technology with old LFM waste. It has to be noted that the facility used during this case study was not designed for treating old landfilled material. Therefore, the choice of the technology in the process was not perfectly optimized for the treatment, and the results of the sorting should be interpreted with care.

The quantity and quality of the LFM material after each mechanical process were determined based on the particle size distributions in each material flow, classifying each sample by hand (Table 1) and analysing physical and chemical characteristics of the fine fractions (<40 mm).

2.5.1 Bulk density

The bulk density of each material flow at SP1, SP2, SP3,

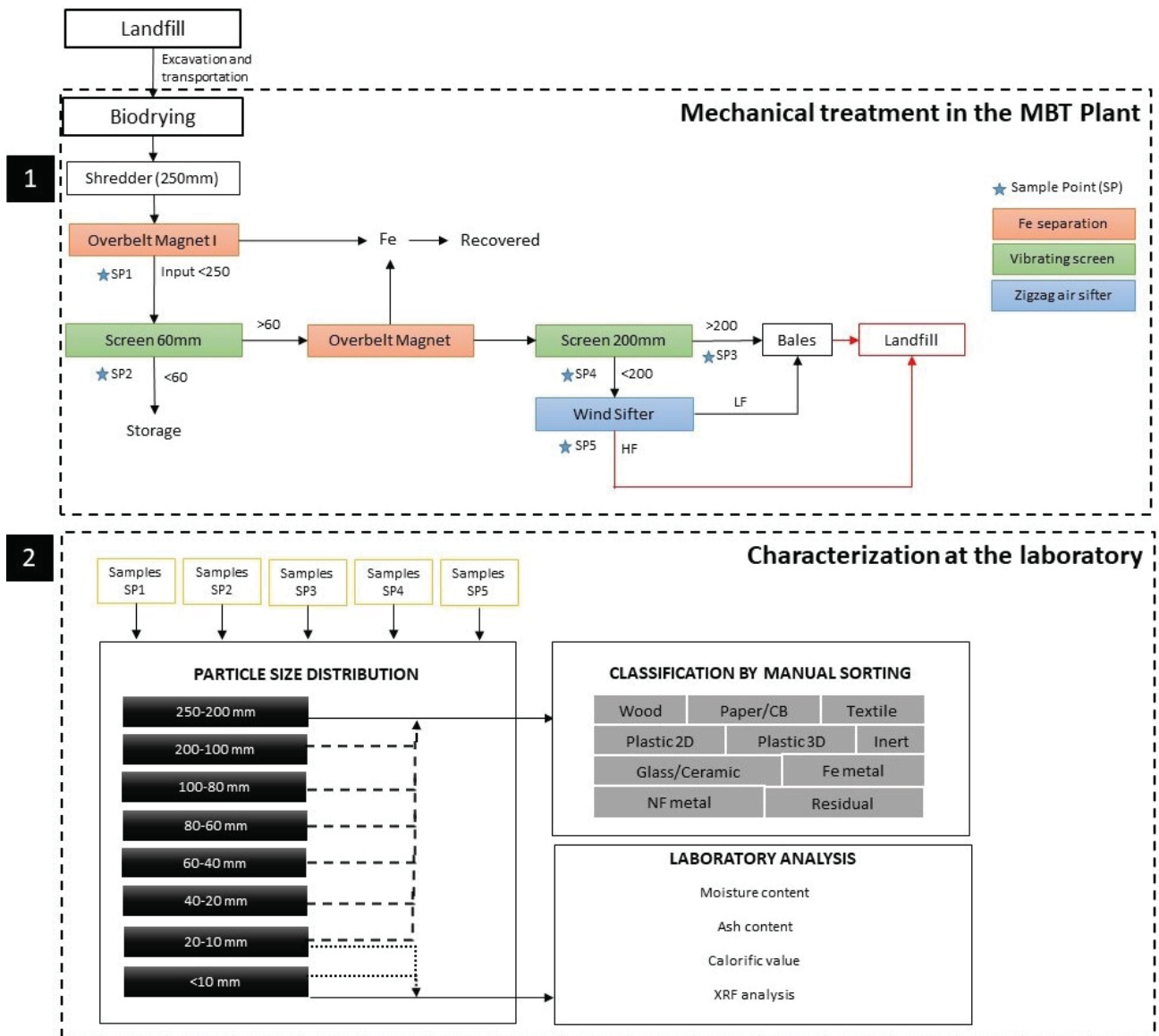


FIGURE 5: Methodology for the characterization of the LFM material in Halbenrain (Part 1: flowchart of the MBT process at the site with sampling points (SPx); Part 2: characterization of the smaller fractions < 40 mm in the laboratory).



FIGURE 6: Input material after a shredder and an overbelt magnet, SP1 (left) and fines from the first screen 60 mm, SP2 (right).

SP4 and SP5 was computed by taking the mean of several filling recipients of 90 L directly from the flow and measuring its weight.

2.5.2 Particle size distribution analysis

Each composite sample from each sampling point was individually sieved for 90 seconds using drum sieves with the following mesh sizes: 200, 100, 80, 60, 40, 20, and 10 mm. The particle size distribution helps to determine in which fractions of the flow desired materials are concentrated.

2.5.3 Manual sorting

The outcome of the drum sieve were eight fractions: >200 mm, 200-100 mm, 100-80 mm, 80-60 mm, 60-40 mm, 40-20 mm, 20-10 mm and <10 mm. Subsequently, all fractions >10 mm were sorted manually and classified into 10 categories (Table 1).

2.6 Characterization at the laboratory: physical-chemical analysis

The fine fractions <40 mm (40-20 mm; 20-10 mm; <10 mm) were reduced in mass based on the German standard given in the previous chapter 2.3 and delivered to the RWTH Aachen University. Further analysis was performed with the objective to estimate the waste-to-energy characteristics (moisture content, ash content, calorific value and heavy metal concentration; Jani et al. 2016). To be able to analyse the last three parameters, the particle of the samples had to be mechanically reduced to <2 mm, and each sample (<40 mm) was separated into 3 subcategories: light fraction (LF), heavy fraction or rest (HF) and metals.

2.6.1 Moisture content

The moisture content of waste is closely related to the amount of organic matter, and it differs with the habits of the population. In the EU and the USA, it ranges from 20-30%, whereas values in China are from 30-60% due to the higher content of kitchen garbage (Jani et al., 2016).

Looking at existing landfills, different factors affect the moisture content, e.g., the type, composition and properties of the waste, climatic conditions, landfill operating system and soil cover layer (Hull et al., 2005). The moisture con-

tent is important when considering the recycling of waste to produce energy through biological and/or thermal treatment (Brunner and Rechberger, 2015), in addition to for sorting the material during the mechanical pretreatment.

The standard DIN EN 14346:2007 "Characterization of waste – Calculation of dry matter by determination of dry residue or water content" suggests to dry the samples at 105 °C. However, volatile fractions would also evaporate at this temperature, making certain plastic particles melt, thus resulting in a less precise analysis. Therefore, the moisture content was determined by drying the samples of each material flow in a ventilated oven at 75°C until reaching a constant temperature.

2.6.2 Particle size reduction (pretreatment)

After the drying process, a reduction of the particle size of three fractions (40-20 mm, 20-10 mm and <10 mm) was necessary to analyse the calorific value and organic content and to determine the heavy metals. Each sample was classified with an air sifter into a light fraction (LF) and a heavy fraction (HF). The metals contained in the sample were sorted previously using a magnet to avoid damage caused by further processing machines. In general, the LF had larger particle sizes than the remaining inerts in the flow. By sieving, using a mesh size of 2 mm, the LF could be freed of the majority of the inerts. The HF was crushed with a hammer mill and afterwards grinded in a disk mill. In the case of LF with a particle size >2 mm, a cryogenic comminution method using liquid nitrogen was used to reduce in size flexible materials such as 2D plastics. The result of comminution was a powder or flakes with sizes <2 mm for the LF and <1 mm for the HF.

This reduction (pretreatment) is needed to provide relatively homogenic material fractions in comparison to the initial material for further tests (ash content, calorific value and XRF analysis). The mass of each fraction (LF, HF/rest and metals) was measured to consider the share of each, in wt%.

2.6.3 Ash content

The ash content/organic content was calculated using 1 g of sample in each fraction, 40-20 mm, 20-10 mm and <10 mm (from SP1), and analysed by using a muffle furnace according to DIN EN 14775.

The volatile compounds calculated as the difference between the initial weight in the test and the weight of the remaining solids after the incineration is an indicator of the organic matter content.

2.6.4 Net calorific value

The calorific value was determined for the same samples as for the organic content. In this case, a bomb calorimeter was used according to the standard DIN 51900. The test consisted of complete combustion with oxygen of approx. 0.5 g of a dried sample in a bomb with a pressure of 40 bars. The heat transmitted to the surrounding water was measured and the net calorific value calculated accordingly.

2.6.5 XRF analysis

The content of heavy metals was determined with a

TABLE 1: Classification by categories.

Category	Material
Wood	All types of wood
Paper	Paper/cardboard/composite carton
Textile	All types of textile
Plastic 2D	Aluminum package/bags (transparent/white/colored)
Plastic 3D	PP/PET/PET Oil/PEAD/PEBD/PVC/PS/Others
Fe metals	Iron
NF metals	Copper/Aluminum can/steel
Inerts	Mineral fraction (stones)
Glass	Colorless glass/green glass/brown glass/others
Residual	Sanitary material, rubber, foam, silicone, melted plastics, sandpaper, electronic plates, hazards, undefined

Niton™ XL3t X-ray fluorescence (XRF) spectrometer. For the analysis, the samples of each fraction (< 10 mm, 10-20 mm and 20-40 mm) of the sampling points (SP1-SP5) were analysed eight times. Afterwards, the mean values for all samples and the standard deviation were computed.

3. RESULTS AND DISCUSSION

3.1 Mass balance of the MBT plant with LFM material

In total, 2786 t of excavated material were treated mechanically, and 3% of Fe metal was recovered. The rest of the output flows with possible recoverable materials were landfilled again. Figure 7 depicts the mass balance of the MBT plant.

3.2 Characterization of the material flows

3.2.1 Bulk density

The bulk density depends on both the density and arrangement (compaction) of the particles in the flow. For instance, the bulk density in the input material flow (SP1), with a particle size 250-0 mm, was 0.25 t/m³ (see Table 2), whereas higher-bulk-density material was found in the fine fraction (<60 mm) of the 60-mm screen, with 0.62 t/m³. The coarses “250-200 mm” had a lower bulk density (0.05 t/m³) compared to the fines “200-60 mm” (0.18 t/m³). This result can be explained with the enrichment of light material types such as foils in the coarses and an increased amount of e.g., inerts and wood in the fines. These shifts in the composition can be explained as a result of the effects of the screening has on the material flow.

TABLE 2: Mean values of the bulk density at each sampling point (SP1-SP5) of the MBT plant.

Sampling point	Bulk density t/m ³
SP1	0,25
SP2	0,62
SP3	0,05
SP4	0,18
SP5	0,27

3.2.2 Composition of the material flows

Input flow of the mechanical treatment (<250 mm) (SP1). The composition of the input flow is decisive for the rest of the flows in the plant, since this is the raw material that shall be classified, sorted by density, magnetism, induction, etc. Figure 8 shows the average composition (wt%), where the largest proportion is the fine fraction (<10 mm), with approx. 50% of the total mass. The fines (<10 mm) are mainly soil, glass shards and mineralized organic matter. In chapter 2.3., “Physical-chemical analysis”, one finds a detailed characterization of this fraction in the input flow (SP1). The content of ferrous metals (Fe), as presented here, must be considered with care, since it is only representative for the material flow after the first magnetic separation unit (overbelt magnet).

It must be considered that the weight of most defilements (fine particles) remains on the manual sorted fractions (wood, paper, plastics, etc.). These defilements not only have the effect of changing the mass balance but can

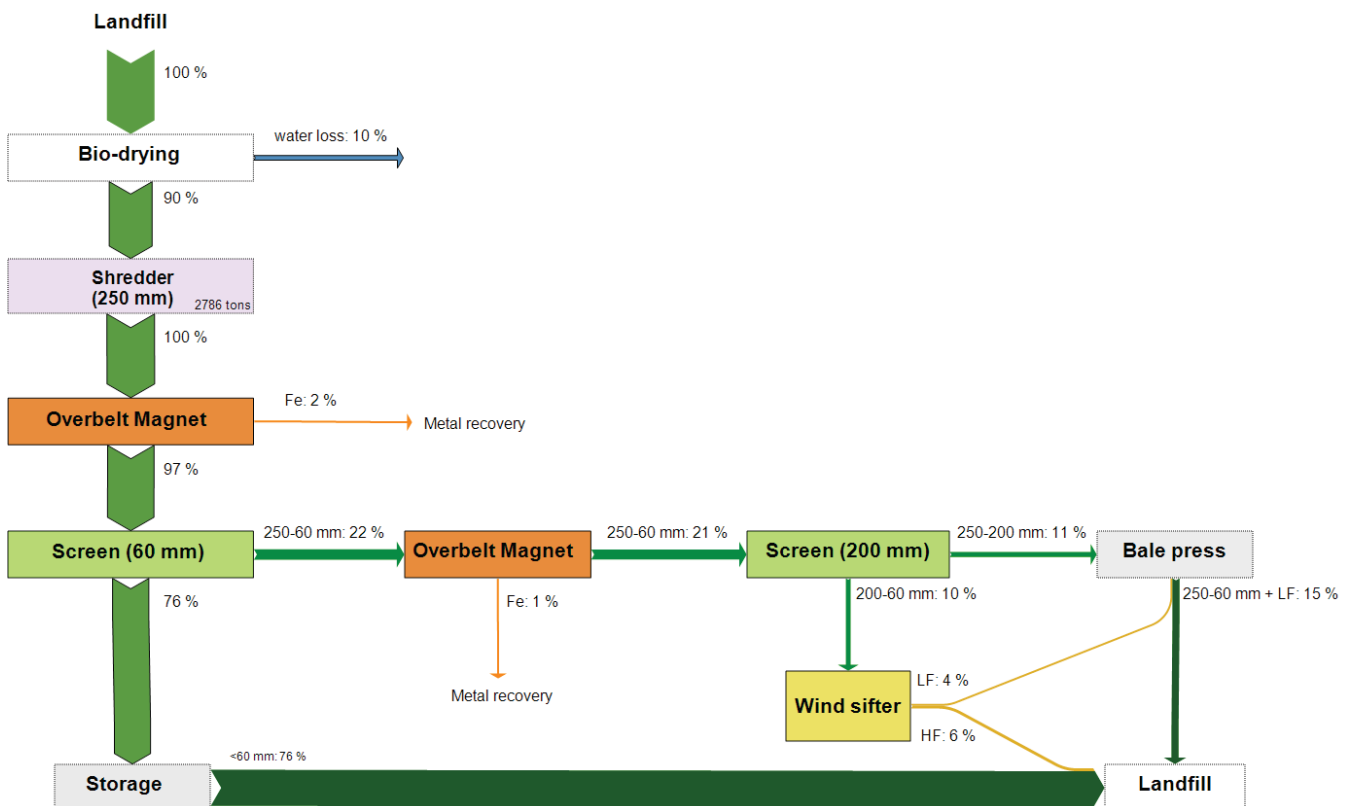


FIGURE 7: Mass balance of the MBT in Halbenrain (Austria).

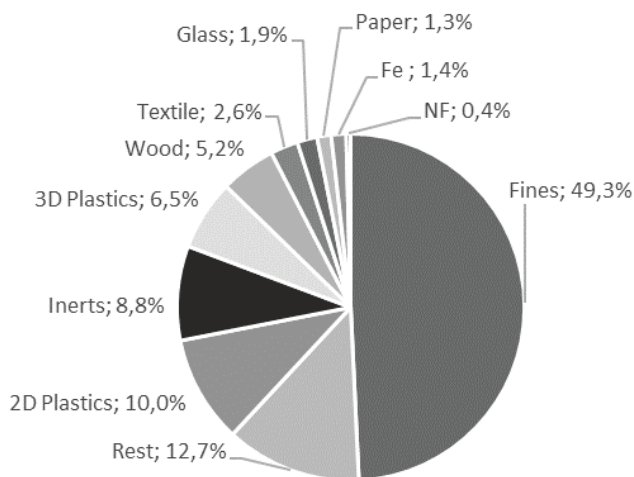


FIGURE 8: Average composition (wt%) of the material supplied in the MBT plant during the sampling campaign after a shredder and a magnet separator, SP1.

also reduce the heating value. The influence of the defilements attached to coarse particles is larger for flat particles (e.g., 2D plastic) since the surface is bigger in comparison to the total weight of a particle than it is for round or cubic objects.

The results from the input composition cannot be used for comparison with earlier studies in a reliable manner since the proceeding in each investigation varies. In this manner, the results are not properly comparable due to differences in properties and pre-processing, e.g., moisture content, analytical approach, mechanical and/or biological treatment. Once a common methodology is used, a proper comparison can be possible. However, the amount of fines (<10 mm) found in Halbenrain, 49%, is comparable to those found in Kuopio, Finland, with 50-54% (Kaartinen et al., 2013); Lower Austria, Austria, with 47% (Wolfsberger et al., 2015); and Remo, Belgium, with 44±12% (Quaghebeur

et al., 2013). Regarding the amount of plastics (2D and 3D plastics), Halbenrain accounts for 16.5%, whereas the amount in Kuopio, Kujape, Lower Austria and Remo are 23%, 22.4% (Bhatnagar et al., 2017), 18%, and 17±10%, respectively.

The variability of the results from 12 samples taken in the same sampling point (SP1) can be observed in Figure 9.

The absolute fluctuation in fines (<10 mm) is greater than in the remaining smaller categories, e.g., Fe, NFe, and glass. In fines (<10 mm), there is a 13% absolute variation, whereas the ferrous content fluctuates 4%, but its relative fluctuation is greater than the one of the fines (<10 mm), resulting in a bigger impact on the amount of product that can be generated from it. In this manner, for example, the potential revenues would rather be affected by ferrous fluctuations since this material type is initially more marketable than the fines (<10 mm).

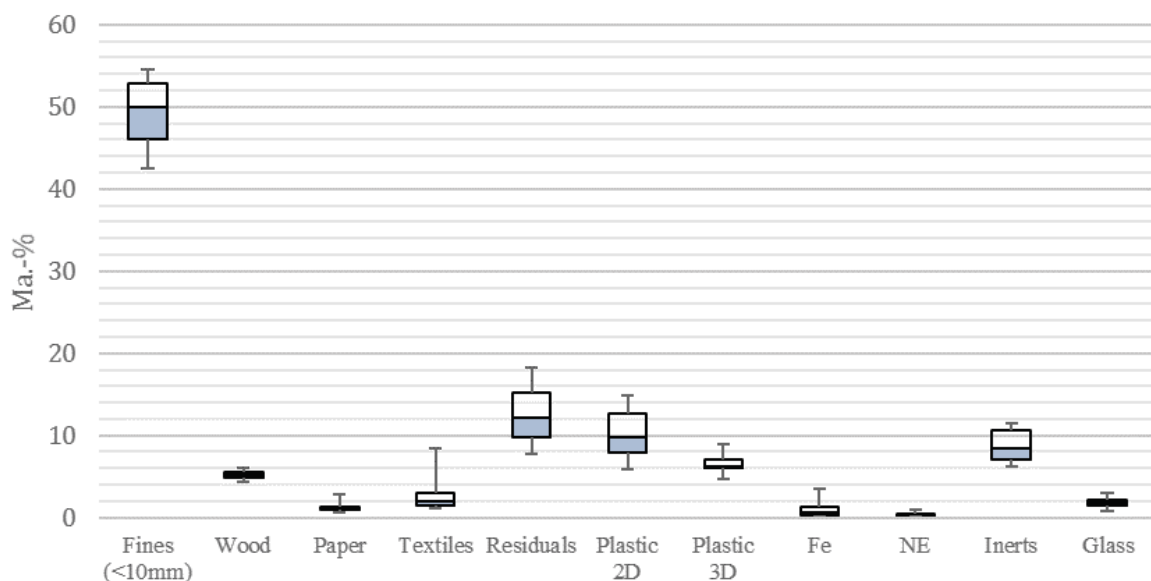


FIGURE 9: Range of the share of different material groups in the input flow of both batches (n=12).

Figure 10 shows the composition of the input material and other sampling points after each mechanical step, %wt semidry basis. See Appendix A for more information.

Output flow of the screen 60 mm - fine fraction (< 60 mm) (SP2). The fines from the 60-mm screen mainly consist of <10 mm fines, which account for approx. 71%; see Figure 10. Impurities in the flow are also found, including plastic particles (6%), glass (3%) and metals (1%). The content of glass in this material flow is greater than in the rest of the examined flows. The screening efficiency turned out to be lower than expected, resulting in an increased amount of fines in the coarses flow. This reduced efficiency can be ascribed to agglomeration of fines.

Output flow of the 200-mm screen - coarse fraction (250-200 mm) (SP3). The coarses of the 60-mm screen (250-60 mm) were sorted by a second magnet separator and sieved with a 200-mm screen. The amounts of fines in the flow are reduced, but there is still a remaining portion of 7.1%, which indicates that screening efficiency and the quality of the material. In the next chapter, regarding the particle size distribution, the efficiency of the screen can be assessed. This flow is characterized by its light fraction of 2D plastics (28.9%), followed by 3D plastics (21.2%), residuals (16.6%) and textiles (13.7%). This is an example that demonstrates the necessity of cleaning the material flow of impurities (mineral fraction) and concentrating the potential RDF (plastics, wood, textiles, and paper) via screening.

Output flow of the 200-mm screen - fine fraction (200-60 mm) (SP4). The fine fraction from the 200-mm screen (200-60 mm) consists of a large share of inerts (20.2%), which could have been part of the covering layer of the landfill. MSW rarely consists of that many medium-sized stones. Apart from inerts, 3D and 2D plastics account for the biggest share in the composition of the flow. Once again, a significant amount of fines (<10 mm), 8.9%, was

found. The screening efficiency could have been improved by using a bigger screen or a mesh size with a bigger opening size surface. The order of the 200- and 60-mm screens should have been switched, performing coarse screening first and afterwards using the 60-mm screen. In this case, the mechanical process was already configured prior the landfill mining project.

Output flow of the windsifter I - heavy fraction (HF 200-60 mm) (SP5). The input material of the windsifter had a particle size of 60-200 mm. The major categories inside the heavy fraction flow are inerts (34.5%), wood (19.6%) and 3D-plastics (24.1%). The LF flow had an enrichment of 2D plastics, paper, textile and fines, which were almost removed from the heavy fraction flow. In addition, a big share of metals was found in the HF flow in comparison to the rest of the material flows. Hypothetically, a magnetic and an eddy current separator, after the windsifter in the heavy fraction, could have recovered 3.2% of Fe metals and 1.7% of NF metals. Instead, these valuable metals were returned to the landfill.

3.2.3 Particle size distribution of the material flows

The results for the particle size distribution demonstrate the efficiency of the screens and other sorting aggregates according to the grain sizes: <10 mm, 10-20 mm, 20-40 mm, 40-60 mm, 60-80 mm, 80-100 mm, 100-200 mm and 200-250 mm. Figure 11 provides an overview of percentage of the total mass by particle and the cumulative screening throughput in the input material flow <250 mm (SP1).

Input material flow (SP1): The composition of the coarses (>40 mm), Table 3, consists of mainly potential RDF (pRDF) materials, which are 2D and 3D plastics, textiles and wood with supposedly high calorific value, whereas the opposite is true for inerts, metals and glass. In addition, the category "residuals" contains a high concentration of combustibles, such as nappies, which could also be val-

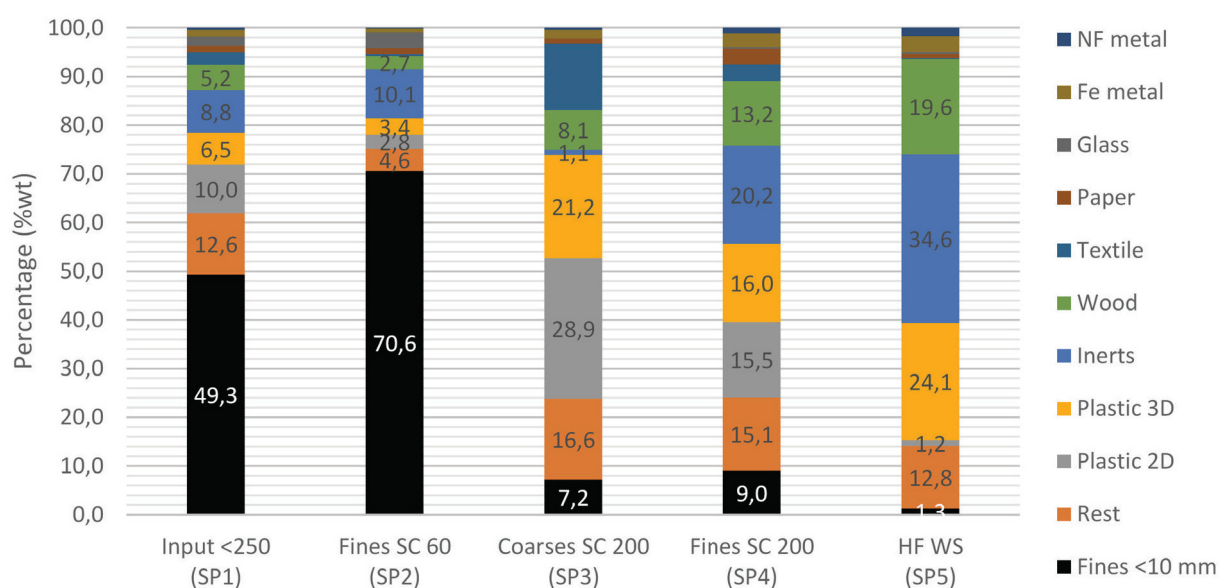


FIGURE 10: Composition of the input material (SP1) and output flows after each mechanical process (SP2, SP3, SP4, SP5).

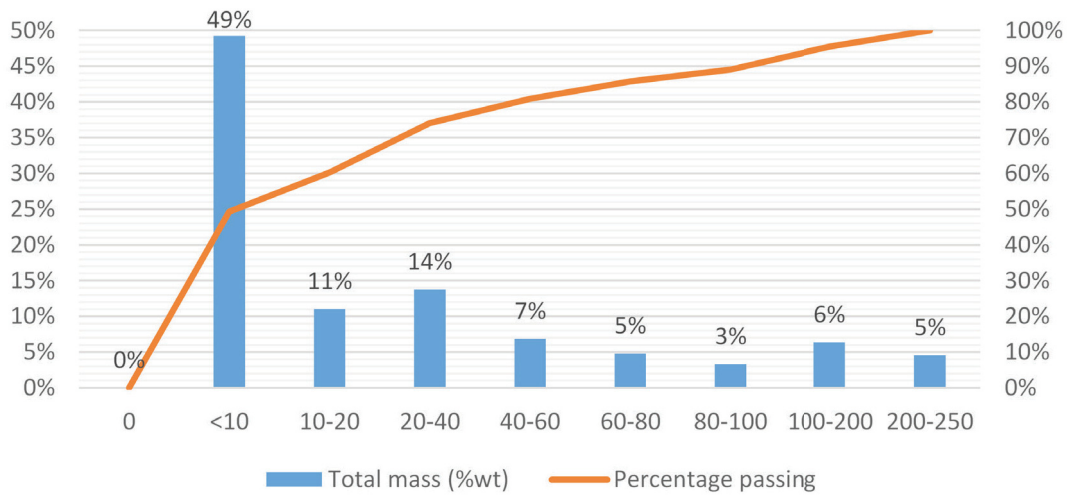


FIGURE 11: Particle size distribution of the input flow (SP1).

orized energetically. The amounts of NF and Fe in the input flow remain relatively low.

The fine fraction (<40 mm) in SP1 represents approx. 74 wt% of the entire input mass flow, being 60% the share of <20 mm and 49% of <10 mm. Similar amounts of fines have been found in previous characterizations of fine fraction mined. For example, the fine fractions (<20 mm) of two MSW landfills in Finland, Lohja and Kuopio, were on average 45%±7% and 58%±11%, respectively (Mönkäre, T. J. et al. 2015), similar to U.S. landfill reclamation projects: at least 50% and 46% of the excavated material were <25 mm in a landfill in New Jersey and one in Delaware, respectively (Hull et al. 2005; Miller et al. 1991), and in a landfill in Pennsylvania and one in Florida, approx. 41% and 60% were <20 mm (Forster 1994; Von Stein et al. 1993).

Table 4 presents the pRDF materials fractions in different particle size ranges. In the case of the coarse fraction, >80 mm, there is a bigger share of plastics and textiles.

Wood and paper have a greater share in the size range of 20-100 mm than in the rest of fractions.

Initially, the composition of the LFM material is not very positive in terms of finding large quantities of recyclables, Table 5, but via biological and mechanical treatment, this complex material can be partly cleaned from impurities (particles <40 mm), and possible desirable materials, e.g., pRDF, metals and soil can be sorted out from the flow for further treatment processes, e.g., thermal valorization, fines treatment, and metal recycling.

As seen from the results of the mechanical processing, the coarse flow of the 200-mm screen (250-200 mm) is an example of enrichment of pRDF. The amount of pRDF in the particle size fraction 100-200 mm of the input material is 7.3 wt%, whereas in the coarses of the 200-mm screens, in the same particle size class, is 28.5 wt%. The treatment of these would reduce the landfill volume that is occupied. Another point of the sieving is to classify the material by

TABLE 3: Comparison of the composition of the particle size classes in the input material flow (SP1), wt%.

Particle size (mm)	<10	10-20	20-40	40-60	60-80	80-100	100-200	200-250
RDF	0	28	43	55	60	64	63	88
Fe	0	2	4	4	1	3	1	2
NF	0	0	1	2	1	2	0	0
Inerts	0	22	23	23	18	8	8	0
Glass	0	9	6	1	1	0	0	0
Residual	0	38	24	16	18	22	28	10
Fines	100	0	0	0	0	0	0	0

TABLE 4: High calorific materials by particle sizes in the input material flow (SP1), wt%.

Particle size (mm)	<10	10-20	20-40	40-60	60-80	80-100	100-200	200-250
Wood	0	9	13	13	15	10	7	0
Paper	0	2	4	4	3	3	1	0
Textile	0	0	1	2	4	7	7	26
Plastic 2D	0	10	13	19	21	25	32	43
Plastic 3D	0	7	12	17	17	20	16	19

TABLE 5: Total mass of the input material flow and percentage by categories in the input material after a magnetic separator, wt%.

Categories	Coarse fraction 250 - 40 mm	Fine fraction <40 mm
Wood	2	3
Paper	1	1
Textile	2	0
2D Plastics	7	3
3D Plastics	5	2
Fe metals*	1*	1*
NFe metals	0	0
Inerts	3	6
Glass	0	2
Rest	5	8
Fines (<10 mm)	0	49
Total	26	74

* Fe metals sum a total of 3% in the initial material feedstock. The amount of Fe-metals in this table is reduced due to the influence of an over-belt magnetic separator prior the sampling point SP1.

size and achieve a higher efficiency in the following mechanical treatment. For example, according to Pretz et al. 2010, for an effective windsifter treatment, the ratio between the maximum and minimum particle sizes should not exceed 3:1. Even though the grain size range of 60-200 mm used in the MBT did not match the recommendations, still, the air sifting process was satisfactory. The windsifter helped to reduce the impurities contained in the fraction with a size from 200-60 mm, from a share of 8.9 wt% of fines (<10 mm) to 1.3 wt%. Furthermore, the windsifter concentrates the heavy fraction, which commonly consists of 3D plastics, inerts and metals. The composition of the HF material flow of the windsifter contains 87 wt% of coarses (200-60 mm), where 45 wt% are pRDF and 37 wt% are inerts, in the form of stones. It is also important to highlight the amount of residuals, between 200-60 mm, in the same material flow, which has a share of 13 wt%.

Based on this information, particle size distributions of the LFM material and the results of this study can be used as guidance for mechanical treatment. Further chemical analyses are mandatory to determine whether the quality of the excavated material, e.g., fines and inerts, fits the standards for its recuperation.

TABLE 6: Mean values and standard deviation (in brackets) of the moisture content, organic content and calorific value of the input material in fine fractions (<10 mm; 10-20 mm; 20-40 mm).

Input (mm)	Moisture (wt% semidry basis)	Composition (wt% dm)			Organic content (wt% dm)			Calorific value (MJ/kg dm *)			Total
		LF	HF	Metal	LF	HF	Metal**	LF	HF	Metal**	
<10	32	7	91	2	78.0 (0.02)	32.0 (0.02)	0.0	25.9 (0.01)	6.0 (0.02)	0.0	7.2
10-20	17	18	77	5	81.0 (0.01)	23.0 (0.00)	0.0	25.0 (0.88)	5.1 (0.01)	0.0	8.5
20-40	20	23	73	4	84.0 (0.01)	29.0 (0.07)	0.0	32.5 (0.56)	6.1 (0.21)	0.0	11.9

* dm: dry matter

** It is assumed the amount of organic content of the metals is 0 wt% dm; therefore, its calorific value is also 0 MJ/kg dm

See Appendix A-B for more results from each sampling point.

3.3 Physical-chemical analysis

Hull et al. pointed out in his study that waste fractions that can absorb moisture such as fines, paper, cardboard, wood and textiles had much higher moisture contents than fractions that cannot absorb water. However, it has to be considered that the size of the fines is another factor that influences the moisture content As can be observed from Table 6, <10 mm has a higher moisture content, 32 wt%, than 10-20 mm and 20-40 mm, 17 wt% and 20%, respectively, due to capillary forces on particles <10 mm.

Even if the results of this chapter are focused on the fines, moisture of samples containing all fractions could be almost equal. The mean moisture content of fines in previous investigations ranges from 16 to 43% (Hull et. al 2005).

The calorific value varies of the samples analysed from 7.2 to 11.9 MJ/kg, depending on the share of organic content (<10 mm: 34.6 wt%, 10-20 mm: 32.3 wt%, 20-40 mm: 40.0 wt%).

The percentage of heavy metals contained in the fine fractions, reported in Table 7, are not below the Austrian limits, at least, to use the fine fraction for compost. In previous characterizations of landfilled material characterizations (Hull et al. 2005), selected trace metals also exceeded soil background levels and recommended levels when applying sewage biosolids to agricultural land.

There is an increase of the heavy metal content according to the diminution of the particle; < 10 mm has a higher concentration of heavy metals than 20-40 mm. Further analysis is mandatory to estimate the potential of this fraction for construction material due to the amount of impurities (metals, glass shards and plastics).

4. CONCLUSIONS

The results from the investigations in Halbenrain landfill show that almost 90 t of ferrous metals could be recovered from 2785 t of mined landfill waste (approx. 3%). However, even combined with the profit from nonferrous metals, the profit would be insufficient to make such a landfill mining project feasible today. This fact is further influenced negatively by the fact that the defilements on plastics that could e.g., be used for thermal valorization

TABLE 7: Mean and standard deviation (in brackets) of the heavy metals contained in the fine fractions: <10 mm, 10-20 mm, 20-40 mm, (% dry basis).

Metals	Fraction			Limit values * (%) [Austria, 2018]
	<10 mm	10-20 mm	20-40 mm	
Pb	0.155 (0.098)	0.112 (0.00)	0.087 (0.000)	0,020
As	0.007 (0.000)	0.007 (0.00)	0.002 (0.000)	-
Zn	0.708 (0.104)	0.490 (0.00)	0.297 (0.000)	0,180
Ni	0.046 (0.002)	0.025 (0.00)	0.026 (0.000)	0,010
Cr	0.220 (0.004)	0.187 (0.00)	0.093 (0.000)	0,025
Cd	0.003 (0.000)	0.003 (0.00)	0.004 (0.000)	<0,001
Cu	0.659 (0.366)	0.395 (0.010)	0.324 (0.020)	0,050

* General requirements for waste-compost, quality class B, in Austria (Bundesrecht konsolidiert: Gesamte Rechtsvorschrift für Kompostverordnung, Fassung vom 05.03.2018, BGBl. II Nr. 292/2001)

reduce the heating value and increase the ash content of such pRDF.

Furthermore, comparisons with previous landfill mining studies could be performed, even though such comparisons are made difficult by differences in landfill composition, preprocessing and the analytical approaches in such projects. However, certain similarities among this and former studies can be noted, such as similar amounts of fines (50 wt%) and plastics (17 wt%). In particular, the amounts of fines, 74 wt% < 40 mm and 50 wt% < 10 mm, represent the biggest share of the excavated material, as Hernández Parrodi et al., 2017 also indicated in his study where this fraction can be as high as 40-80 wt% in various landfills around the world, and they need further investigation in order to reduce the financial burden they are today.

Moreover, fluctuations in the material compositions can be highly problematic. On one hand, these fluctuations can influence the load on different machines, potentially reducing the performance of the whole plant. On the other hand, such fluctuations, even if they might seem relatively small, can reduce the marketable fractions. Even if ferrous or non-ferrous products only make up a small amount of the total LFM material, when this amount varies between 1 and 5 wt%, the amount of marketable product can also fluctuate approximately 500%. Another problem with the mechanical process is the moisture of the material: if the material is not dry or semi-dried, as in this case for biological treatment, the quality of the sorting is lower, the amount of impurities adhered to the surface increases and the mass balance of each category would not be representative for the real composition (e.g., soil-type paper absorbs large amounts of water).

Chemical analysis reveals the presence of heavy metals in specific fractions. Depending on the further treatment of the different output fractions of such an LFM project, the limit values must be considered. Depending on the country

LFM material recovery should be conducted according to the applicable limit values, which can constitute a problematic hurdle and determine whether such a project can be viable.

Another inconvenience of landfill mining is the presence of hazardous materials, in addition to the contaminated soil, which drastically reduces the potential of the landfill as a source of resources. However, this inconvenience should not stop landfill mining activities, since the environmental issue that landfills entail cannot be ignored, and remediation strategies are necessary to avoid future costs.

ACKNOWLEDGEMENTS

This research has received funding from the European Union's Horizon 2020 Program (H2020/2014–2019) under Grant Agreement no. 721185 (MSCA-ETN NEW-MINE).

The authors would like to acknowledge the help from the Chair of Waste Processing Technology and Waste Management of Montanuniversität Leoben (Austria) and the support given by FCC Halbenrain Abfall Service Gesellschaft m.b.H. & Co Nfg KG. This publication reflects only the author's view, exempting the Community from any liability. Project website: <http://new-mine.eu/>.

REFERENCES

- Bhatnagar, A., Kaczala, F., Burlakovs, J., Kriipsalu, M., Hogland, M., & Hogland, W. (2017). Hunting for valuables from landfills and assessing their market opportunities A case study with Kudjape landfill in Estonia. *Waste management & research : the journal of the International Solid Wastes and Public Cleansing Association, ISWA*, 35(6), 627–635.
- Brunner, P. H., & Rechberger, H. (2015). Waste to energy—key element for sustainable waste management. *Waste management (New York, N.Y.)*, 37, 3–12.
- Bundesminister für Land- und Forstwirtschaft, Umwelt und Wasserwirtschaft verordne (2001). Verordnung des Bundesministers für Land- und Forstwirtschaft, Umwelt und Wasserwirtschaft über Qualitätsanforderungen an Komposte aus Abfällen (Kompostverordnung): BGBl. II Nr. 292/2001.
- EURELCO (2017). NEW MINE – EU Training Network for Resource Recovery Through Enhanced Landfill Mining, from European Union's EU Framework Programme for Research and Innovation Horizon 2020: <http://new-mine.eu/>.
- Eurostat (2014a). Classification of treatments: Directive 75/442/EEC.
- Eurostat (2014b). Treatment of waste by waste category, hazardousness and waste operations, from http://appsso.eurostat.ec.europa.eu/nui/show.do?dataset=env_wastrt&lang=en.
- Ferranti, M. P. (op. 1985). *Sorting of household waste and thermal treatment of waste*. London: Elsevier.
- G. A. Forster (1995). *Assessment of Landfill Reclamation and the Effects of Age on the Combustion of Recovered Municipal Solid Waste*.
- Hernández Parrodi, J. C., Höllen, D., Pomberger, R. (2017). Characterization of fine fractions from landfill mining: A review of previous landfill mining investigations. *Proceedings Sardinia 2017*.
- Hull, R. M., Krogmann, U., & Strom, P. F. (2005). Composition and Characteristics of Excavated Materials from a New Jersey Landfill. *Journal of Environmental Engineering*, 131(3), 478–490.
- Jani, Y., Kaczala, F., Marchand, C., Hogland, M., Kriipsalu, M., Hogland, W., & Kihl, A. (2016). Characterisation of excavated fine fraction and waste composition from a Swedish landfill. *Waste management & research : the journal of the International Solid Wastes and Public Cleansing Association, ISWA*, 34(12), 1292–1299.
- Kaartinen, Tommi; Sormunen, Kai; Rintala, Jukka (2013): Case study on sampling, processing and characterization of landfilled municipal solid waste in the view of landfill mining. *En: Journal of Cleaner Production* 55, pág. 56–66. DOI: 10.1016/j.jclepro.2013.02.036.

- Kranert, M., & Cord-Landwehr, K. (2010). Einführung in die Abfallwirtschaft (4., vollständig aktualisierte und erw. Aufl.). Vieweg Studium. Wiesbaden: Vieweg + Teubner.
- Miller, Logan V., Mackey, Robert E., and Flynt, Jim (1991). "Excavation and Recycling Feasibility Study of a Municipal Solid Waste Landfill Utilizing Leachate Recycle. Report to Post Buckley, Schuh, and Jernigan, Inc and The Delaware Solid Waste Authority.
- Ministerium für Umwelt und Forsten Rheinland-Pfalz (Dezember 1983): Grundregeln für die Entnahme von Proben aus Abfällen und abgelagerten Stoffen. Richtlinie für das Vorgehen bei physikalischen und chemischen Untersuchungen im Zusammenhang mit der Beseitigung von Abfällen. LAGA - RL. PN 2/78K.
- Ministerium für Umwelt und Forsten Rheinland-Pfalz (Dezember 2001): Richtlinie für das Vorgehen bei physikalischen, chemischen und biologischen Untersuchungen im Zusammenhang mit der Verwertung/Beseitigung von Abfällen. LAGA PN 98.
- Mönkäre, T. J., Palmroth, M. R. T., & Rintala, J. A. (2016). Characterization of fine fraction mined from two Finnish landfills. Waste management (New York, N.Y.), 47(Pt A), 34–39.
- Quaghebeur, M., Laenen, B., Geysen, D., Nielsen, P., Pontikes, Y., van Gerwen, T., & Spooren, J. (2013). Characterization of landfilled materials: Screening of the enhanced landfill mining potential. Journal of Cleaner Production, 55, 72–83.
- Salerni, E.L. (1995). Landfill Reclamation Manual. Reclaim-95-Landfill Mining, 28–29, SWANA Landfill Reclamation Task Group.
- Von Stein, E. L., Savage, G. M. (1993). Evaluation of the Collier Country, Florida, Landfill Mining Demonstration. EPA/600/R-93/163.
- Wolfsberger, T., Aldrian, A., Sarc, R., Hermann, R., Höllen, D., Budischowsky, A., et al. (2015). Landfill mining: Resource potential of Austrian landfills–Evaluation and quality assessment of recovered municipal solid waste by chemical analyses. Waste management & research : the journal of the International Solid Wastes and Public Cleansing Association, ISWA, 33(11), 962–974.

APPENDIX A: Tables

TABLE i: Minimum number of individual/composite samples according to LAGA PN 98.

Name sampling point	Volume m ³	Theoretically			Sampling campaign		
		Individual samples n	Composite samples n	Sample weight Kg	Individual samples n	Composite samples n	Sample weight Kg
SP1	400	32	8	15	18 *	6 *	21
SP2	30	8	2	15	8	2	12 *
SP3	30	8	2	15	8	2	15
SP4	30	8	2	12	8	2	18
SP5	30	8	2	12	8	2	21

* For technical reasons the number and the amount of the samples were not possible to reach in accordance to the guideline

TABLE ii: Composition by sampling point (%wt semidry basis).

Sampling point	Input <250 (SP1)	Fines SC 60 (SP2)	Coarses SC 200 (SP3)	Fines SC 200 (SP4)	HF WS (SP5)
Fines <10 mm	49,3	70,6	7,2	9	1,3
Rest	12,6	4,6	16,6	15,1	12,8
Plastic 2D	10	2,8	28,9	15,5	1,2
Plastic 3D	6,5	3,4	21,2	16	24,1
Inerts	8,8	10,1	1,1	20,2	34,6
Wood	5,2	2,7	8,1	13,2	19,6
Textile	2,6	0,4	13,7	3,5	0,2
Paper	1,3	1,2	0,9	3,2	0,9
Glass	1,9	3,3	0,1	0,3	0,4
Fe metal	1,4	0,7	1,8	2,9	3,2
NF metal	0,4	0,2	0,4	1,1	1,7

TABLE iii: Comparison of the composition by particle sizes in the fine fraction of the screen 60mm (SP2), wt%.

Particle size (mm)	<10	10-20	20-40	40-60
Fines <10mm	100,0%	0,0%	0,0%	0,0%
RDF	0,0%	28,1%	37,1%	47,3%
NF	0,0%	0,2%	1,1%	1,3%
Fe	0,0%	2,2%	1,9%	3,6%
Inerts	0,0%	37,6%	32,9%	30,5%
Glass	0,0%	16,1%	11,0%	1,3%
Residual	0,0%	15,8%	15,9%	16,1%

TABLE iv: High calorific materials by particle sizes in the fine fraction of the screen 60mm, wt%.

Particle size (mm)	<10	10-20	20-40	40-60
Wood	0,0%	7,2%	9,8%	11,6%
Paper	0,0%	4,5%	3,4%	3,8%
Textile	0,0%	0,6%	1,2%	3,2%
Plastic 2D	0,0%	6,5%	9,9%	14,6%
Plastic 3D	0,0%	9,3%	12,8%	14,1%

TABLE v: Comparison of the composition by particle sizes in the output flow (>200mm) of the screen 200, wt%.

Particle size (mm)	<10	10-20	20-40	40-60	60-80	80-100	100-200	200-250
Fines <10mm	100,0%	0,0%	0,0%	0,0%	0,0%	0,0%	0,0%	0,0%
RDF	0,0%	75,5%	71,4%	69,5%	73,9%	71,1%	79,6%	81,4%
NF	0,0%	0,0%	1,6%	1,2%	1,1%	1,8%	0,4%	0,0%
Fe	0,0%	0,0%	1,5%	0,6%	0,9%	0,1%	1,4%	3,4%
Inerts	0,0%	2,7%	3,1%	11,8%	0,6%	4,7%	0,0%	0,0%
Glass	0,0%	2,9%	1,5%	0,0%	0,0%	0,0%	0,0%	0,0%
Residual	0,0%	18,9%	21,0%	17,0%	23,5%	22,2%	18,6%	15,2%

TABLE vi: High calorific materials by particle sizes in the output flow (>200mm) of the screen 200 mm, wt%.

Particle size (mm)	<10	10-20	20-40	40-60	60-80	80-100	100-200	200-250
Wood	0,0%	31,6%	15,5%	26,1%	17,3%	14,4%	10,5%	0,8%
Paper	0,0%	9,1%	8,1%	3,7%	2,1%	1,2%	0,5%	0,0%
Textile	0,0%	7,1%	6,2%	2,4%	5,3%	6,5%	8,7%	26,9%
Plastic 2D	0,0%	16,8%	16,4%	18,5%	23,5%	23,4%	35,5%	32,9%
Plastic 3D	0,0%	10,9%	25,1%	18,8%	25,6%	25,5%	24,4%	20,8%

TABLE vii: Comparison of the composition by particle sizes in the output flow (<200 mm) of the screen 200, wt%.

Particle size (mm)	<10	10-20	20-40	40-60	60-80	80-100	100-200
Fines <10mm	100,0%	0,0%	0,0%	0,0%	0,0%	0,0%	0,0%
RDF	0,0%	54,5%	64,2%	63,2%	39,2%	48,5%	64,5%
NF	0,0%	1,9%	0,1%	1,7%	1,9%	0,2%	1,5%
Fe	0,0%	2,8%	2,6%	1,3%	0,2%	0,9%	5,7%
Inerts	0,0%	7,4%	5,0%	16,4%	39,4%	35,2%	12,8%
Glass	0,0%	3,5%	1,4%	1,6%	0,3%	0,0%	0,0%
Residual	0,0%	29,8%	26,8%	15,8%	18,9%	15,2%	15,5%

TABLE viii: High calorific materials by particle sizes in the output flow (<200 mm) of the screen 200, wt%.

Particle size (mm)	<10	10-20	20-40	40-60	60-80	80-100	100-200
Wood	0,0%	11,7%	24,5%	25,2%	10,5%	15,4%	12,9%
Paper	0,0%	20,8%	11,6%	6,0%	3,0%	2,7%	2,4%
Textile	0,0%	1,7%	1,3%	1,4%	2,0%	1,3%	6,4%
Plastic 2D	0,0%	11,2%	11,3%	12,2%	10,6%	15,0%	21,6%
Plastic 3D	0,0%	9,2%	15,5%	18,4%	13,1%	14,1%	21,2%

TABLE ix: Comparison of the composition by particle in the heavy fraction flow (HF) of the windsifter I, wt%.

Particle size (mm)	<10	10-20	20-40	40-60	60-80	80-100	100-200
Fines <10mm	100,0%	0,0%	0,0%	0,0%	0,0%	0,0%	0,0%
RDF	0,0%	35,1%	45,6%	58,5%	38,4%	41,7%	55,2%
NF	0,0%	3,1%	0,0%	0,9%	1,8%	0,9%	2,8%
Fe	0,0%	10,2%	9,5%	4,2%	4,8%	2,8%	1,3%
Inerts	0,0%	19,0%	7,6%	28,4%	45,1%	41,5%	24,3%
Glass	0,0%	4,7%	2,8%	1,4%	0,6%	0,0%	0,0%
Residual	0,0%	27,8%	34,5%	6,6%	9,4%	13,0%	16,4%

TABLE x: Comparison of the composition by particle in the heavy fraction flow (HF) of the windsifter I, wt%.

Particle size (mm)	<10	10-20	20-40	40-60	60-80	80-100	100-200
Wood	0,0%	8,2%	18,3%	28,7%	17,5%	20,0%	19,6%
Paper	0,0%	5,2%	4,3%	0,7%	0,5%	1,0%	0,7%
Textile	0,0%	0,7%	0,3%	0,0%	0,1%	0,7%	0,0%
Plastic 2D	0,0%	4,6%	2,2%	1,5%	0,4%	1,7%	1,1%
Plastic 3D	0,0%	16,4%	20,5%	27,6%	19,9%	18,3%	33,8%

APPENDIX B: Figures

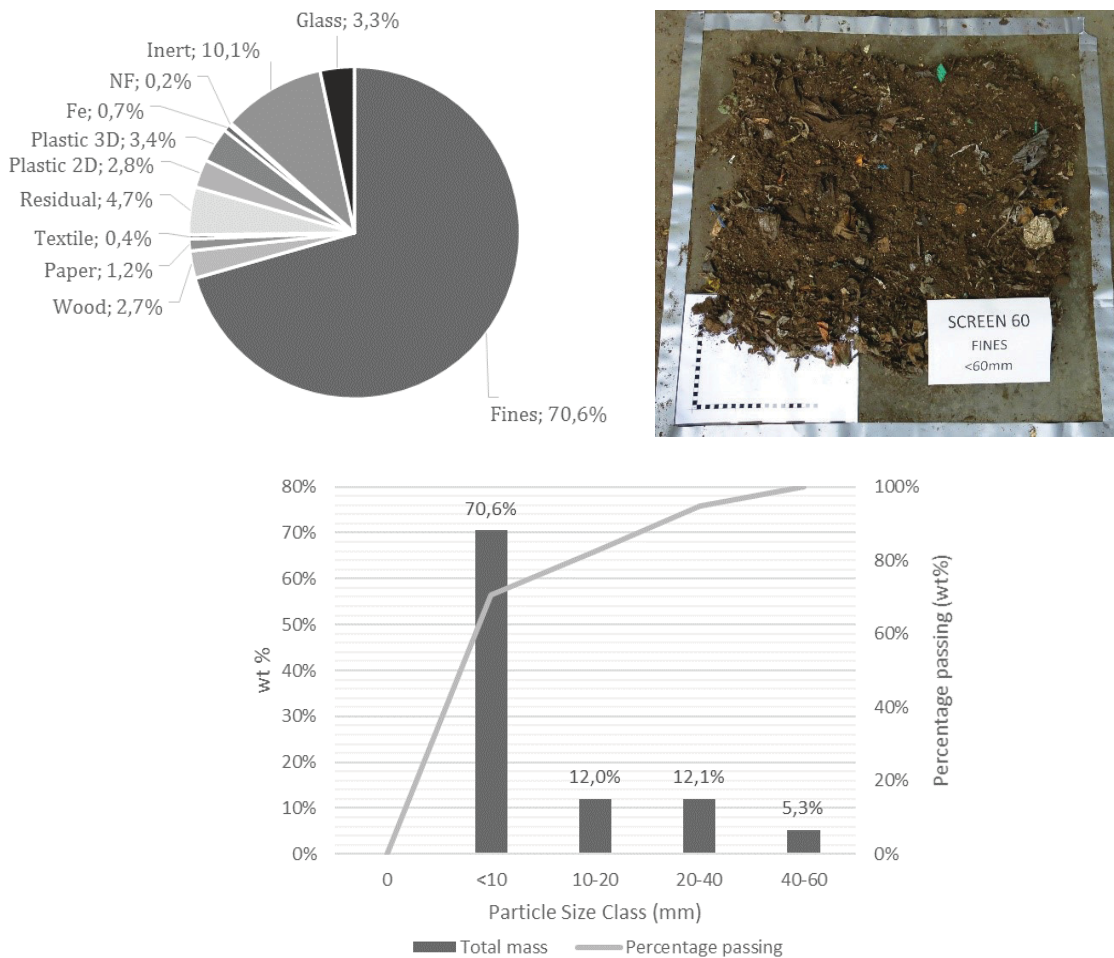


FIGURE i: Average composition of the fine fraction of the screen 60mm, SP2, (up) and its particle size distribution (down).

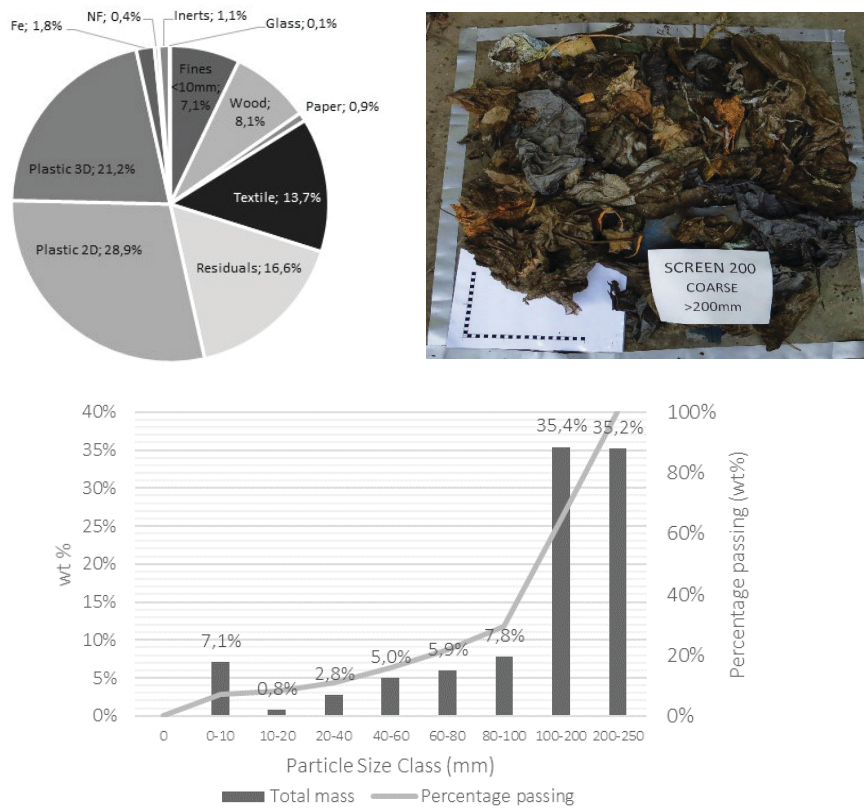


FIGURE ii: Average composition of the coarse fraction (250-200 mm) of the screen 200, SP3, (up) and its particle size distribution (down).

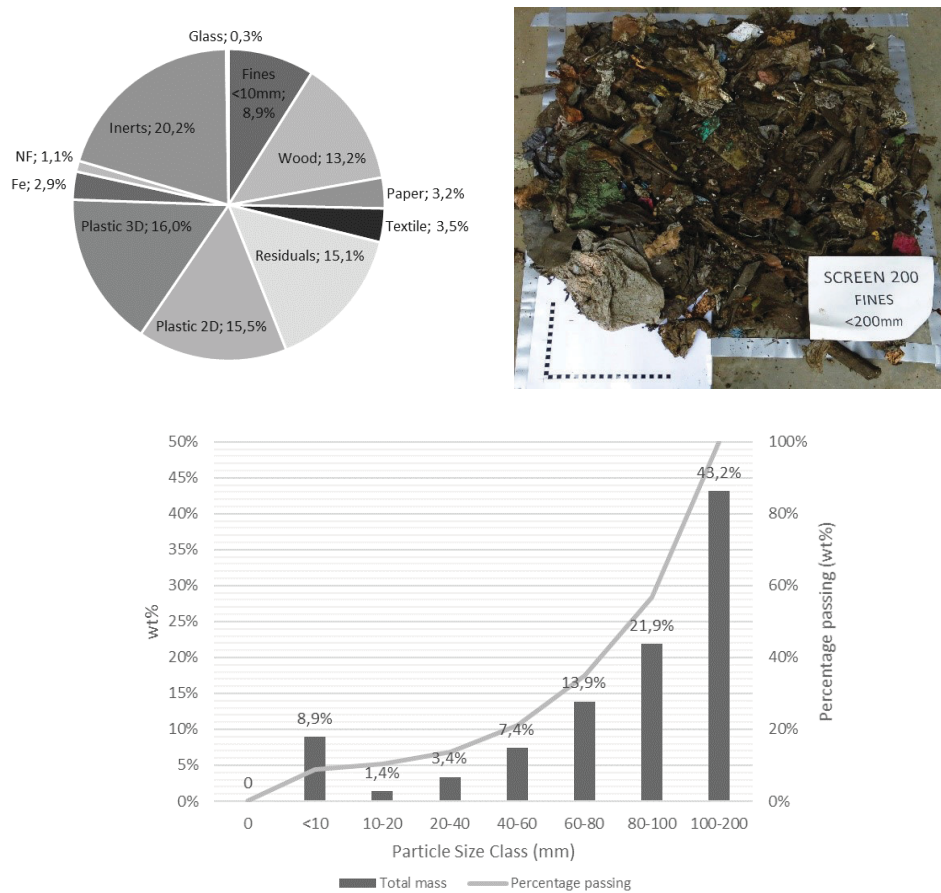


FIGURE iii: Average composition of the fine fraction (<200 mm) of the screen 200, SP4, (up) and its particle size distribution (down).

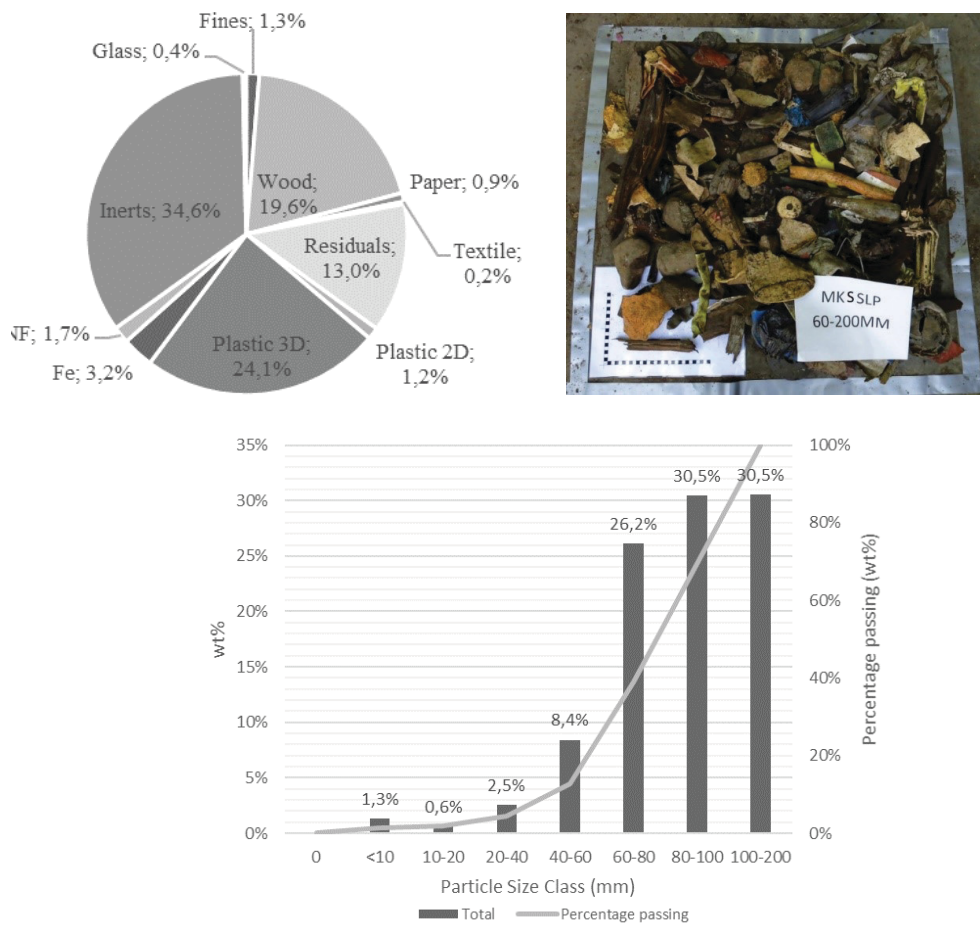


FIGURE iv: Average composition of the heavy fraction (HF) windsifter, SP5, (up) and particle size distribution (down).

3 PUBLICATION 2

Characterization of landfill mining material after ballistic separation to evaluate material and energy recovery

García López C, Ni A, Hernández Parrodi JC, Küppers B, Raulf K, Pretz T (2019) CHARACTERIZATION OF LANDFILL MINING MATERIAL AFTER BALLISTIC SEPARATION TO EVALUATE MATERIAL AND ENERGY RECOVERY POTENTIAL. Detritus In Press. Doi: 10.31025/2611-4135/2019.13780

Annotation on my own contribution to publication 2:

Juan Carlos Hernández Parrodi mainly conducted the planning of the large-scale tests that form the basis of this paper. Juan Carlos Hernández Parrodi, Cristina García López and me, jointly carried out the execution of the on-site tests (sample selection, supervision of excavation, conduction of ballistic-separation tests, development of a sampling plan, sampling and on-site manual separation). Anita Ni supported Cristina García López during follow-up work. I assisted Cristina García López with the analysis and evaluation of the obtained data. All co-authors reviewed the publication.

CHARACTERIZATION OF LANDFILL MINING MATERIAL AFTER BALLISTIC SEPARATION TO EVALUATE MATERIAL AND ENERGY RECOVERY POTENTIAL

Cristina García López ^{1,*}, Anita Ni ¹, Juan Carlos Hernández Parrodi ^{2,3}, Bastian Küppers ³, Karoline Raulf ¹ and Thomas Pretz ¹

¹ Department of Processing and Recycling, RWTH Aachen University, Aachen, 52062, Germany

² Renewi Belgium SA/NV, Gerard Mercatorstraat 8, 3920 Lommel, Belgium

³ Chair of Waste Processing Technology and Waste Management, Montanuniversität Leoben, Leoben, 8700, Austria

Article Info:

Received:

30 October 2018

Revised:

31 January 2019

Accepted:

22 February 2019

Available online:

01 August 2019

Keywords:

Enhanced landfill mining

Refuse derived fuel

Mechanical pretreatment

Ballistic separator

Recycling

Waste-to-energy

Waste-to-material

ABSTRACT

For decades, ballistic separators have been used in Europe as a means of sorting waste to separate mixed waste material streams at material recovery facilities and municipal solid waste treatment plants. Currently, with the growing need to remediate landfill sites, ballistic separators can be employed to recover calorific fractions from excavated landfill material within the framework of enhanced landfill mining. Ballistic separators provide multiple separation steps in one machine: they sort flat two-dimensional materials from rigid three-dimensional materials, while the material is screened to a selected particle size at the same time. The present study shows the results obtained during an investigation performed at the landfill in Mont-Saint-Guibert, Belgium. The main objectives were to acquire first-hand information regarding the efficiency of the ballistic separator in relation to processing old and untreated landfilled material and to study the potential of the landfill as a reservoir of secondary resources. The excavated material was processed through a pre-treatment chain of steps, including material classification and separation, as well as particle size reduction. As a first step, the material was processed with a ballistic separator using two different mesh sizes, 200 mm and 90 mm. Subsequently, the performance of the separator in question was evaluated, especially regarding its effectiveness in the production of refuse derived fuel. The two-dimensional flow was characterized by combustible materials from municipal solid waste and the three-dimensional by construction and demolition waste. As a result, 46% (dry basis) of the input material were fines particles <20 mm, 3% had a calorific value of 22.4 MJ kg⁻¹, 1% 16.0 MJ kg⁻¹ and approximately 1% were magnetic metals that could be recovered by mechanical processes. The results of processing and valorising the potential resources disposed in landfills are essential for the implementation of enhanced landfill mining since revenues from material and energy recovery could contribute to the economic feasibility of the project.

1. INTRODUCTION

As the global demand for raw materials rises, while the availability of natural resources remains limited, alternative sources of materials demand investigation and, therefore, new techniques need to be developed in order to maximize the use of existing materials. A political framework to tackle these challenges was set by the 2020 Strategy of the European Union (EU). This strategy serves as the basis for the 7th Environment Action Programme, which seeks to develop a sustainable, low-carbon and resource-efficient economy where waste is turned into a resource (European Parliament, 2013). Regarding historic waste, it is of major interest to

identify the potential and examine which secondary resources could be recovered from the existing 150,000 to 500,000 landfills that are estimated to be located in the EU (Hogland et al., 2010). This subject is investigated in enhanced landfill mining (ELFM) projects, which aim for “the safe conditioning, excavation and integrated valorisation of (historic and/or future) landfilled waste streams, both as materials (Waste-to-Material, WtM) and energy recovery (Waste-to-Energy, WtE), using innovative transformation technologies and respecting the most stringent social and ecological criteria” (Jones et al., 2013). ELFM contributes to create a circular economy and to reduce the EU’s dependency on imports of raw materials, driven by the goals of reclaiming land, re-



* Corresponding author:

Cristina Garcia Lopez

email: cristina.garcialopez@iar.rwth-aachen.de



Detritus / In press / pages 1-19

<https://doi.org/10.31025/2611-4135/2019.13780>

© 2018 Cisa Publisher. Open access article under CC BY-NC-ND license

IN PRESS

gaining landfill capacity and protecting groundwater, as has previously been achieved by landfill mining (LFM) projects (Hermann et al., 2014; Hernández Parrodi et al., 2018a).

This study focuses on the characterization of landfilled material that was directly processed with a ballistic separator after excavation. Figure 1 shows the working principle of a ballistic separator, which is a standard processing equipment, normally installed in packaging waste treatment plants before sensor-based sorting or after in-feed with subsequent drum screen. Due to the inclination and upward movement of the paddles, three-dimensional (3D) materials (heavy, hard and round particles) move downwards and are separated from the two-dimensional (2D) materials (lighter and soft particles), such as plastics, paper and textiles, which are collected at the top end of the paddles. A third output stream, the under-sieve fraction, is produced due to the screening property of the paddles. The latter can be varied by adjusting the screen of the paddles according to a certain particle size. Material characteristics, such as weight, form, size and elasticity, can influence the movement of the particles and can, therefore, affect the sorting efficiency of the equipment.

A bottom-up approach, in contrast to a top-down approach analysing historical data (Bhatnagar et al., 2017), was chosen in this study. Especially since most older landfill sites did not register the type and amount of material deposited during their active phase (Jones et al., 2013). However, landfilled materials are heterogeneous waste streams that need to be separated and treated before they can be recovered (Quaghebeur et al., 2013). Previous studies provide information on the applicability of full-scale and state-of-the-art technology used currently in waste-treatment plants (García López et al., 2018; Kaartinen et al., 2013; Maul & Pretz, 2016).

The novelty of this case study is the use of a ballistic separator as the first step of the mechanical process prior to shredding. This method allows the recuperation of fractions that are suitable for the production of refuse derived

fuel (RDF) with a high heating value in its original size, in addition to other valuable materials, such as inert, glass and metallic materials.

Landfilled waste from which RDF might be produced includes plastics, paper, wood and textiles (calorific fractions). In addition, metals, glass and perhaps mineral and organic materials could be recovered (Kaartinen et al., 2013; Quaghebeur et al., 2013). The material composition of landfill sites varies according to different factors, such as the time of deposition, the type of stored waste, the meteorological and hydrological conditions of the site, and the collection area, since waste composition is influenced by population density, consumer behaviour and waste-sorting habits (Quaghebeur et al., 2013; Wolfsberger et al., 2015a). Therefore, a holistic characterization of the landfilled waste contributes to assessing the suitability of a site for ELFM, which is determined by the share of usable recyclables from the excavated waste, among others, and to predict the revenue and costs of an ELFM project (Hermann et al., 2014).

The purpose of this study is to evaluate the performance of the ballistic separator "STT 6000"-STADLER@Anlagenbau GmbH" with landfilled material. This evaluation was achieved by characterizing each output stream of the ballistic separator. The materials composing these streams were identified by manual sorting and were subjected to laboratory analyses, such as moisture content, particle-size distribution (PSD), calorific value and ash content, to obtain qualitative and quantitative information and determine the suitability of the calorific fractions for the production of RDF.

2. MATERIALS AND METHODS

2.1 Site description

The examined landfill site is located in the municipality of Mont-Saint-Guibert (MSG) in the province of Walloon Brabant, Belgium. This site was established on a former sand

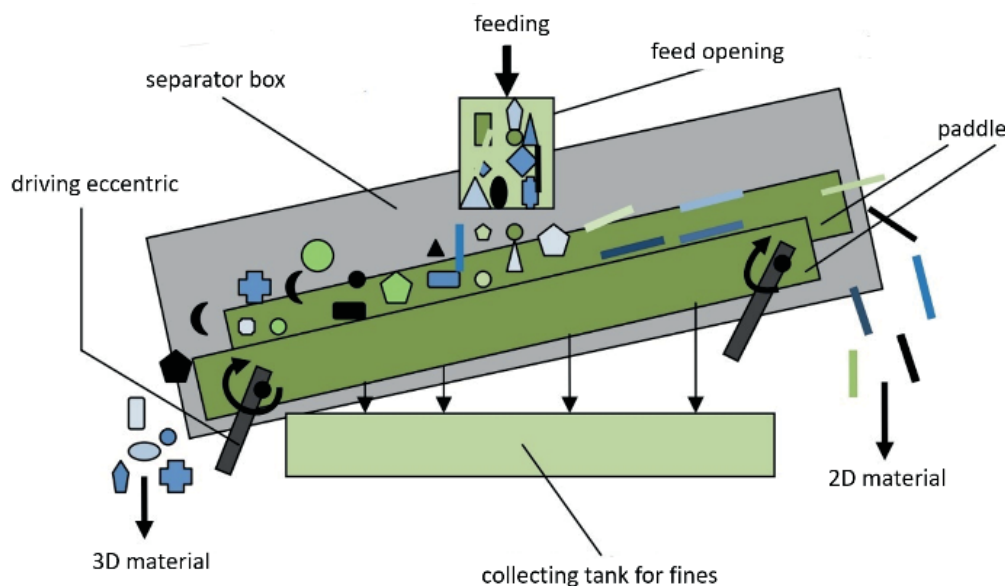


FIGURE 1: Schematic diagram of a ballistic separator (adopted from Martens & Goldmann, 2016).

quarry and has served as one of the main disposal sites of municipal solid waste (MSW), non-hazardous industrial waste and construction and demolition waste (CDW) since 1958 (Bureau d'études greisch, 2002). The site covers an area of approximately 44 ha, of which 26 ha belong to the most recent part and 2 ha to the oldest part. The oldest part of the site has no bottom liner and, nowadays, the biogas collection system has been removed, while the leachate collection system is still in place and operational. The present investigation was carried out in the old part of the landfill, which has an estimated depth between 30 m and 60 m and where at least 5.7 million m³ of waste were deposited between 1958 and 1985 (Hernández Parrodi et al., 2018b).

In September 2017, before the excavation, a geophysical exploration was performed in an area of approximately 2150 m². Using electromagnetic induction, the depth of the cover layer and the soil properties were estimated. Based on the results of the electrical conductivity, the area was then divided into four batches. This paper focusses only on batch 1. A future publication will show the results of all four batches.

As shown in Figure 2, the waste was covered by a clay layer with a thickness of about 4 m. This layer was removed in order to keep it separated from the landfill waste. The processed pit was 5 m long, 5 m wide and 4 m deep; a total volume of 130 m³ was excavated and treated. During the excavation, a layering of different types of materials was observed. From top to bottom: 4 m cover layer, 2 m CDW

and 2 m MSW. For the extraction of the buried material, an excavator with a toothed digging-type bucket was employed, while for the manipulation of the excavated material a wheel loader was used. The weight of the material was measured with a weighing bridge (resolution of 50 kg).

2.2 Mechanical processing and sampling campaign

After the excavation, the material was directly fed into the ballistic separator "STT 6000", the specifications of which are given in the Appendix. The motivation for the choice of this specific equipment was the following: i) the conglomerates of the input material would be loosened due to the agitation (crankshaft eccentricity) on the screen deck, ii) its availability for treating CDW (Sigmund, 2018), iii) no pre-shredding of the input material is needed (saving the wear and energy on the shredders for the infeed material), iv) sorting large items increases sorting quality (large parts can be removed in one piece), v) saving of space on the site due to the separation of 3 fractions in one step (vs. a drum type, by which only particle size can be sorted), and vi) its robust design. Thus, these characteristics could lead to better sorting processes (enhanced mechanical treatment) with respect to effectiveness, wear and energy consumption. Even if previous studies recommend low moisture content (<15%) for an effective sorting process (Giani et al., 2016; Martens & Goldmann, 2016), this study was performed without drying the material prior to the processing.



FIGURE 2: Excavation at the Mont Saint Guibert Landfill, Belgium.

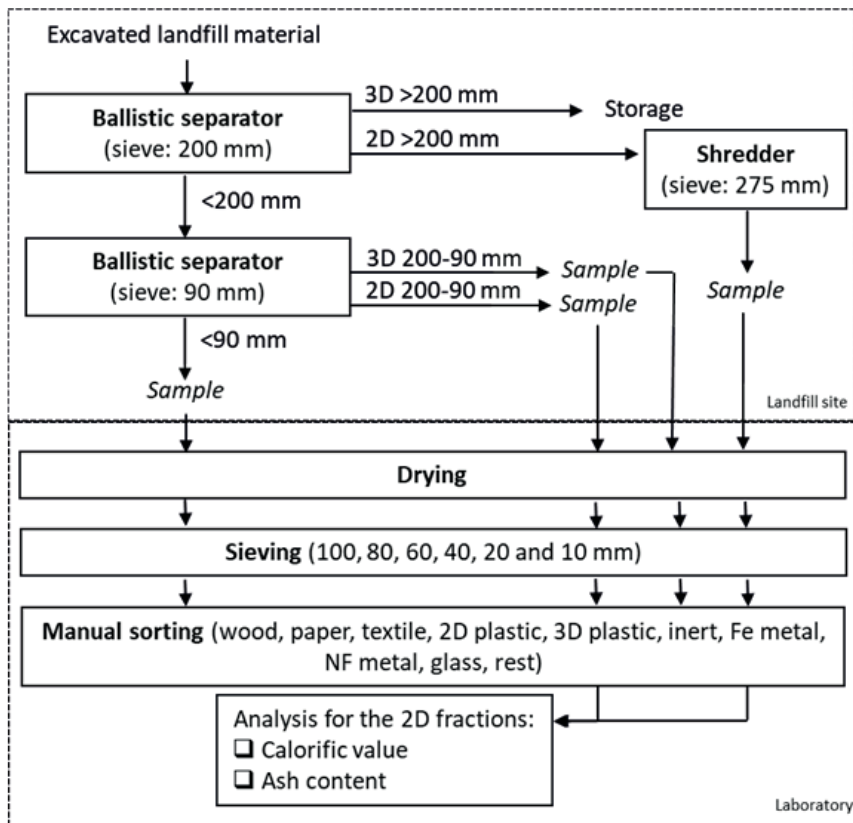


FIGURE 3: Scheme of the mechanical pretreatment, sampling campaign and methodology used in the laboratory.

The landfilled material was first sieved with a mesh size of 200 mm and subsequently with a mesh size of 90 mm, as can be seen in Figure 3. The output “2D >200 mm” was fed into a shredder (sieve: 275 mm) to reduce the particle size down to <275 mm; hereafter, this output stream is referred to as “2D <275 mm”.

The sampling campaign followed the same methodology as in the case study in Halbenrain (García López et al., 2018), based on the German Directives (LAGA PN 78; LAGA PN 98). The “3D >200 mm” output stream was not sampled; instead, all the output material was sorted in situ

into different categories (Table 1). Moreover, 60 m³ of the obtained fraction <200 mm were subsequently processed with the ballistic separator with a mesh size of 90 mm, from which 3 additional output streams were obtained: 2D 200-90 mm, 3D 200-90 mm and <90 mm.

The following numbers of samples were taken exclusively during the mechanical treatment and were adapted to the time of the process to achieve the maximum level of representation: i) 2D <275 mm, 8 samples (n=8), summing to 132 kg, ii) 2D 200-90 mm, 9 samples (n=9), summing to 63 kg, iii) 3D 200-90 mm, 7 samples (n=7),

TABLE 1: Classification of the landfilled material by categories.

Category	Material	Age of site (as of 2018)
I	Wood	All types of wood
II	Paper	Paper, cardboard, composite carton
III	Textile	All types of textiles
IV	Plastic 2D	Bags, foils
V	Plastic 3D	PP, PET, HDPE, LDPE, PVC, PS, others
VI	Fe metals	Iron
VII	NFe metals	Non ferrous metals: copper, aluminium, lead, others
VIII	Inert	Mineral fraction (stones), ceramic
IX	Glass	Colorless glass, green glass, brown glass, others
X	Rest	Rubber, foam, EPS, silicone, melted plastics, sandpaper, hazardous waste (e.g. sanitary material), unidentified, composites
XI	Fines	Particles < 20 mm

summing to 154 kg and iv) <90 mm, 12 samples (n=12), summing to 116 kg. All the figures with fluctuations given in this study are based on the corresponding number of samples. The samples were further characterized in the Department of Processing and Recycling at the RWTH Aachen University.

2.3 Characterization of landfill mining material

2.3.1 Moisture content and particle size distribution

Based on the DIN CEN/TS 15414-1 all samples were dried but at a reduced temperature of 75°C to prevent plastics from melting, which can happen at higher temperatures.

After drying, the samples from the output streams 3D 200-90 mm, 2D 200-90 mm, <90 mm were sieved with a drum sieve and a box sieve at the Department of Processing and Recycling (RWTH Aachen University), except for the ones from 2D <275 mm, which did not provide realistic information regarding the size of the original material. As a result, seven particle size fractions were generated: 200-100 mm, 100-80 mm, 80-60 mm, 60-40 mm, 40-20 mm, 20-10mm and <10 mm.

2.3.2 Material composition by output stream

All the particle size fractions >20 mm from 2D <275 mm, 2D 200-90 mm, 3D 200-90 mm and <90 mm were sorted manually into eleven categories, listed in Table 1. There is no category for organic waste (food scraps, green waste, etc.) because they were not distinguishable after at least 15 years inside the landfill. It is likely that the organic material was degraded to soil-like material (Quaghebeur et al., 2013). At this point, it must be mentioned that no pure and clean materials can be obtained by manual sorting without washing or using other pretreatment due to surface defilement and material agglomeration.

2.3.3 Calorific value and ash content

Such characteristics as calorific value, amount of organic carbon, total carbon, ash content, and hydrogen and nitrogen contents are needed to be measured to assess the efficiency for WtE applications (Quaghebeur et al., 2013). In this case, only the gross calorific value (GCV) and the ash content were determined. These values give information about the recoverable energy and amount of residue produced in the combustion process (Kuchta, Hobohm, & Flamme, 2017). Before conducting the analysis, several mills (hammer mill, disc mill and cutting mill) were used to reduce the size of the particles down to 1 mm. After the particle size reduction of each category in each sample, the GCV was determined according to the DIN 51900-1 and the ash content based on DIN EN 15403. The measurements were only conducted for the 2D output fractions (2D 200-90 mm and 2D <275 mm), which were estimated to have a high heating value. Metals and glass were assumed to have a GCV of 0 J/kg and an ash content of 100%.

3. RESULTS AND DISCUSSION

3.1 Moisture content and particle size distribution

The moisture content landfilled material plays an im-

portant role when considering the material processing (Hull et al., 2005). Previous experiences include that moisture contained in excavated waste did not impede its processability, but it might have an impact on the processing efficiency (Kaartinen et al., 2013). Drying could (i) reduce the amount of surface defilement; increase both the quality of the recyclable materials and the efficiency of sorting processes, (ii) enable a more efficient and precise particle size classification in the screening and sieving processes, (iii) decrease the total amount of material to be processed and perhaps transported and (iv) raise the calorific value (Hernández Parrodi et al., 2018a).

The fluctuations in the moisture content within the samples of every output stream are represented in Figure 4. The similar moisture contents of 2D <275 mm and 2D 200-90 mm, with averages of 31% and 32% respectively, allow a first estimation about their composition, which is described in detail in the section "3.2. Material composition". The output "<90 mm" is characterized by a slightly lower average moisture content of 28%, while "3D 200-90" mm contains considerably less water, showing an average of 12%. The latter correlates with the low capacity to hold water of materials usually found in the 3D output stream of ballistic separators, such as stones, metals, glass, rubber and wood.

It has been reported that the moisture content and amount of organic matter are interrelated and decrease with the age of the waste due to microbiological activity (Quaghebeur et al., 2013). Dating back to the 1960s and 1970s, the investigated waste from MSG can be considered as old. Nevertheless, the amount of water is still notable, with a range of 9-41%, which might be explained by the thick layer of clay used as cover material and the type of waste landfilled. More permeable material, such as compost, leads to higher degradation rates and thus faster water reduction.

Due to this moisture, fine particles likely adhere to surfaces and larger particles which may lead to an increased share of the fine fraction after drying (Kaartinen et al., 2013). Combined with the subsequent sieving, this may contribute to the reduction of surface defilement and as a consequence, compliance with the requirements for other waste treatments, e.g., sensor-based sorting if considered for further processing.

Drying the material is an operational cost but can reduce the total mass being transported and fed into the mechanical processing; hence, the throughput might be increased and transportation costs reduced. Other effects of drying are an increase in the CV and more effective sieving results.

Figure 5 illustrates the total mass (dm%) by particle size (mm) in each sieved output stream from which it can be deduced that a dried sample of landfilled material contains more fine particles than it did under humid conditions. After drying, 51% of the output stream "2D 200-90 mm" is smaller than 80 mm, even though it was first classified as >90 mm by the sieve of the ballistic separator. Moreover, fines <10 mm in this output stream make up 30%, which is almost as high as the share of particles >100 mm (35%).

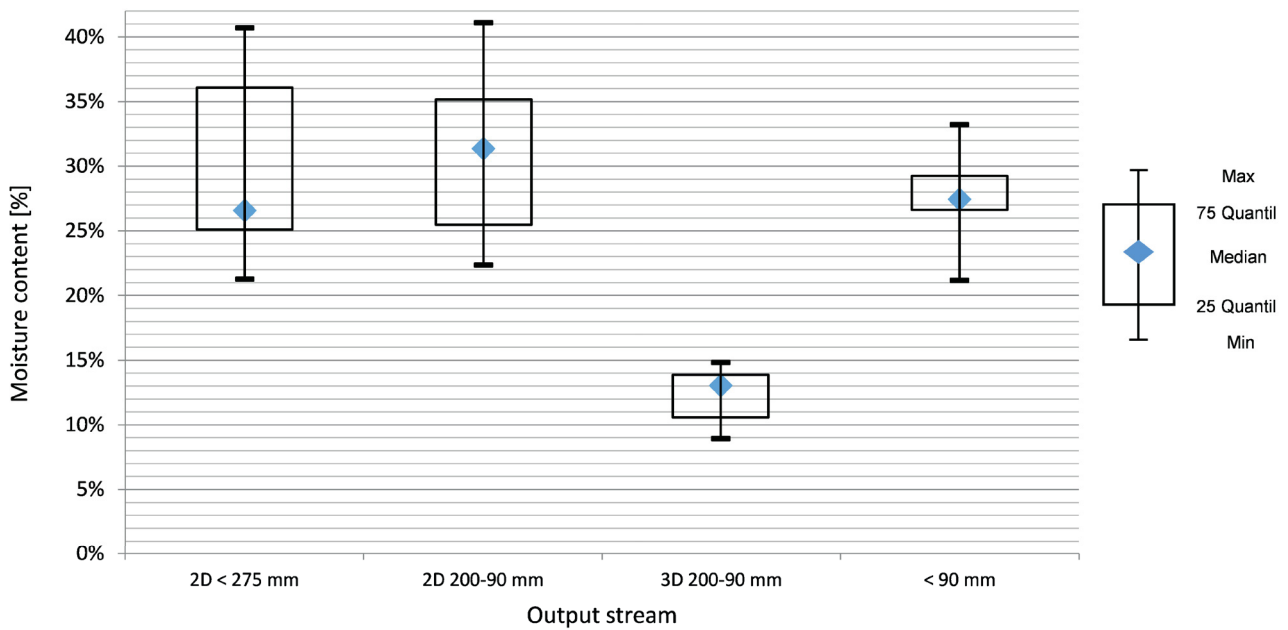


FIGURE 4: Fluctuations in the moisture content by the output stream of the ballistic separator. Number of samples shown, n=8, n=9, n=7, n=12.

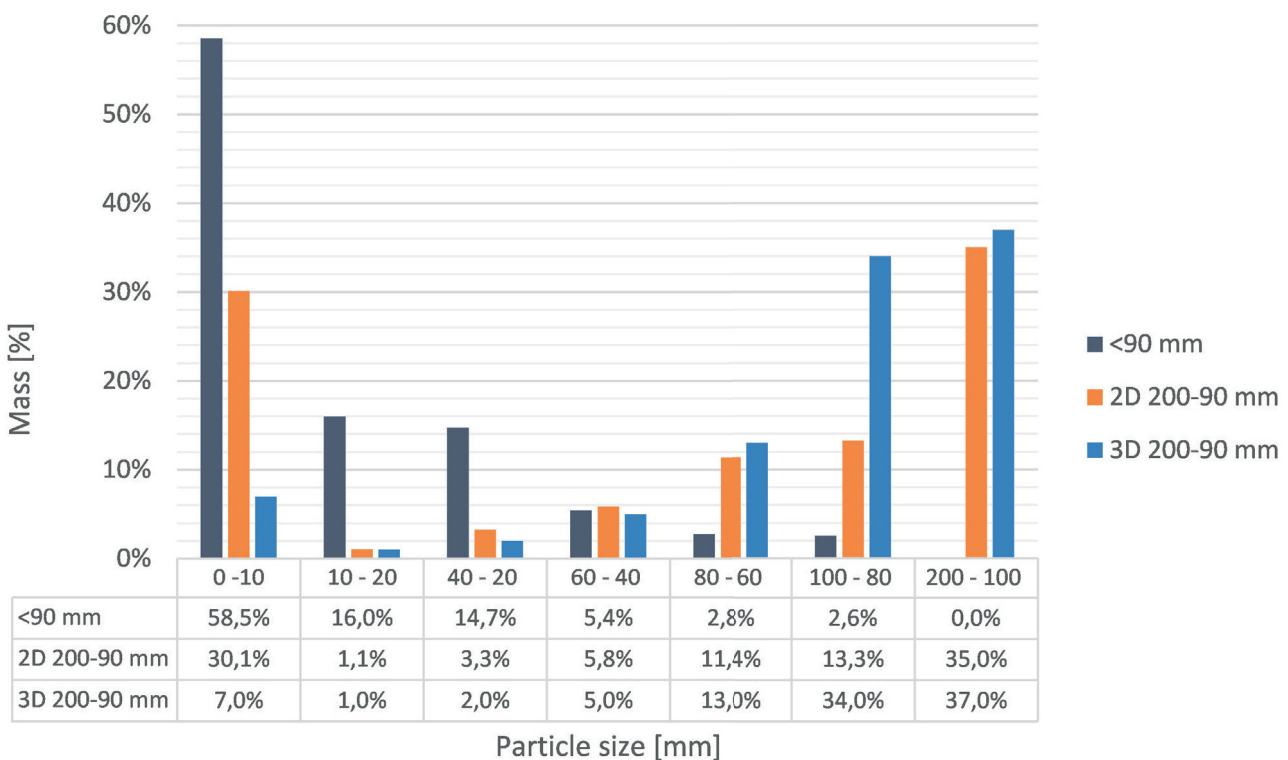


FIGURE 5: Distribution of the total mass (dm%) by particle size in each sieved output stream of the ballistic separator STT 6000 using landfilled waste.

For the “3D 200-90 mm”, 28% is <80 mm. This statement can only be made with some reservations, since some bricks broke during the sieving in the drum sieve, especially in the first run with a mesh size of 100 mm. This means that the actual throughput at particle size 100 mm is lower than indicated in Figure 6 and that the particle-size fraction 200-100 mm composes more than

one third of the whole output stream “3D 200-90 mm”. Besides, more fines than those originally contained in the samples are generated due to abrasion processes while sieving the material.

In addition, there is a concentration of material in the smaller particle size fractions: 34% of “2D 200-90 mm” is < 40 mm and 30% is <10 mm. Regarding the output stream

<90 mm this observation is more significant, with values of 90% and 59%, respectively.

In line with the above-described findings, the moisture content of all samples varies between 9 and 41% and on the average makes up for almost a third of the RDF potential fractions. The PSD reveals a high percentage of fine material, not only in the output stream <90 mm but in all outputs due to the large amount of impurities found between the large particles, which are separated by the drying process.

3.2 Material composition

The excavated waste from MSG (batch 1) consisted of three main categories: inert, fines and plastics. In this study, all particles with a particle size <20 mm are defined as fines. Figure 6 gives an overview of the material distribution in all the output streams generated by the ballistic separator. As expected, most fines are found in the output stream <90 mm, additionally both, 2D >200 mm and 2D 200-90 mm, show considerable amounts of fines. Inert material is concentrated in the 3D output streams (3D >200 mm and 3D 200-90 mm). The ferrous metals (Fe metals) are mainly found in the 3D output streams: 3% in the >200 mm and 5% in the 200-90 mm output, as well as wood with

4% in the both 3D output streams. It must be noted that the mass percentages of "3D >200 mm" are given on a wet matter (wm) basis, while the other streams flows refer to dry matter (dm). Detailed figures (Fig. A.1-3) with the average values of the masses by particle size in each output can be found in the Appendix.

3.2.1 Output stream 3D 200-90 mm

The box whisker diagram in Figure 7 illustrates that the inert fraction is by far the largest with a median of 75%, while the other fractions all range below 10% with tendencies toward 0%; the shares of the categories paper, textile, 2D plastics, Non Ferrous (NFe) metals and glass are less than 1%. The same explanation as above may be considered for the high amount of inert material: the upper layer of the pit consisted of CDW. The second largest fraction is that of fines (8%), followed by Fe metals and wood, 5% and 4% respectively. Regarding Fe metals and wood, it was observed that half of the samples contained compounds of both materials in the fractions 60-40 and 40-20 mm. As the magnetic forces of a magnetic separator attract ferrous materials, wood parts containing nails were categorized as Fe metals. On the other hand, a large piece of wood (100-80 mm) with nails was identified and

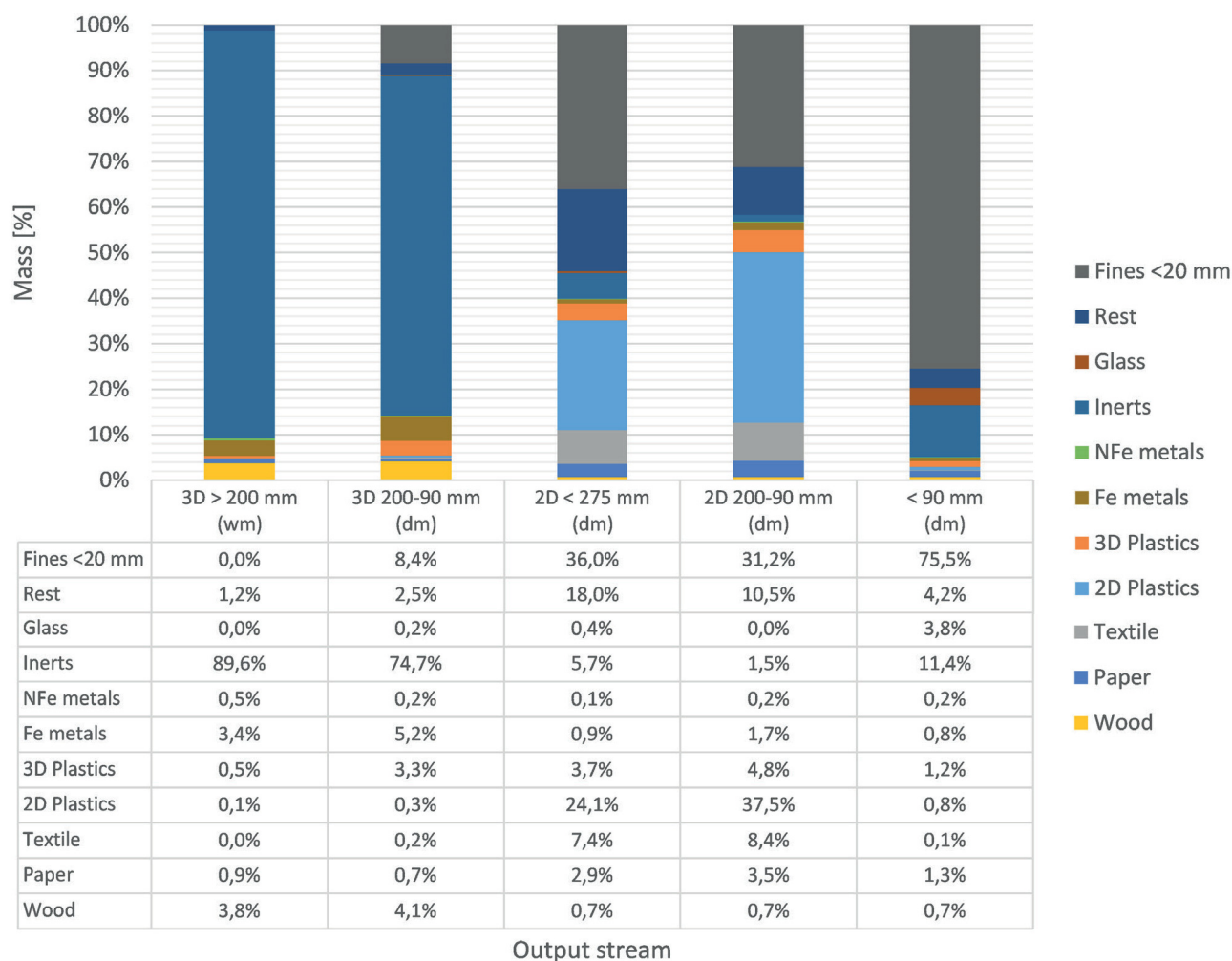


FIGURE 6: Composition of all output streams by categories.

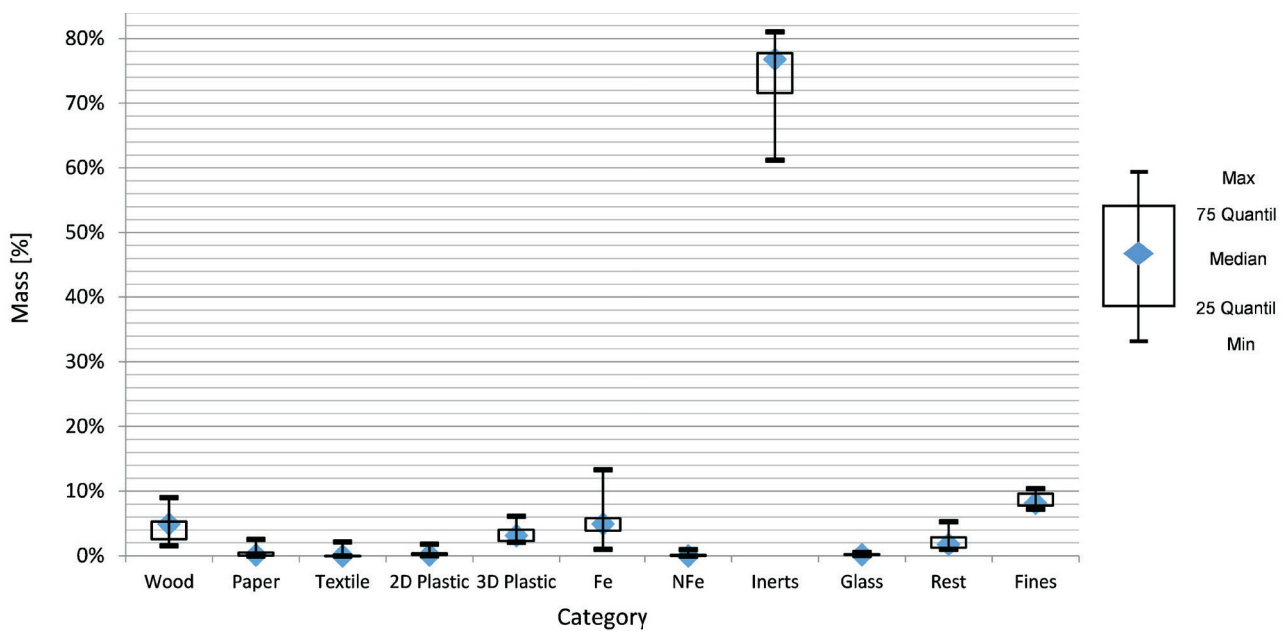


FIGURE 7: Output “3D 200-90 mm”: fluctuations in the material composition, dm % (n=7).

classified as wood. Another compound found was wood with 3D plastic.

The fluctuations indicate that the samples do not differ strongly from each other. The largest variations are observed in the categories wood, Fe metals and inert material, which also correspond to those obtained in previous LFM investigations.

Figure 8 represents the composition of each particle size fraction indicating its weight as it relates to the total weight of the output “3D 200-90 mm”. The two larger coarse fractions make up most of the material, 37% and 34%, but breaking and abrasion in the drum sieve have affected the PSD distribution. Wood presented in the output “3D 200-90 mm” is distributed equally between the three larger particle size fractions, whereas most iron particles are counted in the 100-80 mm fraction (2%). The low quantity of glass (0.2%) might be explained by the fact that glass is likely to break and pass the sieve, both when previously transported and landfilled and during the excavation and mechanical stress in the ballistic separator, finally ending in the output stream <90 mm.

Looking to further processing steps, the enrichment of one material by sieving could result in difficulty due to similar distribution curves. Therefore, different sorting treatments such as magnetic separation, sensor-based separation (Beel, 2017; Martens & Goldmann, 2016), or float-sink separation (Bauer et al., 2018; Kranzinger et al., 2017) could be considered. Generally, the composition resembles the output “3D >200 mm” although it shows an increased number of fines generated in the PSD process (particle breakage and the drying process). Hence, the ballistic separator meets the expectations for enrichment of 3D materials.

3.2.2 Output stream 2D <275 mm

As shown in Figure 9, the output stream 2D <275 mm

has a heterogeneous composition in comparison with 3D 200-90 mm, where the fine fraction (<20 mm) holds the largest share with 36% of the total. These fines are mainly composed of a mix of 2D plastics and soil-like material that may have been generated during the shredding process and due to the high detention time inside the shredder (Figure 10). To prevent losing this part of the combustibles in the fine fraction, sieving with a mesh size of 10 or 5 mm is suggested. Moreover, a considerable number of particles (particle size approximately <3 mm and smaller) were attracted by the magnet, being magnetic soil-like. Comparable findings are also described by Quaghebeur et al., 2013, where the amount of metallic iron in the magnetic fraction was between 8 and 9%.

The second-largest fraction is made up by 2D plastics with an average share of 24%, followed by Rest with 18%. Many particles categorized as Rest during the sorting process are compounds, such as carpets and nappies. They are mainly made of plastic, textile and cellulose, thus this category may be considered as a highly calorific fraction. Another compound that was mainly present in the output stream “2D <275 mm” consists of cables. If the 2D and 3D plastics, Rest, wood, paper and textile are considered highly calorific materials, 57% of the total mass has RDF potential. However, wood is insignificant with less than 1%. The same applies to glass and both Fe and NFe metals. Metals could not be separated completely due to attached pieces of plastic, mostly two-dimensional, textile or other materials.

3.2.3 Output stream 2D 200-90 mm

As it can be seen in Figure 11, the grain-size fractions >60 mm in the 2D 200-90 mm flow are especially rich in plastic foils (>45%). As expected, the main component of this flow are 2D plastics with an average content of 41% (Figure 12). In contrast, 32% were fines (<20 mm), which

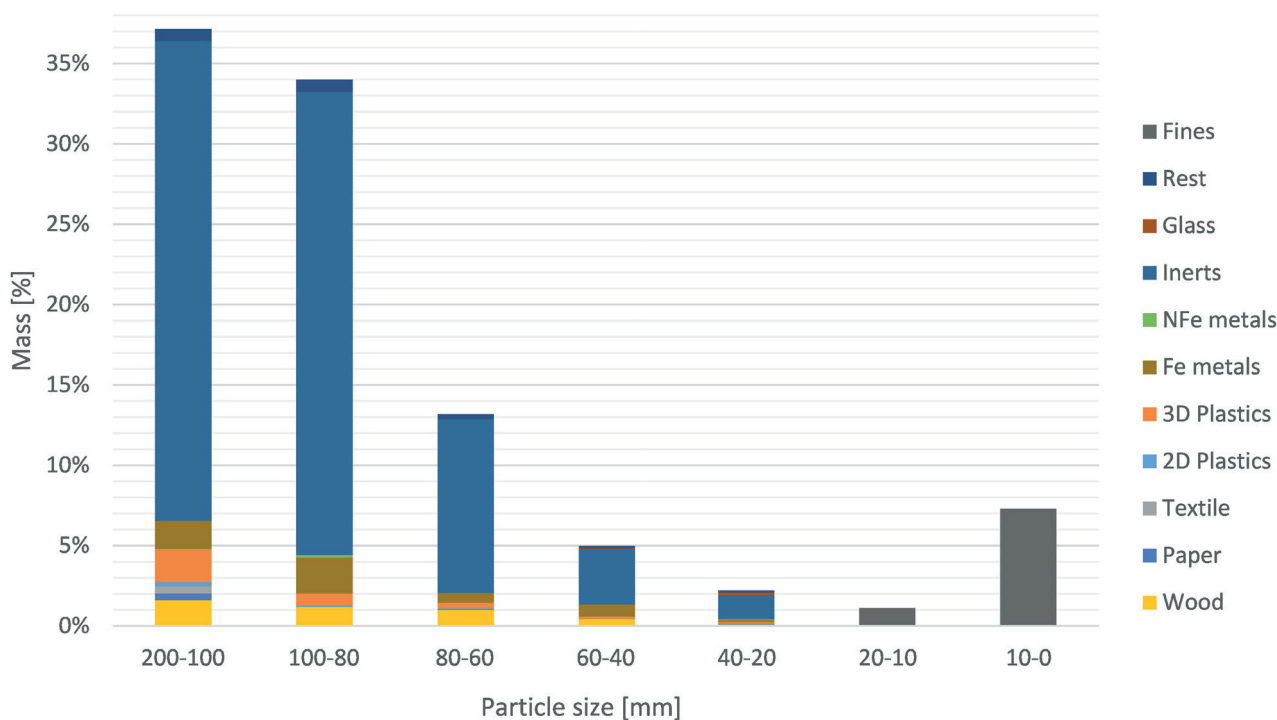


FIGURE 8: Material composition of the output stream "3D 200-90 mm" by particle size.

may reduce the RDF potential drastically. However, the categories Rest and wood could contribute to increase the calorific value with a share of 7% and 6% respectively, since they are considered combustible materials.

Furthermore, it can be said that fraction 40-20 mm has a very heterogeneous composition consisting of all materials except glass, while the other sorted particle sizes are characterized by 2D plastics as the main component.

All inert material can be discharged by sieving with a mesh size of 80 mm, as shown in Figure 15. Apart from wood and fines, all other categories show similar distribution curves, so sieving alone will not be suitable for the enrichment of single categories as it is also the case for 3D 200-90 mm. Regarding the heterogeneous composition of both 2D streams compared to the 3D stream characterized by CDW, it can be deduced that the composition of this stream consists mainly of MSW with a high content of potential combustibles.

3.2.4 Output stream <90 mm

Most of the output stream (75%) consisted of fines <20 mm, Figures 13 and 14. These were not sorted manually, but as a general observation the particle sizes between 20 and 10 mm consisted mainly of glass and those <10 mm of soil-like material, comparable to the Fines of 2D <275 mm and 2D 200-90 mm. Within the categories (>20 mm), inert material makes up the largest part ranging between 5-23% of the total, with an average of 14%. Also worth mentioning is the amount of glass in fraction 40-20 mm (4%). Together with the glass present in fraction 20-10 mm this confirms the previous assumption that glass is likely to break and pass to smaller grain-size fractions.

Looking at the PSD of the materials in Figure 13, a conclusion similar to the other outputs can be made: sieving with a mesh size of 40 mm may yield a material stream poor in glass but further enrichment does not seem realizable with the mesh sizes used in the analysis.

3.2.5 Overview of all output stream

Normally the 3D output streams of ballistic separators used to separate fresh waste contain stones, metals, glass, rubber and wood (H. Martens, 2016). In comparison, the results of the present paper show that the same applies for landfilled CDW and MSW with one exception: glass is only present in the finer fraction of the output stream <90 mm. Thus, considering the enrichment of highly calorific materials in the 2D streams, mostly 2D plastics, the ballistic separator seems to meet the expectations.

Nevertheless, a mass balance of the whole process must be considered to estimate a reliable potential for the whole landfill. This means that the composition of every output stream must be related to its share in the total flow when extrapolating the absolute mass of all materials stored in the landfill. Figure 15 presents the mass balance considering wet and dried material. However, the total water content must be higher than the indicated 25% because the moisture content of the output "3D >200 mm" was not analysed in this study and the water is evaporated during separation. Nevertheless, it points out the high share of particles in the output stream <90 mm, 58% of the input material, compared to 4% (dry) with RDF potential from which the fines separated by sieving must still be subtracted. Two main reasons are considered for the predominant share of fines: the longer the waste is stored, the more organic material can be degraded; thus, the amount of fines

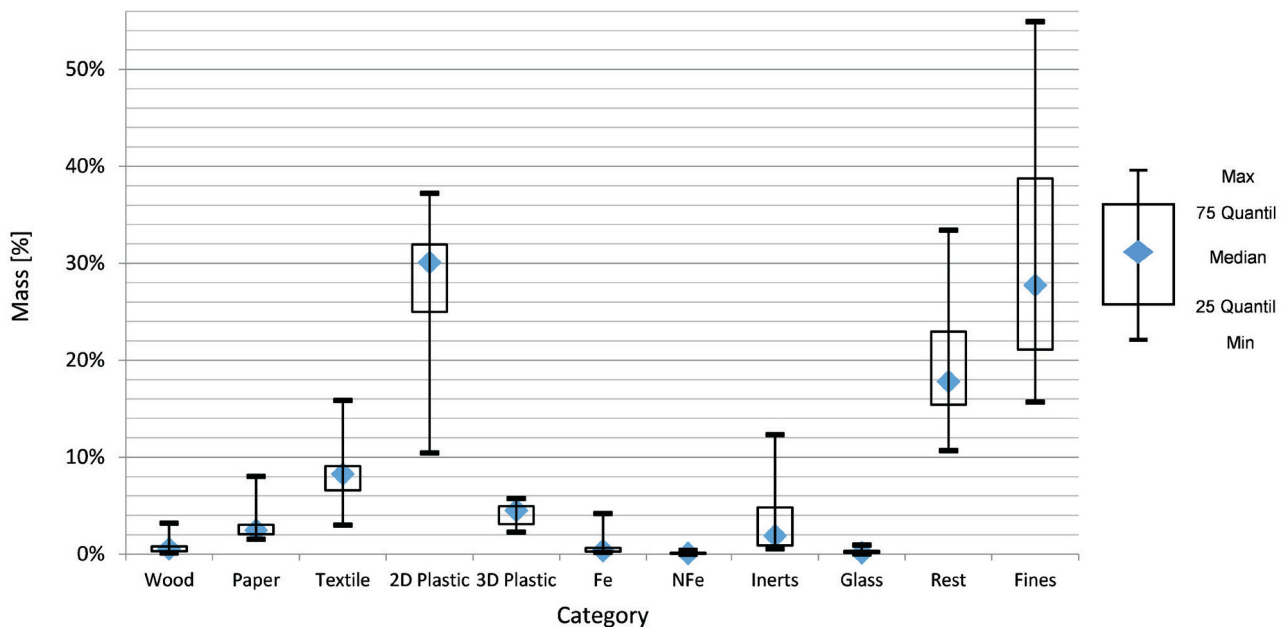


FIGURE 9: Output "2D <275 mm: fluctuations in the material composition, dm % (n=8).



FIGURE 10: Fines (<20 mm) from the output stream "2D <275 mm".

increases with time (Maul et al., 2016). Besides, the cover layer is a source of fines because usually soil is used as a daily cover (Kaartinen et al., 2013).

3.3 Calorific value and ash content

In order to assess the quality of the potential RDF produced by the ballistic separator, Table 2 shows the distribution of the calorific values, the ash content and the mass percentages by material categories in both 2D output stream, 2D <275 mm and 2D 200-90 mm.

As expected, 2D plastic, with a considerable share of

the output streams, is the material with the highest calorific value, 35.1 and 40.9 MJ kg⁻¹, followed by the 3D plastics with an average of 32.4 and 30.6 MJ kg⁻¹. In the case of the Rest, the values are 18.5 and 23.3 MJ kg⁻¹, which reinforce the previous assumption that this category can be regarded as a highly calorific fraction. Compared to the mean net calorific value of 21.9 MJ kg⁻¹ (dry and ash free) for RDF (Phyllis database, 2018), the results of this study range within the same magnitude at 16.0 and 22.4 MJ kg⁻¹. Nevertheless, the influence of the fines is significant since they make up a third of the mass. This means that by separat-

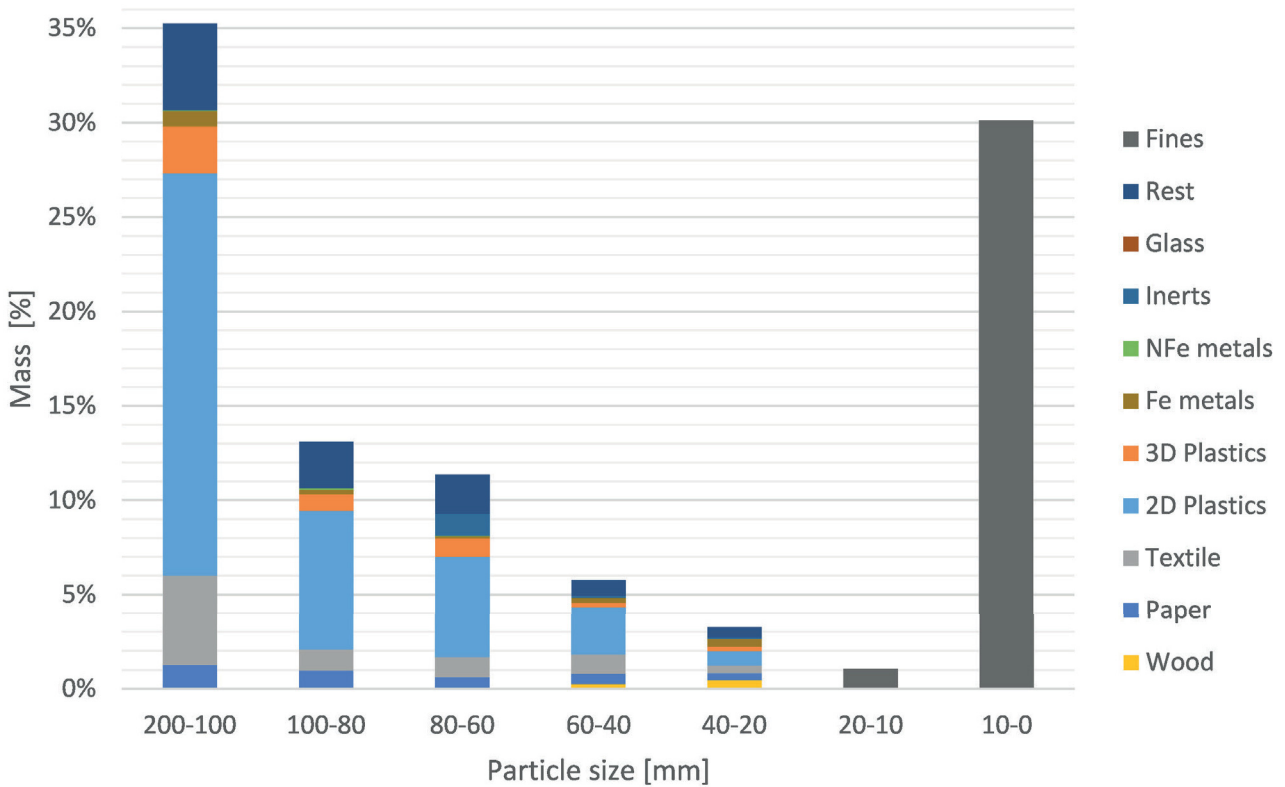


FIGURE 11: Material composition of the output stream "2D 200-90 mm" by particle size.

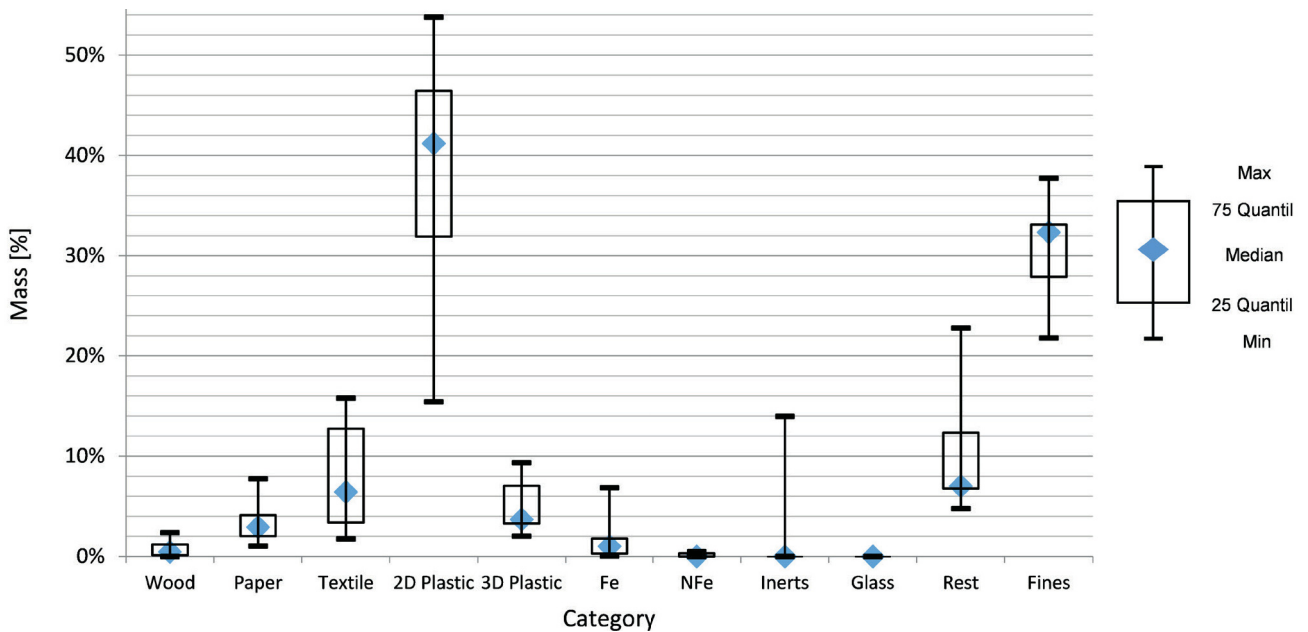


FIGURE 12: Output "2D 200-90 mm": fluctuations in the material composition, dm % (n=9).

ing fines from the stream before combustion, the amount of energy produced could be increased and the ash content could be reduced. In addition, only materials with ash contents <60% can burn autonomously (Seifert & Vehlow, 2017). In this regard, the 2D output streams have an ash content average of 50.5 and 40.4, thereby meeting this requirement. Moreover, low ash contents are also desirable

to reduce the dust loading. It can be deduced from the low amount of materials that are not suitable for RDF (metals, inert and glass) and thus degrade the burning parameters, that the ballistic separator enriches RDF potential materials in the 2D stream as expected since the downgrading fines come from the surface of the RDF particles and were generated in the subsequent drying process.

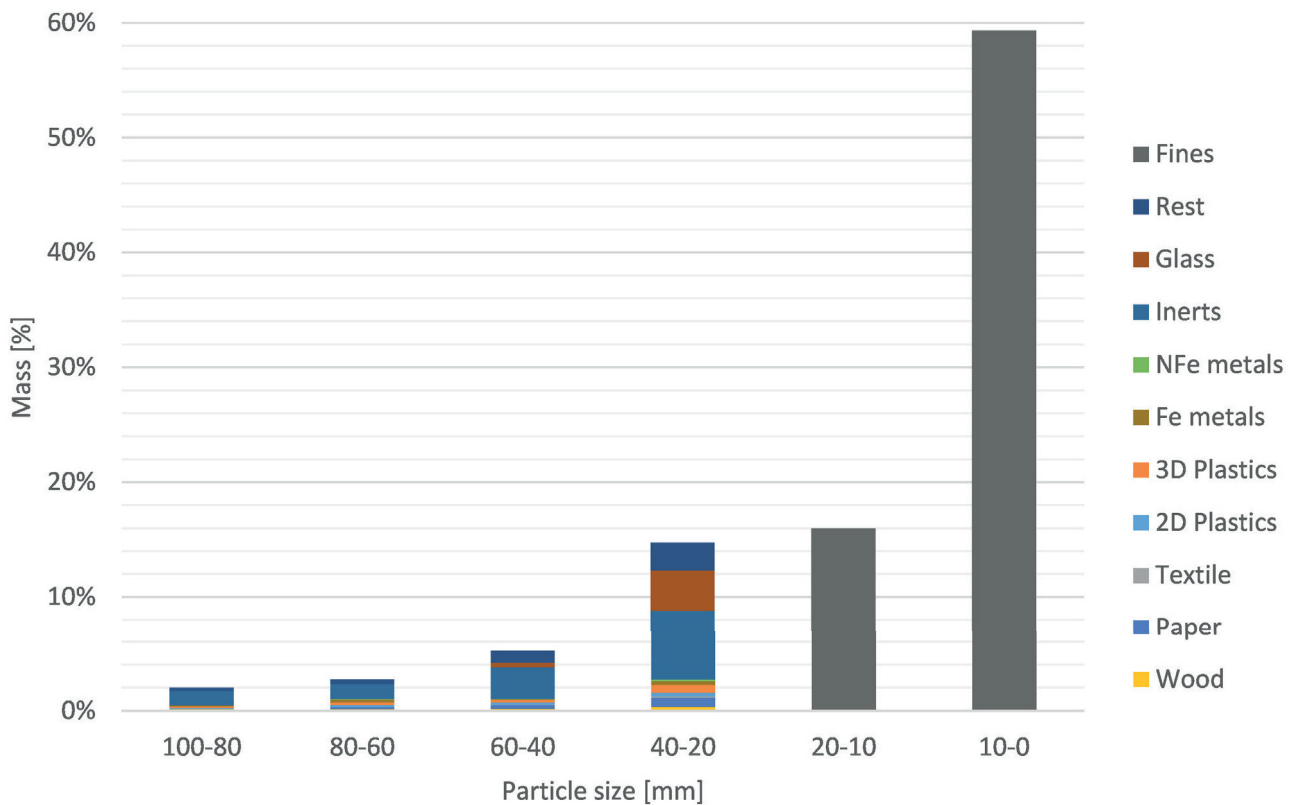


FIGURE 13: Material composition of the output stream "<90 mm" by particle size.

3.4 Comparison with previous LFM investigations

The total range of moisture content was between 9 and 41%, comparable with data in the literature of 18 to 40% for 17 to 40 year old waste (Hernández Parrodi, 2018a), even if data from "3D >200 mm" is missing for a complete comparison. Apart from the age, other important parameters can influence the water content of the material, e.g., geographical location, landfill layering (water permeability), particle size and the type of waste landfilled.

The characteristics of the mined material depend strongly on the type of waste that was initially landfilled. This becomes evident when looking at the material composition indicated on a wet and mass basis from previous studies (Bhatnagar et al., 2017; Jani et al., 2016; Kaartinen et al., 2013; Quaghebeur et al., 2013; Van Vossen & Prent, 2011; Wolfsberger et al., 2015b). In Table 3, the inert fraction (17% in this study) makes up more of the total when CDW was deposited. Municipal landfills, on the other hand, are characterized by 10% of inorganic substance (concrete, stones, and glass), 20-30% highly calorific fraction and 27-54% soil-like materials. Thus, the share of plastics in MSW is considerably higher than the 3% found for mixed waste in this paper. The same holds for household waste materials, such as paper and textiles: the percentages counted are below the values reported in the literature (0.4% and 2-7%, respectively). With a share of approximately 46%, the fines (<20 mm) are in accordance with MSW but different particle sizes are used to define the fines or soil-like materials. The metal concentrations in most LFM projects range below 5%, nevertheless the 1% found seems low because

more metals are expected from CDW, especially structural steel.

Similar to the difficulty encountered when comparing PSD, materials are classified into different categories by different researchers, especially overlapping categories (e.g., for plastics and metals) making comparison more challenging. Moreover, the efficiency of sorting, and therefore the results of the composition, depends on the applied technique: manual, mechanical or sensor-based sorting.

Findings on the GCV and ash content are compared to results presented by Quaghebeur et. al., 2013 for the REMO landfill site in Belgium. It stands out that the calorific value of the main combustible fraction (2D plastics, 35.1 and 40.9 MJ kg⁻¹) is considerably higher than for plastics analysed by Quaghebeur et. al., 2013 (19.0-28.0 MJ kg⁻¹) with an ash content of 20-35% compared to 21,7% and 12,8% (12,8% and 11,8% for 3D plastics), depending on the 2D output stream in this study. Similar differences are noted for the ash content of paper and cardboard, which amounts to 25-61% at the REMO site but is only estimated to be 12% in this study. The CV of paper and cardboard is more conformable in both studies: 6.7-12.0 MJ kg⁻¹ and 15 MJ kg⁻¹, respectively. The results for fines are in accordance with the compared data in which a CV of 1.3-4.8 MJ kg⁻¹ and ash contents of 64.4-87.5% are reported.

Summarizing the above comparison, it can be said that the mixture of CDW in the examined material with MSW influences the RDF potential negatively because MSW land-

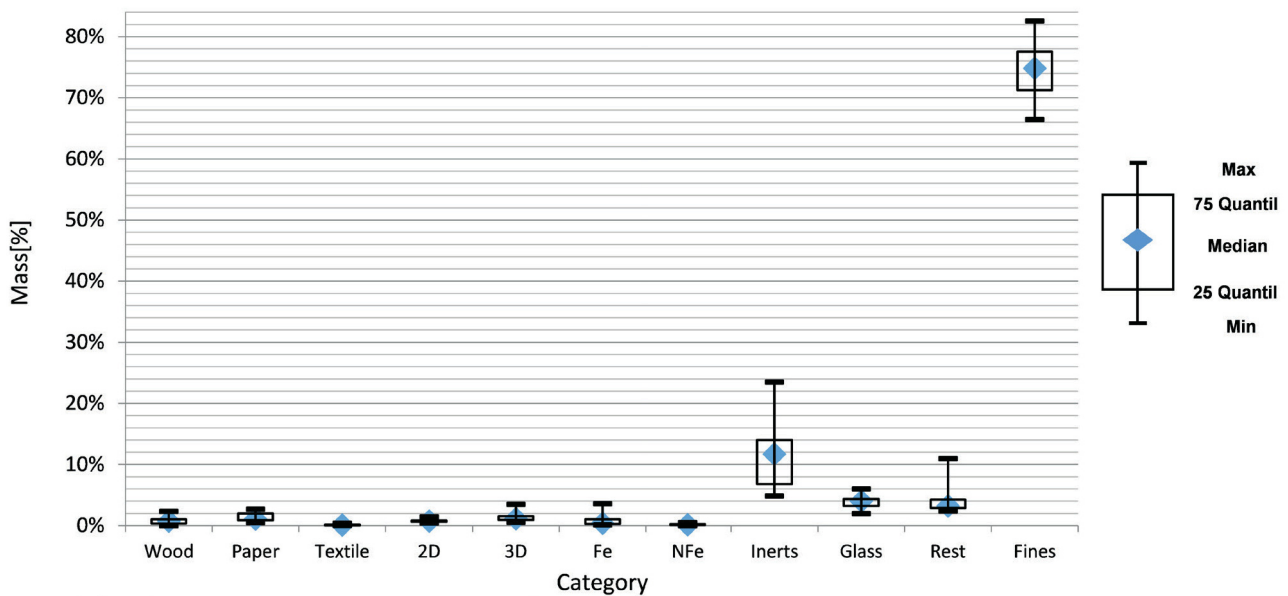


FIGURE 14: Output “<90 mm”: fluctuations in the material composition, dm % (n=12).

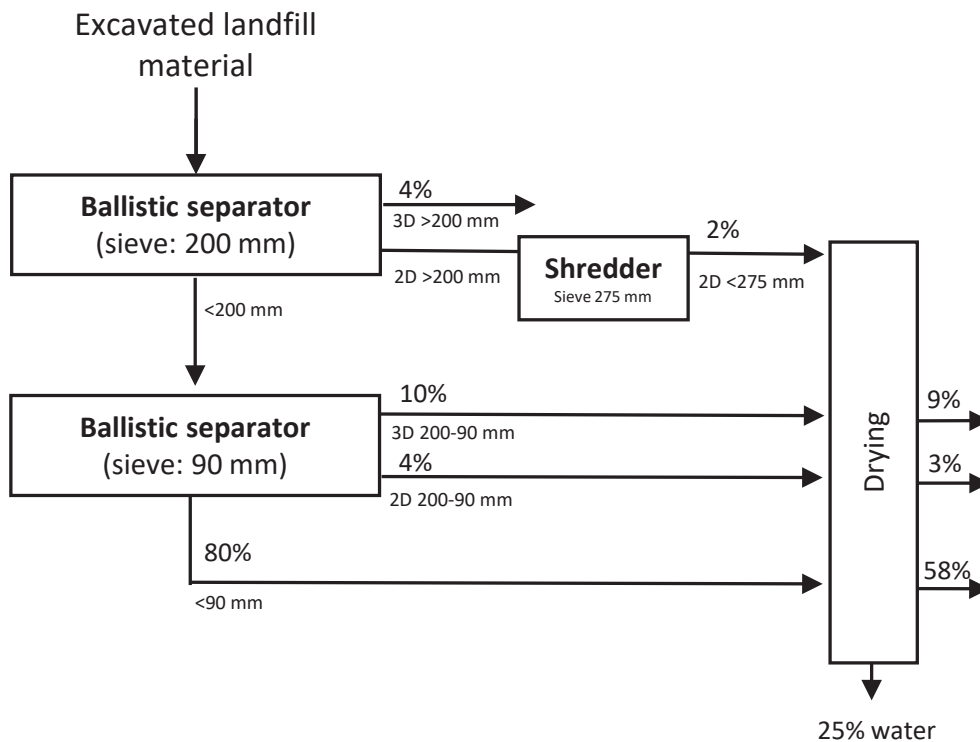


FIGURE 15: Mass balance of the ballistic separator with the two sieving steps of 200 mm and 90 mm (all indications refer to the input 100%).

fills are found to consist of more combustible materials. The high amount of fines described in most LFM projects is similar, whereas the CV and ash content are restricted in their resemblance. Standardized or widely agreed-on material categories and particle size fractions to increase comparability are desirable.

3.5 Recovery options

Generally, two different recovery processes can be dis-

tinguished: WtM, which creates new materials according to the properties of the recovered materials and WtE, which can substitute for the use of fossil fuels. For fresh plastic waste both recovery options are practised. WtM (for plastics) is subdivided into primary recycling without modifications of the polymers, secondary recycling with downgrading and tertiary recycling with depolymerization reactions. Primary and secondary recycling requires high-quality incoming waste. Moreover, the possibility of meeting the

TABLE 2: Average composition, GCV and ash content of the 2D <275 mm and 2D 200-90 mm output streams (n=8, n=9, respectively). Data from the REMO landfill (Quaghebeur et al., 2013) were used to compare the results.

Categories	2D < 275 mm			2D 200-90 mm			REMO, Belgium (2013)	
	Mass	GCV	Ash content	Mass	GCV	Ash content	GCV	Ash content
	[% of total]	[MJ/kg]	[%]	[% of total]	[MJ/kg]	[%]	[MJ/kg]	[%]
Wood	0,7	15,2	10,3	0,7	16,9	10,9	-	-
Paper	2,9	16,0	22,0	3,5	15,2	12	7.3 - 13.0	25.0 - 61.0
Textile	7,4	22,5	32,0	8,4	22,7	19,6	-	-
2D Plastics	24,1	35,1	21,7	37,5	40,9	13,5	19.0 - 28.0	20.0 - 35.0
3D Plastics	3,7	32,4	12,8	4,8	30,6	11,8	-	-
Fe metals	0,9	-	100,0	1,7	-	100	-	-
NFe metals	0,1	-	100,0	0,2	-	-	-	-
Inert	5,7	0,1	98,4	1,5	-	99,6	-	-
Glass	0,4	-	100,0	0,0	-	-	-	-
Rest	18,0	18,5	34,7	10,5	23,3	16,8	-	-
Fines	36,1	2,0	79,0	31,2	1,9	88	2.1 - 5.7	64.4 - 87.5
Total	100,0	16,0	50,5	100,00	22,4	40,4	-	-

limits on heavy metal content must be questioned, taking into account the diverse additives that were used in the past for plastic production. Tertiary recycling seems suitable for landfill-mined plastics but only a few industrial plants applying this process exist in Europe (Quaghebeur et al., 2013). Likewise, the heterogeneity and high level of contamination of paper, textiles and wood would require extensive and expensive treatment for WtM valorisation of those materials. As mentioned above, the Rest of the “2D 200-90 and 2D <275 mm” also appears suitable for WtE. Hence, for most excavated materials WtE valorisation as “Solid recovered fuels (SRF) is the most realistic marketable material” (Bhatnagar et al., 2017). RDF differs from SRF in that the latter guarantees a certain quality of the fuel, since SRF must be produced from non-hazardous waste and fulfil certain fuel qualities (Rotter et al., 2011). Therefore, more parameters, apart from the characteristics presented in this study, are needed to evaluate the efficiency and quality of the RDF generated from landfilled materials and the emissions of the combustion process. Those parameters are the amount of organic carbon, total carbon, hydrogen, nitrogen, sulfur, chlorine, fluorine, bromine and heavy metals (Quaghebeur et al., 2013). It is obligatory to indicate the concentration of chlorine according to the specification DIN EN 15359 due to its corrosive impact and the property of mobilizing some of the metals into the flue gas (Kaartinen et al., 2013). Heavy metals are of special concern for SRF made from pretreated waste (Wolfsberger et al., 2015a). Therefore, information should be gathered about the history and origin of the landfilled waste. The requirements that the above parameters must meet depend on the combustion system used and on applicable laws and authorization procedures (Kuchta et al., 2017).

If metals are not separated during the SRF/RDF production process and are directly valorised as WtM, they can be

recovered from the ash after incineration (Seifert & Vehlow, 2017). As glass is an inert material, WtM is considered for its valorisation providing an efficient separation (Quaghebeur et al., 2013).

Of major importance is the recoverability of the fine fractions, as they make up around half of the total material excavated and have been found to be challenging in previous investigations (Hernández Parrodi et al., 2018; Jones et al., 2013). A WtE application of the fine fractions, as described by Quaghebeur et al., 2013, is not considered to be applicable for the present material because of the age of the waste, the resulting high degree of degradation, the low CV and the high ash content. Thus, WtM options are to be considered.

One possibility is the use of the fine fractions as a cover layer in operating landfills. At the Kudjape landfill, Estonia, the fine fraction was used as a methane degradation layer. This valorisation requires a low degree of contamination (Bhatnagar et al., 2017). The use of fines and conditioned inert materials as filler and construction material generally can be considered if they comply with the limit values for such activities (Quaghebeur et al., 2013).

Heavy metals are especially expected to be found in old landfills and can contribute to decrease the costs of EFLM if recovered (García López et al., 2018). From these findings, the recovery of the major and trace metals from the fine fractions could be an option to meet the globally increasing demand. Conducting leaching tests and XRF analysis can give a more precise composition determination and allow an estimation of the marketable potential. Apart from the potential economic benefit of heavy metals recovery from the fine fractions, another positive effect can be the resulting reduction of their uncontrolled leaching out of the landfill (Hernández Parrodi et al., 2018; Bhatnagar et al., 2017; Quaghebeur et al., 2013; Kaartinen et al., 2013).

TABLE 3: Comparison of the material MSG composition of this study with previous LFM investigations, adapted from Hernández Parrodi, 2018a.

Type of information	This study, 2018 (MSG, Belgium)	Various countries (Van Vossen and Prent, 2011)	Högbyp, Sweden (Jani et al., 2016)	Kuopio, Finland (Kaartinen et al., 2013)	Kudjape, Estonia (Bhatnagar et al., 2017)	Lower Austria, Austria (Wolfsberger et al., 2015)	Houthalen, Belgium (Quaghebeur et al., 2013)
Type of waste	MSW + C&D	Various	MSW + C&D	MSW	MSW	MSW	MSW
Age of waste [y]	40 - 50	Various	5	5 - 10	10	13 - 20	14 - 29
Average moisture content	25%	-	-	-	-	29 - 55%	48 - 66%
Fines/ Soil-like material	46%	55%	27%	50-54%	29%	47%	44% (12)
Stones	-	3%	28%	-	18%	-	-
Inert/minerals	17%	6%	-	-	-	6%	10% (6)
C&D	-	9%	-	-	-	-	-
Limestone	-	-	5%	-	-	-	-
Asphalt	-	-	3%	-	-	-	-
Glass/ceramics	2%	1%	6%	-	5%	1%	1.3% (0.8)
Plastics (3D/2D)	3%	5%	-	23%	22%	18%	17% (10)
Soft plastics	-	-	1%	-	-	-	-
2D plastics	2%	-	-	-	-	-	-
3D plastics	1%	-	-	-	-	-	-
Other plastic/ Composites	-	-	7%	-	-	4%	-
Organic/kitchen waste	-	5%	-	-	-	-	-
Paper/cardboard/ PPC	1%	5%	-	4 - 8%	5%	3%	7.5% (6)
Paper	<1%	-	4%	-	-	-	-
Wood	1%	4%	15%	6 - 7%	5%	-	6.7% (5)
Textile	<1%	2%	3%	7%	-	6%	6.8% (6)
Leather	-	2%	-	-	-	-	-
Rubber	-	-	0%	-	-	-	-
Wood/leather/rubber	-	-	-	-	-	9%	-
Total metals	1%	2%	-	3 - 4%	3%	5%	2.8% (1)
Fe metals	1%	-	0%	-	-	-	-
NFe metals	<1%	-	0%	-	-	-	-
Other/ Rest	3%	3%	-	2%	13%	1%	-
Non-MSW	-	0%	-	-	-	-	-

A third option would be to re-landfill the fine fractions, but this procedure bears costs instead of revenues and is not in line with the introduced goals of ELFM projects (Kaartinen et al., 2013).

Independently of the recovery option chosen for the fine fractions, their separation from other excavated materials by sieving can be essential for further processing, since it raises the purity and CV of the RDF stream and improves the possible efficiency of sensor-based sorting techniques (Hernández Parrodi et al., 2018; Maul et al., 2016). Moreover, the bulk density of the material is a very relevant parameter for the design of the mechanical treatment. Although no quantitative statement was done in this analysis, it can be said that landfilled material presents higher bulk densities than fresh MSW, since the

landfill-mined material showed more fine material than those typical of MSW.

4. CONCLUSIONS

This study found that the 3D-output streams (>200 mm and 200-90 mm) of the ballistic separator consisted mainly of coarse CDW, whereas more heterogeneous MSW was yielded in the 2D-output streams (>200 mm and 200-90 mm). By comparing 57% of the combustible materials (plastics, paper, textiles, leather and wood) in the output "2D <275 mm" and 65% in "2D 200-90 mm" to 75% of inert material in "3D 200-90 mm", the efficiency of the separating process was suitable for the landfilled material. The 2D-output streams were characterized by a higher moisture content (average, 30%) than the 3D streams (12%), which

caused elevated amounts of fines (<20 mm) to adhere to larger particles.

The laboratory analysis showed an average CV of 22 MJ kg⁻¹ and an ash content of 40% for the “2D 200-90 mm”. To fully determine the quality of the produced RDF, further tests that characterize the generated flue gas and remaining ash should be conducted.

A considerable share of the total excavated waste was made up of the output stream <90 mm, which was the greatest output stream of the ballistic separator with a share of 80% (wm). Its amount is expected to increase if the material is dried beforehand. As a further processing step, separating the fines by sieving is advisable to remove inert materials and enrich the WtE-stream with high CV materials, since fines contain a significant amount of inert materials, which are not suitable for RDF production. WtM valorisation of the recovered materials, such as inert materials as construction sand, soil-like materials as cover material for operational landfills or metals for recycling, could be considered for the fine fractions. If the separation of metals, glass and stones is possible, the amount of material that has to be re-landfilled would be decreased significantly.

The results of this study cannot be directly transferred to other landfills because compositions depend on different factors such as the origin of the waste, time of storage and physical conditions of the site. In this study, the ballistic separator shows an enhanced mechanical processing due to the share of CDW, which mostly consists of heavy 3D-materials. Further investigation is required in order to state that different types of waste (industrial waste, MSW and CDW, independently) have the same rate of enrichment of high calorific materials as in this study.

Although this study assesses the technical aspects by characterizing the different output streams generated by the ballistic separator, cost efficiency also needs to be taken into account when considering the feasibility of a full-scale ELFM project. Additionally, a remaining challenge is the assessment of costs and revenues of a recovery process by estimating the total amount of deposited waste and relating it to the market prices of the recoverable materials.

ACKNOWLEDGEMENTS

The authors would like to acknowledge the financial support from the European Union's EU Framework Programme for Research and Innovation Horizon 2020 under Grant Agreement No 721185. Special gratitude is due to the team of Stadler@ Anlagenbau GmbH for the knowledge, expertise and support provided during the material processing with the STT 6000 ballistic separator. The authors are grateful to the personnel from Renewi Belgium SA/NV for their extensive collaboration during the excavation work at the MSG landfill and to Christin Bobe from the Research Group Soil Spatial Inventory Techniques (Ghent University) for its geophysical exploration prior to the excavation that helped to determine the area of interest.

REFERENCES

- Bauer, M., Lehner, M., Schwabl, D., Flachberger, H., Kranzinger, L., Pomberger, R., & Hofer, W. (2018). Sink–float density separation of post-consumer plastics for feedstock recycling. *Journal of Material Cycles and Waste Management*, 20(3), 1781–1791.
- Beel, H. (2017). Sortierung von schwarzen Kunststoffen nach ihrer Polymerklasse mit Hyperspectral-Imaging-Technologie: Recycling und Rohstoffe. Neuruppin: TK Verlag Karl Thomé-Kozmiensky.
- Bhatnagar, A., Kaczala, F., Burlakovs, J., Kriipsalu, M., Hogland, M., & Hogland, W. (2017). Hunting for valuables from landfills and assessing their market opportunities. A case study with Kudjape landfill in Estonia. *Waste management & research : the journal of the International Solid Wastes and Public Cleansing Association, ISWA*, 35(6), 627–635.
- Bureau d'études greisch (2002). Interview with Centre d'Enfouissement Technique de Mont-Saint-Guibert: Etude des conséquences de l'octroi du permis d'urbanisme du 29.10.01 sur les conditions d'exploitation du permis du 16.12.98.
- Department of Processing and Recycling (2014). Retrieved October 13, 2018, from <https://www.iar.rwth-aachen.de/cms/IAR/Forschung/-Experimentelle-Arbeiten/~efnu/Technikum/lidx/1/>.
- DIN 51900-1 (2000). Determination of gross calorific value by the bomb calorimeter and calculation of net calorific value.
- DIN CEN/TS 15414-1 (2010). Solid recovered fuels - Determination of moisture content using the oven dry method.
- DIN EN 15359 (2005). Solid recovered fuels - Specifications and classes.
- Energy research Centre of the Netherlands (2018). Phyllis2, database for biomass and waste, from Energy research Centre of the Netherlands: <https://www.ecn.nl/phyllis2>.
- European Parliament (2013). Decision No 1386/2013/EU of the European Parliament and of the Council of 20 November 2013 on a General Union Environment Action Programme to 2020 Living well, within the limits of our planet Text with EEA relevance. In *Official Journal of the European Union*.
- García López, C., Küppers, B., Clausen, A., & Pretz, T. (2018). Landfill mining: A case study regarding sampling, processing and characterization of excavated waste from an Austrian Landfill. *Detritus*, 2(1), 29.
- Giani, H., Fidalgo Estevez, R., Kaufelf, S., Althaus, M., & Pretz, T. (Eds.). 2016. Technical-economic evaluation of an advanced MBT process to enrich biomass as renewable fuel. Cyprus.
- Hermann, R., Baumgartner, R. J., Sarc, R., Ragossnig, A., Wolfsberger, T., Eisenberger, M., et al. (2014). Landfill mining in Austria: Foundations for an integrated ecological and economic assessment. *Waste management & research : the journal of the International Solid Wastes and Public Cleansing Association, ISWA*, 32(9 Suppl), 48–58.
- Hernández Parrodi, J. C., García López, C., Raulf, K., Pretz, T., Küppers, B., & Vollprecht, D. (2018b). Characterization of Fine Fractions from Landfill Mining - A Case Study of a Landfill Site in Belgium. *VORTRÄGE-Konferenzband zur 14. Recy & DepoTech-Konferenz*. (14), 569–576.
- Hernández Parrodi, J. C., Vollprecht, D., & Pomberger, R. (2018a). Characterization of Fine Fractions from Landfill Mining - A Review of Previous Investigations. *Detritus*, 2(1), 46.
- Hogland, M., Marques, M., 2010. Enhanced Landfill Mining: Material recovery, energy utilisation and economics in the EU (Directive) perspective. In: *Proceedings of the International Academic Symposium on Enhanced Landfill Mining*. Molenheide, Belgium.
- Hull, R. M., Krogmann, U., & Strom, P. F. (2005). Composition and Characteristics of Excavated Materials from a New Jersey Landfill. *Journal of Environmental Engineering*, 131(3), 478–490.
- Jani, Y., & Kaczala, F., Marchand, C., Hogland, M., Kriipsalu, M., Hogland, W., & Kihl, A. (2016). Characterisation of excavated fine fraction and waste composition from a Swedish landfill. *Waste Management & Research*, 34 (12), 1292–1299.
- Jones, P. T., Geysen, D., Tielemans, Y., van Passel, S., Pontikes, Y., Blanpain, B., et al. (2013). Enhanced Landfill Mining in view of multiple resource recovery: A critical review. *Journal of Cleaner Production*, 55, 45–55.
- Kaartinen, T., Sormunen, K., & Rintala, J. (2013). Case study on sampling, processing and characterization of landfilled municipal solid waste in the view of landfill mining. *Journal of Cleaner Production*, 55, 56–66.

- Kranzinger, L., Schopf, K., Pomberger, R., & Punesch, E. (2017). Case study: Is the 'catch-all-plastics bin' useful in unlocking the hidden resource potential in the residual waste collection system? *Waste management & research : the journal of the International Solid Wastes and Public Cleansing Association, ISWA*, 35(2), 155–162.
- Kuchta, K., Hobohm, J., & Flamme, S. (2017). Verwertung von Altprodukten und Abfällen. In: KRANERT, Martin (Hrsg.): Einführung in die Kreislaufwirtschaft : Planung – Recht – Verfahren, 253–293.
- Martens, H., & Goldmann, D. (2016). *Recyclingtechnik: Fachbuch für Lehre und Praxis* (2. Aufl. 2016). Wiesbaden: Springer Fachmedien Wiesbaden.
- Maul, A., & Pretz, T. (2016). Landfill Mining from the processing perspective - a view on mass balance and output streams. *Proceeding "3rd International Academic Symposium on Enhanced Landfill Mining, ELM III"*, Lisboa (Portugal).
- Ministerium für Umwelt und Forsten Rheinland-Pfalz (1983). LAGA - RL. PN 2/78K - Grundregeln für die Entnahme von Proben aus Abfällen und abgelagerten Stoffen. Richtlinie für das Vorgehen bei physikalischen und chemischen Untersuchungen im Zusammenhang mit der Beseitigung von Abfällen.
- Ministerium für Umwelt und Forsten Rheinland-Pfalz (2001). LAGA PN 98 - Richtlinie für das Vorgehen bei physikalischen, chemischen und biologischen Untersuchungen im Zusammenhang mit der Verwertung/Beseitigung von Abfällen.
- Quaghebeur, M., Laenen, B., Geysen, D., Nielsen, P., Pontikes, Y., van Gerwen, T., & Spooren, J. (2013). Characterization of landfilled materials: Screening of the enhanced landfill mining potential. *Journal of Cleaner Production*, 55, 72–83.
- Rotter, V. S., Lehmann, A., Marzi, T., Möhle, E., Schingnitz, D., & Hoffmann, G. (2011). New techniques for the characterization of refuse-derived fuels and solid recovered fuels. *Waste management & research : the journal of the International Solid Wastes and Public Cleansing Association, ISWA*, 29(2), 229–236.
- Seifert, H., & VEHLOW, J. (2017). Thermische Verfahren In: KRANERT, Martin (Hrsg.): Einführung in die Kreislaufwirtschaft : Planung – Recht –, 5 Wiesbaden : Springer Fachmedien Wiesbaden, 423–470.
- Sigmund, U. (2018). Sorting with ballistic separators. *4th International Symposium on Enhanced Landfill Mining*, 89–94.
- van Vossen, W. J., & Prent, O. J. (2011). Feasibility study: Sustainable material and energy recovery from landfills in Europe. *Proceedings Sardinia 2011. Thirteenth International Waste Management and Landfill Symposium*. 3 - 7 Oct., 247–248.
- Wolfsberger, T., Aldrian, A., Sarc, R., Hermann, R., Höllen, D., Budischowsky, A., et al. (2015b). Landfill mining: Resource potential of Austrian landfills-Evaluation and quality assessment of recovered municipal solid waste by chemical analyses. *Waste management & research : the journal of the International Solid Wastes and Public Cleansing Association, ISWA*, 33(11), 962–974.
- Wolfsberger, T., Nispel, J., Sarc, R., Aldrian, A., Hermann, R., Höllen, D., et al. (2015a). Landfill mining: Development of a theoretical method for a preliminary estimate of the raw material potential of landfill sites. *Waste management & research : the journal of the International Solid Wastes and Public Cleansing Association, ISWA*, 33(7), 671–680.

APPENDIX A

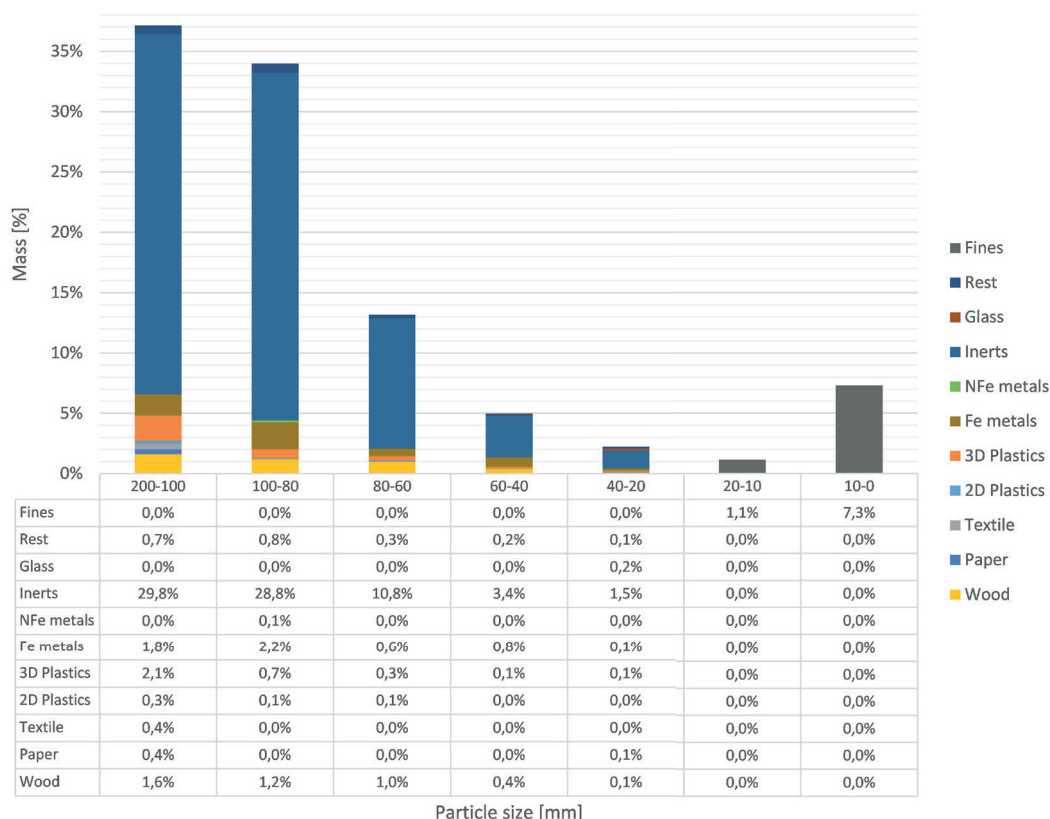


FIGURE A1: Total mass composition, dm %, by particle size of the output "3D 200-90 mm".

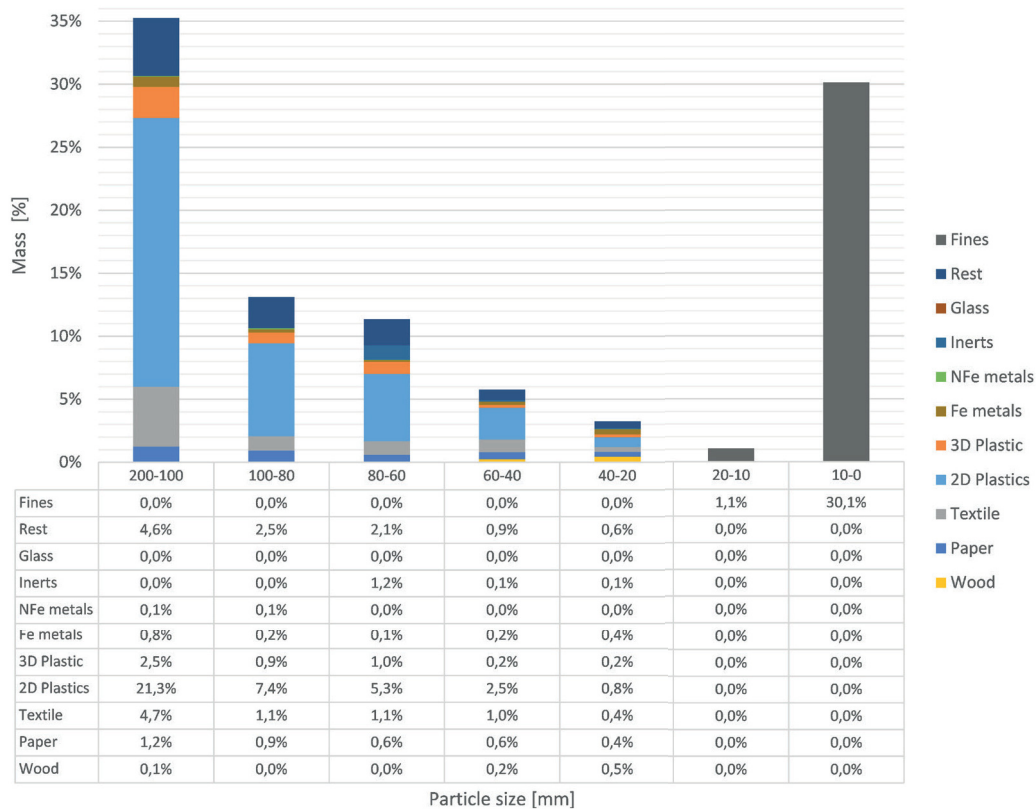


FIGURE A2: Total mass composition, dm %, by particle size of the output "2D 200-90 mr"

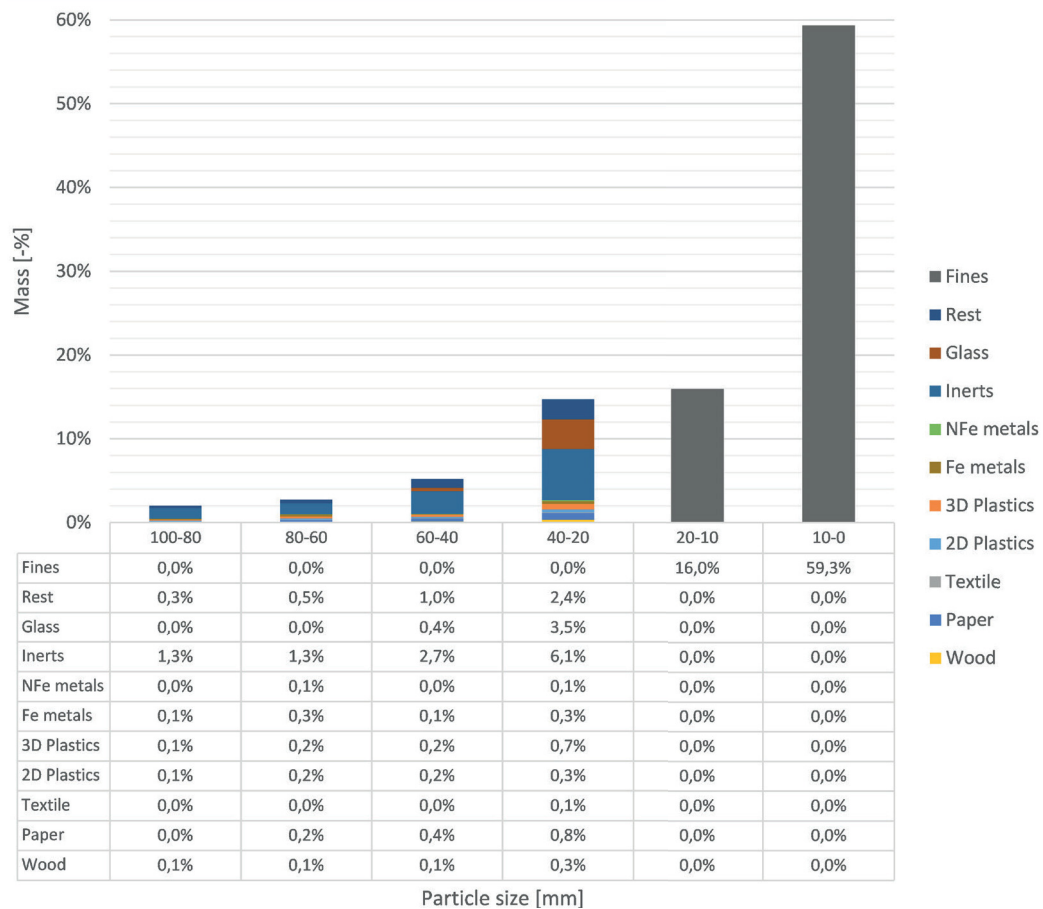


FIGURE A3: Total mass composition, dm %, by particle size of the output "<90 mm".

APPENDIX B

TABLE B1: Technical specifications of the ballistic separator.

Manufacturer	STADLER®
Modell	STT 6000
Dimensions (L x W x H) (mm)	6030x2970x6040
Weight (kg)	25000
Engine output (kW)	30
Adjustable Angle	15°; 17.5°; 20°
Surface (m ²)	14.3
Maximum output (m ³ /h)	200
N° of paddles	5
N° of fans	No fans available

TABLE B2: Technical specifications of the sieves.

	Drum sieve	Box sieve
Manufacturer	Self-made by the Department of Processing and Recycling (RWTH Aachen University)	Siebtechnik
Type of movement	Rotating	Circular Vibratory Screen
Input power (kW)	2.2	0.75
Diameter of drum screen (mm)	1500	-
Installation	Polygonal screen with 8 screen linings	-
Dimensions of screen linings (mm)	950x560	500x500
Revolution	Adjustable	1400 RPM
Mesh sizes (mm)	10; 20; 40; 60; 80; 100 ; 120; 140; 160; 200; 240; 300	1; 2; 4; 6.3; 10; 20 ; 31.5; 40 ; 50; 60; 80 ; 100

*The mesh sizes used during this study are marked in bold.

TABLE B3: Technical specifications of the sieves.

Type of cutting mill	Large cutting mill	Small cutting mill	Disc mill
Manufacturer	Reto	Dreher	Retsch
Input power (kW)	37	2.2	1.75
Rotor peripheral speed (m/s)	9	10	10
Rotor cutting diameter (mm)	350	160	
Rotor length (mm)	450	200	
Mesh sizes (mm)	4; 5; 6; 8; 10 ; 12; 15; 20; 30; 40; 50; 60; 70; 80	1; 2; 3; 4; 5; 6; 8	0.5 ; 0.75; 1; 1.5; 2; 4; 6; 8; 10

*The mesh sizes used during this study are marked in bold.

TABLE B4: Technical specifications of the hammer mills.

	Large hammer mill	Small large mill
Manufacturer	Hazemag	Condux
Type of crusher	High speed	High speed
Main types of loads	-	Impact, Shearing
Weight (kg)	-	30
Input power (kW)	18	3
Revolution	adjustable up to approx.19 m/s	2850 RPM
Mesh sizes (mm)		
Feed grain size (mm, max.)	approx. 360 x 280	100 x 60
Rotor width (mm)	-	150

4 PUBLICATION 3

Influence of surface roughness and surface moisture of plastics on sensor-based sorting in the near infrared range

Küppers B, Schloegl S, Oreski G, Pomberger R, Vollprecht D (2019) Influence of surface roughness and surface moisture of plastics on sensor-based sorting in the near infrared range. *Waste Management & Research* 37(8): 843–850. Doi: 10.1177/0734242X19855433

Annotation on my own contribution to publication 3:

I designed the test series and jointly conducted the experiments in collaboration with Sabine Schloegl. Sabine Schloegl's analysis of the obtained results was guided by me. Gernot Oreski who supported me in the analysis and evaluation of the attained data performed further laboratory analyses. I wrote the publication with decisive support from Sabine Schloegl. All co-authors reviewed the publication. I revised the publication with assistance of Sabine Schloegl.

Influence of surface roughness and surface moisture of plastics on sensor-based sorting in the near infrared range

Waste Management & Research
2019, Vol. 37(8) 843–850
© The Author(s) 2019
Article reuse guidelines:
sagepub.com/journals-permissions
DOI: 10.1177/0734242X19855433
journals.sagepub.com/home/wmr
SAGE

Bastian Küppers¹ , Sabine Schloegl¹, Gernot Oreski²,
Roland Pomberger¹ and Daniel Vollprecht¹

Abstract

In the project ‘NEW-MINE’ the use of sensor-based sorting machinery in the field of ‘landfill mining’ is investigated. Defilements pose a particular challenge in the treatment and sorting of plastics contained in landfills. For this reason, the effects of various pollutants caused by the interactions in the landfill body or the mechanical treatment steps in landfill mining are examined. In the following elaboration, the focus is on the influences of surface moisture and surface roughness of plastics on sensor-based sorting by means of near-infrared technology. Near-infrared radiation (NIR) in a wavelength range of 990 nm to 1500 nm has been used for the detection and classification of plastic particles. The experiments demonstrate that increased surface roughness reduces signal noise and thereby improves the classification of both spectrally similar and transparent plastics, but reduces the yield of low-softening plastics because their sliding speed on a sensor-based chute sorter varies as a result of the heating of the chute. Surface moisture causes the absorption of radiation from 1115 nm (high density polyethylene [HDPE], linear low density polyethylene [LLDPE], polyethylen terephthalate [PET] and polyvinylchloride [PVC]) or from 1230 nm (low density polyethylene [LDPE], polypropylene [PP] and thermoplastic polyurethane [TPU]) up to at least 1680 nm, which causes amplification or attenuation of various extremes in the derivative. However, the influence of surface moisture on the yield of plastics is usually very low and depends on the spectral differences between the different plastics.

Keywords

Sensor-based sorting, hyperspectral imaging, near-infrared spectroscopy, influence of defilements, surface roughness, surface water

Received 10th April 2019, accepted 13th May 2019 by Associate Editor Nemanja Stanisavljevic.

Introduction

Sensor-based sorting units have been used for years in the recycling industry to solve complex sorting tasks. The development of modern sorting technology was initially influenced by the fields of mineral processing and food inspection (Huang et al., 2008; Wotruba and Harbeck, 2010). In contrast to the use of sensor-based sorting machines in the food or mining sector, the material flows in the recycling industry, especially in landfill mining, are characterised by significant contaminations (Maul and Pretz, 2016). These could be caused by fine mineral or biodegradable waste particles contained in municipal solid waste (MSW) (Vujić et al., 2010) or owing to impact factors of storage (e.g. water ingress by rain). Thus, the surface of objects can, among others, be covered with water, dust, grease and oils. In the past, the common doctrine was that the prerequisite for successful sensor-based sorting is a clean and dry surface. Therefore, the recycling technology had to evolve enormously to achieve the goal of producing quality-assured products from waste (Pretz and Julius, 2008; Schug et al., 2007).

A relevant advantage of sensor-based sorting units is the fact that they work non-destructively and have very short measuring times (Eccher-Zerbini, 2005). Since a high material throughput is indispensable in recycling plants, optical in-line measurement, in

particular with near infrared radiation (NIR) measurement technology, are state-of-the-art today. NIR spectroscopy is based on changes in dipole moments creating absorption bands in specific spectral regions. Position and intensity of absorption bands are influenced by molecular composition as well as intramolecular interactions. This allows for conclusions regarding both chemical and physical properties (e.g. crystal structure, density, viscosity and particle size in pulverulent solids) without the necessary sample preparation one usually needs for traditional chemical analysis (Blanco and Villarroya, 2002). Additionally, a NIR sensor is simple to operate after the initial calibration (Büning-Pfaue, 2003).

Another advantage is that, within optical sorting techniques, the sorting criterion is decoupled from the separating force. The separation criteria can be modified so that different characteristic

¹Waste Processing Technology and Waste Management (AVAW), Montanuniversität Leoben, Austria

²Polymer Competence Center Leoben GmbH, Leoben, Austria

Corresponding author:

Bastian Küppers, Waste Processing Technology and Waste Management (AVAW), Montanuniversität Leoben, Franz Josef-Straße 188700 Leoben, Austria.

Email: bastian.kueppers@unileoben.ac.at

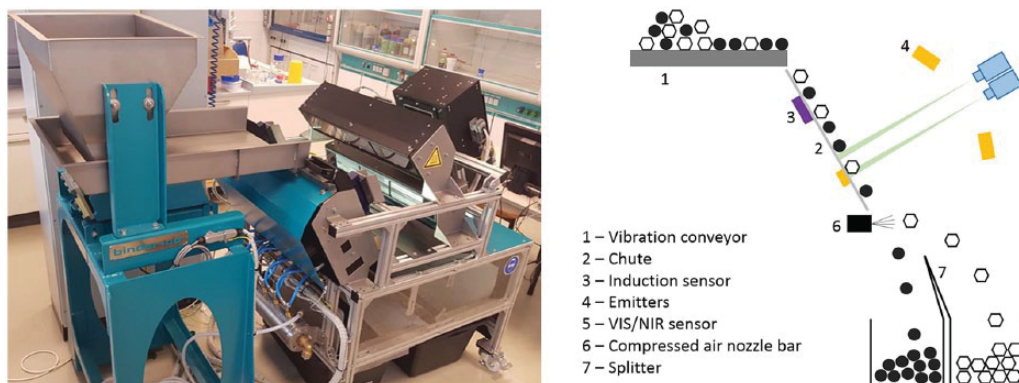


Figure 1. Test stand for sensor-based detection (left) and schematic drawing of the working principle and sensor arrangement (right).

properties of the material are decisive for the sorting decision. As a result of this decision, which is determined by the applied algorithm, the corresponding particle is discharged. Although also X-ray transmission (XRT) (Mesina et al., 2006), X-ray fluorescence (XRF) and laser-induced breakdown spectroscopy (LIBS) are used, common sensor-based sorting systems for sorting of plastics work with NIR technology (Gundupalli et al., 2016). Information obtained from photon-matter interactions (e.g. reflection, absorption, scattering and delayed re-emission of photons) at the particle surface in NIR spectroscopy is used to draw conclusions about the type of plastic enabling sorting decisions (Gschaider and Huber, 2008).

It is well known in the industry that moisture has a negative impact on the identification of materials via NIR technology in sorting plants. Additionally, it is obvious that surface roughness varies significantly depending on the mechanical preprocessing, but no studies on its impact on NIR sorting have been conducted yet. Therefore, the impetus of our research is to enable the improvement of the identification of materials by NIR spectroscopy by providing deeper understanding of the impacts on these surface properties.

In order to be able to qualitatively assess the sorting of different material streams despite contamination, it is necessary to know how the respective contaminants influence the spectrum. The aim of the present study is to evaluate the influence itself and the resulting impact on the sorting decision. The potential of such information may enable optimisations concerning plant designs and therefore improved machine efficiencies. Likewise, the algorithm for sorting particles can be adapted to take into account how different contaminants influence the detectable spectrum of a substance in the NIR range. Despite the importance of the influence of contaminations being well-known, no systematic research has been conducted yet to our knowledge. Consequently, we present the first scientific study covering the effect of surface roughness and moisture on NIR sorting of plastics.

Materials and methods

To investigate the influences of surface moisture and surface roughness on both the spectral information and the efficiency

(i.e. yield and purity) of a sensor-based sorting unit, experiments were carried out with different types of plastic.

A test stand for sensor-based detection and sorting (compare Figure 1) was used for the experiment. In addition to a colour sensor and an induction strip, it contains a NIR sensor (EVK-Helios-G2-NIR1). For the presented experiments only the NIR sensor was used. The working principle of the test stand can be seen in Figure 1. The emitter is a halogen lamp. The emitted radiation interacts with the near-surface molecules of the particles and is reflected, absorbed and/or transmitted depending on the chemical composition and structure of these particles. The dispersedly reflected radiation strikes the NIR sensor and is detected. Subsequently, this radiation (wavelength range 990 nm–1680 nm) is converted into an electrical signal. The spectral resolution of the sensor is 3.18 nm. A spatial pixel is 1.60 mm wide owing to the geometry of the experimental setup. Depending on the sliding speed of the particle on the chute, the length of the pixel may vary but is always smaller than 1.60 mm. The frame rate of the line sensor is always 476 Hz, with an exposure time of 1800 μ s.

To evaluate the influence of contaminants, various series of experiments were carried out. These can be divided as follows.

1. Influence of contamination on the detected near-infrared spectrum.
2. Influence of contamination on classification and yield of plastics.

For the series of tests for both of these aspects, eight different types of plastic were used (see Table 1). Despite the polyethylene terephthalate (PET) and polyvinylchloride (PVC) samples (originating from PET bottles and PVC film) all test specimens were specifically produced via an extrusion process at the Chair of Polymer Processing, Montanuniversitaet Leoben, and subsequently cut into particles with a projection area of approximately 25 cm².

To determine the influence of contaminants, a sorting recipe was created. From the listed materials, example objects were selected to take pictures with the NIR sensor. These recordings contain an NIR spectrum assigned to each object pixel. In order

Table 1. List of the plastics used for the test series.

Name	Abbreviation	Colour
High density polyethylene	HDPE	Grey
Low density polyethylene	LDPE	Red
Low density polyethylene	LDPE	White
Linear low density polyethylene	LLDPE	Turquoise
Polyethylen terephthalate	PET	Green/blue transparent
Polypropylene	PP	Pink
Polyvinylchloride	PVC	Clear
Thermoplastic polyurethane	TPU	Yellow

Table 2. Preprocessing and spectral processing of spectra for classification.

Preprocessing	Spectral processing
<ul style="list-style-type: none"> • Spatial correction • Bad pixel replacement • Intensity calibration • Noise suppression 	<ul style="list-style-type: none"> • 1st derivative • Normalisation • Smoothing

to be able to store a material specific NIR spectrum, at least 60 spectra per material were selected generating an averaged spectrum. The object pixels used for this purpose were grouped in clusters and selected. Care was taken to ensure that the spectra were not located close to atypical object edges or at exceptionally high/low reflecting points. The averaged spectrum serves as a reference spectrum for assigning objects to the substance classes stored in the recipe.

To detect and evaluate all potential changes, the whole spectral range within 990 nm–1500 nm was used for the classification of object pixels. Before the classification of such a spatial pixel, the detected spectrum is pre-processed and spectrally processed (Table 2):

Based on the created recipe, the individual object pixels of particles are classified and provided with false colours. If none of the taught average material spectra fits the NIR spectrum of the object pixel, it is classified as ‘not known’. In this way the image information from the NIR spectrum is classified and thus presented in a simplified version. In addition, the data volume of the spectral information is reduced, enabling fast classification of the objects.

The false colour pixels are used to assign each object to one of the taught material types. For this purpose, the classified object pixels of each material class are added up. Each object is assigned to the material class that prevails in this object. For example, in Figure 2, some high density polyethylene (HDPE) particles are partly misrecognised as PET (white pixels), linear low density polyethylene (LLDPE) (green pixels) or ‘not known’ (yellow pixels). Reasons for misrecognition may include, but are not limited to, polarisation effects. Owing to the large number of HDPE pixels (grey), the particles are correctly classified as HDPE anyway.

As mentioned above, two main aspects were examined in the experiments. To gather information concerning the influence of contaminations on the detected near-infrared spectrum (‘Aspect 1’)

the plastic particles were either roughened via a ‘Bosch PEX 220 A’ random orbital sander equipped with P60 sandpaper or wetted with, on average, 0.76 g water per particle. By usage of the random orbital sander, a severe degree of surface roughening that is expected to be either representative or even exceed the roughening degree a plastic surface can reach during mechanical processing (shredding, mechanical label removal, screening, etc.), was attained. Subsequently, spectral images of the objects (original/rough/wet) were taken to illustrate the influence of the ‘surface roughness’ and ‘surface moisture’. By comparing the spectra of soiled and clean object pixels, the influence of the respective contamination can be determined.

For the evaluation of the influence of contaminations on classification and yield (‘Aspect 2’), the plastics listed in Table 1 were sorted. Fifty particles of each material were scanned individually and discharged with compressed air (3 bar). Misses could be attributed to misrecognition or mechanical errors (e.g. different sliding speeds of the different types of material). These experiments were carried out at thresholds between the arbitrary units 10 and 100, with higher thresholds allowing larger deviations of the considered spectrum from the taught spectra for classification. Both the particle-related output (yield) and the number of correctly and incorrectly classified pixels were recorded.

Additional UV/VIS/NIR measurements were performed using a Lambda 950 ultraviolet (UV)/visible spectrum(VIS)/NIR spectrometer with integrating sphere (Perkin Elmer, Waltham, USA). Spectra were recorded from 250 to 2500 nm in 5 nm steps. The Spectralon-coated Ulbricht sphere had a diameter of 15 cm. Hemispherical as well as diffuse transmittance and reflectance spectra were used to evaluate the effect of surface roughness (Figure 3).

Results and discussion

In this section, obtained results of the influence of water and surface roughness on the detected NIR spectra are presented and discussed, followed by an evaluation of this impact on the classification and yield.

Influence on the detected NIR spectra

Surface roughness. The influence of increased surface roughness can be summarised in three observations.

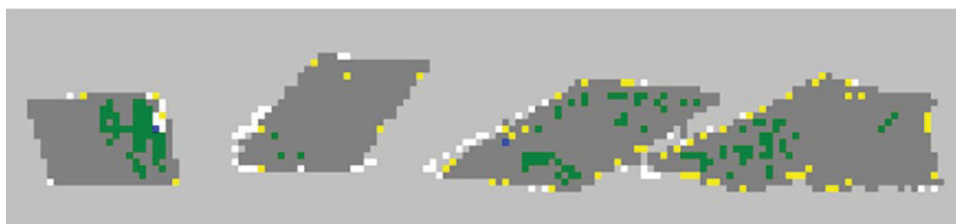


Figure 2. Correct classified HDPE particles (grey), including partially false classified pixels as PET (white) or LLDPE (green) and unknown pixels (yellow).



Figure 3. Measurement of direct, hemispheric and diffuse transmittance.

1. The intensity of the raw spectrum detected by the sensor is increased for all plastics except HDPE.
2. Extrema in the raw spectrum are amplified.
3. The spectral variation decreases owing to roughening of transparent particles.

A higher intensity of the detected raw spectrum is characterised by a better ‘spectral data basis’ per pixel. Owing to the higher amount of radiation detected per time interval, a better-founded set of spectra is created for each object pixel. This could also be proven in laboratory experiments, whereby the largest effect was observed with transparent plastics. Thus, the diffuse reflection of transparent PVC could be increased by almost 500%, while the direct reflection was reduced by 95%, from 5.9% to 0.3%.

The larger extremes in the raw spectrum, of for example PET, have the consequence that there are fewer fluctuations in the normalised derivative, relevant for the sorting decision (Figures 4 and 5). This relationship ensues from the fact that the normalisation of the spectrum is performed with respect to the absolute minimum and the absolute maximum of the spectrum. A raw spectrum, with a small difference between the absolute minimum and the absolute maximum, is stretched more than it is in the case of a large difference. Therefore, a smaller difference results in larger fluctuations in the derivative.

Surface moisture. Surface moisture has two different influences on the detected spectrum of the examined plastics.

1. Absorption of the reflected radiation starting from 1115 nm (HDPE, LLDPE, PET, PVC) or from 1230 nm (low density polyethylene (LDPE), polypropylene (PP), thermoplastic polyurethane (TPU)).
2. (Partial) smoothing of the raw spectrum.

Exemplarily, the PP spectra (with and without surface moisture) as well as the associated derived, smoothed and normalised

spectra are shown in Figure 6. It can be seen that the ‘raw spectrum wet’ has a generally lower intensity. From a wavelength of about 1230 nm on, the intensity of the spectrum continues to decrease in comparison with the ‘raw dry spectrum’. This is owing to the increased absorption of the radiation owing to surface water. Similar effects can be observed in food with high water contents. The strongest absorption of pure water samples is at 1400–1410 nm (Büning-Pfaue, 2003).

The increasing absorption of the radiation with increasing wavelength has the consequence that individual extremes in the derivative are formed stronger or weaker (see Figure 3: Ranges 1, 2 and 4). The larger the slope at the inflection point of the raw spectrum in the marked areas, the stronger the corresponding extremum which is formed in the derivative. As a result, the extremum at 1360 nm (Point A) no longer represents the absolute minimum, as it is the case with the ‘derivative normalised dry’, but the extremum at 1140 nm (Point B). Thus, a reduction of the minimum at 1360 nm takes place during normalisation.

In addition, in ‘Range 3’, a smoothing of the raw spectrum owing to the influence of water can be observed. As a consequence, the extrema of ‘derivative normalised wet’ are attenuated in comparison with the ‘derivative normalised dry’.

Influence on classification and yield

In order to investigate these results with regard to their significance for the sorting, the influence on classification and yield of both types of contamination were examined.

Surface roughness. The following observations concerning the influence of surface roughness were made.

1. Neither the classification nor the output of most plastics is significantly affected (exceptions: TPU and LDPE_red/white).
2. The number of detected object pixels of the PVC and PET particles has increased.

Since the influence of surface roughness hardly changes the raw spectrum of most plastics, the influence on the classification is very low. Only the classification and yield of transparent plastics (PET and PVC) at low thresholds (≤ 30) is improved, as the fluctuation ranges of the derived spectra are significantly reduced. Relevance for sorting therefore exists primarily if such materials need to be distinguished from materials that generate a coinciding

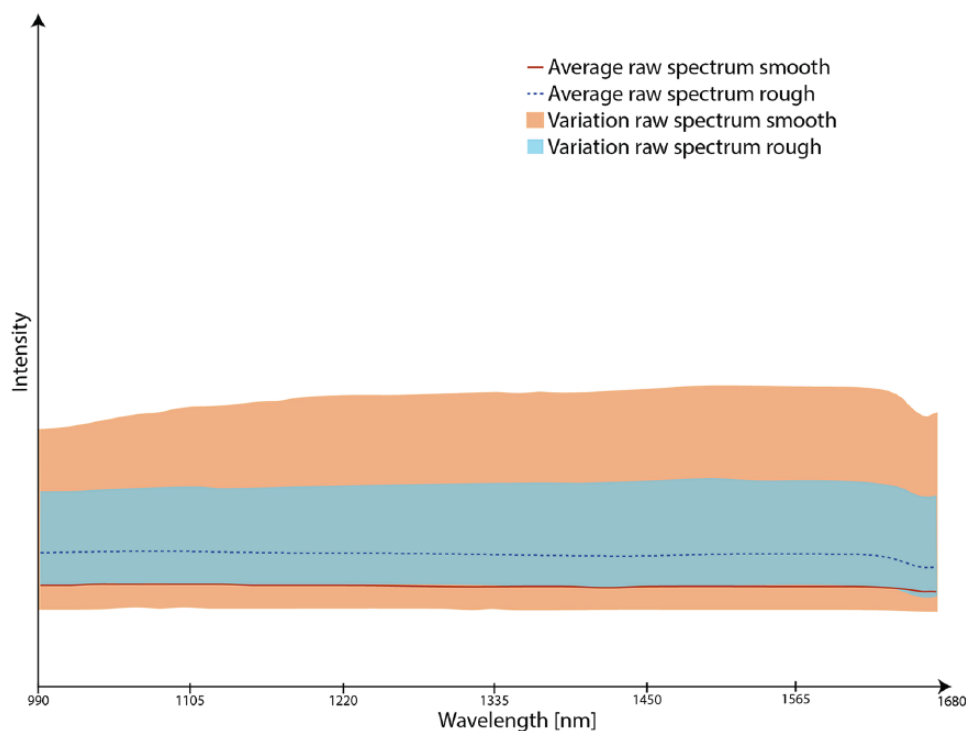


Figure 4. Average raw spectra and variations of PET spectra, rough and smooth in comparison.

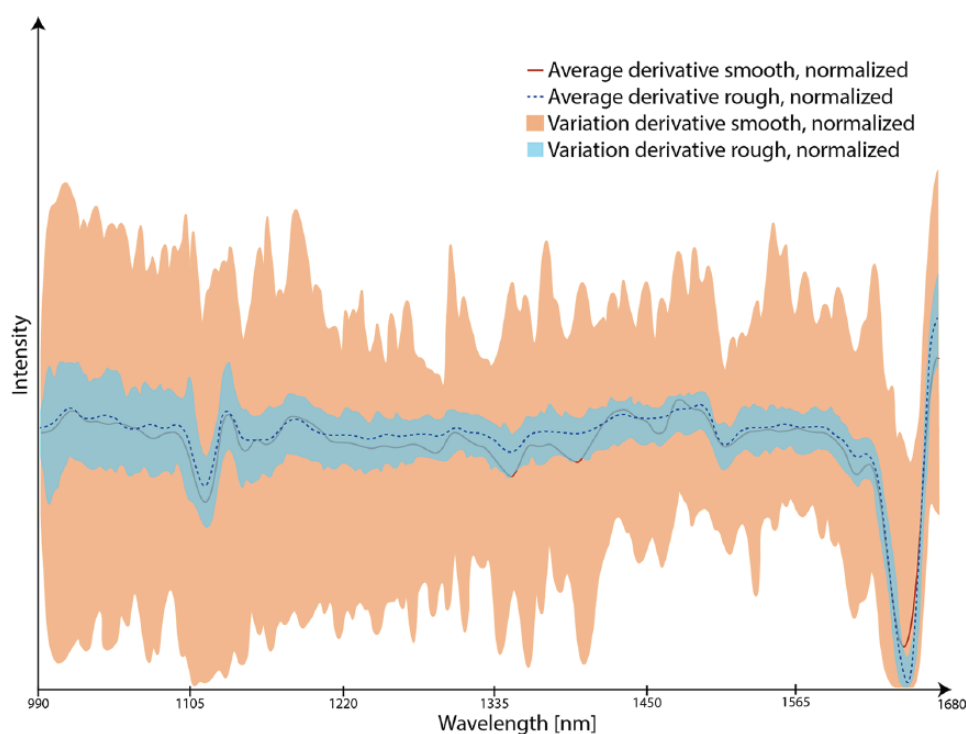


Figure 5. Average derivatives and variations of PET spectra, rough and smooth in comparison.

NIR spectrum, for example when differentiating between different types of PET.

In contrast, the results for roughened TPU and LDPE_red/white are impaired. The reduced yield of TPU particles is caused by two main factors: First, the misrecognition of roughened TPU pixels as PP is above a threshold of 30 at about 8.3% (rough)

instead of 1.0% (smooth). As a consequence, the maximum yield is reduced from 99.2% to 94.7% (Figure 7).

Second, it has been observed that the yield of TPU is temperature dependent. The surface of the chute (see Figure 1) was heated up to 58 °C by the infrared radiation. In the course of this warming, despite the constant recognition of the correctness of

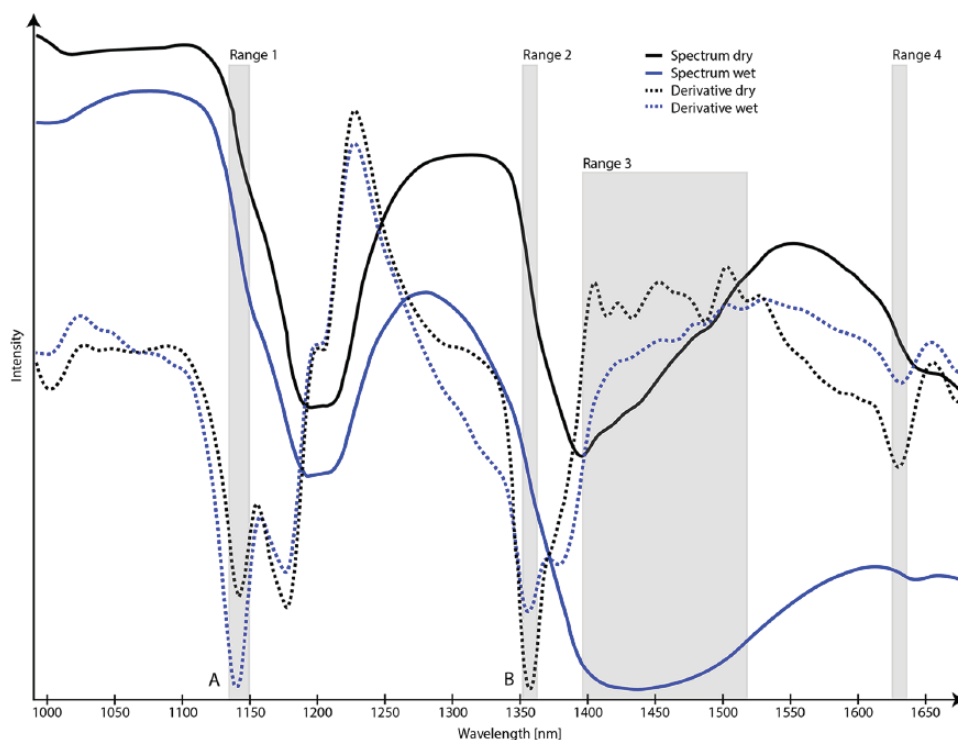


Figure 6. Comparison of raw spectrum and derivative (smoothed and normalised) of the PP spectrum with and without water influence.

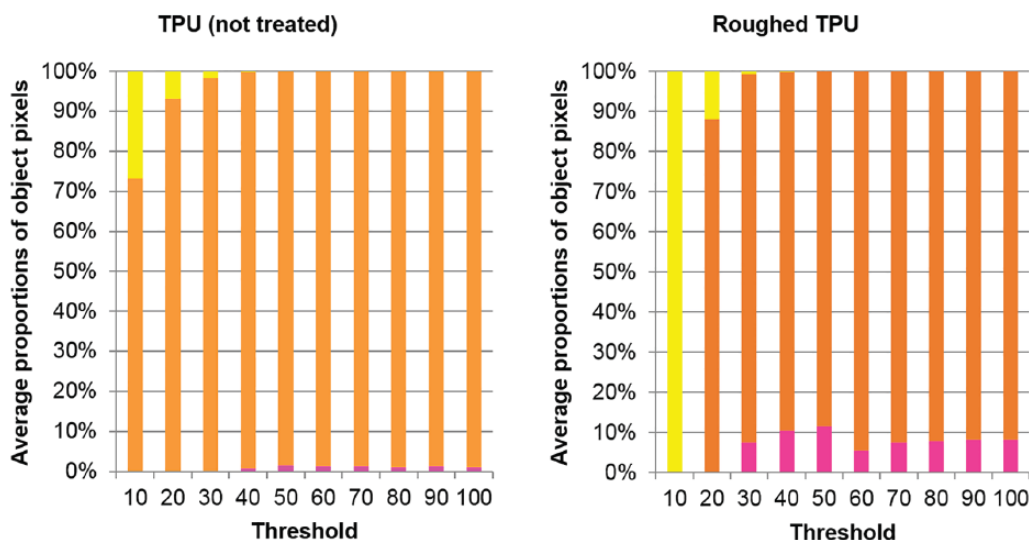


Figure 7. Average proportions of object pixels: TPU (orange), PP (pink) and unknown (yellow).

the TPU pixels, the yield dropped from approximately 96% to 71%. One explanation for this issue may be the low softening temperature of TPU; that is, the plastic fibres produced by the roughening on the object surface of the TPU particles can heat up faster and thus melt on the contact surfaces to the chute, so that higher adhesive forces between chute and TPU particles arise. This results in a non-uniform sliding speed and thus a reduced discharge of the roughened TPU particles.

Another effect of roughening the particles occurs in the distinction between LDPE_red and LDPE_white. The roughened LDPE_red particles show a slight shift in the derivative. This

change means that fewer object pixels are recognised correctly. This reduces the yield from 76.7% to 44.7%.

The improved detection of the PVC object pixels (138%) and PET particles (64%) is owing to the higher intensity of the reflected raw spectrum after roughening the surface, owing to dispersive radiation. With smooth PVC/PET particles, a distinction of the objects from the background might be problematic. Therefore, object pixels of particles with a roughened surface are rather classified as the material than as background. This effect has also been proven: In an additional experiment with a smooth PVC particle, only 2% of the reflected radiation measured as

diffusely reflected radiation. Using a roughened PVC particle, the diffuse share was 8%.

Surface moisture. The extent of the influence of surface moisture on the classification and yield depends on two factors.

1. Share of the object surface that is wetted.
2. Influence of the water layer on the reflected spectrum.

The larger the wetted surface of an object, the more object pixels can be misclassified by spectral changes. This is significantly influenced by the hydrophobic/hydrophilic properties and shape of the material. Whether this misclassification takes place, depends on how strong the influence of water is on the respective spectrum and how different the spectra of materials to be distinguished are. The average share of object pixels that is incorrectly classified can be found in Table 3.

It can be stated that most of the plastics (HDPE, PET, TPU, PVC) are partially misidentified as PP owing to the influence of water and thus classified worse overall. Exceptions are LLDPE, as well as LDPE_red and LDPE_white. As one can see in Figure 8, the effects of a moistened surface is restricted to the areas of accrued water drops. The remaining surface is correctly classified.

LLDPE was misidentified as both PP and HDPE by the influence of water. Again, the number of correctly recognised object pixels has dropped significantly. The only type of plastic whose number of correctly recognised object pixels has been improved by the water entry is LDPE_red (Table 3). It should be noted, however, that the correct recognition of the LDPE_white pixels has decreased accordingly.

Table 3. Average share of incorrectly classified pixels that can be traced back to the influence of water.

Material type	Pixel losses owing to water influence
HDPE	1.20%
LDPE_Red	-7.38%
LDPE_White	5.60%
LLDPE	2.26%
PET	10.27%
PP	0.87%
PVC	5.28%
TPU	6.66%

The yield of the investigated types of plastic has usually been reduced by the introduction of water. Exceptions are the plastics PET, LDPE_red and PVC. The improved yield of PET is owing to the shape of the test pieces. Since bent, thin-walled PET parts were used, the trials with dry material showed an average maximum yield of about 72%. This comparatively low yield is owing to uneven slippage and soaring of the particles. Wetting with water increased the particle weight of the PET objects and allowed a smoother sliding of the particles. This explains the improved yield.

The increased LDPE_red output can be explained by the higher correct classification of object pixels. The improved PVC yield owing to water entry is in contradiction to the deteriorated classification of the PVC object pixels. A possible explanation for this might be the reuse of the same particles for the experiments with dry material, while more particles had to be used for the experiments on water influence, so that a drying of the objects already used could be ensured. It can be expected that the repeated use of the dry PVC particles has led to a steady heating of the PVC parts, which promotes a more uneven sliding, explaining the reduced yield on the used chute sorter.

Implications on overall waste management

The increasing demand for recycling and the resulting ongoing propagation of sensor-based sorting machines in waste treatment and sorting plants reveal the relevance of this technology. Especially NIR technology is used to separate plastic types (Gundupalli et al. 2016), enabling, for example, material recycling and the production of refuse-derived fuels.

Common problems in such sorting steps occur in the form of false classification of plastics owing to the influence of external factors (e.g. defilements, such as surface water and roughness), resulting in potentially reduced recovery rates and quality reduction of products (Gundupalli et al., 2016). To identify such potentially problematic sorting tasks and to subsequently counteract occurring undesired effects, underlying algorithms for sorting have to be adapted.

This study provides insights into the effects of two common influencing factors (surface moisture and surface roughness) on sorting steps in waste sorting plants. By studying specific spectral

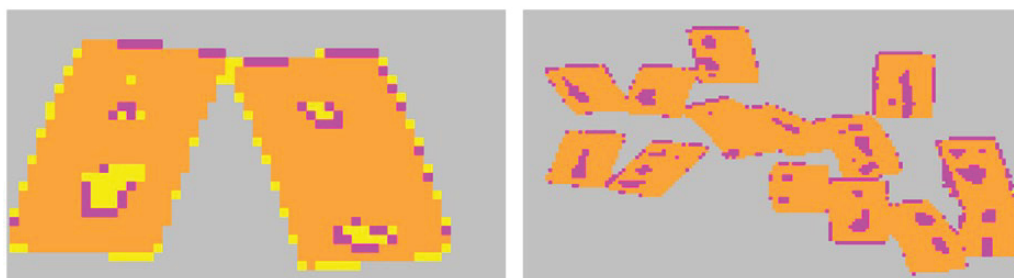


Figure 8. Misclassification of object pixels owing to water drops on TPU particles (orange): PP (pink) and unknown (yellow).

changes (in the derivatives), caused by wetting and roughening of the surface of the investigated particles, a deeper understanding of their effects with regards to application-oriented sorting algorithms can be gained. Our results show that the influence of water in obtained spectra is limited to specific wavelength ranges (1115–1680 nm or 1230–1680 nm). The given findings can be used to correctly classify defiled materials whose characteristic peaks are present in the ranges.

Furthermore, obtained knowledge may be used to indirectly improve sorting rates by changing material properties via implementing mechanical processing steps prior to sorting. Roughening of the material surface increases the amount of disperse-reflected radiation, which reduces the background noise in the derivative of the spectrum, used for the classification. By choosing the appropriate technology, for example, during shredding, a roughening of the surface can be enhanced, resulting in a raised sorting efficiency.

By following this differentiated approach for sensor-based sorting, this technology can be applied more efficiently, which improves product qualities and reduces material losses.

Conclusion and outlook

In summary, the following conclusions can be drawn from the experiments carried out.

- Higher surface roughness results in more diffusely reflected radiation, providing more raw data for processing the near-infrared spectrum.
- Increased surface roughness makes extremes in the raw spectrum more prominent, reducing signal noise in the lead, especially in the signal evaluation of clear plastic resulting in reduced spectral variation in the normalised derivative.
- The surface roughness has mostly a small influence on the classification of plastics, as long as no spectrally similar (LDPE grades or similar) or transparent material is detected and classified.
- Increased surface roughness reduces the yield of low-softening plastics on chute sorters because the sliding speed of these plastics varies as a result of the heating of the chute.
- Surface moisture causes the absorption of radiation from 1115 nm (HDPE, LLDPE, PET, PVC) or from 1230 nm (LDPE, PP, TPU) up to at least 1680 nm, which causes amplification or attenuation of various extremes in the derivative.
- Surface moisture causes at least partial smoothing of the raw spectrum, which reduces extremes in the relevant derivative of the spectrum for the evaluation.
- The influence of surface moisture on the yield of plastics is usually very low and dependent on the spectral differences between the different plastics.

By implementing the obtained information in existing or new sorting algorithms, the influence of surface water and surface

roughness could be reduced significantly or used to an advantage. The examined topics show potential for further studies to generate a deeper understanding of, for example, the role of polarisation effects and distinctive interactions of moisture or roughness and edge effects on incorrect classification. This could be especially valuable information for sorting of material with small particle sizes, showing higher proportions of edge pixels.

Declaration of conflicting interests

The authors declared no potential conflicts of interest with respect to the research, authorship, and/or publication of this article.

Funding

The authors disclosed receipt of the following financial support for the research, authorship, and/or publication of this article: The project NEW-MINE has received funding from the European Union's EU Framework Programme for Research and Innovation Horizon 2020 under Grant Agreement No 721185.

ORCID iD

Bastian Küppers  <https://orcid.org/0000-0002-0367-4786>

References

- Blanco M and Villarroya I (2002) NIR spectroscopy: A rapid-response analytical tool. *Trends in Analytical Chemistry* 4: 240–250.
- Büning-Pfaue H (2003) Analysis of water in food by near infrared spectroscopy. *Food Chemistry* 82: S107–115.
- Eccher-Zerbini P (2005) Emerging technologies for non-destructive quality evaluation of fruit. *Journal of Fruit and Ornamental Plant Research* 14: 12–22.
- Gschaider HJ and Huber R (2008) Neue Entwicklungen in der optischen Sortierung. *Berg- und Hüttenmännische Monatshefte* 153: 217–220.
- Gundupalli SP, Hait S and Thakur A (2016) A review on automated sorting of source-separated municipal solid waste for recycling. *Waste Management* 60: 56–74.
- Huang H, Yu H, Xu H, et al. (2008) Near infrared spectroscopy for on/in-line monitoring of quality in foods and beverages: A review. *Journal of Food Engineering* 87: S303–313.
- Maul A and Pretz T (2016) Landfill mining from the processing perspective – a view on mass balance and output streams. In: Proceedings of 3rd International Symposium on Enhanced Landfill Mining, 8–10 February 2016, Lisbon.
- Mesina MB, de Jong TPT and Dalmijn WL (2006) Automatic sorting of scrap metals with a combined electromagnetic and dual energy X-ray transmission sensor. *International Journal of Mineral Processing* 82: 222–232.
- Pretz T and Julius J (2008) Stand der Technik und Entwicklung bei der berührungslosen Sortierung von Abfällen. *Österreichischer Wasser- und Abfallwirtschaftsverband* 60: 105–112.
- Schug H, Eickenbusch H, Marscheider-Weidemann F, et al. (2007) Zukunftsmarkt Stofferkennung und -trennung; Fallstudie im Auftrag des Umweltbundesamtes im Rahmen des Forschungsprojektes Innovative Umweltpolitik in wichtigen Handlungsfeldern Available at: <https://www.umweltbundesamt.de/sites/default/files/medien/publikation/long/3456.pdf>.
- Vujić G, Jovičić N, Redžić N, et al. (2010) A fast method for the analysis of municipal solid waste in developing countries – case study of Serbia. *Environmental Engineering and Management Journal* 9(8): 1021–1029.
- Wotruba H and Harbeck H (2010) Sensor-based sorting. In: *Ullmann's Encyclopedia of Industrial Chemistry*, Wiley-VCH Verlag GmbH & Co. KGaA. DOI: 10.1002/14356007.

5 PUBLICATION 4

Influences and consequences of mechanical delabelling on PET recycling

Küppers B, Chen X, Seidler I, Friedrich K, Raulf K, Pretz T, Feil A, Pomberger R, Vollprecht D (2019) INFLUENCES AND CONSEQUENCES OF MECHANICAL DELABELLING ON PET RECYCLING. Detritus Volume 06: 39-46. Doi: 10.31025/2611-4135/2018.13664

Annotation on my own contribution to publication 4:

I primarily designed and planned the experiments, which this publication is based on. The experiments consisted of sampling the input material for the delabelling tests, performing, monitoring and analysing the experiments and the output fractions. The experiments were jointly conducted by Irina Seidler, Karl Friedrich and me. Xiaozheng Chen, Irina Seidler, Karl Friedrich and Daniel Vollprecht provided a meaningful contribution to my analysis of the results. I received guidance of Karoline Raulf, Thomas Pretz and Alexander Feil and support from Xiaozheng Chen while writing the publication. I revised the publication, which was reviewed by all co-authors.

INFLUENCES AND CONSEQUENCES OF MECHANICAL DELABELLING ON PET RECYCLING

Bastian Küppers^{1,*}, Xiaozheng Chen², Irina Seidler¹, Karl Friedrich¹, Karoline Raulf², Thomas Pretz², Alexander Feil², Roland Pomberger¹ and Daniel Vollprecht¹

¹ Montanuniversitaet Leoben, Chair of Waste Processing Technology and Waste Management, Austria

² Rheinisch Westfälische Technische Hochschule Aachen, Department of Processing and Recycling, Germany

Article Info:

Received:
17 January 2019
Revised:
26 April 2019
Accepted:
3 May 2019
Available online:
24 May 2019

Keywords:

PET recycling
Sensor-based sorting
Label
Roughness
NIR Spectroscopy

ABSTRACT

The recycling of polyethylene terephthalate (PET) is an important issue of today's society. Mechanical recycling makes more sense from an ecological point of view than chemical PET recycling. However, mechanical recycling still is highly susceptible to defilements. Therefore, intensive pre-treatment is necessary to ensure the mechanical production of high-quality recycled PET. An important step in this process is to separate the PET bottles from their labels/sleeves. For this purpose, a newly developed label remover was studied. In this study, it was found that the machine had a delabelling efficiency of 90 w%. The PET bottles that were not sufficiently delabelled (10 wt.%) on average had a significantly smaller bottle size. This means that a sharp screening step, prior to delabelling, could improve the delabelling efficiency furthermore. Additionally, the applicability of near-infrared sorting technology was tested to find out, whether it can be used for quality control. Tests showed that state-of-the-art technology could differentiate between labelled and delabelled PET bottles, enabling separation of labelled PET bottles from delabelled bottles via sensor-based sorting. Hence, the proportion of contaminated PET bottles could be reduced furthermore with additional processing steps.

1. INTRODUCTION

Polyethylene terephthalate (PET) is one of the most common and prevalent thermoplastic polymers in today's society. It is used for the production of beverage bottles, fibres, moldings, sheets and other packaging material. Especially its worldwide usage as a container for beverages can be explained by the, in comparison to other plastic types, superior properties such as chemical, physical, mechanical, oxygen and carbon dioxide barrier features. The high clarity of PET constitutes a major advantage in comparison to many other packaging polymers. These properties contributed to the increased consumption of PET since the 1950s (Shen et al., 2010; Burat et al., 2009; Welle, 2011).

Due to the high quantities of PET bottles, this material presents a significant amount of today's waste. Since PET is not degradable under normal conditions and therefore occurs in aged waste excavated during landfill mining, expensive procedures would be needed in order to degrade PET biologically. In contrast, recycling processes constitute a relatively cost-effective method to reduce landfilling or incineration of PET waste. Therefore, its recycling is driven forward constantly (Awaja and Pavel, 2005).

Usually for recycling, first, mechanical pre-processing

steps are applied to generate PET flakes that can be recycled chemically via depolymerisation or mechanically via extrusion. Chemical recycling offers the advantage that the recycled PET (RPET) has better properties than mechanically recycled PET, enabling a wide-ranging variety of possible applications. These superior properties come at the cost of a worse environmental profile of the chemical recycling process. During this process, the PET polymer is stripped down into monomers or oligomers using depolymerisation, resulting in an economically inferior process (Shen et al., 2010).

To receive better product qualities of mechanically manufactured recycled PET (RPET), the quality of their PET flakes must be improved. One of the main influencing factors on quality is the number of contaminants that enter RPET. These contaminants can be reduced by sorting out other materials, such as polyethylene (PE), polypropylene (PP) as well as metals. In order to separate PE and PP that are used for labels and sleeves from PET, pre-conditioning in form of delabelling can be necessary. (Awaja and Pavel, 2005).

Especially due to marketing requirements, labels and sleeves become more popular and their size is often in-

* Corresponding author:
Bastian Küppers
email: bastian.kueppers@unileoben.ac.at

creased for promotional actions like enhancing packaging decoration. The variety of labels used on PET bottles is significant. Mainly low-density polyethylene (LDPE) and/or polyvinyl chloride (PVC) labels are used. Nevertheless, also labels and sleeves made out of 2-phenylphenol, polypropylene, and polystyrene can be found on the market. Such labels cannot only have an enormous effect on the quality of RPET but also affect the mechanical processing and sorting of PET bottles resulting in decreased machine efficiencies and recycling rates. If labels and sleeves are successfully removed from the PET bottles, they can be sold as by-products or be incinerated. The separation of labels/sleeves and bottles can also be accomplished by a washing process (Shen et al. 2010; Cotrep, 2012).

In this work, the separation efficiency of an innovative delabelling stage is tested and assessed at the pilot scale. Furthermore, its intelligent utilization in combination with sensor-based sorting machines is discussed. At last, the effects of the delabelling stage on the efficiency of downstream sensor-based sorting machines, applying near-infrared (NIR) technology, are studied.

2. PET RECYCLING - AN OVERVIEW

In order to recycle PET bottles, they have to be collected first. In Europe, this usually happens under schemes which follow the rule of producer responsibility. In some countries, PET bottles are collected within the household waste or via deposit-refund systems like in Germany. Either way, the collection of PET bottles is carried out on a local scale to transport the PET bottles to separation centres (Arena et al., 2003).

In waste separation centres, the bottles undergo several mechanical processing steps. Since the bottles often arrive in bales, a bale opener is used to disperse the bottles. Afterwards, either pre-washing or delabelling is necessary to remove labels and sleeves, enabling successful and efficient sorting of the bottles. In case of a washing step, an 80°C hot solution with 2% NaOH can be used. In the dry mechanical delabelling step, assessed in this study, mechanical friction is applied to tear the label or sleeve of the PET bottles (Awaja and Pavel, 2005).

The sorting of the material is often conducted via sensor-based sorting machines but can also be done manually. Magnetic and eddy current separators can be used to separate ferrous and non-ferrous metals. After separating undesirable materials and contaminants, the bottles can be sorted, e.g. according to their colour. At last the bottles are shredded into flakes, washed and have to be dried carefully. For the final washing step of the PET flakes, solvent washing with tetrachloroethylene is suitable. Since the minimization of the moisture content is most important to reduce hydrolytic degradation, the drying stage is essential after washing. Usually drying temperatures between 140 and 170°C, with a retention time between 3 and 7 hours are chosen in order to reach < 50 ppm water in PET flakes. To ensure the required purity of the PET flakes, a sensor-based sorting step might be necessary (Shen et al., 2010; Kranert, 2017; Awaja and Pavel, 2005; Assadi et al., 2004).

In this way, about 75 w.% of the baled PET bottles are

processed to PET flakes and can be used for mechanical or chemical recycling. Losses occur during mechanical treatment, e.g. in the form of defilements, plastic and paper labels/sleeves, PE-/PP-caps and metals. 11-14 w.% of these fractions can be sold as by-products (PE caps, PVC/LDPE sleeves, etc.) while 14-18 w.% resemble solid waste and have to be treated furthermore (Shen et al., 2010).

The described mechanical pre-processing steps are necessary to prepare the PET for its further processing. Especially the quality characteristics of PET flakes must be achieved to ensure successful mechanical recycling. In Table 1, the minimum requirements for RPET flakes are given.

The degradation of RPET is increased by contaminants such as polyolefins or PVC, causing a reduction of the molecular weight and intrinsic viscosity of PET. This leads to a deterioration of the RPET properties. Reinforcing fillers and toughening modifiers then have to be applied to counteract the drop in molecular weight. (Srithep et al., 2011; Awaja and Pavel, 2005)

Once the minimum requirements for RPET flakes are met, they can be converted to granules or finished products at 280°C via melt extrusion. In comparison to chemical recycling, extrusion is a relatively simple, environmentally friendly and cost-effective process. However, to reduce the main disadvantage of mechanical recycling (reduction of molecular weight), mechanical processing must be improved (Shen et al., 2010).

In accordance with the topic of this study, a special focus lies on the influence of labels and sleeves on the recycling process of PET bottles despite their negative impact on RPET quality. During the sorting stage, labels and sleeves often remain on the PET bottles and can end up in the PET stream as well as in the PE or waste stream. Depending on the type of plastic used for the labels/sleeves, their thickness and size, PET bottles might not be identified correctly as PET and could be sorted out wrongly as undesirables. In this case, the PET yield would be significantly decreased since e.g. all full-sleeve PET bottles might be lost. Because of this reduction of the PET yield Cotrep (the technical committee for recycling of plastic packaging in France) recommends the use of partial labels and sleeves (Cotrep, 2012).

PVC labels are classified as unfavourable because PVC has a significant negative impact on RPET. It decomposes

TABLE 1: Minimum requirements for post-consumer-PET flakes to be reprocessed (Awaja and Pavel).

Property	Value
Viscosity [η]	> 0.7 dl g ⁻¹
Melting point [T_m]	> 240°C
Water content	< 0.02 wt. %
Flake size	0.4 mm < D < 8 mm
Dye content	< 10 ppm
Yellowing index	< 20
Metal content	< 3 ppm
PVC content	< 50 ppm
Polyolefin content	< 10 ppm

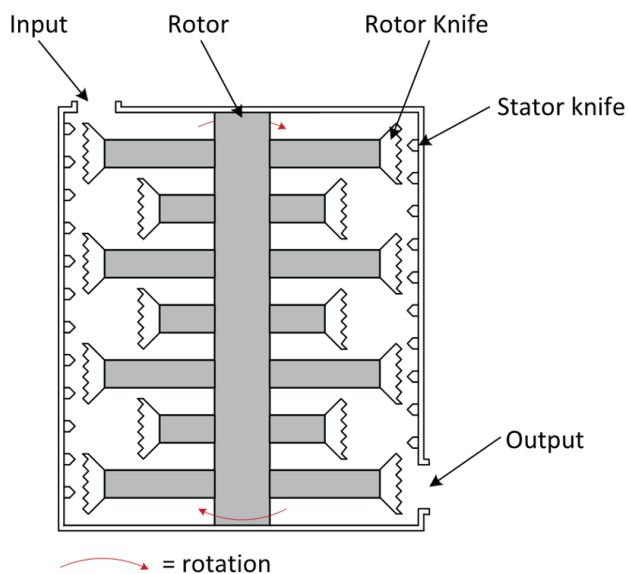
during extrusion, clogs extruder fillers and causes further quality problems. Hence, if a PVC flake is detected in the PET flake stream, the separation of PVC has to be ensured. For a singular separated PVC flake up to 100 flakes are ejected. Because of this, more losses are generated and the amount of waste to be disposed of is rising (Cotrep, 2012). Cotrep recommends that labels and sleeves that are made out of polystyrene (PS) and PET-G should be substituted because they tend to deteriorate, form impurities (PS) and create yellowing (PS and PET-G) in RPET. Shrink LDPE labels are classified as favourable since they do not disrupt the recycling process significantly (Cotrep, 2012).

3. MATERIAL AND METHODS

PET bottles from a public collection system were obtained as input material for the delabelling trials. To generate reliable data, only empty bottles with fully attached



FIGURE 1: Input material for delabelling trials - PET bottles from the public collection system.



labels were chosen for the trials. In total 98 kg of PET bottles with labels or sleeves were handpicked. An exemplary picture of the handpicked PET bottles is given in Figure 1. One can be seen that most of the bottles are deformed or crushed. The samples had a bulk density of around 50 kg/m³.

Delabelling trials were conducted with the “STADLER label remover” (max. throughput 8 t/h, dimensions 2,733 × 1,862 × 2,317 mm (L x W x H) stator diameter of 1,600 mm and drive power of 37 kW, rotor speed of 200 rpm) at the Stadler Technology Centre in Krško, Slovenia. As can be seen in Figure 2, the label remover is equipped with rotating arms that have jagged knives made from high-tensile steel. The length of these arms can be adjusted via slot holes. So, the distances between the knives on the rotating arms and the knives on the inner wall can be adjusted to fit the size of the input material. The general principle is that less space between the knives causes more delabelling at the risk of bottles being torn. Two types of knives are mounted to the inner wall:

- Vertically mounted knives
- Knives with an adjustable angle

The knives with adjustable angle enable the machine operator to modify the retention time of the input material: the more obtuse the angle, the longer the retention time.

For the trials, the input material was divided into two equally sized samples each weighing 49 kg. Two trials were run at a throughput of about 4 t/h. In the first and last seconds of each round, a continuous feed into the label remover could not be ensured. Particles at the beginning and the end of a round could falsify the results due to higher retention times. Therefore, only the delabelled product that was generated while a steady feed of the machine could be ensured was further studied. As a result of this approach, of the 49.0 kg input material per trial, 33.2 kg and 34.9 kg could be analysed respectively. It has to be mentioned, that



FIGURE 2: Scheme of the grinding chamber and picture of the “STADLER label remover”.

the separated labels were not weighed after the trials since too many of them would remain in the delabeller or be lost throughout the trials to make sufficiently sound conclusions.

To evaluate the influence of the delabelling process, samples were taken before as well as after the trials and screened with a laboratory polygonal drum sieve. These screenings were conducted at a mesh size of 80 mm for 90 seconds since this is the typical screening time of packaging material in a technical drum screen of 10 m length (Go et al., 2018). The mesh size of 80 mm was chosen because this screen cut is used industrially to enrich PET bottles in the coarse fraction. PET bottles with a volume of 0.5 l and less can be lost into the fines. Therefore, the number of bottles in the coarse and fine fraction provides information about the predominant bottle size in the screened sample and potential shredding effects of the delabeller. Additionally, the delabelled bottles were sorted manually after the trials and divided into three different categories:

- Good: > 98% of the labels/sleeves were separated from the respective bottles (sufficient)
- Middle: 90-98% of the labels/sleeves were separated from the respective bottles (sufficient)
- Bad: < 90% of the labels/sleeves were separated from the respective bottles (insufficient)

The allocation of the delabelled bottles to these three categories was carried out by manual separation after the trials. Bottles that ended up in category 1 either contained no label at all or only small label pieces at the joins. Category 2 mainly contains bottles with label pieces on the joins. Bottles in category 3 primarily showed labels that were ripped open or sleeves that were sliced in pieces but not separated from the bottle. After the delabelling trials, samples of each category were taken and a screening analysis was conducted with a mesh size of 80 mm.

Before and after the delabelling process, samples of bottles were taken for further investigations with NIR (near infrared) technology. For these analyses, a sensor-based sorting machine from Binder+Co AG, equipped with a hyperspectral imaging (HIS) NIR sensor from EVK (HELIOS NIR G2 320) with a wavelength range from 950 nm to 1700 nm was used. Pictures of the samples, taken before and after the delabelling trials, were captured to analyse the raw spectra of the samples and to classify the different materials contained in the samples using state of the art algorithms. These algorithms consist of the processing steps given in Table 2.

For a classification of each object pixel, the y-values of each spectral band (width of one band is approx. 3.2 nm)

TABLE 2: Preprocessing and spectral processing steps of spectra for classification.

Preprocessing	Spectral Processing
Spatial correction	1st Derivative
Bad pixel replacement	Normalization
Intensity Calibration	Smoothing
Noise suppression	

were compared with the material specific spectral information implemented in the algorithm. This way, each pixel can be provided with a false colour and less computing power for the evaluation of each particle is necessary. Hence, the classification of each bottle can be performed.

4. RESULTS AND DISCUSSION

The delabelling efficiency results from the composition of the output of the delabelling trials. The results are given in Table 3.

After visual inspection of the output, it could be found that about 90 wt.% of the bottles were delabelled sufficiently (60 wt.% Good, 30 wt.% Middle), meaning, the number of labels on PET bottles was reduced drastically. About 10 wt.% of the bottles were not delabelled successfully. The visual result can also be withdrawn from Figure 4.

An apparently large number of small bottles was sorted into category 3 (Figure 3). The visual observation can be confirmed with the results of the screening analyses presented in Figure 4. It can be seen, that compared to the

TABLE 3: Output composition - label remover.

	Good	Middle	Bad
Trial 1	62 wt. %	29 wt. %	9 wt. %
Trial 2	59 wt. %	33 wt. %	8 wt. %



FIGURE 3: Output fraction of the delabeller - from left to right: category 1 (Good), category 2 (Middle), category 3 (Bad).

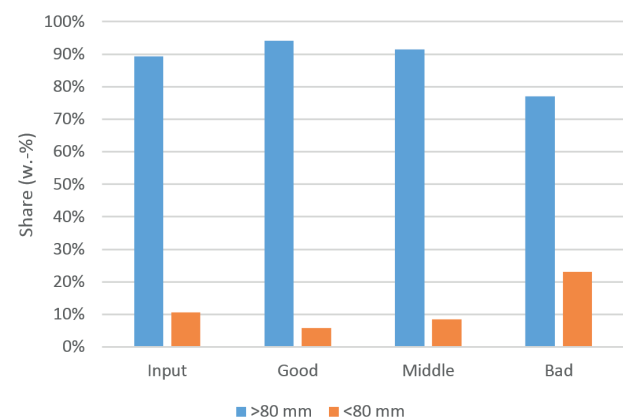


FIGURE 4: Results of screening analyses before and after delabelling.

input analysis, bottles in categories 1 and 2 (Good and Middle) show smaller amounts of material <80 mm (less than 10 wt.%) while category 3 contains more than 20 wt.% of bottles <80 mm.

It must be stated, that no shredded or compacted bottles were found. This suggests that most small bottles were delabelled insufficiently while most big bottles (>0.5 l) were processed successfully. The inverse conclusion of this is that a sieving step prior to the delabelling step would increase the efficiency of the delabeller furthermore, which is in accordance with findings of Go et al., 2018. Additionally, it must be mentioned that the input for the above-shown trials consisting of 100% labelled bottles is not the case in reality. This affects the quality of the output positively by increasing the percentage amount of label-free bottles in the output of the delabelling stage. Besides that, fully affixed paper labels underwent little to no change during the treatment. An example is given in Figure 5.

To determine the impact of labels and of the delabeller on the detection as well as classification of PET bottles, HSI NIR pictures of the bottles, prior and after delabelling, were taken. The different average spectra that were used to distinguish PET from PET covered with a label (PETL) and bottle caps are given in Figure 6. Significant differences between HDPE and the other spectra can be registered. To distinguish PET from PETL pixels, two different spectra for PETL had to be included due to variations concerning the intensity of the peaks, typical for PETL. Therefore, a



FIGURE 5: Impact of delabeller on the fully affixed paper label.

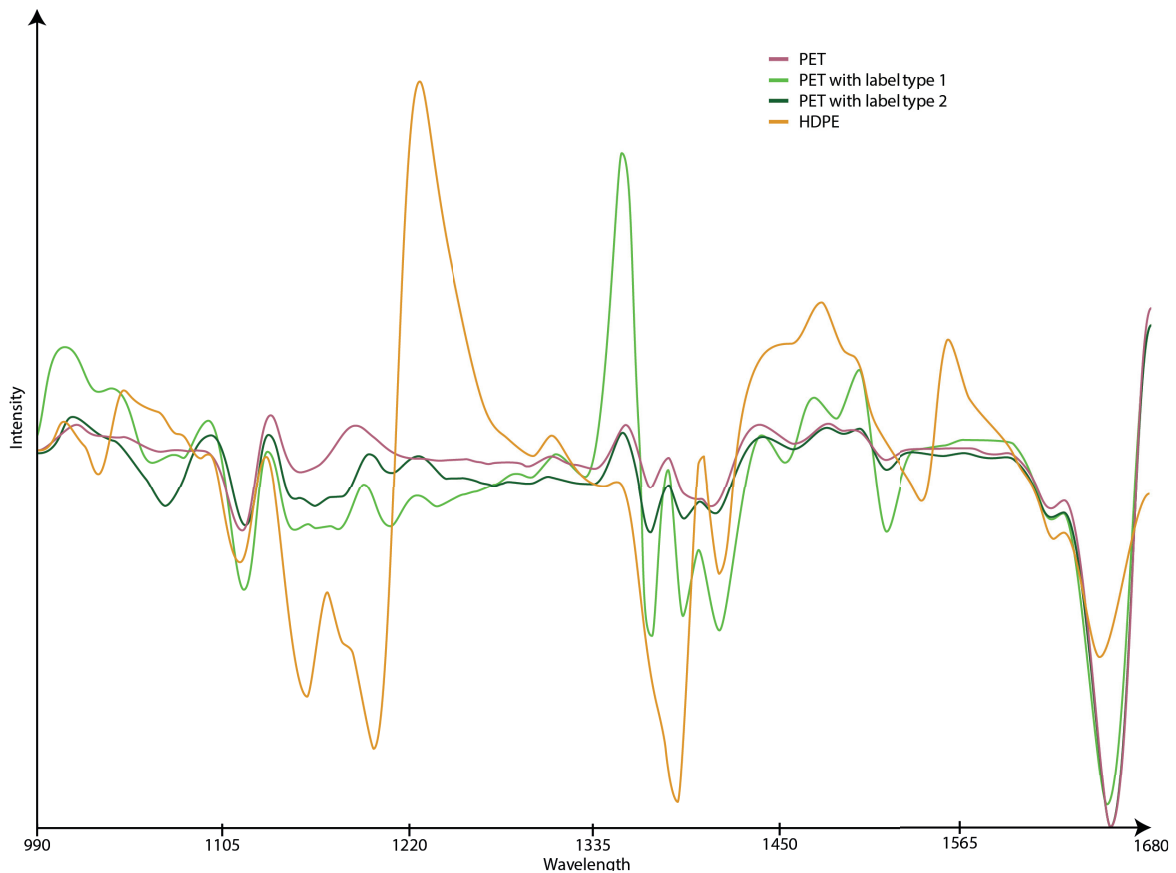


FIGURE 6: Qualitative spectral course (first derivative, normalized) of PET, PET with label type 1, PET with label type 2 and HDPE.

classifier with four different spectra was developed to distinguish between PET, PET with label and HDPE.

Examples for classified bottles are given in Figure 7. It can be seen that PET, HDPE and PETL can be distinguished from each other very well. It should be noted that even though some pixels of the fifth bottle were wrongly classified due to the influence of water, in this trial, all labelled bottles could be correctly classified as such.

To double-check the functionality of the created classifier, pictures of delabelled bottles were taken and classified as well. The result can be seen in Figure 8. All bottles are classified as not labelled PET and the caps (on bottles 1 and 4) are also correctly classified as HDPE. Only a few pixels on the edges of objects in Figure 7 and 8 are falsely classified as PETL due to edge effects. The amount of incorrectly classified pixels is insignificant and differentiation between PET bottles with and without labels can be expected.

Additionally, the extent of the PET spectrum before and after delabelling was analysed as well as the signal-to-noise ratio. In total 60,096 spectra were analysed for this purpose. The results are given in Figures 9 and 10. The spectra before and after delabelling are displayed. Apart from outliers (grey), it can be seen that 90% of the derived spectra (interquartile deviation) show significantly higher extents and marginally higher averaged standard devia-

tions after the delabelling process than before. Prior to delabelling, the characteristic and most important absorption for classification of PET at a wavelength of about 1650 nm is barely noticeable let alone smaller peaks, e.g. between 1110 nm and 1180 nm. This complicates the classification significantly because the spectra have to be normalized for consistent sorting efficiency, which results in enhanced background noise.

Despite the fact that correct classification before and after delabelling is possible, mechanical treatment during label removal simplifies the classification and therefore enhances sorting of PET bottles. The trials showed that the differentiation between labelled and delabelled PET bottles is possible. This can be used for processes aiming for high product purities by installing a downstream sensor-based sorting unit after the delabelling step. The downstream sensor-based sorting unit separates the remaining labelled PET bottles from the delabelled bottles to recirculate them as input for the delabelling step once again.

5. CONCLUSION

For mechanical recycling of PET bottles with the aim of high-quality RPET production, the reduction of defilements is of utmost importance. An important part of this process is the separation of the labels and sleeves from the PET

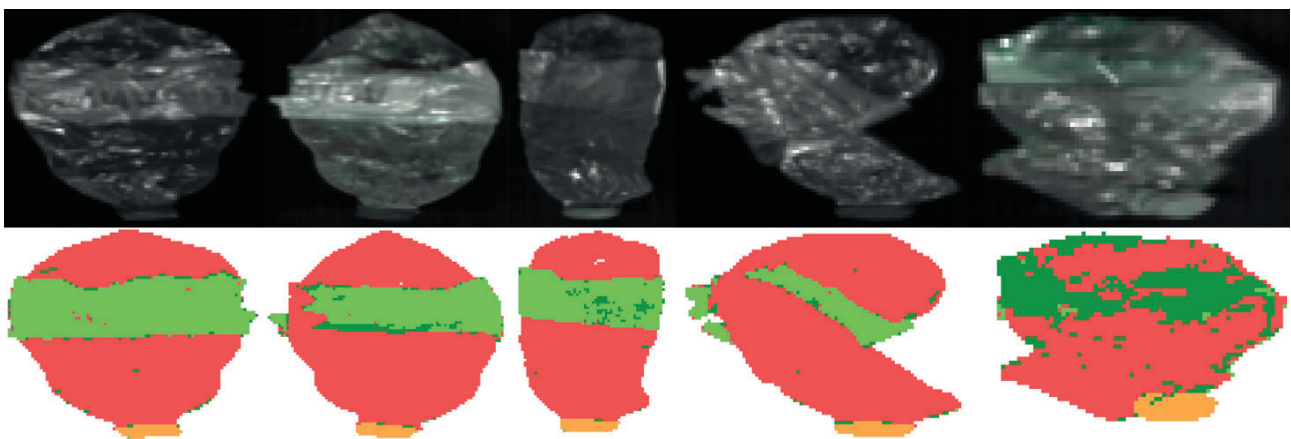


FIGURE 7: Comparison of live picture (upper row) and classified picture with false colours (lower row) of labelled PET bottles; red=PET, green=PETL, orange=HDPE.

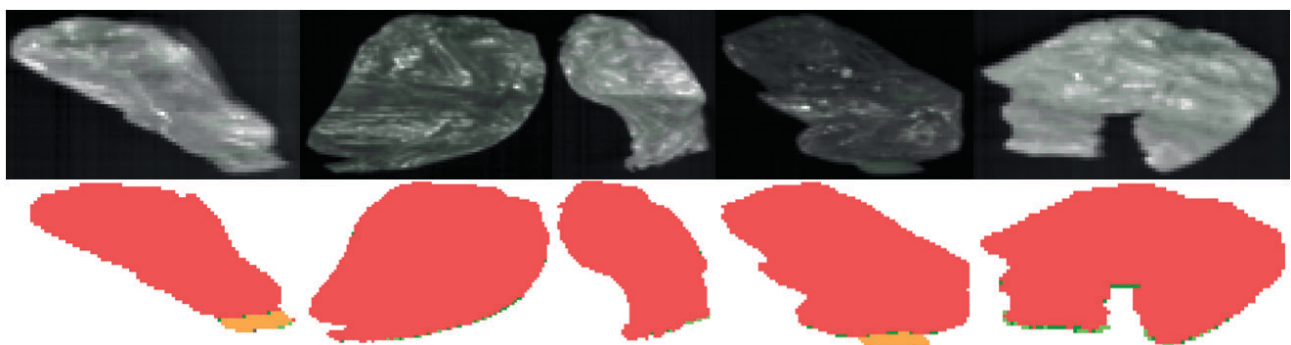


FIGURE 8: Comparison of live picture (upper row) and classified picture with false colours (lower row) of delabelled PET bottles; red=PET, green=PET with label, orange=HDPE.

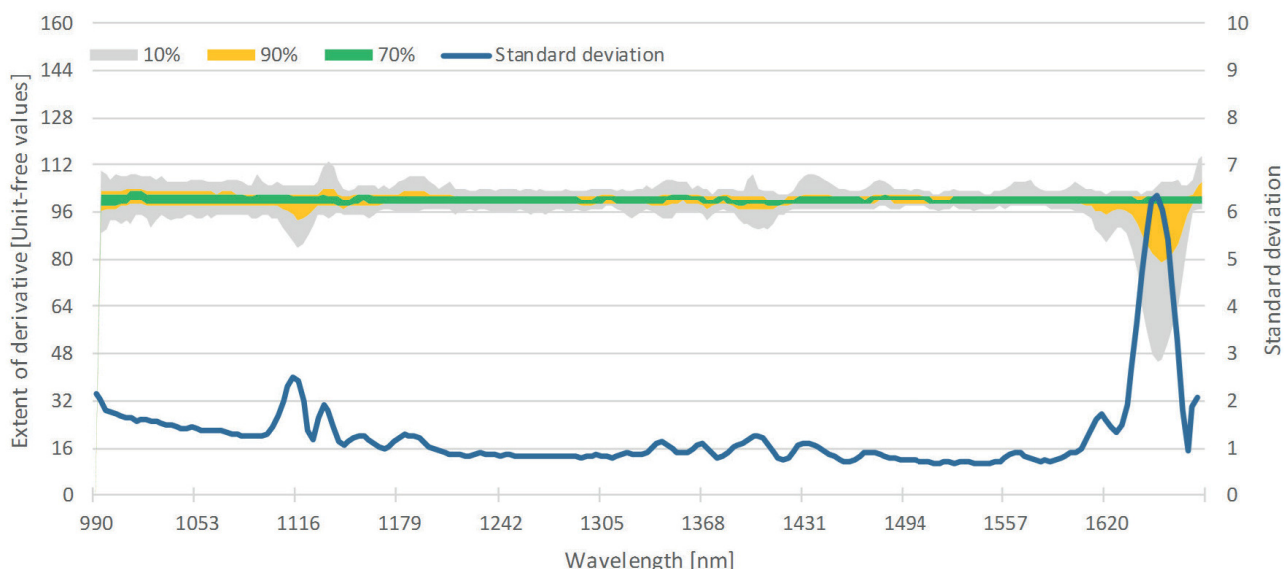


FIGURE 9: Interquartiles (90%, 70%) and outliers (10%) of derivatives basing on the raw spectra, recorded of PET pixels prior to delabelling (primary axis) and standard deviation of derivatives (secondary axis).

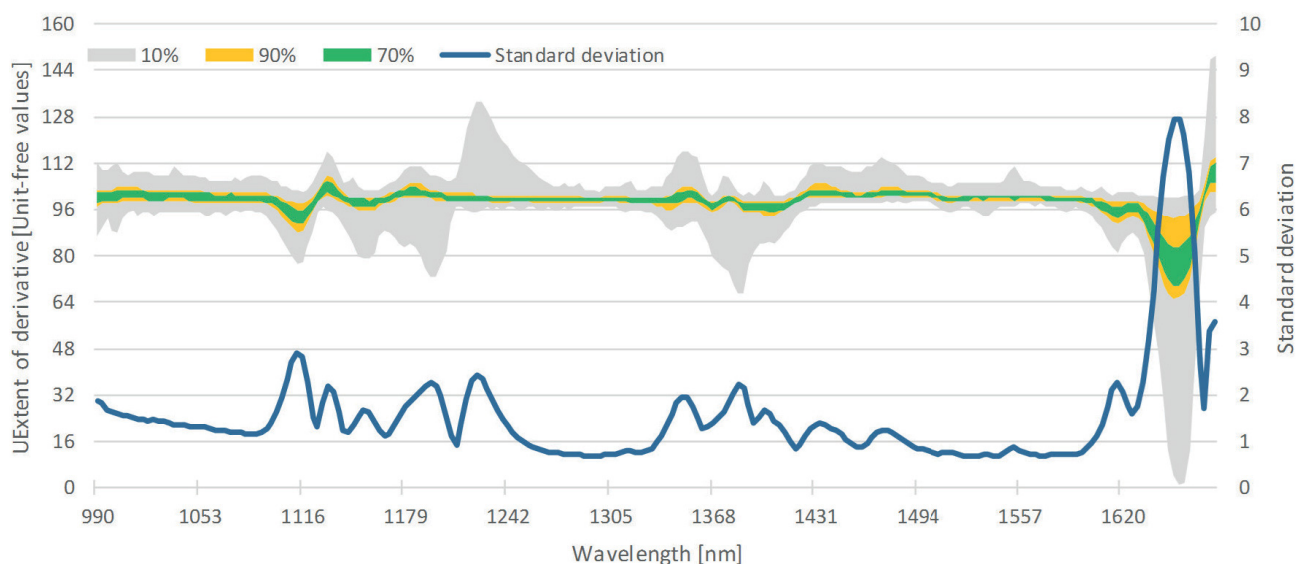


FIGURE 10: Interquartiles (90%, 70%) and outliers (10%) of derivatives basing on the raw spectra, recorded of PET pixels after delabelling (primary axis) and standard deviation of derivatives (secondary axis).

bottles. This can be achieved by the application of a mechanical delabelling step.

The studied “STADLER label remover” showed a delabelling efficiency of 90% at a throughput of about 4 t/h. It was found that the number of bottles unsuccessfully treated was strongly affected by the number of small bottles, <0.5 l filling volume. Therefore, in an industrial process, a screening step prior to delabelling would improve the efficiency of the delabeller furthermore.

Findings showed that the bottles were neither shredded nor significantly deformed during delabelling, enabling high efficiencies of downstream machinery, e.g. sensor-based sorting units. It was found that PET bottles with and without labels/sleeves could be classified and separated when applying HSI NIR technology. A sensor-based sorting unit

could be installed downstream a delabeller to sort out PET bottles still containing labels, improving the purity of the PET stream. Additionally, it was found that the mechanical treatment roughens the bottle surface, resulting in an enhanced peak extension and, consequently, improved PET bottle classification.

ACKNOWLEDGEMENTS

This research has been funded by the European Union’s Horizon 2020 research and innovation programme under the Marie Skłodowska-Curie grant agreement No. 721185 “NEW-MINE” (EU Training Network for Resource Recovery through Enhanced Landfill Mining; www.new-mine.eu). The authors wish to express their special gratitude to Renewi

Belgium SA/NV, Stadler Anlagenbau GmbH and the Department of Processing and Recycling (IAR) of the RWTH Aachen University for their straightforward collaboration and support.

REFERENCES

- Arena, U., Mastellone, M.L. and Perugini, F. (2003), "Life Cycle assessment of a plastic packaging recycling system", *The International Journal of Life Cycle Assessment*, Vol. 8 No. 2, pp. 92–98.
- Assadi, R., Colin, X. and Verdu, J. (2004), "Irreversible structural changes during PET recycling by extrusion", *Polymer*, Vol. 45 No. 13, pp. 4403–4412.
- Awaja, F. and Pavel, D. (2005), "Recycling of PET", *European Polymer Journal*, Vol. 41 No. 7, pp. 1453–1477.
- Burat, F., Güney, A. and Olgaç Kangal, M. (2009), "Selective separation of virgin and post-consumer polymers (PET and PVC) by flotation method", *Waste management (New York, N.Y.)*, Vol. 29 No. 6, pp. 1807–1813.
- Go, N., Thoden van Velzen, Eggo Ulphard, Althaus, M., Feil, A. and Pretz, T. (2018), "The influence of plastic packaging shape on recycling efficiency".
- Kranert, M. (2017), *Einführung in die Kreislaufwirtschaft*, Springer Fachmedien Wiesbaden, Wiesbaden.
- Shen, L., Worrell, E. and Patel, M.K. (2010), "Open-loop recycling. A LCA case study of PET bottle-to-fibre recycling", *Resources, Conservation and Recycling*, Vol. 55 No. 1, pp. 34–52.
- Srithep, Y., Javadi, A., Pilla, S., Turng, L.-S., Gong, S., Clemons, C. and Peng, J. (2011), "Processing and characterization of recycled poly(ethylene terephthalate) blends with chain extenders, thermoplastic elastomer, and/or poly(butylene adipate-co-terephthalate)", *Polymer Engineering & Science*, Vol. 51 No. 6, pp. 1023–1032.
- Cotrep (2012), "Bottles - PET and HDPE - general information on labels and sleeves - AG12", www.cotrep.fr/en/technical-study/
- Welle, F. (2011), "Twenty years of PET bottle to bottle recycling—An overview", *Resources, Conservation and Recycling*, Vol. 55 No. 11, pp. 865–875.

6 PUBLICATION 5

X-ray fluorescence sorting of non-ferrous metal fractions from municipal solid waste incineration bottom ash processing depending on particle surface properties

Pfandl K, Küppers B, Scheiber S, Stockinger G, Holzer J, Pomberger R, Antrekowitsch H, Vollprecht D (2019) X-ray fluorescence sorting of non-ferrous metal fractions from municipal solid waste incineration bottom ash processing depending on particle surface properties. Waste Management & Research 1-11. Doi: 10.1177/0734242X19879225

Annotation on my own contribution to publication 5:

The test series, on which this publication is based, was decisively designed by Kerstin Pfandl in consultation with me. Gerhard Stockinger provided the material for the experiments. Kerstin Pfandl conducted the test series with technical support of Johannes Holzer and me. The sampling of the output fractions from XRF-based sorting stages for subsequent analysis was conducted by Kerstin Pfandl. Stefanie Scheiber conducted the analyses. Kerstin Pfandl conducted the evaluation of the chemical and metallurgical analyses with support from Daniel Vollprecht and me. Kerstin Pfandl wrote the publication with assistance from Daniel Vollprecht and me. All co-authors reviewed the publication, which was revised by Kerstin Pfandl.

X-ray fluorescence sorting of non-ferrous metal fractions from municipal solid waste incineration bottom ash processing depending on particle surface properties

Waste Management & Research

1–11

© The Author(s) 2019

Article reuse guidelines:

sagepub.com/journals-permissions

DOI: 10.1177/0734242X19879225

journals.sagepub.com/home/wmr



Kerstin Pfandl¹ , Bastian Küppers¹ , Stefanie Scheiber²,
Gerhard Stockinger³, Johannes Holzer⁴, Roland Pomberger¹,
Helmut Antrekowitsch² and Daniel Vollprecht¹

Abstract

A heavy non-ferrous metal fraction (<50 mm) of municipal solid waste incineration bottom ashes from wet-mechanical treatment was separated by screening, magnetic separation and eddy-current separation into ferrous metals, non-ferrous metals and residual sub-fractions. The non-ferrous metal fractions were divided and subjected to (i) a washing process, (ii) dry abrasion and (iii) no mechanical pre-treatment to study the effect of resulting different surface properties on a subsequent X-ray fluorescence sorting into precious metals, zinc, copper, brass, stainless steel and a residual fraction. The qualities of the X-ray fluorescence output fractions were investigated by chemical analyses (precious metal fraction and the residual fraction), pyrometallurgical tests and subsequent chemical analyses of the metals and slags produced by the melting processes (zinc, copper, brass and stainless steel fraction). Screening directs brass and stainless steel primarily into the coarser fractions, while copper and residual elements were rather transferred into the finer fractions. X-ray fluorescence sorting yielded zinc, copper, brass, stainless steel and precious metals fractions in marketable qualities. Neither a negative nor a positive impact of mechanical pre-treatment on the composition of these fractions was identified. Solely the yield of the brass fraction in the grain size 16–20 mm decreased with increasing mechanical pre-treatment. The pre-treatment also had no impact on yield and quality of the products of pyrometallurgical tests.

Keywords

Bottom ash, X-ray fluorescence sorting, metal recovery, mechanical processing, surface properties, municipal solid waste incineration residues, metal recycling, heavy non-ferrous metals

Received 24th July 2019, accepted 5th September 2019 by Associate Editor Mario Grosso.

Introduction

The number of municipal solid waste incineration (MSWI) plants increases worldwide. Since 2015, more than 200 new plants with an overall annual capacity of more than 50 million tonnes have been put into operation. By the end of 2017, 2450 plants, with a capacity of 330 million tonnes per year, were operating, of which the majority (about 75%) are grate furnace plants, about 20% are fluidised bed plants and about 5% run on alternative technologies (ecoprog GmbH, 2018).

In grate furnace plants, between 150 and 250 kg MSWI bottom ash per tonne of input material are produced (Kranert and Cord-Landwehr, 2010). Normally, MSWI bottom ash is discharged via a water bath. The water content of wetly discharged bottom ash accounts for about 20 wt% (Simon and Holm, 2013). Bottom ash contains, besides (earth) alkaline metals, chlorides, silicates and sulphates, ferrous and non-ferrous metals and metal compounds. The mineral fraction adds up to 85–90 wt%, the

metals (scrap) 7–10 wt% and the residues (not or only partly combusted) 1–5 wt% (Gillner et al., 2011). The main constituents of the metal fraction are iron, aluminium, copper, brass and stainless steel (Bunge, 2016). Furthermore, bottom ash contains a number of critical raw materials according to the definition of the European Commission (2017), for example rare earth elements,

¹Chair of Waste Processing Technology and Waste Management (AVAW), Montanuniversität Leoben, Leoben, Austria

²Chair of Nonferrous Metallurgy (NEM), Montanuniversität Leoben, Leoben, Austria

³Brantner Gruppe GmbH, Krems an der Donau, Austria

⁴REDWAVE a division of BT-Wolfgang Binder GmbH, Eggersdorf bei Graz, Austria

Corresponding author:

Kerstin Pfandl, Chair of Waste Processing Technology and Waste Management (AVAW), Montanuniversität Leoben, Franz Josef-Str. 18, 8700 Leoben, Austria.

Email: kerstin.pfandl@unileoben.ac.at

antimony, vanadium, cobalt, gallium, tungsten, niobium, tantalum, beryllium, germanium, indium, rhodium, palladium, ruthenium (ordered according to the average contents) in MSWI ashes in descending order according to Pfandl et al. (2018), Allegrini et al. (2014), Bayuseno and Schmahl (2010), Funari et al. (2015), Johnson and Huter (2010), Jung and Osako (2007), BOKU (2010) and Zhang et al. (2001) and phosphorus (Pan et al. 2008; Wang et al. 2016). Although, copper and zinc are not defined as critical raw material, they have a high economic importance compared with other raw materials according to the European Commission (2017). Furthermore, zinc is considered as potentially critical raw material in Austria (Bundesministerium für Verkehr, Innovation und Technologie, 2018).

MSWI bottom ashes are mostly subjected to mechanical processing in order to recover at least the metals and partly also to recycle the mineral fraction. Although the composition of bottom ash is similar in different geographic regions, no two processing plants are identical. Even plants in the same region and accordingly with the same legislation often use different technologies, which suggests that there is still optimisation potential in bottom ash processing (Bunge, 2016).

According to Bunge (2014, 2016), the value of the potentially recoverable metals accounts for approximately €60 per tonne of bottom ash. Owing to increasing raw material prices, the separation of metals provides benefits not only from an environmental, but also from a financial point of view. Besides energy savings, compared with the mining of primary raw materials, the primary raw material consumption and accompanied waste generation during production can be reduced (Simon and Holm, 2013).

The processes for separation of metallic and mineral constituents of bottom ash are comparable with those that are used in mineral processing of primary raw materials. The disagglomeration of metal–mineral intergrowths (sintering) can be achieved by comminution, for example by impact mills (Simon and Holm, 2013). An alternative technology, which offers potential for further research, is electrodynamic fragmentation (Dittrich et al., 2016). The classification of bottom ash is conducted by using different screens, for example bar sizer, drum screen and flip-flop screen (Bunge, 2016). Ferrous metals are normally separated by magnetic separators of different design, non-ferrous metals by eddy-current separators (Gillner et al., 2011). In mechanical processing plants, jigs are used to enrich material groups based on density separation in different output flows (Pfandl et al., 2018). A dry-mechanical alternative to swim-sink-separation is density separation via X-ray transmission (XRT) (Gisbertz and Friedrich, 2015).

Sensor-based sorting is increasingly used for the sorting of non-ferrous metals (e.g. copper, brass, stainless steel). The potential suitability of X-ray fluorescence (XRF) sorting in bottom ash processing has been demonstrated several times (Gisbertz and Friedrich, 2015; Kollegger and Berghofer, 2017). XRF, though, is limited to the particle surface and especially for bottom ash processing, the influence of surface defilements must be considered (Gisbertz and Friedrich, 2015). These can be significantly

impacted by factors, such as mechanical stress during the processing steps. However, currently there is no meaningful scientific information on the influence of particle surface properties of bottom ash on the XRF sorting efficiency.

Thus, in this study, a set of experiments was conducted to investigate the impact of different mechanical treatment procedures and resulting particle surface properties on the XRF sorting efficiency. Obtained results serve as a basis for an optimised sorting and thereby may lead to an increased recycling of bottom ash.

Materials and methods

Waste origin and sampling

Among others, the company Brantner operates a wet-mechanical bottom ash processing plant that uses the Brantner Wet Slag (BWS) process, presented in Figure 1.

In the first step, oversized pieces are removed via pre-screening at mesh size 50 mm and subsequently magnetic constituents are separated by an overbelt magnet. The core aggregate of the BWS process is a jig that splits the bottom ash into four fractions: (1) a swimming fraction (e.g. plastics, paper and textiles), (2) a heavy non-ferrous (HNF) fraction (e.g. non-ferrous metals, precious metals and stainless steel), (3) a light fraction (e.g. minerals and aluminium) and (4) a sludge fraction. From the light fraction (3), an aluminium and a non-ferrous metals concentrate is produced by eddy current separation with previous magnetic separation of ferrous metals. The separation of the HNF metals in the grain size range 0.02–2 mm (5) is realised in the Fine Slag Treatment Plant (FSTP). The fractions ‘magnetic bottom ash’ and ‘bottom ash’, as well as the ‘sludge’ from jiggling, are currently landfilled.

Each year about 40,000 t of waste incineration bottom ash is processed in the BWS process. For the experiments, the HNF metals from the jig and the FSTP (grain size 0–50 mm; ~0.5 wt% of the plant input) were chosen as the sample material. Sampling was conducted based on ÖNORM S 2127 (Österreichisches Normungsinstitut, 2011) and yielded a sample weight of about 2 t.

The conducted work is summarised in Figure 2 and described in detail in the following.

Mechanical processing

To prepare the HNF metals 0–50 mm for XRF sorting, the sample was subdivided into grain sizes of 0–6.3 mm, 6.3–10 mm, 10–16 mm, 16–20 mm and 20–50 mm in batch mode using the following screen types and linings.

- Waste screen Type SM 800×2450 FV, IFE Aufbereitungstechnik GmbH, standard mesh, mesh size 20 mm;
- Waste screen Type SM 800×2450 FV, IFE Aufbereitungstechnik GmbH, finger screen lining, mesh size 16 mm;
- Flip-flop screen ST 800×3600 F, IFE Aufbereitungstechnik GmbH, screen mat, mesh size 10 mm.

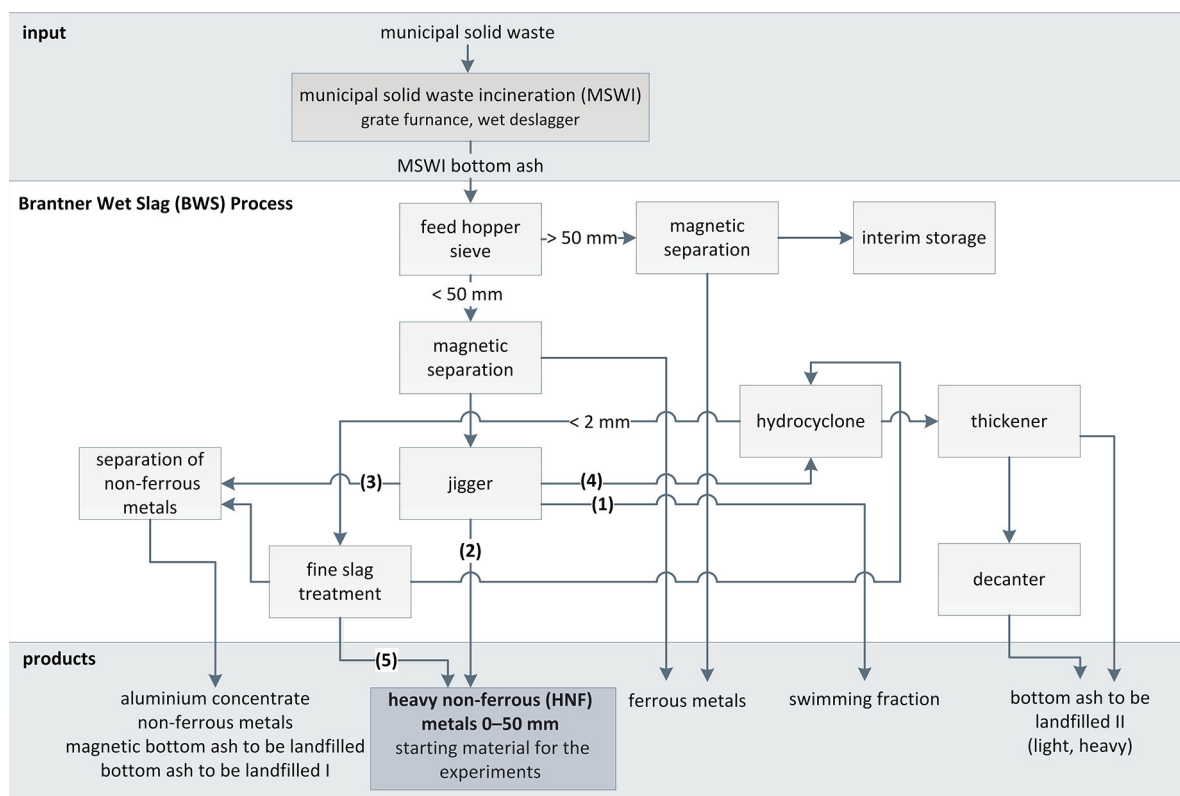


Figure 1. Brantner Wet Slag (BWS) process – modified and updated after Pfandl et al. (2018) and Stockinger (2016).

- Screen UE 500×1330 FSV LM645T, IFE Aufbereitungstechnik GmbH, screen lining, mesh size 6.3 mm.

Material feeding was conducted via feeding trays. Magnetic constituents of the produced grain size fractions 6.3–10 mm, 10–16 mm and 16–20 mm were separated using a drum magnet (HPG 500×650/13, barium ferrite magnets, brimming feeding), non-ferrous metals (NF fractions) by eddy current separation (INPXS 650×500/36). Owing to the grain size limits of the REDWAVE sorter used (see *XRF sorting*), the grain size fractions 0–6.3 mm and 20–50 mm were not further processed.

Surface pre-treatment

For the study of the influence of particle surface treatment on the XRF sorting result, the NF fractions 6.3–10 mm, 10–16 mm and 16–20 mm from mechanical processing were divided into three parts (i) surface treatment, dry, (ii) surface treatment, wet and (iii) no surface treatment. The pre-treatment was conducted batch-wise (maximum 80 kg) in a commercial concrete mixer (ATIKA BM 125 S). During dry-mechanical processing, the material remained in the mixer under continuous stirring for 20 min. For the wet-mechanical processing, 9 L water was added after 15 min of dry stirring. After a further 5 min of rotating, the water was discharged and another 9 L of water was added. The entire content of the drum was discharged and the water was collected separately.

XRF sorting

Altogether nine NF fractions (6.3–10 mm: (i) dry, (ii) wet, (ii) not pre-treated; 10–16 mm: (i) dry, (ii) wet, (ii) not pre-treated and 16–20 mm: (i) dry, (ii) wet, (ii) not pre-treated) with a total mass of 442 kg were sorted via XRF sorting in batch mode (REDWAVE 1350 XRF chute, sorting width 450 mm with X-ray tube and detectors). The material was discharged with 12 valves and 48 nozzles via compressed air.

Precious metals (gold, silver, palladium, platinum), zinc, copper and brass were separated as ejects subsequently in the respective order (positive sorting), namely the reject of the first run were fed again to the sorter and the subsequent eject was separated in the next run, etc. (first run: ejection of precious metals, reject fed again to the sorter, second run: ejection of copper, . . .). For the separation of a stainless steel fraction, the method of negative sorting was applied, namely all particles were ejected containing elements that are not allocated to the stainless steel fraction (last run). The working steps described above were repeated for the six NF fractions 10–16 mm and 16–20 mm. Owing to the small amounts of stainless steel present in the three NF fractions 6.3–10 mm (shown by previous analyses), only precious metals, zinc, copper and brass were separated from the fractions in this grain size range.

The detection of metals was conducted at the following energies of characteristic X-rays: copper: 8.05 keV; zinc: 8.64 keV; gold: 9.71 keV; silver: 22.16 keV; palladium: 21.18 keV; platinum: 9.44 keV. The following minimum contents constitute the

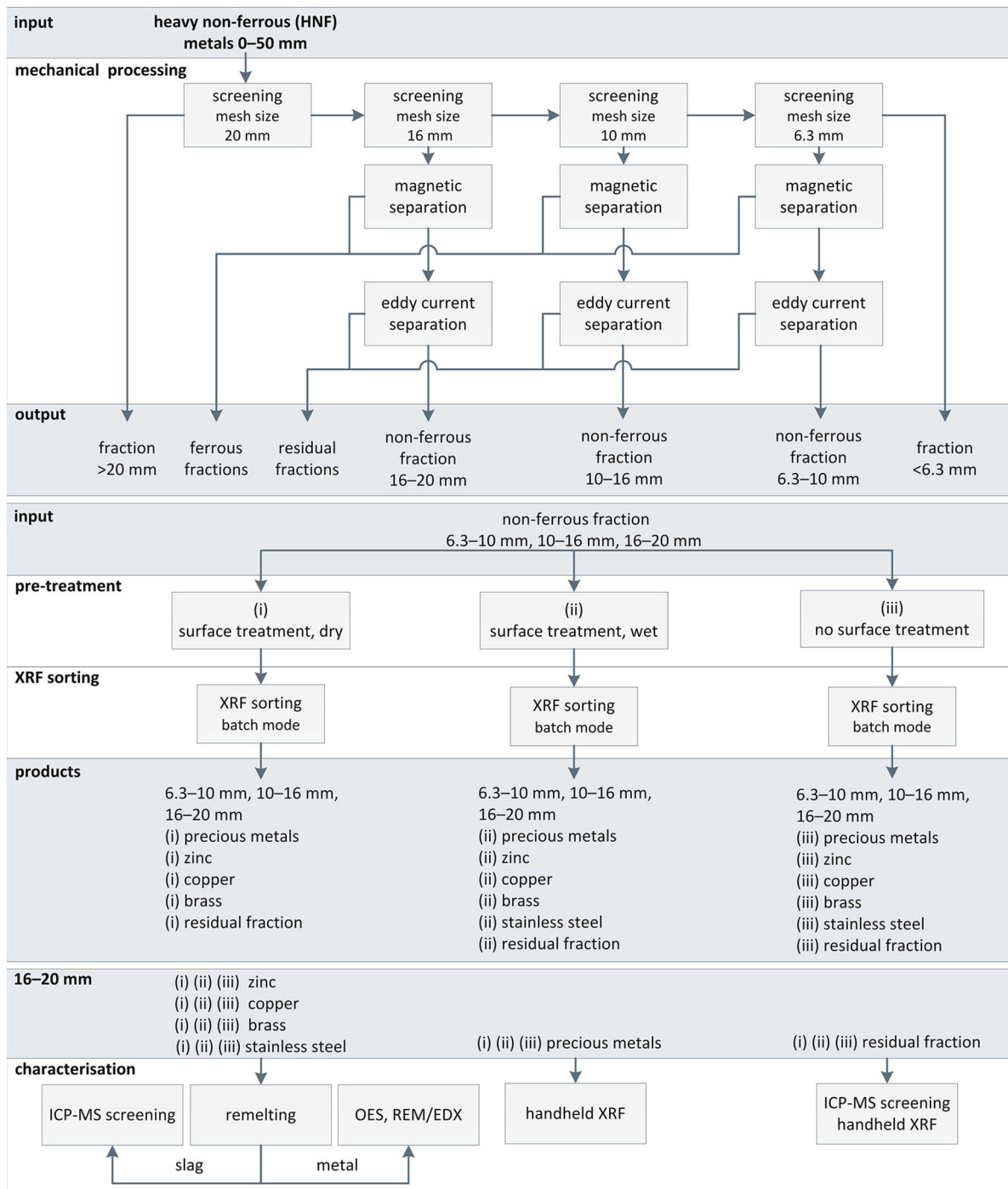


Figure 2. Conducted work, overview on methodology.

thresholds for the allocation of a particle to a fraction: copper >85%; zinc >85%; brass: copper >60% zinc >20%; precious metals: >1%.

Melting tests

In order to homogenise the chemical composition of XRF sorting products, two samples of each fraction in the range of 16–20 mm (zinc, copper and stainless steel) were remolten in an induction furnace (Indutherm MU 700). The used input weights amounted to 1500g. Graphite crucibles were used for all experiments.

Additionally, a condenser was used to collect the evaporating elements and to determine their masses. The experimental temperature was chosen sufficiently high to melt the desired metal and sufficiently low to avoid the volatilisation of alloying elements, for example zinc from brass (550°C for zinc, 950°C for brass, 1150°C for copper and 1550°C for stainless steel). The holding period for zinc and copper melts accounted for 30 min and aimed for the dissolution of accompanying elements in the metal phase. The brass and stainless steel fractions were kept at the desired temperature for 10 min to avoid excessive volatilisation of zinc and to keep the erosion of the crucible and the combustion of

graphite low. The slags were skimmed from the metal melt. The respective metal was first cast in suitable sample shapes for subsequent analyses, the remaining metal melt was cast into bar shapes. The corresponding input fractions and the solidified melts and skimmed slags were weighed. Owing to their low weights and their inhomogeneity, the precious metal fractions were not remelted. However, their chemical composition was determined using a handheld XRF (see *Chemical analyses*).

Chemical analyses

The elemental composition of the remelted metal fraction (zinc, copper, brass, stainless steel) was determined by scanning electron microscopy using energy-dispersive X-ray spectroscopy (SEM/EDX, Jeol JSM-IT300) and via optical emission spectroscopy (OES, spark spectrometer SPECTROMAXx). Because of the good homogenisation owing to electromagnetic stirring in the induction furnace, only one sample of each melt was poured into a round steel mould. After metallographic preparation, including grinding with SiC papers of divers grain sizes and polishing with diamond suspension of 1 µm, the samples were analysed at three different areas using SEM/EDX analysis. Besides, OES analyses were applied at four different positions of each sample. From these values, the mean and the standard deviations were determined.

The slags from the melting experiments were processed (comminution with a jaw crusher, mortar and pestle to <2.5 mm, rejuvenation, homogenisation) and digested by aqua regia according to ÖNORM EN 13657(6.3) (Österreichisches Normungsinstitut, 2002b) or totally according to ÖNORM EN 13656 (Österreichisches Normungsinstitut, 2002a). Digested samples were analysed for silver, aluminium, gold, calcium, cobalt, chromium, copper, iron, potassium, magnesium, manganese, molybdenum, sodium, niobium, nickel, lead, palladium, platinum, antimony, silicon, tin, vanadium, tungsten and zinc by inductively coupled plasma mass spectrometry (ICP-MS screening, Agilent 7500ce) following ÖNORM EN ISO 17294-2 (Österreichisches Normungsinstitut, 2017).

A handheld XRF (X-ray fluorescence analysis, Bruker Magnum Metal-ceramic S1 Titan S/N: 600N3361) was used to determine the elemental composition of the precious metals fraction. Up to 100 particles were analysed, weighed and the composition was determined considering the masses of each analysed particle.

The residual fractions from XRF sorting were comminuted by a vibratory disc mill to <5 mm, subsequently rejuvenated, homogenised and digested with aqua regia (ÖNORM EN 13657(6.3), Österreichisches Normungsinstitut, 2002b). The dry substance was determined according to ÖNORM EN 14346 (Österreichisches Normungsinstitut, 2007) – procedure A. The samples were analysed for silver, gold, cobalt, chromium, copper, iron, manganese, niobium, nickel, lead, palladium, platinum, antimony, tin, vanadium and zinc using the ICP-MS screening method following ÖNORM EN ISO 17294-2 (Österreichisches Normungsinstitut,

2017). Molybdenum and tungsten were determined by inductively coupled plasma optical emission spectroscopy (ICP-OES, Varian Vista-MPX CCD) according to ÖNORM EN ISO 11885 (Österreichisches Normungsinstitut, 2009).

Calculations

The yields of XRF sorting and melting experiments were calculated according to equation (1) (R yield in wt%; M mass of desired or residual fraction from XRF sorting and of metal or slag from melting experiments, respectively, in kilograms; M_{input} input mass for XRF sorting and melting experiments, respectively, in kilograms):

$$R = \frac{M}{M_{input}} * 100 \quad (1)$$

The content of the elements i in the output fraction of XRF sorting and consequently the elemental composition of the desired fractions zinc, copper, brass and stainless steel were calculated based on the results of chemical analyses of metals and slags according to equation (2) (c_i content of element i in the desired fraction in per cent; R_m , R_s yield of metal and slag, respectively, in wt% during melting of the desired fraction; $c_{i,m}$, $c_{i,s}$ content of element i in the metal and in the slag, respectively, in wt%). The elementary contents c_i in the residual fractions were calculated from ICP-MS results, those in the precious metals fraction from XRF results (compare *Chemical analyses*):

$$c_i = \frac{R_m * c_{i,m} + R_s * c_{i,s}}{100} \quad (2)$$

To show the distribution of the elements copper, zinc, iron and lead across the XRF output fractions, equation (3) was used (R_i yield of element i in wt%; M mass of desired/residual fraction in kilograms; c_i content of element i in the desired/residual fraction in wt%; $M_{i,input}$ total mass of element i in the input of XRF sorting in kilograms):

$$R_i = \frac{M * c_i}{M_{i,input}} \quad (3)$$

Results and discussion

Mechanical processing

NF fractions for XRF sorting were produced by screening and the subsequent magnetic and eddy current separation. However, the NF fractions 6.3–10 mm and 10–16 mm had to be re-screened manually (analytical screens HAVER&BOECKER DIN ISO 3310-1, mesh size 5 mm and 10 mm) because too fine bottom ash particles for XRF sorting (minimum grain size 6 mm) were present in the products of mechanical processing as a result of the transport of the samples. Owing to manual screening, the mass losses are considered in further evaluations (6.3–10 mm: about 27 wt%, 10–16 mm: about 75 wt%). Re-screening of the fraction 16–20 mm was not necessary. The share of the NF fractions

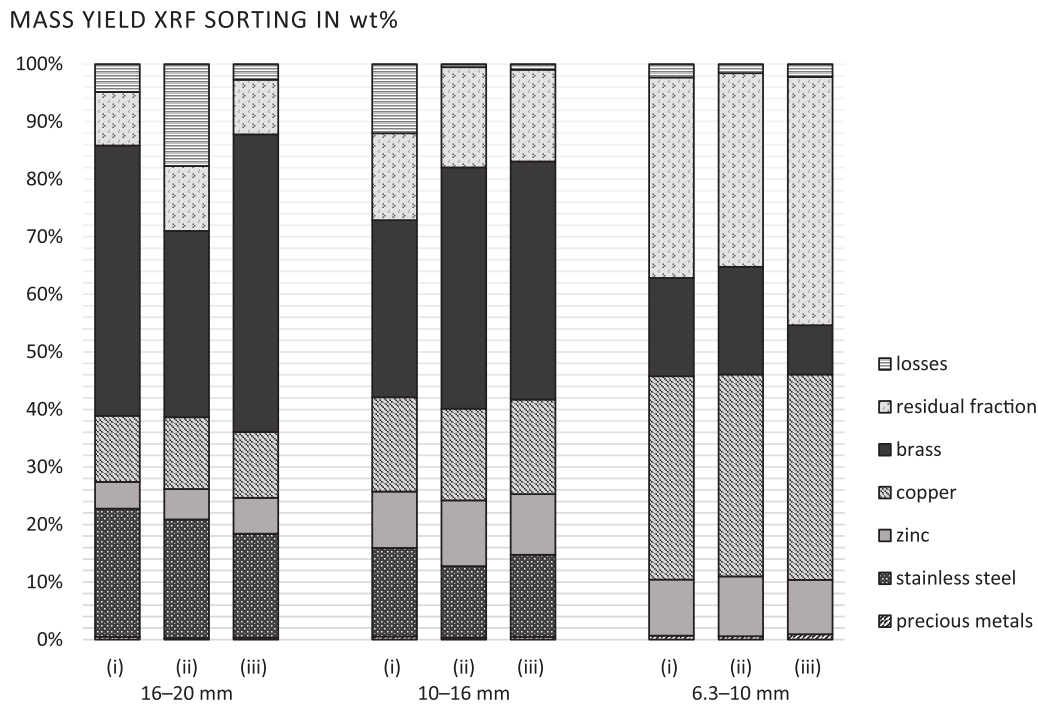


Figure 3. XRF sorting of the NF fractions 16–20, 10–16 and 6.3–10 mm – Yield for the experiments with (i) dry, (ii) wet and (iii) without surface treatment of the NF fractions.

6.3–20 mm on the fraction HNF metals 0–50 mm from the BWS process accounts for about 41 wt% (16–20 mm: 11 wt%, 10–16 mm: 17 wt%, 6.3–10 mm: 13 wt%). The content of ferrous metals accounted for about 16 wt% (16–20 mm: 5 wt%, 10–16 mm: 7 wt%, 6.3–10 mm: 4 wt%).

Surface pre-treatment and XRF sorting

Figure 3 illustrates the yield of the desired fractions precious metals, zinc, copper, brass and stainless steel of XRF sorting under consideration of the pre-treatment of the NF fractions, namely (i) drily pre-treated, (ii) wetly pre-treated and (iii) not pre-treated.

Whereas the yield of stainless steel and brass tends to increase with increasing grain size, the yield of zinc, copper and precious metals increases with decreasing grain size. The comparably large amounts of residual fractions in the grain size range 6.3–10 mm mainly result from the fact that no stainless steel was sorted out in the experiments. There is neither a positive nor a negative effect of pre-treatment on the yield of the desired fractions in XRF sorting. An exception is the brass fraction 16–20 mm, whose yield is reduced for increasing intensity of the pre-treatment. The mass losses across all sorted fractions were relatively low. They decrease proportionally with the grain size, explained partially by the fact that losses of smaller particles during the sorting process have smaller effects on the mass losses than losses of larger particles. For the differences between the various kinds of pre-treatment – (i) dry, (ii) wet or (iii) or no pre-treatment – no systematic correlation could be observed. Screening at a mesh size of 16 mm is not required

from a processing point of view as the ideal grain size range for sensor-based sorting is a ratio of 1:4 according to Bunge (2012). This is supported by the congruent results for the yield in the considered grain size ranges.

Figure 4 shows the elemental composition of the output fractions of XRF sorting in the grain size range 16–20 mm. No matter if the experiments were conducted with or without pre-treatment of the particle surface, all desired fractions have similar qualities. As the yield for stainless steel during re-melting of the drily pre-processed fraction exceeded 100% (see below) for the subsequent summary, a value of 100% was assumed.

Zinc: (i) 83.6% zinc (ii) 87.3% zinc (iii) 81.1% zinc

Copper: (i) 83.6% copper (ii) 86.2% copper (iii) 80.9% copper

Brass: (i) 58.3% copper; 33.0% zinc (ii) 56.0% copper; 34.7% zinc (iii) 56.9% copper; 33.4% zinc

Stainless steel: (i) 64.2% iron (ii) 63.6% iron (iii) 64.6% iron

Precious metals: (i) 18.0% silver (ii) 14.1% silver (iii) 12.6% silver

Copper, zinc, lead and iron were identified as the main constituents of the residual fraction for the three experiments (i)–(iii) (47.1–50.9% copper, 17.1–22.4% zinc, 7.9–10.0% lead and 1.1–2.7% iron).

The content of the elements copper and zinc (supposed to accumulate in the product fractions) in the residual fractions rises with increasing intensity of mechanical processing. This observation suggests decreased oxygen contents and consequently less oxide compounds in the residual fraction, if the bottom ash is

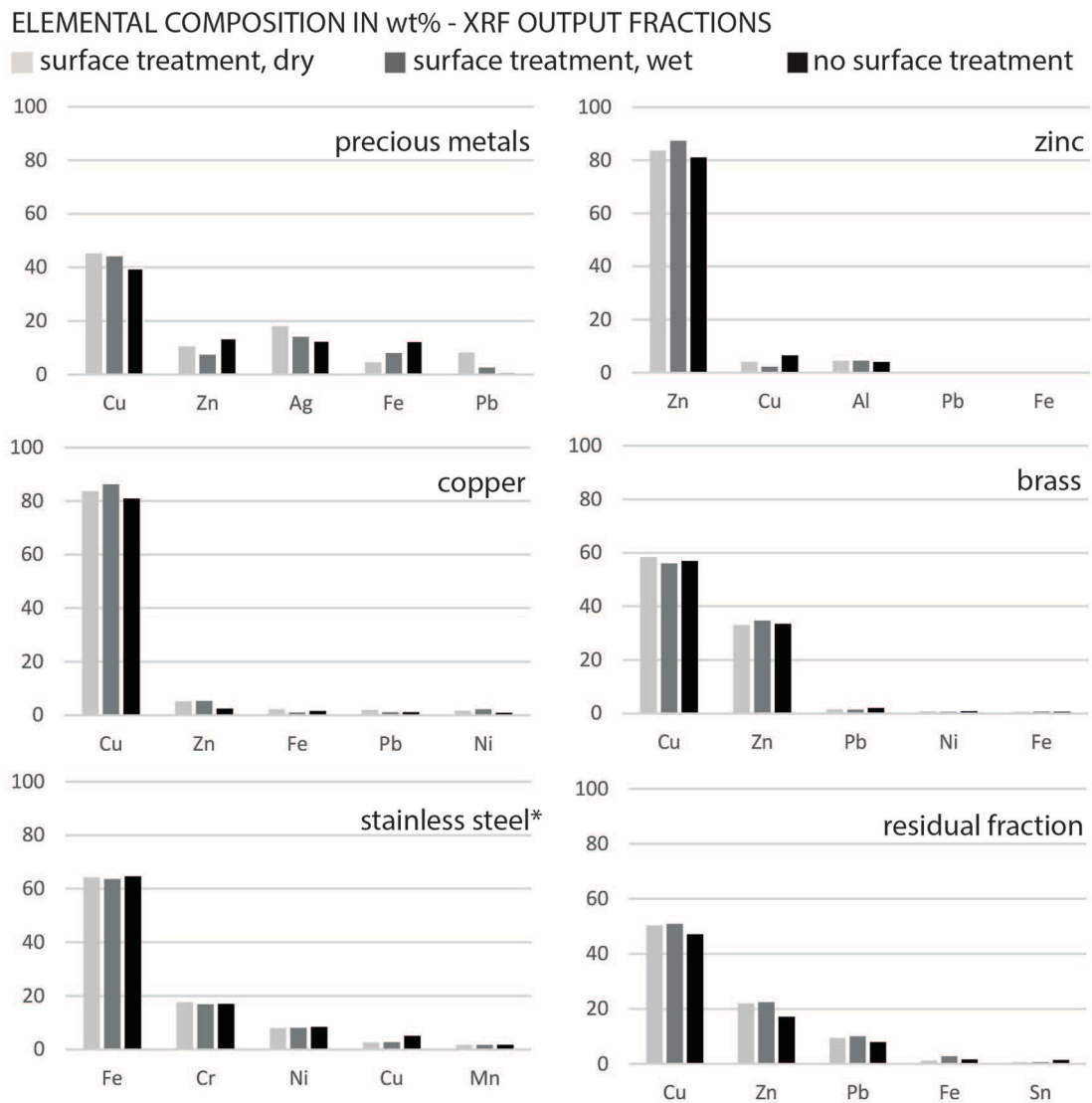


Figure 4. Elemental composition of the output fractions of XRF sorting experiments with (i) dry, (ii) wet and (iii) without surface treatment of the NF fractions 16–20 mm.

*The composition of the drily pre-treated stainless steel fraction (i) refers to a yield of $R_m = 100\%$.

pre-treated wetly or drily. Furthermore, this result suggests that by pre-treatment of the bottom ash corroded constituents, which are enriched in the slag during re-melting, are separated.

Figure 5 illustrates the distribution of the elements copper, zinc, iron and lead among the output flows of XRF sorting (grain size range 16–20 mm). Most of the copper from the input fractions is enriched in the copper and brass fractions (corresponds to $\leq 86.8\%$ of the entire copper contained in the input fractions). Up to 16.3% of the copper are lost with the residual fraction. Of the zinc contained in the input, 58.8% to 71.1% ends up in the brass fractions, 17.7% to 24.3% in the zinc fractions and 6.7% to 13.3% in the residual fractions. This is in general agreement with the statement of Bunge (2014), that zinc in pure form occurs in bottom ash only in minor amounts (0.2 wt%) and the majority is alloyed with copper as brass. The distribution of copper and zinc among the output flows of sensor-based sorting as well as the element composition of the output flows (see Figure 4), suggest that there is still optimisation potential regarding the yield of

brass, copper and zinc. Regarding an improvement or decline of the yield of copper and zinc depending on the pre-processing, no trend is visible. The majority of iron was yielded successfully into the stainless steel fraction ($>94.6\%$). Contrary, lead is enriched in the residual and brass fractions. Owing to the lead addition in copper–tin alloys, the lead content of the brass fraction is accordingly high (Deutsches Kupfer-Institut e.V., 2007). By the use of lead, the machinability of copper and copper alloys is improved (Deutsches Kupfer-Institut e.V., 2012).

Melting experiments

The achieved metal yield in melting experiments is 72%–84% for zinc, 73%–89% for copper, 60%–92% for brass and 92%–102% for stainless steel. The excess over 100% in the experiment with stainless steel can be explained by the uptake of carbon from the graphite crucible by the steel melt. The amount of volatilised elements that were separated in the condenser is zero for all

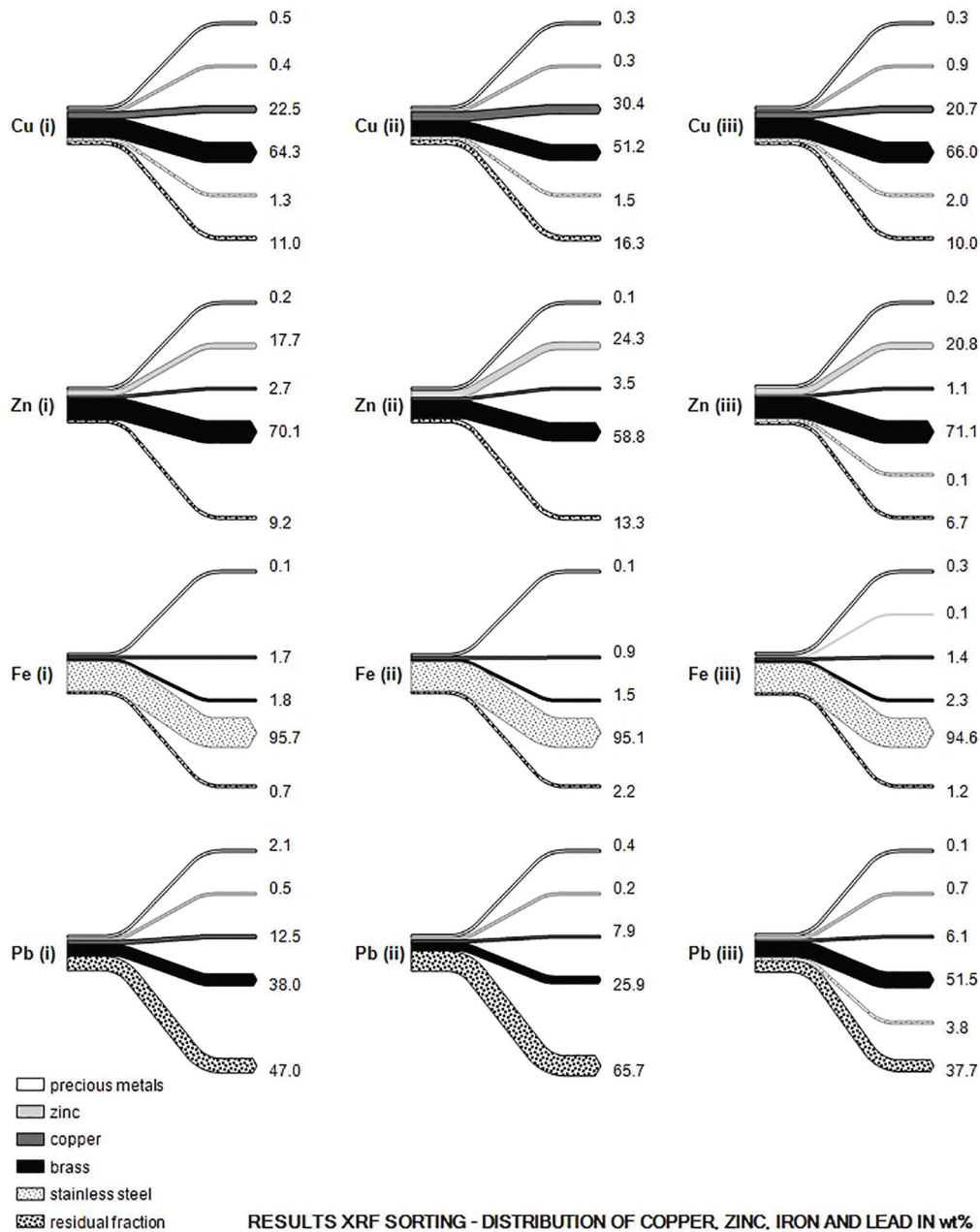


Figure 5. XRF sorting – Distribution of elements among the output fractions of XRF sorting in wt% [(i) surface treatment, dry, (ii) surface treatment, wet and (iii) no surface treatment].

fractions apart from those from the experiments with stainless steel. In the last case, metallic zinc sublimated because of the high temperatures. Owing to the oxygen in the atmosphere, zinc oxidised to ZnO and re-sublimated at the condenser. The losses are in the range of 1% to 8% (except for stainless steel where a weight increase of up to 4% was observed, see also the discussion of the yield). They can be traced back to metal residues on the skimmer or in the crucible. In case of the wetly pre-processed brass fraction and the wetly pre-processed stainless steel fraction, the experiments were conducted in triplicate owing to deviations between the results of the first two experiments to validate the results. Regarding the metal yield, no trend depending on the surface pre-treatment, for example (i) drily pre-treated, (ii) wetly pre-treated and (iii) not pre-treated, was recognised. Table 1

indicates the composition of the re-melted metals based on SEM/EDX investigations. The results from SEM/EDX and OES agree with each other. However, for the zinc samples, copper, lead and aluminium were outside the calibration range of the OES measurement. For the stainless steel samples, this affected partly the lead and carbon contents.

The re-melted zinc fraction contains between 86.8% and 91.4% zinc. The main alloying element is aluminium, with up to 4.8%. The copper content varies considerably within the individual fractions with identical pre-treatment. Overall, the content of accompanying elements does not depend on the kind of pre-treatment. In Germany, hard zinc as well as zinc top and bottom drosses from galvanisation industry with zinc contents >90% are used for the production of zinc oxide (Th, 2016). Hence, the

Table 1. Excerpt – Composition of the re-melted metals zinc, copper, brass and lead (SEM/EDX, (i) surface treatment, dry, (ii) surface treatment, wet, (iii) no surface treatment). Remark: Each sample was analysed three times and thereof the mean μ and the standard deviation σ was calculated. Values below the quantification limit (<0.1 wt%) are shown as ‘—’.

			Cu	Zn	Fe	Ni	Pb	Sn	C	O	Cr	Mn	Al		
Zinc	(i)	μ	2.7	90.2	—	—	—	—	0.8	1.3	—	—	4.8		
		σ	0	0.3	—	—	—	—	0.4	0.1	—	—	0.2		
	(ii)	μ	4.9	87.3	—	0.1	—	—	1.2	1.8	—	—	4.7		
		σ	0.2	0.1	—	0.2	—	—	0.1	0	—	—	0		
	(iii)	μ	2.2	91.4	—	—	—	—	0.5	1.2	—	—	4.6		
		σ	0.1	0.1	—	—	—	—	0.1	0.1	—	—	0.2		
	Copper	(i)	μ	3.7	88.1	—	0.1	1	—	1	1.3	—	—	4.8	
			σ	0	0.6	—	0.2	0.1	—	0.4	0.1	—	—	0.1	
		(ii)	μ	2.4	90.6	—	—	—	—	1	1.4	—	—	4.6	
			σ	0	0.2	—	—	—	—	0.2	0.2	—	—	0.1	
		(iii)	μ	6.4	86.8	—	—	—	—	0.8	1.2	—	—	4.7	
			σ	0.1	0.1	—	—	—	—	0.1	0	—	—	0.1	
Brass		(i)	μ	88.7	5.5	0.8	1.7	1.5	0.7	0.3	0.4	—	—	0.3	
			σ	0.3	0.1	0	0	0.2	0.1	0.1	0.1	0.4	—	—	0
		(ii)	μ	89.1	5.1	0.6	2.2	0.8	0.6	0.6	0.6	0.6	—	—	0.4
			σ	0.9	0.2	0	0.1	0.1	0.1	0.7	0.1	0.1	—	—	0.1
		(iii)	μ	88.8	5.4	0.7	2.4	1.1	0.5	0.2	0.5	—	—	0.4	
			σ	0.2	0.1	0	0.1	0.1	0.1	0.1	0.1	—	—	0.1	
	Stainless steel	(i)	μ	86.7	7.6	0.5	3.1	0.4	0.5	0.3	0.5	—	—	0.4	
			σ	0.3	0.2	0	0	0.4	0.1	0.1	0.1	0.4	—	—	0.1
		(ii)	μ	90.3	2.6	0.9	1	1.2	0.4	2.6	0.7	—	—	—	
			σ	3.4	0.1	0	0.1	0.1	0.1	2.7	0.2	—	—	—	
		(iii)	μ	88.9	5.3	0.4	2.4	0.8	0.7	0.4	0.6	—	—	0.4	
			σ	0.1	0.1	0	0	0.2	0.1	0.2	0	—	—	0	
Stainless steel		(i)	μ	62.5	31.9	0.4	0.8	1.6	0.5	1.4	0.7	—	—	—	
			σ	0.3	0.3	0	0	0	0	0	0	—	—	—	
		(ii)	μ	61.9	32.2	0.4	0.7	1.5	0.4	1.9	0.7	—	—	0.1	
			σ	0.3	0.3	0	0	0.2	0	0.3	0.1	—	—	0.2	
		(iii)	μ	61.7	34	0.3	0.6	1.5	0.4	0.8	0.6	—	—	—	
			σ	0.3	0.6	0	0	0.1	0	0.3	0	—	—	—	
	Stainless steel	(i)	μ	60.9	33.6	0.4	0.3	1.7	0.4	1.8	0.8	—	—	—	
			σ	0.4	0.3	0	0.3	0.2	0	0.5	0	—	—	—	
		(ii)	μ	62	31.5	0.4	0.7	1.6	0.5	2.4	0.7	—	—	—	
			σ	0.4	0.1	0	0	0.1	0.1	0.4	0	—	—	—	
		(iii)	μ	60.6	33.1	0.3	0.8	2.1	0.4	1.7	0.7	—	—	—	
			σ	0.4	0.2	0	0.1	0.1	0.1	0.2	0.1	—	—	—	
Stainless steel		(i)	μ	60.8	32.4	0.4	0.4	2.1	0.3	2.8	0.6	—	—	—	
			σ	0.3	0.1	0	0.4	0.2	0	0.3	0	—	—	—	
		(ii)	μ	2.5	—	64.2	7.9	—	—	5	—	17.6	1.6	—	
			σ	0.1	—	0.5	0.1	—	—	0.3	—	0.6	0.1	—	
		(iii)	μ	1.2	—	64.2	8.1	—	—	6.2	—	17.2	1.4	0.2	
			σ	0.1	—	0.4	0.1	—	—	0.4	—	0.2	0.1	0	
	Stainless steel	(i)	μ	2.6	—	63.9	8.1	—	—	4.9	—	17	1.7	0.3	
			σ	0.1	—	0.5	0.2	—	—	0.6	—	0.1	0	0	
		(ii)	μ	1.4	—	64.9	7.6	—	—	5.5	—	16.8	2.2	0.2	
			σ	0.1	—	0.3	0.2	—	—	0.6	—	0.1	0.1	0	
		(iii)	μ	3.8	—	65.1	8.5	—	—	1.4	—	17	2.3	0.6	
			σ	0.2	—	0.2	0.2	—	—	0.2	—	0.3	0.1	0	
Stainless steel		(i)	μ	4.1	—	66.5	8.7	—	—	0.3	—	17.6	1.7	—	
			σ	0.2	—	0.4	0.2	—	—	0.4	—	0.3	0.1	—	
		(ii)	μ	3.8	—	62.5	7.7	—	—	5.2	—	16.5	2.2	—	
			σ	0.1	—	0.4	0.3	—	—	0.3	—	0.1	0.1	—	

recycling of the zinc fractions produced in this project seems realistic, for example by the French process (Worrell and Reuter, 2014). Furthermore, electric arc furnace dusts with 40% zinc can

be recycled pyrometallurgically (Lin et al., 2017). Aluminium (3.8%–4.2%) and copper (0.7%–1.1% in case of the Zamak alloy ZL0410) are used as alloying elements for casting alloys.

Aluminium improves for example the processability, tensile strength, fracture elongation and impact bending toughness of zinc, whereas copper has a positive impact on the tensile strength and hardness of the metal (Röhr, 2017). However, the quality requirements according to ÖNORM EN 13283 (Österreichisches Normungsinstitut, 2003) for secondary zinc (>97.5% for quality ZS2) and according to ÖNORM EN 1774 (Österreichisches Normungsinstitut, 1997) for casting alloys (sort-specific, very strict limit values for accompanying elements) are not reached.

The main constituent of the copper fractions is copper (86.7%–90.3%). The main accompanying elements are zinc and nickel. Additionally, lead, iron and zinc were identified as accompanying elements. In contrast, the concentration of single alloying elements in low-alloy copper material is limited to a percentage of 1%–2%, in total 5% (Deutsches Kupfer-Institut e.V., 2012). Corresponding refining steps would be necessary to increase the electrical conductivity for electric and electronic applications (Deutsches Kupfer-Institut e.V., 2000).

The brass blocks produced in the melting experiments consist mainly of two parts of copper and one part of zinc (copper: 60.6%–62.5%, zinc: 31.9%–33.6%). According to the German Copper Institute (Deutsches Kupfer-Institut e.V., 2007) common copper–zinc alloys contain, besides copper, also 5 to 45 wt% zinc.

The iron contents of the stainless steel fraction range from 62.5 wt% to 66.5 wt%. The main alloying element is chromium with 16.5–17.6 wt% followed by nickel with 7.6–8.7 wt%. Manganese is present with about 2 wt%. Iron alloys with $\geq 10.5\%$ chromium and $\leq 1.2\%$ carbon belong to the group of stainless steel (Informationsstelle Edelstahl Rostfrei, 2008). Owing to the high temperatures and erosion of carbon crucible by stirring of melt, carbon is dissolved in the steel melt. With decreasing temperature during solidification, the solubility of carbon significantly decreases resulting in a large number of carbides formed in the material. Consequently, the carbon content rises to 6.2 wt%. In the case of stainless steels, chromium carbides preferentially form, which lead to a decrease of corrosion resistance. Besides, the materials embrittle and the weldability sinks (Angerer N.D.; Kinzel, 1952).

The composition of all re-melted samples corresponds to the respective desired fractions from XRF sorting. Only the contained lead has to be removed to obtain better saleable products. The maximum allowed concentration for lead for homogeneous materials is 0.1 wt% according to article 4 of the European guideline 2011/65/EU (The European Parliament and the Council of the European Union, 2011). The surface pre-treatment has no impact on the purity and the composition of the products from melting experiments. The slags from the experiments are no homogeneous liquid phases, but crumbly to doughy surface layers.

Summary

In this study, mixed non-ferrous metals fractions from wet processing of MSWI bottom ash, which are currently directly

recycled metallurgically, are further separated mechanically to recover besides copper also brass, zinc, stainless steel and precious metals.

The conducted experiments demonstrate that zinc, copper, brass, stainless steel and precious metals fractions can be produced in a marketable quality by XRF sorting. Neither a positive nor a negative effect of surface pre-treatment (wet, dry) on the purity of the desired fractions could be proven. Only the yield of the brass fraction in the grain size range 16–20 mm decreased with increasing mechanical treatment intensity.

Regarding the metal yield and the quality of the re-melted metals, the surface cleaning of the particles prior to XRF sorting had no effect. The produced melt products had marketable qualities (zinc: 86.8–91.4% zinc; copper: 86.7–90.3% copper; brass: 60.6–62.5% copper and 31.5–34.0% zinc; stainless steel: 62.5–66.5% iron).

In order to obtain better saleable products (metals and alloys), it is recommended to separate the lead contained in the re-melted fractions, which could be achieved by an additional XRF sorting step (depending on whether the lead in the non-ferrous bottom ash is present as metal or alloy and the related mass distribution). In addition, further pyrometallurgical and hydrometallurgical processes could be used to refine the products and to lower lead contents in the re-melted fractions, respectively. However, further experiments have to be performed to make reliable scientific statements.

Acknowledgements

The authors thank the Austrian Research Promotion Agency (FFG) for funding the project, as well as all contributing research and industrial partners and Alexia Aldrian (Montanuniversität Leoben) and her team for the chemical analyses.

Declaration of conflicting interests


The authors declared no potential conflicts of interest with respect to the research, authorship, and/or publication of this article.

Funding

The authors disclosed receipt of the following financial support for the research, authorship, and/or publication of this article: The authors thank the Austrian Research Promotion Agency (FFG) for funding the project AKRosA II [No. 848621].

ORCID iDs

Kerstin Pfandl  <https://orcid.org/0000-0002-8103-4784>

Bastian Küppers  <https://orcid.org/0000-0002-0367-4786>

References

- Allegrini E, Maresca A, Olsson ME, et al. (2014) Quantification of the resource recovery potential of municipal solid waste incineration bottom ashes. *Waste Management* 34: 1627–1636.
- Angerer M (N.D.) Stahl – Einfluss der Legierungselemente. Available at: <http://www.maschinenbau-wissen.de/skript3/werkstofftechnik/stahl-eisen/38-einfluss-legierungselemente-stahl> (accessed 22 July 2019).
- Bayuseno AP and Schmah WW (2010) Understanding the chemical and mineralogical properties of the inorganic portion of MSWI bottom ash. *Waste Management* 30: 1509–1520.

- BOKU (2010) Institut für Abfallwirtschaft, Universität für Bodenkultur Wien. Grundlagen für die Verwertung von MV-Rostasche: Teil A: Entwicklung des Österreichischen Behandlungsgrundsatzes. Available at: https://www.bmmt.gv.at/dam/jcr:3e990e78-f77d-4d52-b9a1-b3b5ffe5630a/BOKU_Grundsatz_Teil_A_Rostasche.pdf+&cd=1&hl=de&ct=clnk&gl=at&client=firefox-b-d (accessed 23 July 2019).
- Bundesministerium für Verkehr, Innovation und Technologie (2018) Definition: Kritische Rohstoffe und potenziell kritische Rohstoffe mit Bezug zu Österreich. Available at: https://www.ffg.at/sites/default/files/allgemeine_downloads/thematische%20programme/Produktion/rohstoffdefinition_28as_pdz_2018.pdf (accessed 25 March 2019).
- Bunge R (2012) *Mechanische Aufbereitung: Primär- und Sekundärrohstoffe*, 1st edn. Weinheim, Germany: Wiley-VCH Verlag & Co. KGaA, pp.206.
- Bunge R (2014) Wieviel Metall steckt im Abfall? In: Thomé-Kozmiensky KJ (ed.) *Mineralische Nebenprodukte und Abfälle*, Neuruppin, DE: TK Verlag Karl Thomé-Kozmiensky, pp.91–103.
- Bunge R (2016) Aufbereitung von Abfallverbrennungssaschen – eine Übersicht. In: Thomé-Kozmiensky KJ (ed.) *Mineralische Nebenprodukte und Abfälle*, vol 3. Neuruppin, DE: TK Verlag Karl Thomé-Kozmiensky, pp.141–161.
- Dittrich S, Thome V, Seifert S, et al. (2016) Effektive Aufbereitung von Müllverbrennungsschlacken mittels Hochspannungsimpulsen. *Chemie Ingenieur Technik* 88: 461–468.
- Deutsches Kupfer-Institut e.V. (2000) Kupfer in der Elektrotechnik – Kabel und Leitungen. Available at: https://www.kupferinstitut.de/fileadmin/user_upload/kupferinstitut.de/de/Documents/Shop/Verlag/Downloads/Anwendung/Elektrotechnik/brosch09.pdf (accessed 15 March 2019).
- Deutsches Kupfer-Institut e.V. (2007) Kupfer-Zink-Legierungen (Messing und Sondermessing). Available at: https://www.kupferinstitut.de/fileadmin/user_upload/kupferinstitut.de/de/Documents/Shop/Verlag/Downloads/Werkstoffe/i005.pdf (accessed 22 March 2019).
- Deutsches Kupfer-Institut e.V. (2012) Niedriglegierte Kupferwerkstoffe: Eigenschaften Verarbeitung Verwendung. Available at: https://www.kupferinstitut.de/fileadmin/user_upload/kupferinstitut.de/de/Documents/Shop/Verlag/Downloads/Werkstoffe/i008.pdf (accessed 11 March 2019).
- European Commission (2017) Study on the review of the list of critical raw materials: Final report. Available at: <http://hytechcycling.eu/wp-content/uploads/Study-on-the-review-of-the-list-of-Critical-Raw-Materials.pdf> (accessed 13 June 2019).
- ecoprog GmbH (2018) Dynamic development of waste-to-energy market continues. Available at: https://www.ecoprog.com/fileadmin/user_upload/pressemitteilungen/ecoprog_press_release_Waste_to_Energy_2017-2018.pdf (accessed 13 June 2019).
- Funari V, Braga R, Bokhari SNH, et al. (2015) Solid residues from Italian municipal solid waste incinerators: A source for “critical” raw materials. *Waste Management* 45: 206–216.
- Gillner R, Pretz T, Rombach E, et al. (2011) NE-Metallpotenzial in Rostaschen aus Müllverbrennungsanlagen. *Word of Metallurgy – ERZMETALL* 64: 5–13.
- Gisbertz K and Friedrich B (2015) VeMRec – Metallurgische Herausforderungen beim Recycling von NE-Metallkonzentraten aus Abfallverbrennungs-Rostasche. In: Thomé-Kozmiensky KJ (ed.) *Mineralische Nebenprodukte und Abfälle*. Neuruppin, DE: TK Verlag Karl Thomé-Kozmiensky, pp.227–253.
- Informationsstelle Edelstahl Rostfrei (2008) Merkblatt 803: Was ist nichtrostender Stahl? Available at: <https://www.edelstahl-rostofffrei.de/page.asp?pageID=1576> (accessed 26 June 2019).
- Johnson A and Huter C (2010) Characterization and geochemical properties of selected incineration residues. In: Schenk K (ed.) *KVA-Rückstände in der Schweiz: Der Rohstoff mit Mehrwert*. Bern: Bundesamt für Umwelt, pp.145–151.
- Jung C-H and Osako M (2007) Thermodynamic behavior of rare metals in the melting process of municipal solid waste (MSW) incineration residues. *Chemosphere* 69: 279–288.
- Kinzel AB (1952) Chromium carbide in stainless steel. *JOM* 4: 469–448.
- Kollegger P and Berghofer M (2017) Optimierte sensorgestützte Mineraliensortierung durch mineralogisch-petrographische Prozesskontrolle. *Berg Huettenmaennische Monatshefte* 162: 457–459.
- Kranert M and Cord-Landwehr K (eds) (2010) *Einführung in die Abfallwirtschaft*, 4th edn, updated and expanded. Wiesbaden, Germany: Vieweg und Teubner Verlag, pp.316–117.
- Lin X, Peng Z, Yan J, et al. (2017) Pyrometallurgical recycling of electric arc furnace dust. *Journal of Cleaner Production* 149: 1079–1100.
- Österreichisches Normungsinstitut (1997) ÖNORM EN 1774 Zink und Zinklegierungen – In Blockform und in flüssiger Form.
- Österreichisches Normungsinstitut (2002a) ÖNORM EN 13656 Charakterisierung von Abfällen – Aufschluss mittels Mikrowellengerät mit einem Gemisch aus Fluorwasserstoffsäure (HF), Salpetersäure (HNO₃) und Salzsäure (HCl) für die anschließende Bestimmung der Elemente im Abfall.
- Österreichisches Normungsinstitut (2002b) ÖNORM EN 13657 Charakterisierung von Abfällen – Aufschluss zur anschließenden Bestimmung des in Königwasser löslichen Anteils an Elementen in Abfällen.
- Österreichisches Normungsinstitut (2003) ÖNORM EN 13283 Zink und Zinklegierungen – Sekundärzink.
- Österreichisches Normungsinstitut (2007) ÖNORM EN 14346 Charakterisierung von Abfällen – Berechnung der Trockenmasse durch Bestimmung des Trockenrückstandes oder des Wassergehaltes.
- Österreichisches Normungsinstitut (2009) ÖNORM EN ISO 11885 Wasserbeschaffenheit – Bestimmung von ausgewählten Elementen durch induktiv gekoppelte Plasma-Atom-Emissionsspektrometrie (ICP-OES).
- Österreichisches Normungsinstitut (2011) ÖNORM S 2127 Grundlegende Charakterisierung von Abfallhaufen oder von festen Abfällen aus Behältnissen und Transportfahrzeugen.
- Österreichisches Normungsinstitut (2017) ÖNORM EN ISO 17294-2 Wasserbeschaffenheit – Anwendung der induktiv gekoppelten Plasma-Massenspektrometrie (ICP-MS) Teil 2: Bestimmung von ausgewählten Elementen einschließlich Uran-Isotope.
- Pan JR, Huang C, Kuo J-J, et al. (2008) Recycling MSWI bottom and fly ash as raw materials for Portland cement. *Waste Management* 28: 1113–1118.
- Pfandl K, Dobra T and Pomberger R (2018) Potential von Müllverbrennungsrostaschen für die Rückgewinnung kritischer Rohstoffe. In: Bockreis A, Faulstich M, Flamme S, et al. (eds) *8. Wissenschaftskongress Abfall- und Ressourcenwirtschaft*, 15–16 March, Universität für Bodenkultur (BOKU) Wien, Austria, 1st edn. Innsbruck, AT: Innsbruck University Press pp.245–252.
- Röhr G (2017) Zinklegierungen – genormte Qualität aus primären und sekundären Rohstoffen. In: Verband Deutscher Metallhändler e.V. (ed.) *VDM Magazin II/2017 (675)*, pp.10–11.
- Simon F-G and Holm O (2013) Aufschluss, Trennung und Rückgewinnung von Metallen aus Rückständen thermischer Prozesse: Verdoppelung der Metallausbeute aus MVA-Rostasche. In: Thomé-Kozmiensky KJ (ed.) *Aschen, Schlacken, Stäube: Aus Abfallverbrennung und Metallurgie*. Neuruppin, DE: TK Verlag Karl Thomé-Kozmiensky, pp.297–310.
- Stockinger G (2016) Innovative Aufbereitung von Müllverbrennungsschlacke. In: Pomberger R, Adam J, Aldrian A, et al. (eds) *Recy & DepoTech 2016*, 8–11 November, Montanuniversität Leoben. Austria, Leoben, AT: self-published by AVAW, pp.237–242.
- Th (2016) Zinkverbindungen aus Recycling-Rohstoffen: Erfolgreiche Kreislaufwirtschaft bei der Zinkgewinnung. Available at: <https://www.giesserei-praxis.de/news/news/14822-zinkverbindungen-aus-recycling-rohstoffen/> (accessed 22 July 2019).
- The European Parliament and the Council of the European Union (2011) DIRECTIVE 2011/65/EU OF THE EUROPEAN PARLIAMENT AND OF THE COUNCIL: of 8 June 2011 on the restriction of the use of certain hazardous substances in electrical and electronic equipment. Available at: <https://eur-lex.europa.eu/legal-content/EN/TXT/PDF/?uri=CELEX:32011L0065&from=DE> (accessed 4 July 2019).
- Wang Y, Huang L and Lau R (2016) Conversion of municipal solid waste incineration bottom ash to sorbent material: Effect of ash particle size. *Journal of the Taiwan Institute of Chemical Engineers* 68: 351–359.
- Worrell E and Reuter MA (eds.) (2014) *Handbook of Recycling: State-of-the-Art for Practitioners, Analysts, and Scientists*. Amsterdam, Boston, Heidelberg, London, New York, Oxford, Paris, San Diego, San Francisco, Sydney, Tokyo: Elsevier, pp.133–124.
- Zhang F-S, Yamasaki S and Kimura K (2001) Rare earth element content in various waste ashes and the potential risk to Japanese soils. *Environment International* 27: 393–398.

7 Publication 6

Influence of Throughput Rate and Input Composition on Sensor-Based Sorting Efficiency

Küppers B, Seidler I, Koinig G, Pomberger R, Vollprecht D (accepted in 2019) Influence of Throughput Rate and Input Composition on Sensor-Based Sorting Efficiency. Accepted by Detritus

Annotation on my own contribution to publication 6:

I predominantly designed and planned the series of experiments which this publication is based on. Gerald Koinig and I jointly prepared, conducted and analysed the experiments. I evaluated and interpreted the results with support of Irina Seidler, Gerald Koinig and Daniel Vollprecht. The publication was jointly written by Irina Seidler and me. All co-authors reviewed the publication, and I revised it.

Abstract

According to the Directive (EU) 2018/851 of the European Union, higher recycling rates for municipal waste will have to be met in the near future. Beside improvements to the collection systems, the efficiency of mechanical processing and sorting will have to be increased to reach the EU's targets. Sensor-based sorting (SBS) plants constitute an integral part of today's sorting processes. Two main factors determine the sorting performance: throughput rate and input composition. To improve recycling efficiencies, especially SBS machines need to be optimized. Three evaluation criteria are used to describe the performance of these processes: recovery (content of input material – both eject and reject material discharged into the product fraction) or product quantity (amount of product generated via sorting within a specific interval – calculated by multiplying throughput rate and yield), yield (amount of eject material discharged into the product fraction), and product purity. For this study, 160 sorting experiments each with 1,000 red and white low-density polyethylene (LDPE) chips were conducted to investigate the effects of throughput rate and input composition on sorting processes. This simplified approach reduced the influence of other factors on the sorting performance, giving precise information on the effect of throughput rate and input composition. The testing results can enter process optimization. With increasing throughput rates, product quantity rises following a saturation graph (despite exponential decrease in recovery). In the experiments a higher throughput rate also resulted in an exponential decrease of the yield while a change to the input composition had no such effect. The third evaluation criteria, product purity, decreases linearly with increasing occupation density. The slope of this function depends on the input composition.

Introduction

16.3 million tons (170 kg/capita) of plastic packaging waste (PPW) are produced in the European Union (EU) per year, out of which as little as 42 wt% were recycled in 2016 according to Eurostat, 2019. E. g. by 2025, the EU also aims to increase the rate for preparing for re-use and the recycling of municipal waste to 55 wt% (The European Parliament and of the Council of the European Union, 2018).

PPW-recycling requires separation into individual plastic types (International Organization for Standardization, 2008). Plastics are usually separated using sensor-based sorting (SBS) (Gundupalli et al., 2017; Jansen et al., 2012). Spectral imaging techniques including NIR (near-infrared, 750 – 1100 nm (Workman and Springsteen, 1998)), VIS (visual image spectroscopy, 380 – 750 nm (Workman and Springsteen, 1998)) and HSI (hyperspectral imaging) are most commonly applied though laser-induced-breakdown-spectroscopy and X-ray-sorting are available as well (Table 1).

Table 1: Sorting techniques applicable to different types of waste (mod. Gundupalli et al., 2017)

	Eddy current	LIBS	X-ray sort	Optical sort	Spectral sort
metal	✓	✓	✓	✓	✓
Plastic		✓	✓		✓
Paper				✓	
Glass				✓	✓
Wood		✓	✓		

SBS techniques have been utilised by various industries during the last years. Additionally, research results were published in many papers. SBS is mostly applied in recycling (Gundupalli et al., 2017; Mesina et al., 2007; Rahman et al., 2014), mining (Knapp et al., 2014; Lessard et al., 2014; Dalm et al., 2014) and food (Alaya et al., 2019; Cubero et al., 2011; Tu et al., 2007) processing plants. Sound information on the sorting performance of such technologies is limited, however.

One key parameter found fluctuating in industrial SBS plants is their throughput rate adversely affecting their sorting efficiency (Feil et al., 2016). The throughput rate, in tons per hour, is related to the occupation density (the relative size of the detection zone in an SBS unit that is covered with particles), in %. With respect to SBS, the occupation density is a better indicator of capacity than the throughput rate. The reason is that an SBS unit operates differently from other processing technology. Objects must here be presented separately to a sensor enabling a particle-specific sorting decision (eject or reject) by the computing technology. The spatial separation of objects is therefore of utmost importance. Their mass, high or low, in comparison to other particles in the material stream, is irrelevant. The performance of an SBS unit is accordingly related to the space particles occupy in the detection zone and only indirectly correlated with the throughput rate. This paper therefore applies, the occupation density rather than the throughput rate as a reference parameter to describe the capacity of an SBS machine. For industrial applications, conversion into throughput rates considering material-specific grammages is otherwise required.

Fluctuations of the occupation density mostly result from batch processes integrated into an SBS plant, e. g. opening packages or bales. A second key parameter found fluctuating in SBS plants is input composition, because of the delivery of input material from different (urban/rural) regions.

Variations in occupation density and input composition, as well as other factors like surface moisture and roughness (Küppers et al., 2019b), and mechanical stress (Küppers et al., 2019a) can affect the purity and recovery of products in two ways:

- Errors in detection, recognition and classification of particles (sensor and algorithm)
- Errors in mechanical discharge (conveyor belt, chute, pressurized air nozzle bar)

On the one hand, a high occupation density, or throughput rate, may impact the recovery and purity of the output as overlapping particles impede the analysis of the underlying material. Restrictions and a significantly reduced belt speed on standard sorting machines are required especially for sorting light and flat materials, such as films, because of their low weight and high surface coverage (Beel, 2017). On the other hand, high throughput rates are desirable to produce large amounts of products in a short time to be economically sound. No systematic study on the effects of occupation density on SBS of plastics has been conducted yet, however.

The two main factors affecting SBS efficiency, i. e. input composition and occupation density, were addressed in systematic testing series. Data hereby obtained provides insight for better understanding of the efficiency of SBS processes.

Material and Methods

Material

1,000 rectangular LDPE chips (white and red) were used as input material, each featuring an investigated visible surface area of approx. 18.3 cm², a width of 30 mm, an average length of 61 mm and a thickness of 3 mm (Figure 1).

The grammage of these chips amounts to 0.27 g/cm² and the average particle weight is 4.9 g. In the conducted experiments, white particles were regarded as 'eject' and supposed to be discharged via air shocks while red particles were considered as 'reject' and not supposed to be discharged.

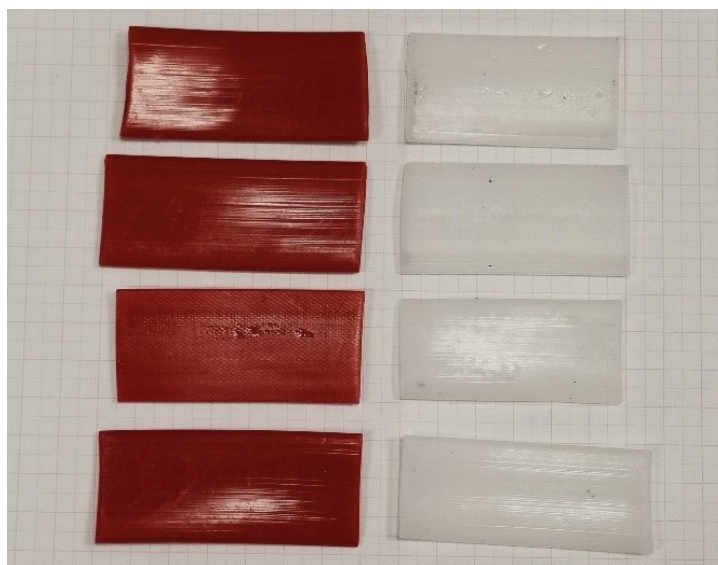


Figure 1: Testing material for sorting experiments – red (reject, left) and white (eject, right) LDPE chips

Equipment

An experimental SBS setup, engineered by Binder+Co AG, was utilized to conduct a total of 160 sorting experiments. As shown in Figure 2, this testing setup consisted of a chute sorter, of a work width and length of 500 mm and 455 mm, respectively, and an upstream vibrating conveyor to feed the sample material. The resolution of the colour sensor is to 0.523 mm x 0.473 mm/px. The valve resolution is 6.25 mm.

Once on the chute, the bulk material was detected using the built in VIS sensor and then classified by means of colour, intensity and brightness. If classified eject material, the respective object was discharged via the compressed air nozzle bar. Any detected object >35 mm, e.g. multiple particles overlapping, was digitally divided into several objects and then classified individually to be rejected or ejected.

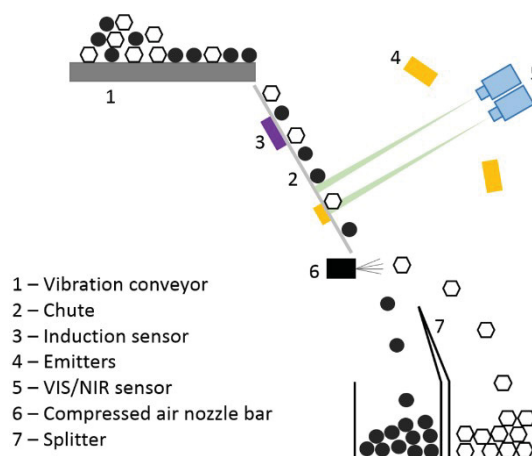
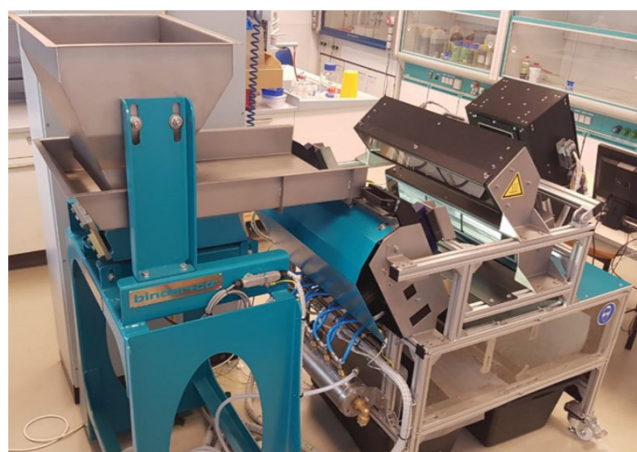


Figure 2: Setup for SBS sorting experiments

Preliminary Tests

Preliminary detection tests were carried out to evaluate the content of falsely classified pixels of reject (red) and eject (white) particles. A series of five trial runs was conducted featuring 1,000 particles for each particle type (eject/reject). Each time, the content of correctly and incorrectly classified pixels was recorded.

Additionally preliminary ejection tests were carried out to determine the average amount of incorrect discharges based on variable sliding speeds, sideways movement, erratic bouncing, etc. on the chute. For this purpose, in five runs each including 1,000 particles supposed to be discharged, were fed to the sorting machine and overlapping of particles was avoided by feeding the particles one by one to the vibration conveyor, ensuring 100 % particle separation. As a result of this approach, the occupation density remained below 2.8 % for all preliminary ejection tests. This enabled assessing the effect of purely mechanically-based sorting errors. The results of the preliminary tests were evaluated by counting the number of falsely rejected and correctly ejected particles.

Main Experiments

To study the effects of input composition on sorting efficiency, eight samples of different composition were created (see Table 2), each containing a total of 1,000 chips.

Table 2: Generated samples and their composition

Sample number	Sample name	Red particles	White particles
1	(95/5)	950	50
2	(90/10)	900	100
3	(85/15)	850	150
4	(80/20)	800	200
5	(70/30)	700	300
6	(60/40)	600	400
7	(50/50)	500	500
8	(20/80)	200	800

On average, this resulted in 5,500,000 detected object pixels per test run, with a standard deviation of about 200,000 pixels, provided that no particles overlapped. The standard deviation σ was calculated using the following equation, where x is the sample mean, \bar{x} is the arithmetic mean and n is the sample size.

$$\sigma = \sqrt{\frac{\sum(x - \bar{x})}{(n - 1)}}$$

Each of the eight samples was sorted 20 times at varying throughput rates. For each experiment, the respective sample mixture of 1,000 particles was placed on the vibration conveyor and fed to the sorting machine by starting the vibration conveyor after adjusting its potentiometer to the intended testing period. After each experiment the number of ejected and rejected particles (red and white) was determined by manual sorting.

Each experiment required a steady feed, since fluctuations of the throughput rate would have resulted in shifting occupation densities, compromising analysis of the results. The testing period of each experiment could therefore deviate slightly from the intended value. The testing periods of the 20 experiments were as evenly distributed as possible for each input composition, ranging from 1.0 s to 70.6 s. Table 3 shows the relationship of testing period, occupation density and throughput rate per metre of working width.

Table 3: Overview of testing period, occupation density and throughput rates

Test duration [s]	Occupation density [%]	Throughput rate [t/(h*m)]
1	278.6	35.02
2	139.3	17.51
3	92.9	11.67
4	69.6	8.75
5	55.7	7.00
6	46.4	5.84
7	39.8	5.00
8	34.8	4.38
9	31.0	3.89
10	27.9	3.50
20	13.9	1.75
30	9.3	1.17
40	7.0	0.88
50	5.6	0.70
60	4.6	0.58
70	4.0	0.50
80	3.5	0.44
90	3.1	0.39
100	2.8	0.35

The occupation density is defined as the ratio of detected object area and available space on the detection area for the testing period. Available space is calculated using the following equation with A=available area, u=sliding speed of particles at the point of detection (1321 mm/s), t=testing period (cf. Table 3) and w=working width (500 mm).

$$A = v * t * w [m^2]$$

After each experiment the particles were thoroughly mixed to generate a uniform blend of all 1,000 particles designed as input material for the next experiment.

Evaluation of Results

The results were analysed based on three evaluation criteria attained at the respective throughput rate of each trial:

- Recovery (directly related to product quantity)
- Yield
- Purity

Recovery (R) is defined as the ratio of complete product mass (m_{eject}) and total input mass (m_{input}) per time unit, providing information on the product quantity generated at a respective throughput rate:

$$R = \frac{m_{eject} \left[\frac{t}{h} \right]}{m_{input} \left[\frac{t}{h} \right]} * 100 \%$$

Product quantity is directly related to recovery, expressed by the mathematical product of throughput rate (Table 3) and recovery (Figure 4) for a given occupation density:

$$P = m_{input} \left[\frac{t}{h} \right] * R$$

The yield (R_w) is based on the amount of the desired component (eject) in the feed material and calculated from the ratio of the mathematical product of determined mass flow (m_{output}) and substance concentration (c_{output}) of the respective sorting product (output) to the respective product of mass (m_{input}) and substance concentration (c_{input} , defined as the content of eject material in the input material) of the feed material (input). It is calculated as follows: (Feil et al., 2016)

$$R_w = \frac{m_{output} \left[\frac{t}{h} \right] * c_{output} [\%]}{m_{input} \left[\frac{t}{h} \right] * c_{input} [\%]} * 100 \%$$

According to Feil et al. (2016), the purity (P_m) of a material is defined as the content of correctly ejected material in the sorting product. It is calculated as follows:

$$P_m = \frac{m_{recyclable\ material} \left[\frac{t}{h} \right]}{m_{impurity} \left[\frac{t}{h} \right] + m_{recyclable\ material} \left[\frac{t}{h} \right]} * 100 \%$$

All three performance indicators are usually mass-specific [w%]. When evaluating SBS sorting experiments, however, particle-related [p%] information is more useful, meaning that a sorting stage is evaluated based on the number of particles contained in each output fraction (reject and eject) and not on the mass of the respective fraction. Conclusions on mass-specific evaluation criteria can be obtained by providing the average particle-specific mass. Particle-related evaluation criteria are displayed accordingly in this paper.

Results and Discussion

Preliminary Tests

During the preliminary detection tests, an average of 0.87 % of the pixels of white objects and 0.65 % of the pixels of red objects were falsely classified, the edges of objects being most commonly affected. Since all objects containing >50 % pixels of the eject material are discharged and misclassification is evenly distributed among all particles, the misclassification rate is not significant for the discharge of objects.

Although misclassification did not result in a rejection of particles, 0.28 % to 0.44 % of all eject particles were rejected in the preliminary ejection test. These amounts of falsely rejected particles were only the result of mechanical errors, because quite low throughput rates had been chosen, overlapping cannot be a reason for rejection. The contents of incorrectly detected and incorrectly rejected particles were therefore insignificant for the used experimental setup. The subsequently conducted main experiments thus allow statements to be made about the best operation conditions of sorting stages in treatment plants applying SBS machinery that are based on input composition and occupation density of a sorting stage only.

Recovery and Product Quantity

The effects of occupation density on the recovery for different input compositions are displayed in Figure 3. Evidently the recovery decreases with increasing occupation density. For rising eject shares of input, maximum recovery increases (usually at the lowest occupation density).

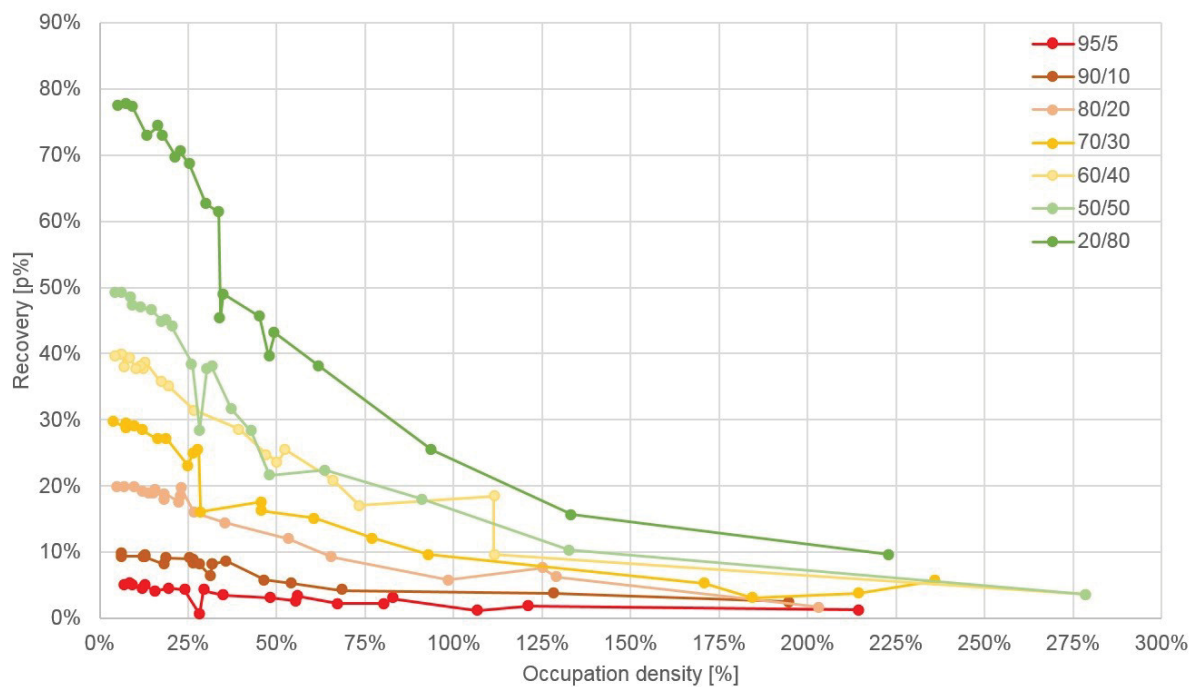


Figure 3: Effects of occupation density on recovery for different input compositions – occupation density <300 %

Since industrial applications most often run at quite low occupation densities the graphs for recovery and product quantity in Figure 4 are displayed for occupation densities <100 %. Despite decreasing recovery, product quantity evidently rises with increasing occupation density following a saturation graph.

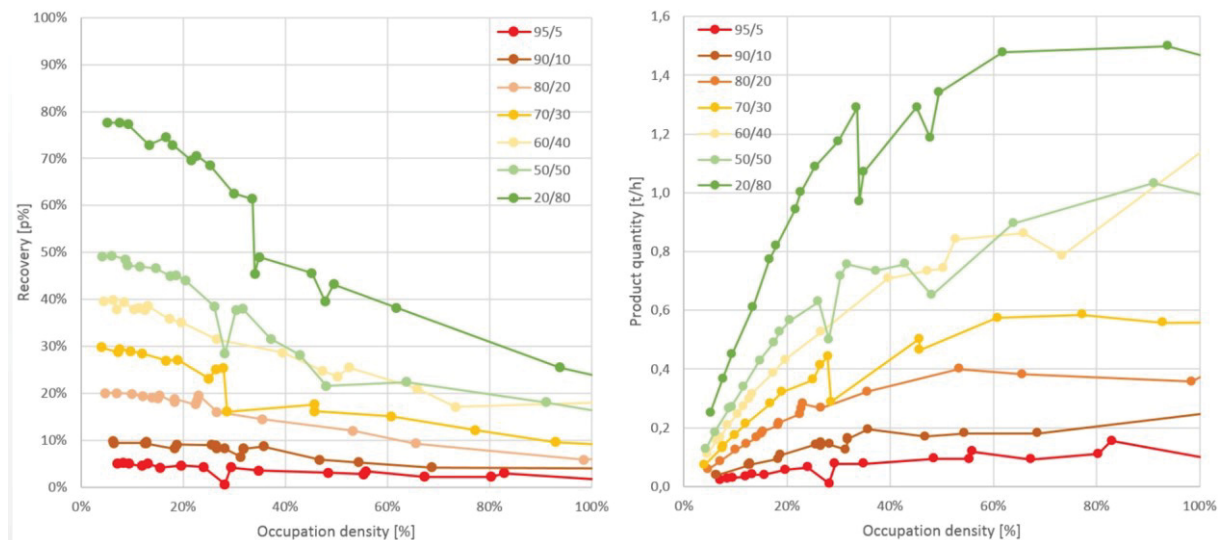


Figure 4: Effects of occupation density on recovery (left) and product quantity (right) for different input composition – occupation density <100 %

The slope of shown saturation graphs most often approaches zero when occupation densities reach 40 % to 60 %. The higher the content of reject particles in the input, the earlier saturation is reached. The slopes of well-balanced inputs (50/50 and 60/40) drop for higher occupation densities. When considering the option of increasing throughput, the result indicates that sorting at high throughput rates may only be reasonable for input material of a balanced composition with regard to product quantity. For other input compositions, high occupation densities show less benefit in this regard.

In general, there are direct correlations observed between recovery and both occupation density and input composition (the content of particle-related eject in input) which may permit forecasting the product quantity as a function of influencing factors. Use Figure 4 to determine the occupation density that is most suitable for a reasonable product quantity, depending on the respective input composition. Note that reject quantity increases with eject quantity.

Yield

The effect of occupation density on yield for different input compositions is given in Figure 5. With rising occupation density, the yield decreases exponentially from approx. 98 p% to approx. 10 p% for all input compositions identically.

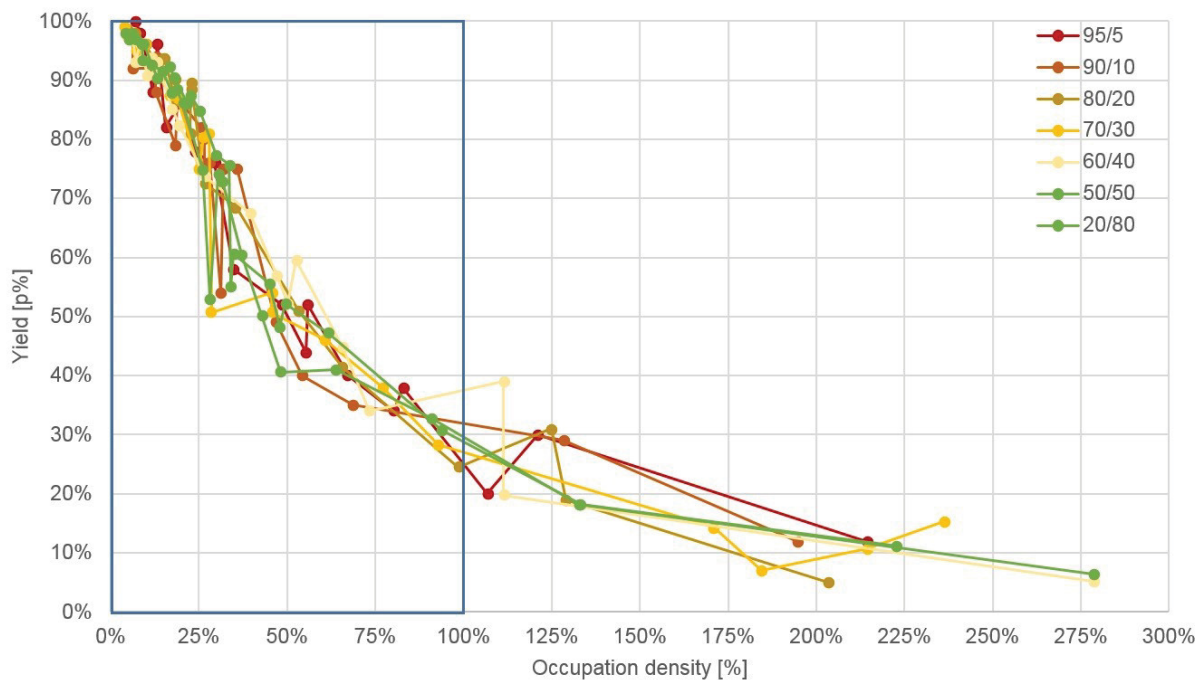


Figure 5: Composition-related effects of occupation density on yield

Since industrial applications most often run at occupation densities <<100 %, only the selected area shown in Figure 5 (blue frame), was taken into account for further analysis. Figure 6, therefore, gives the graph of the yield for all experiments at an occupation density <100 %.

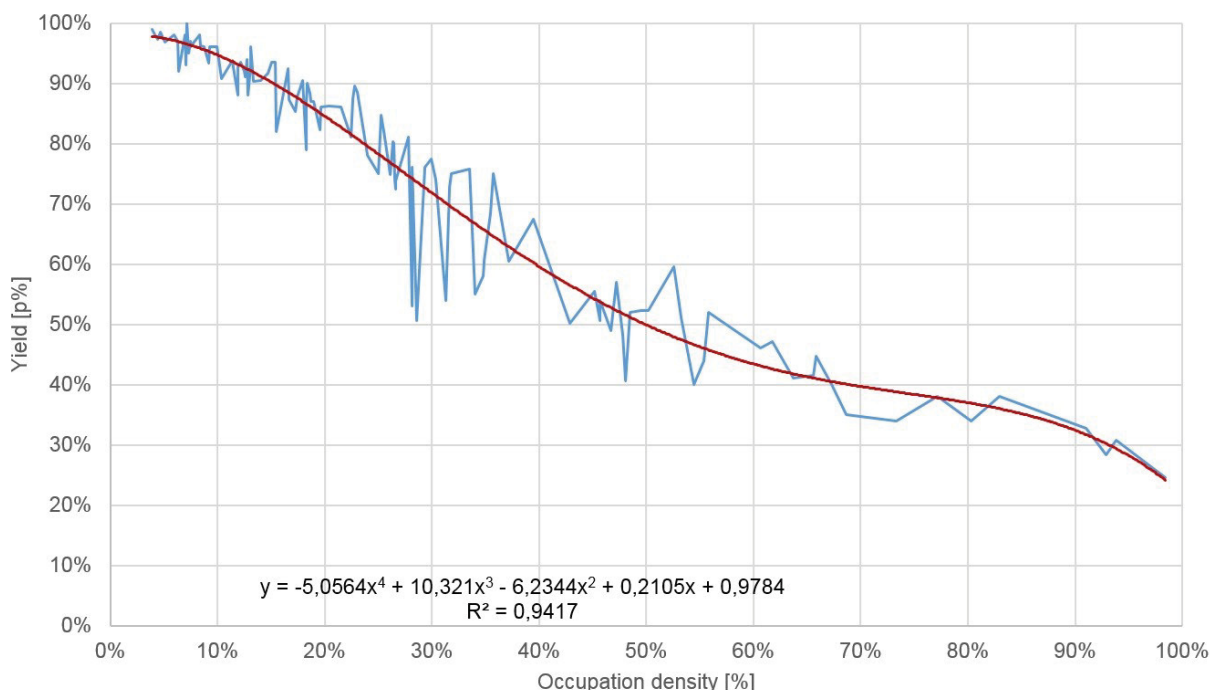


Figure 6: Average effect of occupation density on yield - occupation density <100 %

Additionally, the average yield is shown (red) as a polynomial function of the fourth degree with a coefficient of determination of $R^2=0.9417$. The inflection points of this approximation function are located at occupation densities of 27.6 % and 74.5 %. The first inflection point is reached at an occupation density of about 30 % where its rising value impairs the yield very much. The

second inflection point is reached at an occupation density of 75 % when changes to its value have a much smaller impact on the yield. This is consistent with a range of occupation densities chosen for calculating the average yield. Up to an occupation density of 100 %, the yield decreases constantly. Beyond, the decrease subsides. If values >100 % were included for the occupation density when calculating the approximation function, there was no drop of the polynomial function at an occupation density of 100 %.

Figure 6 shows that the occupation density affects the separation of eject particles while the input composition has no effect on the yield. This information helps to determine the highest occupation density while still achieving acceptable eject losses that may be controlled by, e.g., a quota, independent of the input composition.

Note that fluctuations of the yield increase significantly at occupation densities >27 %. This can be traced back to the elevated potential for overlapping as occupation densities increase since overlapping can either lead to eject losses (reject particles covering eject particles leading to reduced yield by rejection of both particles) or to a discharge of reject particles (eject particles

Effects on the Sorting of Rejects - Purity

The effects of changes to the input composition and occupation density on the absolute number of reject particles wrongly sorted into the eject fraction are displayed in Figure 8. Up to 35 red particles were sorted incorrectly. For clarity purposes, only trend lines (saturation curves) are shown alongside the raw data in Figure 7 covering reject particles leading to increased yield by ejection of both particles).

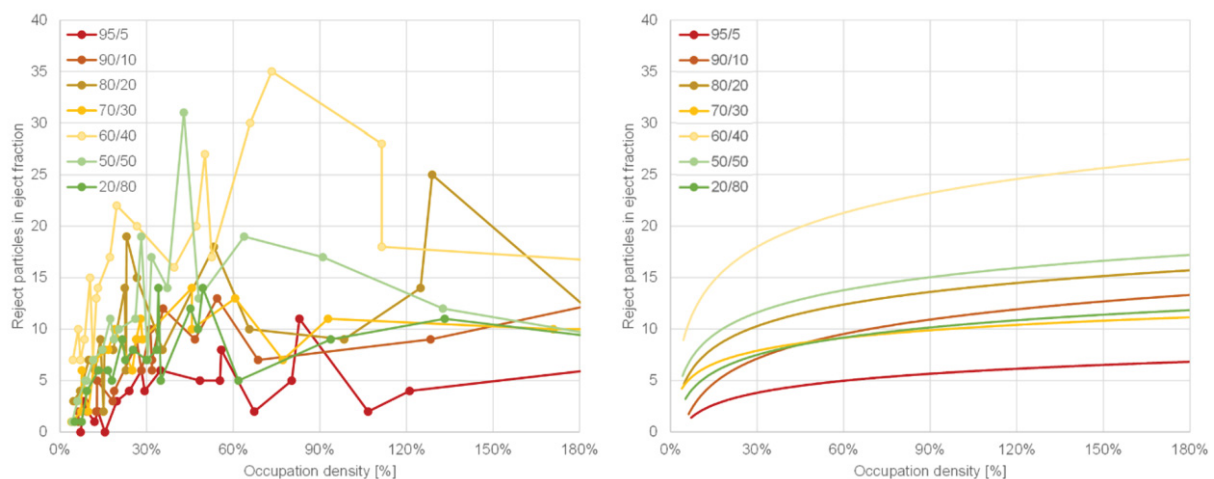


Figure 7: Influence of occupation density on the ejection of reject particles for different input compositions (left: raw data, right: mathematical fit) – occupation density <180 %

The highest number of misclassifications was recorded for the quite balanced mixing ratios of 60/40, 50/50 and 70/30, while the number of falsely ejected reject particles is smaller for imbalanced input compositions. In general, the slope of all graphs is much reduced at

occupation densities of around 30 %. This means that the absolute number of incorrectly ejected reject particles is significantly less prone to increasing with rising occupation densities if the general level is $> 30\%$.

As a result of the exponential decrease of recovery and the concave increase of the number of falsely ejected reject particles, a linear decrease of purity in the eject fractions can be observed for increasing occupation densities (see Figure 8).

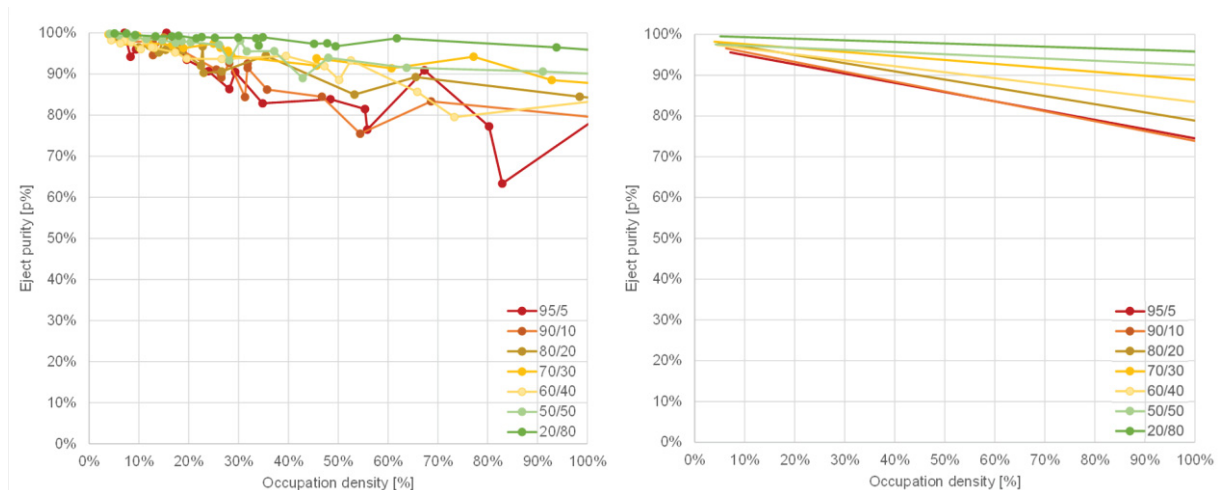


Figure 8: Effects of occupation density on eject purity for different input compositions

A tendency to greater volatility can be observed for the input material if the content of eject particles is small. This trend is consistent with the sample size used for all experiments. For input samples with low contents of eject particles, even small numbers of falsely ejected reject particles constitute quite large amounts of impurities in the eject fraction. Fluctuations of the absolute numbers of incorrectly ejected reject particles therefore rather affect the graphs of input samples with high content of reject particles than vice versa.

Figure 8 shows that, as eject content of the input of a sorting stage increases, the slope of the resulting linear graph softens. While the negative gradient of the linear functions in principle increases with the reject content in the input, the magnitude of this change is not consistent. The graphs of the input samples 70/30 and 60/40 display an anomaly concerning the otherwise consistently increasing negative gradient of the linear graphs.

Economic Potential

This paper highlights the effects of input composition and throughput rate on recovery/product quantity, yield, and purity of the eject fraction from SBS stages. Better knowledge of the interdependence of these variables was also acquired.

Where the accuracy of sensory detection and mechanical efficiency is known, both datasets can be combined to assess the efficiency of SBS steps. Each input composition imposes an upper limit on the achievable recovery, the yield, and purity. This upper limit cannot be raised

by changes to the experimental setup, say, by applying a better sensor, since it is a function only of the ratio of eject to reject particles in the input stream.

To demonstrate the value of the ascertained results, Figure 9 shows a simplified sample application. The graphs (yellow= yield, red=eject purity and green=product quantity) are displayed for a certain input composition.

It was assumed that the eject fraction, produced during this exemplary sorting stage, can be sold for different prices (100/80/60 €/t), depending on its purity (95/90/85 wt%) achieved by sorting. For simplification purposes, assume that the mass balance is in accordance with particle related composition.

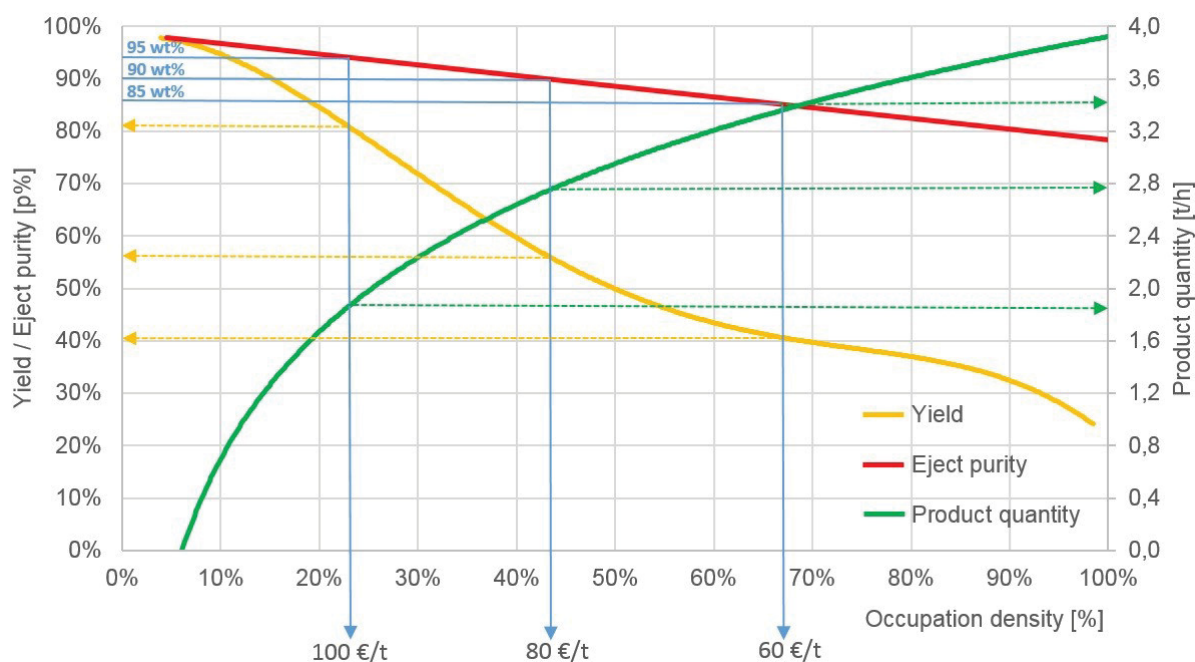


Figure 9: Graphs of yield (yellow), eject purity (red) and product quantity (green) for an sample case; blue arrows – material value for a specific quality; yellow arrows – obtainable yield for a specific eject purity; green arrow – obtainable product quantity for a specific eject purity

Purity, quantity, and possible losses of the potential product must be considered to find out at which occupation density (throughput rate) the highest profit per hour is made. For every input material whose sorting step can be described with the graphs shown in Figure 9, the price and quality of the respective maximum product quantity can therefore be located at the secondary axis of Figure 10 (green arrows). In Table 4, the best occupation densities for meeting the quality requirements are given, including the corresponding product price, yield, product quantity and arising profit per hour.

Table 4: Profit per hour with respective process and product parameters

Occupation density	Quality requirement	Product price	Yield	Product quantity	Profit
23 %	95 wt%	100 €/t	81 wt%	1,85 t/h	185 €/h
44 %	90 wt%	80 €/t	56 wt%	2,78 t/h	222 €/h
67 %	80 wt%	60 €/t	41 wt%	3,45 t/h	207 €/h

Evidently, the highest obtainable profit is found at an occupation density of 44 %, even though the generated product quantity is highest at an occupation density of 67 % and the highest yield would be generated at an occupation density of 23 %. Therefore, knowing the interdependencies of the described factors may help optimizing a sorting stage in the first place.

Conclusion

Evaluating the efficiency of an SBS machine without running sorting experiments, depends on a multitude of influencing factors. These factors can be divided into two categories that do not influence each other.

- Factors affecting the functionality of built-in sensors, reducing the content of particles that can be detected, recognised, and classified
- Factors related to mechanical discharge issues, reducing the efficiency of an SBS machine independent of the accuracy and suitability of built-in sensors

The scientific results shown here provide a basis for assessing the efficiency of SBS units in sorting plants. Displayed data comprises the predominant influencing factors (input composition and occupation density) affecting mechanical discharge issues.

When combined with the sensor-specific efficiency (depending on what a sensor is used for), these data can be used to predict the efficiency of a machine and maybe even the efficiency of many connected SBS machines.

The influence of input composition and throughput rate on sorting efficiency has been established using model mixtures sorted in an experimental setup at various throughput rates. The following main conclusions are based on the experimental series run with homogeneously shaped particles, evenly distributed particle weights and uniform particle size for eject and reject particles:

- Input composition does not affect the yield for any throughput rate/occupation density.
- With increasing occupation density/throughput rate, the yield decreases exponentially from approx. 98 p% to approx. 10 p%.
- The average yield, a function of the occupation density/throughput rate, can be shown as a polynomial function of the fourth degree for occupation densities <100 % (Figure 6).

- As occupation density/throughput rate rises, product quantity increases (despite a decrease in recovery) following a saturation curve that reaches maximum for an occupation density of approx. 60% (Figure 4).
- Eject purity can be plotted as a descending linear function of occupation density/throughput rate. The slope of this function is related to the input composition.
- The higher the eject content in the input composition of an SBS stage, the smaller the slope of the related descending linear function (see Figure 8).

Profounder datasets may be obtained in large scale experimental series using stable input compositions and longer test durations are advisable. Other influencing factors like grain size distribution of the input material, particle shape, and machine design should be examined to expand the dataset presented in this paper.

Actually material flows in sorting plants are subject to powerful fluctuations due to changes to the input composition and irregular material discharge of upstream processing machinery. As has been shown here, such temporarily fluctuating throughput rates can painfully reduce the sorting efficiency of SBS stages. Choosing processing machinery to regulate input rates and to discharge the output fractions regularly can enhance the performance of downstream sorting stages at the same overall throughput rate. Another option of how to reduce fluctuating input rates is using bunkers. Depending on the scope of fluctuations, the required bunker volume may vary, causing high investment costs. This approach may not be feasible for material streams like light-weight packaging waste that, due to its non-bulk properties, could generate a blockage when stored in a bunker.

References

- Alaya, M.A., Tóth, Z. and Géczy, A. (2019), “Applied Color Sensor Based Solution for Sorting in Food Industry Processing”, *Periodica Polytechnica Electrical Engineering and Computer Science*, Vol. 63 No. 1, pp. 16–22.
- Cubero, S., Aleixos, N., Moltó, E., Gómez-Sanchis, J. and Blasco, J. (2011), “Advances in Machine Vision Applications for Automatic Inspection and Quality Evaluation of Fruits and Vegetables”, *Food and Bioprocess Technology*, Vol. 4 No. 4, pp. 487–504.
- Dalm, M., Buxton, M.W.N., van Ruitenbeek, F.J.A. and Voncken, J.H.L. (2014), “Application of near-infrared spectroscopy to sensor based sorting of a porphyry copper ore”, *Minerals Engineering*, Vol. 58, pp. 7–16.
- Eurostat (2019), “Packaging waste statistics. Statistics Explained”, available at: <https://ec.europa.eu/eurostat/statistics-explained/pdfscache/10547.pdf> (accessed 17 July 2019).
- Feil, A., Thoden van Velzen, E. U., Jansen, M., Vitz, P., Go, N. and Pretz, T. (2016), “Technical assessment of processing plants as exemplified by the sorting of beverage cartons from lightweight packaging wastes”, *Waste Management*, Vol. 48, pp. 95–105.
- Gundupalli, S.P., Hait, S. and Thakur, A. (2017), “A review on automated sorting of source-separated municipal solid waste for recycling”, *Waste Management*, Vol. 60, pp. 56–74.

- International Organization for Standardization (2008), *Plastics - Guidelines for the recovery and recycling of plastics waste* No. 15270:2008.
- Jansen, M., Feil, A. and Pretz, T. (2012), "Recovery of Plastics from Household Waste by Mechanical Separation", in Thomé-Kozmiensky, K.J. and Thiel, S. (Eds.), *Waste management: Volume 3, Recycling and Recovery*, TK-Verl. Thomé-Kozmiensky, Neuruppin.
- Knapp, H., Neubert, K., Schropp, C. and Wotruba, H. (2014), "Viable Applications of Sensor-Based Sorting for the Processing of Mineral Resources", *ChemBioEng Reviews*, Vol. 1 No. 3, pp. 86–95.
- Küppers, B., Chen, X., Seidler, I., Friedrich, K., Raulf, K., Pretz, T., Feil, A., Pomberger, R. and Vollprecht, D. (2019a), "Influences and consequences of mechanical delabelling on PET recycling", *Detritus*, No. 0, p. 8.
- Küppers, B., Schloegl, S., Oreski, G., Pomberger, R. and Vollprecht, D. (2019b), "Influence of surface roughness and surface moisture of plastics on sensor-based sorting in the near infrared range", *Waste Management & Research*.
- Lessard, J., Bakker, J. de and McHugh, L. (2014), "Development of ore sorting and its impact on mineral processing economics", *Minerals Engineering*, Vol. 65, pp. 88–97.
- Mesina, M.B., Jong, T.P.R. de and Dalmijn, W.L. (2007), "Automatic sorting of scrap metals with a combined electromagnetic and dual energy X-ray transmission sensor", *International Journal of Mineral Processing*, Vol. 82 No. 4, pp. 222–232.
- Rahman, M.O., Hussain, A. and Basri, H. (2014), "A critical review on waste paper sorting techniques", *International Journal of Environmental Science and Technology*, Vol. 11 No. 2, pp. 551–564.
- The European Parliament and of the Council of the European Union (2018), *Directive (EU) 2018/ of the European Parliament and of the Council of 30 May 2018 amending Directive 2008/98/EC on waste*.
- Tu, S.S., Choi, Y.J., McCarthy, M.J. and McCarthy, K.L. (2007), "Tomato quality evaluation by peak force and NMR spin–spin relaxation time", *Postharvest Biology and Technology*, Vol. 44 No. 2, pp. 157–164.
- Workman, J. and Springsteen, A.W. (1998), *Applied spectroscopy: A compact reference for practitioners*, Academic Press, San Diego.

8 PUBLICATION 7

Potential of Sensor-Based Sorting in Enhanced Landfill Mining

Küppers B, Hernández Parrodi JC, García López C, Pomberger R, Vollprecht, D (accepted)
Potential of Sensor-Based Sorting in Enhanced Landfill Mining. Accepted by Detritus

Annotation on my own contribution to publication 7:

I designed and planned the experiment series with support of Juan Carlos Hernández Parrodi and Cristina García López. I supervised the SBS experiments, which were conducted by Juan Carlos Hernández Parrodi and Cristina García López. The results were analysed by Juan Carlos Hernández Parrodi and Cristina García López and evaluated by me with regard to the potential of SBS in ELFM. I wrote the publication under the guidance of Daniel Vollprecht. All co-authors reviewed the publication, which was revised by Juan Carlos Hernández Parrodi and me.

POTENTIAL OF SENSOR-BASED SORTING IN ENHANCED LANDFILL MINING

Bastian Küppers¹, Juan Carlos Hernández Parrodi², Cristina Garcia Lopez³, Roland Pomberger¹ and Daniel Vollprecht¹

¹ Montanuniversität Leoben, Franz-Josef-Str., Leoben 8700, Austria

² Renewi Belgium SA/NV, New-Mine project; Montanuniversität Leoben, Department of Environmental and Energy Process Engineering

³ RWTH Aachen University - Institut für Aufbereitung und Recycling, Wüllnerstrasse 15, Aachen 52062, Germany

Article Info:

Received:

27 May 2019

Revised:

26 July 2019

Accepted:

19 August 2019

Available online:

xxxx 2019

Keywords:

Enhanced Landfill Mining

Sensor-based Sorting

NIR Spectroscopy

ABSTRACT

In landfill mining, simple technologies and processing chains are frequently applied to excavated material in order to extract recyclable metals and high-calorific fractions used in energy recovery. Sensor-based sorting is one way to extract more and better material from a landfill. Two testing series have been performed using state-of-the-art technology to assess the technical feasibility of classifying and sorting landfill material with the aid of near-infrared spectroscopy. Fractions were classified as inert and combustible and sorted by particle sizes ranging from 90-30 mm, from 30-10 mm and from 10-4.5 mm for water content levels of 0 wt% and of 15 wt%, respectively. Additional tests applied different landfill mining materials. Polypropylene (PP), polyethylene (PE) and polyvinyl chloride (PVC) products were produced, using sensor-based sorting, from a mixed fraction of particle sizes ranging from 60-200 mm. Both test series applied air-classified heavy fractions gained from two distinct processing schemes of landfill mining projects in Belgium and in Austria. Results show that the separation and classification of inert and combustibles is feasible, enriching inert fractions with purities of 97.7 wt% to 99.6 wt% derived from inputs whose inert contents achieved 85.6 to 98.8 wt%. Efficient sorting is a function of the level of pre-processing, water content, relative amounts of adhesive fines, input composition and particle size ranges of the input material. Results from the second test series show that PP, PE, PVC and other materials can be successfully distinguished, achieving correct classification and ejection into respective product fractions of 91.8-99.7 wt%.

1. INTRODUCTION

In the past, landfills were considered cost-effective and final means of waste disposal (Krook, J. et al., 2012). Nowadays such landfills pose both a problem and a chance. Spatial constraints, landfill-based hazards like leachate and methane emissions (Danthurebandara, M. et al., 2015) and shortage of landfill volume (Wörrle, J., 2018) can be arguments in favour of landfill mining (LFM) activities (Quahebeur, M. et al., 2013, Mor, S. et al., 2006, Sormunen, K. et al., 2008).

LFM is usually expensive and not economically feasible. Economic feasibility could be achieved, however, by using mechanical processing to recover marketable valuable materials. Since the 1950s, LFM projects have mostly applied simplified process chains using a screening stage and optional subsequent air classification and magnetic

separation, among other processes, to render mechanical processing as cost-effective as possible (Krook, J. et al., 2012). As a consequence, only limited amounts of landfill resources (metals and refuse-derived fuel (RDF)) could be recovered in the past (Krook, J. et al., 2012). This limitation may be due to the fact that the reduction of environmental impacts and landfill remediation has commonly been given preference to the recovery of land or of landfill volume (Danthurebandara, M. et al., 2015).

By contrast, the design of enhanced landfill mining (ELFM) is targeting the extraction of valuable materials for recycling (waste-to-material, WtM) and for energy production (waste-to-energy, WtE). The TönsLM project, for instance, has developed and examined scenarios based on rather complex process chains and innovative technologies. In addition to comminution, ballistic separators, screening and magnetic separation, also eddy current separators and



* Corresponding author:

Bastian Küppers

email: bastian.kueppers@unileoben.ac.at



Detritus / Volume 08 - 2019 / pages 1-7

<https://doi.org/xxxxxxxxxxxxxxxx>

© 2019 Cisa Publisher. Open access article under CC BY-NC-ND license

near-infrared (NIR) sorters were considered in processing (Breitenstein et al. 2016), enabling higher and purer yields of recyclables. This resulted in better market prices, facilitating economically improved mining.

Studies have shown that ELFM is mainly inspired by the recovery of landfill volume and by the extraction of metals and of high-quality combustible fractions (Danthurebandara, M. et al., 2015; Jones, P. et al., 2013; Kieckhäfer, K. et al. 2017). Most published ELFM projects so far are still at the planning stage, however. One main caveat of any practical implementation of (E)LFM projects is the risk that expected costs may exceed the achievable profit (Kieckhäfer et al. 2017). If framework conditions for ELFM should change, this programme will become more attractive to landfill operators (Kieckhäfer, K. et al, 2017). This paper intends to shed more light on the potential recovery of recyclable and energetically valuable materials.

Utilization of the high-calorific fraction derived from (E) LFM has been practically tested in the recent past (Rotheut, M. and Quicker, P., 2017, Wolfsberger, T. et al, 2015). The relative amount of heavy metals contained in a high-calorific fraction limits its use in Austrian co-incineration plants (Wolfsberger et al, 2015). Since the distribution of heavy metals in the individual groups of substances and particle size ranges may vary significantly, suitable pre-treatment (separation of fractions contaminated with heavy metals) can prevent exceeding the limit values (Wolfsberger, T. et al, 2015, García López, C. et al., 2018).

Studies of Rotheut, M. and Quicker, P. (2017) concerning the energetic utilisation of RDF from LFM have shown that also the RDF's properties may vary a lot, affecting in particular calorific value, water and ash contents. Material from the 'Pohlsche Heide' landfill was excavated, for example, and processed in a state-of-the-art mechanical-biological waste treatment plant. Once the metals had been removed, the light fraction recovered using air classification was thermally converted into RDF. Calorific values between 9.2 and 23.9 MJ/kg, ash contents of up to 49.6 % and water contents of 9.1 % to 30 % were observed. These findings as well as the sometimes high chlorine content caused the fuel properties of the examined material to be ranked as troubling.

Regarding mono-combustion of high-calorific fractions from LFM, the relative amounts of HCl and SO₂ included in the raw gas have been observed to exceed customary process values. In addition, the generation of steam has varied strongly while the bottom ash has shown finer particle size distributions and increased contents of Cl in the eluate. In clean gas, the only elevated readings related to the relative amount of HCl. Based on these and further experiments the authors conclude that co-combustion of RDF from LFM with RDF from municipal solid waste (MSW) in a 1:1 ratio seems feasible while mono-combustion of non-pre-treated material remains troubling (Rotheut, M. and Quicker, P., 2017).

Mechanical recycling and other options, such as gasification, pyrolysis and hydrogenation, can only be pursued if more elaborate pre-treatment (cleaning, drying, comminution and thorough sorting) takes place (Zhou, C. et al., 2014). The waste-to-energy (WtE) route is expected to be

a plausible method of utilising high-calorific fractions from (E)LFM (García López, C. et al., 2018, Quaghebeur, M. et al., 2013) while a waste-to-material (WtM) route is not considered promising due to the increased levels of contaminants in recyclables (Quaghebeur, M. et al., 2013). Generating potential RDF (pRDF) of a quality sufficient for (co-) combustion from (E)LFM requires the separation of material classes containing contaminants like PVC (chlorine), minerals (increased ash content) and metals.

Compared to the calorific fractions, recycling inert constituents such as metals, glass, ceramics and stone is estimated to be more promising (Quaghebeur, M. et al., 2013). Mechanical processing, e.g. the separation of wood, paper and plastics from inerts, is required in this case, either to reduce the TOC or the chloride content of fractions intended for construction aggregates.

Sensor-based sorting (SBS) can be utilised to separate impurities from the respective fractions (pRDF and inert) in order to comply with the boundaries of both the high-calorific fraction and the inert fraction. One promising approach is the treatment of 3D or heavy fractions derived from air classification or ballistic separation. Generating suitable products from an ELFM process may require carrying out not only single but also multi-stage sorting steps (cascading application of SBS technology). This way, several types of plastics can be separated, resulting in pure product fractions. Near-infrared technology was found helpful both for distinguishing inert from pRDF and for differentiating types of plastic that then could be separated using compressed air blasts (Kieckhäfer, K. et al., 2017) (Beel, H., 2017).

Flawless functioning of SBS units is achieved by pre-treating LFM material. An important step of preconditioning is drying the landfill material, hopefully to improve subsequent mechanical processing (García López, C. et al., 2018). Contaminants such as fine adhesions and coarse particles should be separated and fractions of processable particle size ranges produced using pre-classification. The resulting particle size ranges have to match machine requirements of subsequent processing units. In addition, this classification can be used to subdivide the material flow into volume and mass flows suitable for further treatment, preventing overloading of the downstream processing equipment. Pre-processing can also be used to enrich the valuable substances or to separate contaminants into specific grain size ranges and material flows (Pretz, T.; and Julius, J., 2008).

If the treatment is carried out on a landfill site, SBS technology must be adapted to adverse environmental conditions. The treatment can be affected by weather conditions or by dust, raising the risk of e. g. soiling on light bulbs that would cause malfunction or impairment of the SBS equipment (Gundupalli, S. et al., 2017).

This paper discusses near-infrared-(NIR)-based sorting since this technology provides a wide range of possible applications. However, NIR sensors can only analyse the surface of particles and are therefore particularly susceptible to external contamination and adhesions (Pomberger and Küppers, 2017). That is why research regarding the application of this technology in LFM is of particular interest. Two applications for NIR SBS technology are examined:

- Enrichment of the inert fraction using the separation of combustibles (plastics, paper, cardboard, wood, etc.)
- Distinction and separation of various types of plastic from a LFM process to create unpolluted fractions

To verify the technical feasibility of these applications, the distinctness of combustibles, inerts and impurities is examined and quantified.

2. MATERIALS AND METHODS

ELFM projects were conducted at Mont-Saint-Guibert (MSG), Belgium, and on the Halbenrain landfill, Austria. Excavations and mechanical processing in MSG were carried out to verify the suitability of a ballistic separator as the first processing unit in the mechanical processing of LFM material. In Halbenrain, the purpose of on-site examinations was to test whether the available mechanical biological treatment plant was able to process LFM material.

At the MSG landfill, municipal solid waste (MSW) and construction and demolition (C&D) waste were disposed of between 1958 and 1985. For the purposes of this examination, the top clay layer was removed first. Next, a total of about 425 m³ of landfill material was excavated in four batches and treated with the ballistic separator (STADLER STT 6000). The LFM material was processed in two stages, using mesh sizes of 200 mm and 90 mm to produce five output streams (cf. Figure 1). Detailed information concerning landfill site, processing, sampling and landfill composition is provided by García López et al. (submitted) and Hernández Parrodi et al. (submitted).

The fine fraction samples (<90 mm), gained during ballistic separation, were divided into two fractions and treated at two different water content levels (0 wt% and 15 wt%) or using screening into the grain size ranges of 90-30 mm, 30-10 mm, 10-4.5 mm and <4.5 mm, followed by air classification. Heavy fractions from air classification (90-30 mm, 30-10 mm and 10-4.5 mm) yielded input material for SBS experiments and were therefore drawn on during the examination.

At the Austrian Halbenrain landfill, about 500 t of LFM material were excavated and processed in an on-site mechanical and biological treatment plant in 2016 to study op-

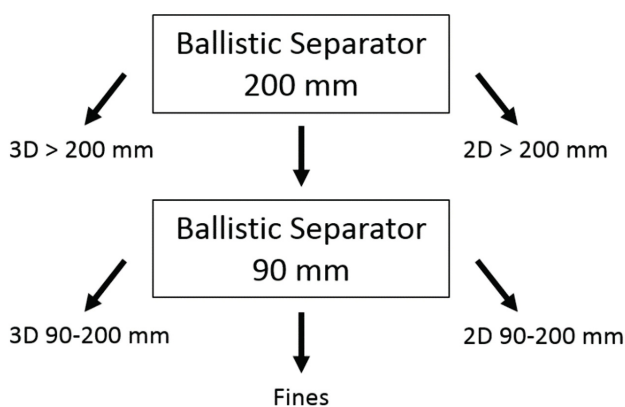


FIGURE 1: Procedure for mechanical treatment of landfill material in MSG

tions for RDF and metal recovery. The treatment included three to four weeks of biological drying in rotting boxes, followed by shredding, multiple screening stages (screen cuts: 200 mm, 60 mm, 14 mm), separation of ferrous and non-ferrous metals using magnetic and eddy current separation and, finally, air classification. More detailed information is provided by García et al., 2018.

For SBS examinations, samples were taken from the heavy fraction of 200-60 mm. These samples were hand-picked and all particles (1377 pieces) categorised by visual inspection and Fourier Transformed Infrared Spectroscopy (FTIR, Agilent Technologies, Cary 630) according to material types: polypropylene (PP), polyethylene (PE), polystyrene (PS), polyvinyl chloride (PVC), polyethylene terephthalate (PET), and residuals.

A hyperspectral imaging (HIS) near-infrared chute sorter (sensor: EVK HELIOS NIR G2 320, spectral range 990-1700 nm) was used for performing the SBS experiments. The spectral resolution of the sensor was 3.18 nm, its spatial pixel width being 1.60 mm. The frame rate of the line sensor was 476 Hz for an exposure time of 1800 μs. During the experiments, the side of a spatial pixel in the direction of movement was always less than 1.6 mm long. Sorting recipes were created by recording sample objects of each material class. Two recipes emerged:

- Recipe 1 – for treating fractions of 90-30 mm, 30-10 mm and 10-4.5 mm from MSG (objective: separation of combustible from inert materials of the heavy fractions)
- Recipe 2 – for treating air-classified heavy fractions from the Halbenrain landfill (objective: distinction of plastic types PP, PE, and PVC from PS, PET and residuals)

Recordings of the recipes contained spectra allocated to pixels on all sample objects. Spectra from several pixels were collected and an average spectrum for each material was created. These spectra were used as references for classifying object pixels. The classification of different materials was improved by including only such wavelength ranges that displayed significant differences (cf. Figures 2 and 3). As a result, a pseudo-colour was allocated to each object pixel. All objects were then assigned to the material class represented by the predominant pseudo-colour. Particles were separated using air blasts from a compressed air nozzle bar to validate the sorting efficiency of the recipes. Low throughputs were applied to avoid overlapping objects, allowing to quantify correct classification rates unaffected by variations of the throughput.

The spectra used in recipe 1 are given in Figure 2. In total, 16 spectra of pulp-based materials (wood, paper and cardboard) and bone (red), plastics (green) and inerts (blue) were used for this recipe. Wavelength ranges included in the classification cover 1120-1273 nm, 1342-1527 nm and 1618-1674 nm (areas marked red in Figure 2). Soot-blackened plastics cannot be classified by spectral data reflected in the NIR range since they absorb much of the irradiation. Their classification as plastics was facilitated by using the low intensity of reflected radiation.

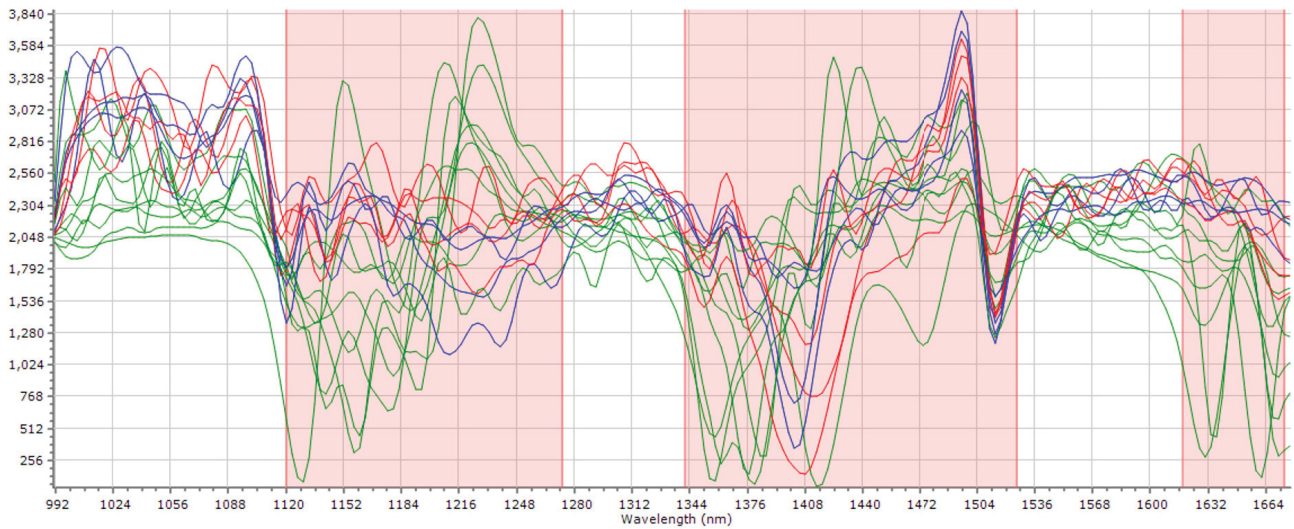


FIGURE 2: Spectral data used to distinguish inerts (blue) and combustibles, consisting of pulp (red) and plastics (green).

For evaluating the results of trials based on recipe 1, an enrichment ratio was calculated to assess the separation efficiency of combustibles and inerts. For this purpose, the purity of a product fraction (inert content in inert product or combustibles content in combustibles product) was divided by the content of the respective material class in the input fraction. If the enrichment ratio was 1 or higher, the material class was enriched via sorting.

Spectra used for the constituent separation of PP, PE and PVC from PS, PET and residuals based on recipe 2 are given in Figure 3. In total, 7 spectra of PP (blue), PE (red) and PVC (green) were applied. Wavelength ranges included in the classification cover 1120-1242 nm, 1339-1414 nm and 1636-1671 nm (areas marked red in Figure 3). To prevent erroneous classification of PVC as PP or PE, soot-blackened plastic was always classified as PVC, based on the low intensity of radiation reflected by such particles. Neither spectra of PS nor of PET or residuals were stored in recipe 2.

For assessing the correct classification rates based on recipe 2, both mass-based (wt%) and particle-based (p%) approaches were examined. For the mass-based approach, the weight of each material class in the eject and reject fraction entered the calculation of yield by material. For the particle-based approach, the numbers of particles in the eject and reject fractions were counted and entered the calculation of yields by material type in a product. Multiple experiments were performed to reduce the effects of outliers due to atypical positioning and mechanical errors from atypical motions of objects during the sorting process. For each trial, all particles were analysed and sorted anew.

3. RESULTS AND DISCUSSION

The results of trials separating inerts and combustibles are given in Table 1. Data on the composition of input and output fractions is given separately for trials based on wa-

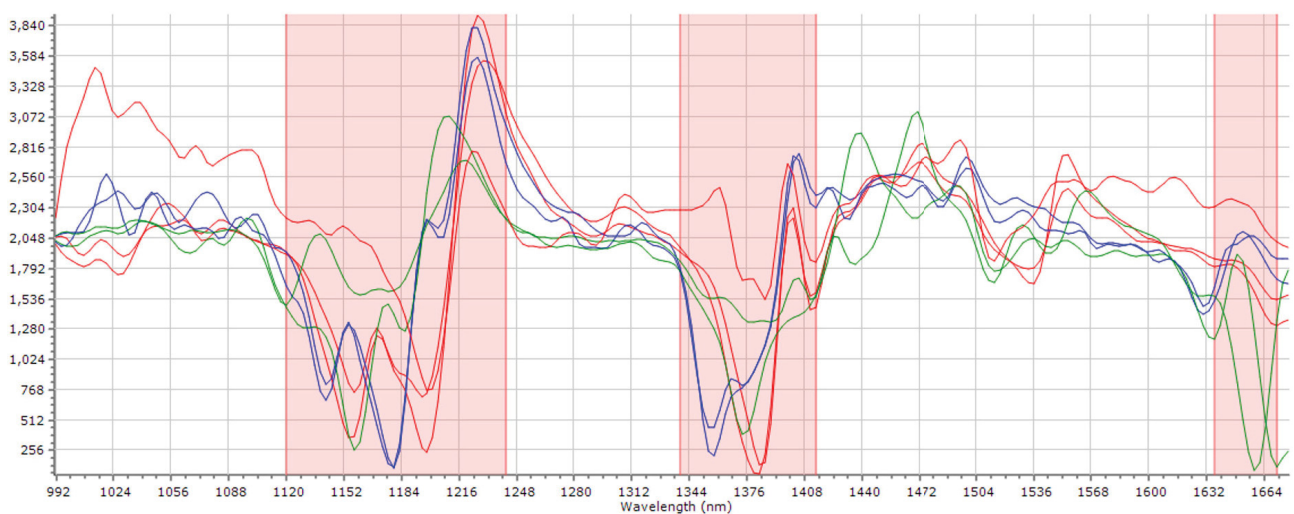


FIGURE 3: Spectral data stored in recipe 2 for distinguishing PP (blue), PE (red) and PVC (green) from PS, PET and residuals.

TABLE 1: Results of sorting trials with Recipe 1.

Water Content [wt%]	0			15		
Size [mm]	90-30	30-10	10-4.5	90-30	30-10	10-4.5
Input						
Inert content [wt%]	88.2	97.1	98.1	85.6	93.7	98.8
Combustibles content [wt%]	11.8	2.9	1.9	14.4	6.3	1.2
Reject - Inert Fractions						
Purity - Inert [wt%]	99.3	99.7	98.8	99.6	97.7	99.4
Yield of inerts [wt%]	99.7	97.8	99.0	99.8	95.1	99.5
Enrichment ratio	1.126	1.027	1.007	1.164	1.043	1.006
Eject - Combustibles Fractions						
Purity - Combustibles [wt%]	62.0	26.3	36.3	68.9	31.3	49.5
Yield of combustibles [wt%]	94.7	72.2	99.0	97.4	66.8	53.6
Enrichment ratio	5.254	9.069	19.105	4.785	4.968	41.250

ter contents of 0 wt% and of 15 wt%, respectively. Comparing the composition of all input fractions demonstrates that the inert content rises with decreasing particle size range for both water content levels. Especially material in the fraction of 90-30 mm contains significantly more combustibles than material in smaller particle size ranges.

The relative content of combustibles in the input is higher for the water content of 15 wt% in particle size ranges of 90-30 mm and of 30-10 mm than in samples containing a water content of 0 wt%. This observation can be explained by higher water absorption in combustibles compared to inerts and increased content of adhesive fines due to the wet surface of combustibles.

All trials achieved high purities for inert fractions (97.7-99.7 wt%) while the purity of combustible fractions was comparatively low (26.3-68.9 wt%). Yet enrichment ratios are low for inert (1,006-1,164) and high for combustibles (4.785-41.250). These results can be attributed to the low content of combustibles in all input fractions, enabling high enrichment ratios, while high inert contents in the input fractions limit enrichment ratios. Rather low purities of combustibles in the respective product fractions can be explained by inert losses wrongly classified and ejected as combustibles. Due to the high amounts of inerts in input fractions, even minor loss of inerts can strongly impact the combustible fractions. The purity of generated combustible fractions could be further improved by applying multiple sorting stages, enriching the combustible fraction even more; the economic feasibility of this approach, however, is in doubt.

The enrichment ratios for inert fractions decrease with particle size while the enrichment ratios of combustibles increase. This is mainly associated with the decreasing relative amount of combustibles in the input for small particle size ranges. For instance, a water content of 0 wt% produced neither a lesser yield of inerts nor of combustibles for the particle size range of 10-4.5 mm, compared to the sorting results of the 90-30 mm fraction. Still, the enrichment ratio of inerts drops with decreasing particle size while the enrichment ratio of combustibles rises.

Although a water content of 15 wt% produces a proportionally lesser yield of combustibles with decreasing particle size, the combustibles enrichment ratio for the particle size range of 10-4.5 mm is highest at 41.250, which is more than twice the respective value for a water content of 0 wt%. This is mostly due to the fact that the lower combustibles content in the input and the 0.5 wt% higher yield of inerts for a water content of 15 wt% have more impact on the sorting efficiency than the yield of combustibles would.

Misclassification, mostly of combustibles but to some extent also of inert, can mainly be referred to faulty classification of pulp material. These particles were characterised by high amounts of adhesive fines on the surface. Such adhesives can impair the spectra, e. g. of paper, resulting in a mixed spectrum of inert and paper. This effect can also be observed in Figure 2 as spectra of pulp-based particles look similar to inert spectra due to their contamination with adhesive fines. The adverse effect of adhesives on SBS is best demonstrated for a water content of 15 wt%, due to increased amounts of adhesives. The yield of combustibles drops with particle size. Especially for the fraction of 10-4.5 mm, major quantities of adhesive fines could be observed on particle surfaces (compare Figure 4).

The sorting results of all trials involving Halbenrain material are given in Table 2. To evaluate the classification and sorting efficiency independently from input composition, only the yield of PP, PE and PVC products is given for each fraction. Results show the average yield of each material class over five runs.

Results of sorting trials show that the particle- and mass-related yields correlate significantly. Differences can be attributed to differing particle masses.

While generating the PP product, neither PVC, PS nor PET were wrongly classified and sorted. Less than 0.8 p% (0.6 wt%) of PE and residuals were falsely ejected.

When sorting out the PE product, the primary misclassification observed was that of PP as PE (3.2 p%/2.1 wt%) while the ejection of PVC, PS and residuals stayed always below a level of 0.8 p% (0.3 wt%), partly due to gliding particles (PS). No misclassification of PET was observed.



FIGURE 4: Reject (left) and eject (right) from SBS trial, water content 15 wt%, fraction 10-4.5 mm.

While producing the PVC product, an increased misclassification of PP (4.4 p%/2.7 wt%), PE (11.0 p%/8.8 wt%) and residuals (5.1 p%/3.5 wt%) was observed which can be attributed to the classification of soot-blackened particles as PVC. No PET was misclassified and discharged as PVC.

An overall distinction between plastic types and separation of such material fractions from LFM could be performed using SBS technology. The relatively high accuracy rates achieved, despite misclassification due to soot-blackened particles, can be explained by the preceding comprehensive biological and mechanical processing as well as by the coarse particle grain size of the examined material, resulting in low amounts of water and adhesives on particle surfaces and enabling mostly correct classification and sorting results.

TABLE 2: Yield of PP, PE and PVC products from Halbenrain LFM air-classified heavy fraction – average of 5 runs.

	PP product	PE product	PVC product
PP yield	94.1 p%	3.2 p%	4.4 p%
	94.8 wt%	2.1 wt%	2.7 wt%
PE yield	0.8 p%	92.9 p%	11.0 p%
	0.6 wt%	91.8 wt%	8.8 wt%
PVC yield	0.0 p%	0.2 p%	95.2 p%
	0.0 wt%	0.1 wt%	99.7 wt%
PS yield	0.0 p%	0.8 p%	0.8 p%
	0.0 wt%	0.3 wt%	0.7 wt%
PET yield	0.0 p%	0.0 p%	0.0 p%
	0.0 wt%	0.0 wt%	0.0 wt%
Residuals yield	0.4 p%	0.4 p%	5.1 p%
	0.3 wt%	0.2 wt%	3.5 wt%

However, further multiple sorting stages and treatments (cleaning, drying, etc.) will be necessary to meet the requirements of recycling and not only those of WtE.

4. CONCLUSIONS

NIR-based SBS trials using pre-treated landfill material show promising results for the application of this technology in EFLM. The separation of inert and combustibles and the distinction between specific types of waste plastic was successfully demonstrated. Sorting efficiency is affected by the level of pre-processing, the water content and the relative amount of adhesive fines, the material composition and the range of particle sizes of the input material at the SBS stage.

While a decent identification of plastic types (except for soot-blackened plastics) using NIR spectroscopy is possible, detecting pulp-based particles and distinguishing them from inerts was sometimes impaired for particle size ranges <30 mm due to adhesive fines, particularly when water was present.

Whether any long-term stability of a sufficiently effective SBS process can be achieved under plausible processing conditions has to be tested large-scale. Problems, e. g. due to dust formation or various degradation states of plastics, may decrease the efficiency rates attained so far. In such cases it might be necessary to adapt the algorithm for material classification.

REFERENCES

- Beel, H.: Sortierung von schwarzen Kunststoffen nach ihrer Polymerklasse mit Hyperspectral-Imaging-Technologie. In: Thomé-Kozmiensky, K. J.: Berliner Recycling- und Rohstoffkonferenz 2017.
- Breitenstein, A; Kieckhäfer, K; Spengler, T.: TönsLM – Rückgewinnung von Wertstoffen aus Siedlungsabfall- und Schlackendeponien. In: Recycling und Rohstoffe, Band 9. 2016.

- Danthurebandara, M.; van Passel, S.; Vanderreydt, I.; van Acker, K.: Assessment of environmental and economic feasibility of Enhanced Landfill Mining. In: *Waste management (New York, N.Y.)* 45. 2015. S. 434–447. Doi: 10.1016/j.wasman.2015.01.041.
- García López, C.; Küppers, B.; Clausen, A.; Pretz, T.: Landfill Mining. A case study regarding sampling, processing and characterization of excavated waste from an Austrian landfill. In: *Detritus* 2 (1), 2018. S. 29. Doi: 10.31025/2611-4135/2018.13664.
- García López, C.; Hernandez Parrodi, J.; Pretz, T.; Raulf, Karoline; Küppers, B.: Landfill mining. Characterization of landfill mining material after ballistic separation to evaluate material and energy recovery. In: *Detritus*, submitted.
- Gundupalli, S.; Hait, S.; Thakur, A.: A review on automated sorting of source-separated municipal solid waste for recycling. In: *Waste management (New York, N.Y.)* 60. 2017. S. 56–74. Doi: 10.1016/j.wasman.2016.09.015.
- Hernández Parrodi, J.; García López, C.; Küppers, B.; Raulf, K.; Vollprecht, D.; Pretz, T.; Pomberger, R.: Case Study on Enhanced Landfill Mining at Mont-Saint-Guibert Landfill in Belgium: Characterization and Potential of Fine Fractions. In *Detritus*, submitted for special issue.
- Jones, P.; Geysen, D.; Tielemans, Y.; van Passel, S.; Pontikes, Y.; Blanpain, B.: Enhanced Landfill Mining in view of multiple resource recovery. A critical review. In: *Journal of Cleaner Production* 55. 2013. S. 45–55. Doi: 10.1016/j.jclepro.2012.05.021.
- Kieckhäfer, K.; Breitenstein, A.; Spengler, T.: Material flow-based economic assessment of landfill mining processes. In: *Waste management (New York, N.Y.)* 60. 2017. S. 748–764. Doi: 10.1016/j.wasman.2016.06.012.
- Krook, J.; Svensson, N.; Eklund, M.: Landfill mining. A critical review of two decades of research. In: *Waste management (New York, N.Y.)* 32 (3). 2012. S. 513–520. Doi: 10.1016/j.wasman.2011.10.015.
- Mor, S.; Ravindra, K.; de Visscher, A.; Dahiya, R.; Chandra, A.: Municipal solid waste characterization and its assessment for potential methane generation. A case study. In: *The Science of the total environment* 371 (1-3). 2006. S. 1–10. Doi: 10.1016/j.scitotenv.2006.04.014.
- Pomberger, R.; Küppers, B. (2017): Entwicklungen in der sensorgestützten Sortiertechnik. In: *Österreichische Abfallwirtschaftstagung 2017*.
- Pretz, T.; Julius, J.: Stand der Technik und Entwicklung bei der berührungslosen Sortierung von Abfällen. In: *Österreichische Abfallwirtschaftstagung* 60 (7-8). 2008. S. 105–112.
- Quaghebeur, M.; Laenen, B.; Geysen, D.; Nielsen, P.; Pontikes, Y.; van Gerven, T.; Spooren, J.: Characterization of landfilled materials. Screening of the enhanced landfill mining potential. In: *Journal of Cleaner Production* 55. 2013. S. 72–83. Doi: 10.1016/j.jclepro.2012.06.012.
- Rotheut, M.; Quicker, P.: Energetic utilisation of refuse derived fuels from landfill mining. In: *Waste management (New York, N.Y.)* 62. 2017. S. 101–117. Doi: 10.1016/j.wasman.2017.02.002.
- Sormunen, K.; Ettala, M.; Rintala, J.: Detailed Internal Characterisation of Two Finnish Landfills by Waste Sampling. In: *Waste management (New York, N.Y.)* 28. 2008. Doi: 10.1016/j.wasman.2007.01.003.
- Wolfsberger, T., Aldrian, A., Sarc, R., Hermann, R., Höllen, D., Budischowsky, A., Zöschner, A., Ragoßnig, A. & Pomberger, R.: LANDFILL MINING: Resource potential of Austrian landfills – Evaluation and quality assessment of recovered MSW by chemical analyses. In: *Waste Management & Research*, 2015. S. 962-974. DOI:10.1177/0734242X15600051.
- Wörle, J.: Immer mehr Bauabfälle: Deponien am Limit. In: *Deutsche Handwerkszeitung*. 2018.
- Zhou, C.; Fang, W.; Xu, W.; Cao, A.; Wang, R.: Characteristics and the recovery potential of plastic wastes obtained from landfill mining. In: *Journal of Cleaner Production* 80. 2014. S. 80–86. Doi: 10.1016/j.jclepro.2014.05.083.

9 SUMMARY

This doctoral thesis contains seven research papers, subdivided into three subject areas that build on one another. The research questions, defined in the subchapters of chapter 1.2, are answered based on the results from these peer-reviewed papers.

Publication 1

Based on the findings of this study, the technical and economic feasibility of utilizing the MBT plant located at the Halbenrain landfill in Austria for the treatment of landfill material was assessed.

Large-scale tests showed that biological drying is required to enable the mechanical processing of landfilled waste. Metal fractions constitute material outputs with the highest economic value in most (E)LFM projects. In this case study, it was found that the share of Fe- and NF-metals, gained via mechanical processing, does not account for enough material (e.g. 3 % Fe-share of the total input material) to achieve an economical treatment of the landfill material in Halbenrain today. In addition, the physical-chemical analysis revealed significant defilement on plastics, resulting in reduced heating values and increased ash content of the potential refuse derived fuel (RDF) fraction. Especially due to the high share of fines (49.3 % <14 mm) in the landfill material, an economical (E)LFM is only attainable if further marketable material fractions can be gained from the fines.

The composition of the excavated landfill material is subject to fluctuations, which can reduce the performance of both singular processing units and the whole processing chain. Therefore, the fluctuations can result in impaired quality and reduced quantity of the marketable output fractions. Furthermore, the humidity of the input material was found to impair the functioning of the entire processing chain, so that the biological drying prior to mechanical processing is mandatory. The biological drying not only reduces the risk of clogging but also the share of adhesive fines and defilements on particles, preventing reduced purities of marketable output fractions. The chemical analyses revealed that heavy metals were present in the fine fractions <10 mm, 10-20 mm and 20-40 mm. The marketing of such fine fractions as waste-compost in Austria, for instance, could face problematic hurdles since it must comply with country-specific limit values. The analyses of the named fine fractions showed that the values of Pb, As, Zn, Ni, Cr, Cd and Cu exceeded the Austrian limit values.

Research question 1:

Which output fractions of a mechanical-biological treatment plant, used for the processing of landfill material, show potential for sensor-based sorting?

To identify suitable output fractions from a MBT process of landfill material for SBS, the results of publication 1 are assessed in this doctoral thesis. Two factors are considered.

First, the characteristics of the material fraction must meet the requirements of the SBS unit to ensure the functional capability of the sorting machine. This includes an appropriate grain size distribution and a material composition that can be processed by the built-in sensor. Due to the broad grain size distribution of the input material of the MBT plant and of the fraction <60 mm, these fractions were ruled out as possible input material for a SBS sorting stage (cf. Figure 10 in publication 1). Only after further mechanical processing steps (separation of fines via screening), the <60 mm fraction could be considered for SBS. The air-classifier light fraction and the fraction >200 mm were enriched in 2D-particles, significantly reducing the performance of SBS machinery. Therefore, only the air-classifier heavy fraction was recognized as suitable for SBS.

Second, an increase in value of the material fraction must be attainable via SBS. For this purpose, one or more potentially marketable output fractions must be producible. Considering the composition of the air-classifier heavy fraction “HF WS” (24.1 wt% plastics 3D, 34.6 wt% inert materials, 19.6 wt% wood, 12.8 wt% rest, 8.9 wt% other material fractions) two possible applications can be targeted: by separating inert materials and combustibles, inert materials can be used for material recycling, while combustibles bare potential for energy recovery. Producing plastic pre-concentrate from the combustibles forms the second application of SBS, allowing for chemical recycling of specific plastic types (depolymerisation). To this end, a second cleaning stage would be necessary, i.e. separating the plastics for chemical recycling from the combustibles that also contain impurities for chemical recycling such as PVC. The distinction of various plastic types must be accomplished both to separate combustibles from inert materials and to sort plastics for chemical recycling.

Publication 2

In this study, the applicability of the ballistic separator “STT 6000” to the mechanical processing of landfill material without any pre-treatment was tested. The manual analyses of the output fractions of this process allow characterizing the processed landfill material and assessing the ballistic separator performance.

The largest output is the <90 mm fraction with a share of 80 wt%, followed by the 3D 200-90 mm fraction with 10 wt%. The 2D 200-90 mm and 3D >200 mm fractions each account for 4 wt%, while the 2D >200 mm fractions constitute 2 wt% of the mass of the input material.

The moisture content in the 2D fractions and <90 mm fraction is 26-32 wt% while the moisture content in the 3D 200-90 mm fraction is significantly lower (median: 13 wt%). By comparison, the biggest fluctuations of moisture content were observed in the 2D fractions.

Both 3D output fractions >200 mm and 200-90 mm were primarily characterised by high shares of inert materials (89.6 wt% and 74.7 wt%), Fe metals (3.4 wt% and 5.2 wt%) and wood (3.8

wt% and 4.1 wt%). While fines (defined as material <20 mm) and 3D plastics were almost completely absent in the 3D >200 mm fraction, in the 3D 200-90 mm fraction shares of 8.4 wt% of fines and 3.3 wt% of 3D plastics were recorded.

In both 2D output fractions, major shares of 2D plastics (24.1 wt% and 37.5 %), fines (36.0 wt% and 31.2 wt%), rest (18.0 wt% and 10.5 wt%) and textiles (7.4 wt% and 8.4 wt%) were found. The rest fraction was composed of plastic compounds, textiles and cellulose, such as carpets and diapers, which constitute high-calorific fractions and are therefore desired in the 2D fraction. The high amount of fines in the 2D fraction can be traced back to the increased share of adhesions that stick to the large surface areas of plastic films and foils, in contrast to 3D materials. Even though the 2D fractions contain significant amounts of fines, which reduce the heating value of these fractions, both can be regarded as high-calorific fractions.

The main components of the <90 mm fraction are fines <20 mm (75.5 wt%), inert materials (11.4 wt%), rest (4.2 wt%) and glass (3.8 wt%). Due to the large share of the <90 mm fraction in the landfill material, the relatively low share of high calorific fractions (4.1 wt% of plastics, textile, paper and wood) still accounts for a significant amount of combustibles (3,28 wt%) in relation to the total amount of the landfill material. Therefore, the combustibles in the <90 mm fraction have the potential to be extracted as additional combustible material.

Based on the given results, the ballistic separator is regarded as suitable for the processing of landfill material to separate enriched combustible fractions (2D fractions) from enriched inert fractions (3D fractions). To create usable output fractions from the fraction <90 mm, in form of calorific fractions or for the recycling of materials, further treatment of this large material stream is necessary.

Research question 2:

What output fractions of a simplified LFM treatment process show potential for sensor-based sorting?

The results of publication 2 allow identifying material streams originating from a simplified LFM process that are suitable for SBS.

Due to the high amounts of 2D material (35 wt% of 2D plastics and 45 wt% of textiles), whose aerodynamic properties significantly decrease the sortability when using SBS, the material streams are expected to cause low throughput rates on SBS units in the 2D fractions of the ballistic separator. Hence, they are classified as unsuitable for the processing with SBS machinery. By contrast, the 3D fractions were selected for SBS experiments due to their material composition and the higher grammage of their particles. A possible scope of application could be the separation of combustibles and inert materials to create RDF and/or construction materials. The aim of this sorting task is to comply with the respective limit values for such fractions, e.g. the maximum combustible shares in construction and demolition aggregates. The same approach could be adopted for the fine fraction, if further preconditioning, such as screening and air classification, was conducted. In this case, the

resulting material streams would show grain size distributions and grammages suitable for SBS.

Publication 3

In this publication, the impact of increased surface roughness and surface water of plastics on SBS was investigated.

It was found that increased surface roughness results in more diffusely reflected radiation per lit local unit, yielding a lower signal noise in the first derivative of the spectrum, which improves sorting decisions and consequently the recognition of all material types. This effect is most prominent for clear plastics. Particles that show low signal noise in the first place are less affected.

Furthermore, it was found that increased surface roughness can reduce the yield of low-softening plastics on chute sorters. The reason for this is that the sliding speed of these particles at chute sorters was partially reduced as a result of infrared-induced partial melting of the rougher surface. This leads to wrongly calculated delay times for the compressed air nozzles and thus a reduced yield of low-softening plastics.

Surface moisture causes wavelength specific absorption of the infrared radiation. The resulting spectral changes amplify or attenuate peaks in the first derivative of the spectra reflected from wet particles. If new absolute minima are formed, a systematic shift of the whole respective spectrum occurs. In addition, partial smoothing of the raw spectrum can be observed, reducing the extremes in the first derivative of the spectrum.

The knowledge of the effects that surface roughness and water have on the NIR spectrum can be used to improve the sorting efficiency of SBS machinery. Since increased surface roughness has positive effects on the detected spectra by reinforcing existing peaks, the pre-treatment of plastic waste can be adapted accordingly, e.g. by choosing processing technology that roughens the surface of the particles contained in the material stream. On the other hand, the knowledge that water on the surface of particles induces the formation of new minima and that this leads to a different shape of the first derivative of the material specific spectrum of a particle, can be taken into account when creating a sorting recipe. Hence, the classification of particles can be enhanced and improve the sorting efficiency of a SBS unit.

Research question 3:

What effects do increased surface roughness and water have in principle on sensor-based sorting with NIR technology?

The effects of surface roughness and water on NIR-based sorting technology can be assessed based on the results from the laboratory trials in publication 3.

Increased surface roughness was found to enhance the amount of disperse radiation that is detected by a NIR sensor. This pre-processed spectral information showed to be more stable

and contain less signal noise, potentially enabling improved classification and separation of materials. This effect is especially prominent for clear plastics such as PET bottles.

Surface water induces the absorption of NIR radiation, resulting in the formation of new minima or, if these minima already exist in a spectrum, in the enhancement of such minima in the first derivative of the spectrum specific to the material. If maxima exist in the pertinent spectral regions, these can be offset. It is possible that such changes result in the formation of new absolute minima in the normalized first derivative of the spectrum, which would entail a shift of the whole spectrum. The extent of the changes in a spectrum due to the humidity highly depends on the shape of the material-specific spectrum and on the amount of water that covers the particle surface. The described effects can lead to a significantly reduced sorting performance due to misclassification. If the described effects are accounted for in a sorting recipe, the amount of losses due to water-induced misclassification can be limited.

Publication 4

In this publication, the effects of increased surface roughness on the SBS sorting performance were investigated, not only under laboratory but also under realistic conditions.

A delabeller was tested for the delabelling of PET bottles and showed a performance of 90 % (PET bottles of which more than 90 % of the label was delabelled) at a throughput rate of approx. 4 t/h. Only smaller bottles (≤ 0.5 L volume) were not delabelled accordingly. A primary screening stage was found to further increase the performance of the tested delabeller.

Delabelling PET bottles increased their surface roughness. In experiments with state-of-the-art NIR sensor technology, the spectral data of the delabelled bottles showed an enhanced peak extension of the material specific NIR-spectrum and consequently improved PET bottle classification. The characteristic PET peak at approx. 1650 nm in the first derivative (not normalized) showed in 30 % of the object pixels of not delabelled PET bottles, while this peak was distinguishable in more than 90 % of the object pixels of delabelled PET bottles. In addition, it was found that the extent of further minima and maxima in the spectral range of 1100-1200 nm increased significantly. These findings suggest that the delabelling prior to NIR-SBS improves the identification of PET bottles, potentially resulting in an improved sorting performance.

The recognition of PET bottles despite labelling proved to be possible based on the characteristic PET peak at approx. 1650 nm wavelength, provided that the spectral information of PET, altered by the label, can be included in the sorting recipe. Furthermore, the distinguishability of labelled and unlabelled PET bottles was proven based on the alteration of the PET spectrum due to the influence of attached labels. However, the presence of water can lead to partial misclassification of object pixels of unlabelled PET so that they are classified as labelled PET.

Research question 4:

Can the observed effects of increased surface roughness be transferred from laboratory testing to real waste fractions?

The positive effects of surface roughening on the detected PET spectrum, found in publication 3, can also be established under realistic conditions. A significant peak extension in the first derivative (not normalized) of the PET-specific NIR spectrum can be noted due to surface roughening via delabelling. This effect translates to reduced signal noise after normalizing it.

The observed increase of detectable object pixels in publication 3 could not be confirmed under realistic conditions. This can be explained with various factors:

- The PET bottles in waste are subject to mechanical stress prior to mechanical processing (e.g. friction during transportation). The mechanical stress results in minor surface roughening and therefore increased peak extension and reduced signal noise in the normalized first derivative of the PET spectrum. This increases the disperse radiation that is reflected and detectable by the NIR sensor in the SBS machine and enables the correct object pixel detection.
- In contrast to the trials in publication 3, when sorting whole PET bottles, the emitted NIR radiation encounters not only one but two or more material layers, resulting in less transmitted and more disperse reflected radiation. This leads to more detectable reflected radiation (an improved data basis) per object pixel and therefore to increased peak extension and reduced signal noise in the normalized first derivative of the PET spectrum. As a result, the object pixels can be detected correctly.

Publication 5

In this study, XRF sorting was tested for the recovery of metals from MSWI ash that are currently not separately obtained. In addition, information about the effect of oxide layers and surface treatment (wet- and dry-mechanical) on the sorting performance can be derived.

In general, the compositions of all output fractions from the sorting trials correspond to the respective desired fractions. The conducted experiments demonstrate that zinc, copper, brass, stainless steel and precious metal fractions can be enriched in product fractions with marketable quality via XRF sorting. Pyrometallurgical tests generated products with marketable purities (zinc: 86.8–91.4 % zinc; copper: 86.7–90.3 % copper; brass: 60.6–62.5 % copper and 31.5–34.0 % zinc; stainless steel: 62.5– 66.5 % iron). Both the residual fraction and the precious metals fraction of XRF sorting show increased quantities of copper and zinc. This is due to the fact that both metals represent large shares in the input fraction, either as copper and zinc or as the alloy brass. Accordingly, in relative terms, even small losses can result in comparatively large amounts of these metals within other, especially in small material fractions.

Lead was found in the respective metal products. If removed from these fractions, better product qualities could be generated. This could be achieved by separating lead in an additional XRF sorting step. Along with this, the sensor sensitivity could be accordingly adjusted for the conducted sorting steps. However, this would bear the risk of material losses.

The purity of the generated metal fractions was not noticeably affected by dry or wet mechanical treatment when compared with each other. Primarily the pre-treatment significantly increased the yield of lead into the residual fraction. More particularly, wet-mechanical treatment increases the yield of lead more (+28 %) than dry-mechanical treatment (+9.3 %). Accordingly, the mechanical pre-treatment reduced the lead yielded into the brass fraction. In addition, the yield of copper and zinc into the brass fraction slightly decreased while the yield of both metals into the residual fraction rose. This suggests that not the pure lead but brass alloys were wrongly classified as “residuals” and accordingly sorted. Consequently, not the misclassification of mechanically pre-treated lead particles but the misclassification of mechanically pre-treated brass particles could be the reason for the shift of lead from the brass fraction into the residual fraction. For copper and zinc, this shift is less prominent than for lead because the lead content in the input material is significantly lower than the copper and zinc contents. Furthermore, only a relatively small share of brass alloys, maybe enriched in lead, was affected by the pre-treatment. The general validity of these observations should be verified on the basis of further comprehensive trials.

Research question 5:

What influence do oxide layers and (wet) mechanical surface treatment have on XRF-based sorting of heavy metal fractions from bottom ash?

The research question can be answered based on the experimental results, obtained in publication 5 of this PhD thesis.

Zinc, copper, brass, stainless steel and precious metals were successfully separated by XRF sorting. The compositions of the product fractions do not significantly differ from each other as a result of the pre-treatment.

However, the pre-treatment partly influenced the material yield of the metals. The biggest effect is seen in the shift of lead. With increasing pre-treatment (none, dry, wet) more brass is sorted into the residual fraction (yields: 37.7 %, 47.0 %, and 65.7 %) and less lead is yielded into the brass fraction (yields: 51.5 %, 38.0 % and 25.9 %). Furthermore, the yield of copper (yields: 66.0 %, 64.3 % and 51.2 %) and zinc (yields: 71.1 %, 70.1 % and 58.8 %) into the brass fraction decreases and the respective yield into the residual fraction increases. This indicates that not different particles of lead, copper and zinc are differently classified and sorted but that the separation of brass alloys is affected by surface pre-treatment.

An explanation for this phenomenon could be the selective leaching of lead, which is less noble than copper and zinc. This could cause decreased lead contents in the outer layer of brass particles prior to the pre-treatment and XRF sorting. The thresholds of the copper content

(>60 %) and zinc content (>20 %) for the classification of brass would need to be accordingly adjusted to these relatively low brass contents. As a result of the pre-treatment, in particular the wet pre-treatment, the low-leaded outer layer/oxide layer could be ablated and hence reveal higher lead contents which indicates the classification of "high-leaded" brass particles as "residuals".

Publication 6

The performance of SBS units can be influenced by two factors. Either the functionality of the built-in sensor technology is impaired in terms of reducing the share of particles that can be correctly detected, recognised and classified, or the mechanical discharge of correctly identified particles is impeded. This impaired mechanical discharge reduces the efficiency of any SBS machine, independent of the installed sensor technology. Two predominant influencing factors were identified in the field of mechanical discharge errors – the input composition and the throughput rate/occupation density of the material in the detection area of a SBS machine. The occupation density strongly correlates with the throughput rate, whereby the grammage of the material fractions within the input stream of the sorting unit influences the relation between occupation density and throughput rate.

The conducted trials do not indicate any influence of the input composition on the product yield at any occupation density. However, with increasing occupation density, the product yield decreases exponentially from 98 p% (occupation density ~4 %) to about 10 p% (occupation density ~200 %). The average product yield, depending on the occupation density, is displayed as a polynomial function of the fourth degree (in this case $y = -5.0564x^4 + 10.321x^3 - 6.2344x^2 + 0.2105x + 0.9784$) for occupation densities <100 % with a coefficient of determination of $R^2=0.9417$.

The yield rises with increasing eject share in the input composition. At a specific eject share, the yield decreases with increasing occupation density, while the product share increases in form of a saturation curve, reaching a maximum at an occupation density of approx. 60 %.

The eject purity can be plotted as falling linear functions of the occupation density for each input composition. The slope of this function depends on the input composition: with decreasing eject share the negative slope steepens.

Based on the obtained results, the principle relationship between input composition/occupation density and SBS efficiency were assessed for various mixtures of similar materials. On this basis, the prediction of the sorting performance was improved. Whether the quantitative evaluation of the displayed interdependencies apply to sorting machinery in general needs to be examined in further experiments. In addition, the influence of other material or factors specific to the machine (grain size distribution of the input material, foil content, particle shape, nozzle size, etc.) bares potential for further studies.

Research question 6:

How do input composition and throughput rate of a material stream influence the performance of a sensor-based sorting machine?

While the composition of a material stream does not change the product yield of a sensor-based sorting machine, the rising throughput rate decreases it exponentially from approx. 98 p% at an occupation density of approx. 4 p% to about 10 p% at an occupation density of approx. 200 %. The average product yield of the sorting machine utilized in the conducted sorting trials can be displayed as a polynomial function of the fourth degree over the occupation density for occupation densities <100 %.

The yield achieved in a sorting step correlates with the product yield but relates to the total amount of material that is fed into the sorting machine. Therefore, the yield decreases exponentially. This decrease does not only account for eject material that is successfully separated but also for reject material that is wrongly ejected. Since the yield is related to the complete input material, a high eject share in the input composition results in an accordingly high yield for low occupation densities. The higher the occupation density, the more the yields of different input compositions converge. Despite the decreasing yield over rising occupation density, the product quantity (in mass per hour) increases in form of a saturation curve, reaching its maximum at an occupation density of approx. 60 %. The value of this maximum depends on the eject share in the input composition and the average particle weight.

To evaluate the quality of an eject fraction separated with a SBS unit, the eject purity can be utilized as the evaluation criterion. As general principle, a high eject share in the input material results in a high eject share (and high eject purity) in the eject fraction at a specific occupation density. At low occupation densities, the product qualities of sorting trials with differing input compositions show relatively similar eject compositions. With rising occupation density, the eject purity declines linearly. The slope of such falling linear functions is steeper for lower eject shares in the input material, resulting in increasingly differing product qualities over rising occupation densities.

Publication 7

Based on publications 1 and 2, material fractions that are potentially suitable for SBS were identified. Samples of these fractions were taken and used for sorting trials. The results of these sorting trials were published in publication 7 alongside with the analyses and assessment of the sorting efficiencies achievable via SBS.

The focus of this study is the application of NIR sensor technology to the separation of combustibles and inert materials as well as to the separation of plastic types.

Trials on the separation of combustibles and inert materials showed that inert fractions could be generated with purities of 97.7-99.7 wt%. This was possible because the pre-treatment consisted of ballistic separation and screening stages, ferrous and non-ferrous separation and

air-classification, generating pre-concentrated inert fractions. As a result, the enrichment ratios of inert materials in all fractions were relatively low (1,006-1,164) while the enrichment ratios of combustibles were higher (4.785-41.250). Accordingly, due to the low combustible content in the input material of SBS, the combustible fractions of SBS showed relatively low purities. The correct recognition of soot-blackened plastics proved to be problematic with NIR technology. However, most misclassification occurred for combustibles due to pulp material that was covered with adhesive fines. Increased water contents were found to reinforce this effect. Based on these results, it was affirmed that NIR-based sorting of fine fractions from LFM (4.5-90 mm) is technically feasible to separate combustibles and inert materials.

The trials on the distinction and separation of various commodity plastic types (polypropylene (PP), polyethylene (PE), PVC, polystyrene (PS), PET) and residual materials, that are contained in air-classifier heavy fraction from a MBT process of landfill material, showed that the distinction of the named material types is possible. For PP, PE and PVC the yield amounted to >91 % while the yield for all remaining material types consistently remained <5.1 %. The sorting of PVC yielded more misclassification and, as a result, more wrong separation of further plastics. The reason for this error is that the material-specific classification of soot-blackened plastics is not possible via NIR technology. Therefore, all soot-blackened plastics were defined as PVC, ensuring the maximum PVC yield.

Since the composition of the output fraction highly depends on the input composition, only the yield of each material type was investigated for a specific sorting task. To circumvent the problem of wrong classification due to overlapping particles, all trials were conducted at low throughput rates, ensuring the singling of all particles.

Research question 7:

Is the application of sensor-based sorting technology in ELFM technically feasible?

The commodity plastics (PP, PE, PVC, PS, PET), found in the heavy fractions >60 mm from mechanical processing of landfill material in a MBT plant were successfully distinguished and separated from each other and from residual materials via state-of-the-art SBS technology. The sorting efficiency is affected by the level of pre-processing, the water content and the relative amount of adhesive fines in the input material of the SBS stage.

In general, the separation of combustibles and inert materials is possible. The detection and distinctiveness of pulp-based particles was impaired for particle size ranges <30 mm due to adhesive fines, particularly in the presence of water.

Based on these results, the basic suitability of NIR-SBS machinery for the distinction and separation of plastics and for the sorting of combustibles and inert materials has been confirmed. Whether the long-term stability of a sufficiently effective SBS process can be achieved under realistic processing conditions has to be tested in large-scale trials. Problems, e.g., due to dust formation or various degradation states of plastics, may decrease the attained

efficiency rates. In such cases, it might be necessary to adapt the algorithm of material classification.

10 DISCUSSION

In publications 1 and 2, the air-classifier heavy fraction (case study Halbenrain) and the 3D fraction of ballistic separation (case study Mont-Saint Guibert) were found to be suitable for further processing with SBS technology in ELFM. For this task, NIR sensor technology was chosen for the separation of combustibles and inert materials. The separated fractions might be sold as RDF and construction aggregate (Parrodi et al., 2018a), respectively, after further processing (e.g. shredding, screening, washing). In addition, polyolefines from the 3D-/heavy fraction could be separated for, e.g., chemical recycling (Bauer et al., 2017).

In publications 3 and 4, two major factors influencing the performance of NIR sensors were investigated, allowing for optimised application of this technology to ELFM. Increased surface roughness was found to improve the performance of NIR sensors, while surface water can distort material specific spectra. This distortion can be counteracted by adapting the sorting algorithm accordingly. In LFM, the positive effect of increased surface roughness entails improved performance of NIR sorting.

In publication 5, it was demonstrated that oxide coatings have only limited impact on the performance of XRF sorting machinery for metal distinction. The limited impact indicates that this technology could also be used for the recognition and separation of aged metal fractions from landfills. To further assess the influence of other influencing factors on XRF sorting in LFM, additional experiments must be conducted.

In publication 6, the impact of the input composition and throughput rate on the sorting performance was investigated. A quantitative description of the relationship between these factors was developed, which allows adjusting the throughput rate for optimal yield and purity.

In publication 7, the technical feasibility of SBS machinery in ELFM was shown. In accordance with the findings from publications 1 and 2, the 3D and heavy fractions from landfill mining activities were chosen for sorting trials with NIR based sorting machinery. By considering the results of publications 3 and 4, the sorting algorithm for the landfill material was appropriately adjusted. As a result, the technical feasibility of NIR-based sorting technology for distinct landfill material fractions was proven. Enriched combustibles and inert fractions could be generated from the processed fines of MSG. The plastics in the air-classifier heavy fraction from Halbenrain were successfully separated from each other. Due to the influence of the input composition and necessary throughput rate on the sorting performance, multi-stage sorting might be necessary to attain the respective target product qualities.

Landfill mining yields excavated materials which can be partly processed by traditional technologies, like shredding, ballistic separation, air classification, screening, magnetic separation and eddy current separation, and thus generate marketable output fractions. Hence, the 2D fraction of ballistic separation or the air-classifier light fraction, the ferrous products of magnetic separation and the non-ferrous metals products of eddy current

separation can be directly recycled. These fractions represent the resource potential using state-of-the-art technologies.

A second fraction, the fine fraction, represents a share of landfill material that is neither feasible to be treated with conventional mechanical processing technology nor with SBS technology due to the insufficient spatial resolution of state-of-the-art sorting technology.

However, there is a third group of fractions derived from traditional processing technologies. These fractions are suitable for SBS and cannot be recycled without further processing in form of material specific separation, e.g. by SBS. They are defined as non-metallic materials, i.e. a mixture of various calorific fractions (3D plastics, textiles, paper, wood) and inert fractions (rocks, ceramics, concrete, glass), which would be yielded into a 3D or heavy fraction from ballistic separation or air-classification while exhibiting a grain size of at least 5 mm. This third category represents the “additional resource potential” which can be unlocked by SBS as considered by Parrodi et al. (2018a). Together with the first category, these materials present all potentially recyclable and recoverable energy materials (REM) as defined by Wolfsberger et al. (2015).

The quantity of REM depends on the composition of a landfill. Eight exemplary landfills, on which LFM activities have been conducted, were contemplated for the possible usage of SBS. In table 1 the average composition of each landfill is displayed.

Table 1: Exemplary composition of eight different landfills [wt%] (Parrodi et al., 2018b; Quaghebeur et al., 2013b)

	Landfill 1	Landfill 2	Landfill 3	Landfill 4	Landfill 5	Landfill 6	Landfill 7	Landfill 8
Inert	10%	17%	11%	20%	42%	0%	22%	7%
Metal	6%	2%	3%	2%	1%	4%	3%	5%
Textile	8%	2%	7%	2%	3%	7%	0%	6%
Wood	8%	7%	7%	4%	15%	7%	5%	0%
Paper/cardboard	3%	7%	8%	5%	5%	6%	5%	3%
Plastic/rubber/foam	31%	4%	17%	5%	8%	23%	22%	18%
Fines/Soil	34%	60%	44%	55%	27%	52%	29%	47%
Others	0%	1%	4%	9%	0%	2%	14%	14%

Several assumptions are made to evaluate the resource potential through SBS in ELFM:

1. The “Fines” fraction is too fine for SBS and therefore not sortable with SBS technology. However, the minimum particle size suitable for SBS is 5 mm, and in many of the cited studies larger cut-off-diameters (up to 90 mm) were used to define the fine fraction.
2. Metals are separated with magnets and/or eddy current separators.
3. The separation of 2D/light and 3D/heavy particles is carried out in form of ballistic separation or air-classification. This results in a 2D-/light fraction that could be used for (co-)incineration without further treatment.

- a. Plastic foils and textiles are discharged into the 2D-/light fraction. This fraction is not feasible for SBS due to the form factor of the particles.
 - b. 50 % of all plastics are foils, the other 50 % are considered to be 3D-/heavy particles, therefore yielded into the 3D-/heavy fraction.
 - c. As demonstrated in publication 7, successful separation of combustibles and inert fraction in the 3D-/heavy fraction is possible.
4. 3D-/heavy combustibles (paper, cardboard, 3D-plastics and wood) are directed into the 3D-/heavy fraction together with inert materials such as glass, stones, bricks, concrete, and asphalt.
 5. After the separation of combustibles and inert fraction(s) with SBS technology the combustibles can be used for energy recovery, while the inert fraction(s) can be recycled as construction aggregates. In both cases further processing (e.g. washing, shredding, and screening) might be necessary, depending on the quality requirements for the respective recycling/energetic recovery path.
 6. For the calculation of the resource potential (share of LFM material that could be exploited through recycling or energy recovery) market prices for the respective fraction are not taken into account.

Based on the given assumptions, the material fractions in Table 1 can be allocated to the three groups mentioned above:

The first category “not recoverable” consists of the fractions “Soil” and “Others” since no recycling option is given for these fractions by conventional mechanical processing or SBS (“Soil”), or the characteristics and recycling paths of the included material fractions are unknown (“Others”).

The second category “recoverable via mechanical processing” contains materials that could be accumulated in marketable output fractions with conventional mechanical processing technology. Therefore, metals (for recycling) as well as plastic foils and textiles (for energy recovery) fall into this category. These fractions can be generated via magnetic separation/eddy-current separation (metals) and ballistic separation/air-classification (plastic foils and textiles).

The third category, “recoverable with SBS technology”, consists of inert and glass as well as combustibles (wood, paper/cardboard and 3D-plastics). These fractions are expected to be yielded into a 3D-/heavy fraction by either ballistic separation or air-classification. Due to the mixture of both, carbon-based and inert materials, this fraction would have to be re-landfilled since its organic content is a critical factor and (Parrodi et al., 2018a) expected to be too high for recycling as construction aggregates, and the heating value is too low for energy recovery.

The contents of all three material categories in each exemplary landfill are displayed in Figure 2.

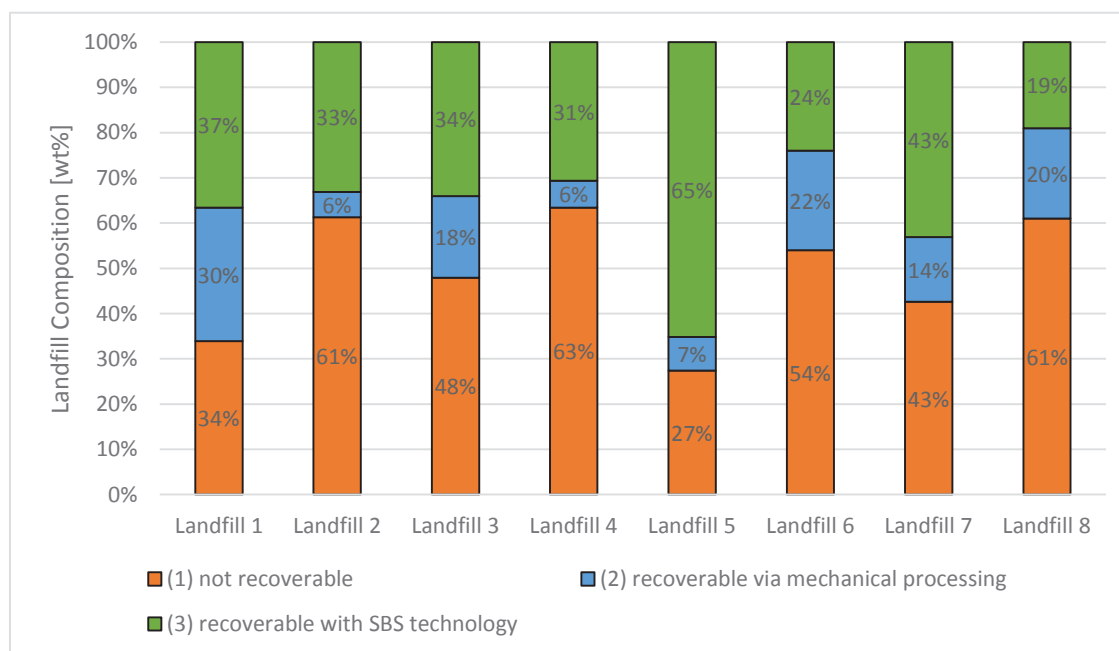


Figure 1: Classification of landfill material shares according to the resource potential that (1) cannot be unlocked, (2) that can be unlocked with conventional mechanical processing technology or (3) that can be unlocked via SBS technology.

On average, 49 wt% of the presented landfill materials are graded as “not recoverable”, fluctuating between 27-63 wt%, mostly due to varying “Soil” shares in the landfills. Overall, this category constitutes the largest shares of all landfill materials taken into consideration.

The overall share of landfill material whose recovery can be achieved with conventional mechanical processing technology amounts to approx. 15 wt%, varying between 6 wt% and 30 wt% between landfills in total. On average, this category consists of about 3 wt% metals, 4 wt% textiles and 8 wt% plastic foils. Depending on the landfill, the share of metal, textiles and plastic foils varies between 1-6 wt%, 0-8 wt% and 2-16 wt% respectively.

The average resource potential that can be unlocked with SBS machinery amounts to 36 wt% of the landfill materials, fluctuating between 19 wt% and 65 wt%. The average shares of inert, combustibles and 3D-plastics expected in the 3D-/heavy fractions are 16 wt%, 12 wt% and 16 wt% respectively. The material shares in the landfills vary between 0-42 wt% for inert, 3-20 wt% for combustibles and 0-8 wt% for 3D-plastics. The exceptionally high resource potential of landfill 5 is explained by the large shares of inert (42 wt%) and wood (15 wt%) while, compared to the other landfills, the fines content (27 wt%) is relatively low.

The resource potential for a specific landfill highly depends on its composition. The average content of the 3D-/heavy fraction of 36 wt% outlines the overall resource potential. Depending on the workload on a SBS stage, its performance can be reduced, as demonstrated in publication 6, which accordingly influences the composition of the respective output fractions. Multiple sorting stages can be necessary for sufficient enrichment of combustibles and inert in the respective fractions. The quality requirements for such output fractions depend on the scope of application and national legislation.

When taking into consideration the average resource potential that can be unlocked with SBS (36 wt%) and the resource potential that can be attained with conventional mechanical processing technology (15 wt%), about 51 wt% of the landfill constituents could in total be recovered. This share corresponds to the findings of Wolfsberger et al. (2015) who estimate that “the total resource potential in household and municipal solid waste landfills of central and northern Europe can be roughly given at 20 to 52 wt%”. Since the separation efficiency of processing machinery is <100 %, the technically feasible resource potential is expected to be notably lower, i.e. 21 % for Fe and 22 % for NF extraction were achieved by Wolfsberger et al. (2015).

11 OUTLOOK AND FUTURE RESEARCH

The results of this doctoral thesis demonstrate the basic functioning of NIR-based sorting technology in ELFM. The resource potential that could be unlocked with SBS is estimated at 36 wt% for municipal solid waste landfills on average. Depending on the efficiency of SBS and upstream processing machinery, the technically feasible resource potential is minor.

Three main topics and associated research questions with potential for further studies, arose from the doctoral thesis at hand:

- Although the basic functioning of NIR-based sorting technology for sorting landfill material was demonstrated, long-term stability under the adverse conditions of ELFM must be proven in large-scale SBS trials to make a definitive assessment.
 - o What kind of pre-processing is sufficient/optimal for the successful implementation of SBS in ELFM on-site?
 - o How does state-of-the-art sorting machinery function under the conditions of ELFM?
 - o What measures must be taken to enable long-term stability of SBS machinery in ELFM?
- The ageing effects, in particular the deterioration, of plastics on the recyclability and on SBS must be studied to assess the potential of different recycling options such as mechanical or chemical recycling.
 - o Does ageing of plastics lead to altered material specific spectra in the NIR range?
 - o Is it possible to distinguish deteriorated plastics from unaltered plastics with state-of-the-art technology?
 - o Can the impaired properties of plastics from ageing be quantified based on state-of-the-art NIR sensor technology?
- In connection with influences of input composition and throughput rate on sorting efficiency, further parameters, specific to the material or the machine, affect the performance of SBS machines. Additional comprehensive investigations in this field would enable more profound understanding of the sorting process, potentially allowing for application-specific and target-optimized process operation.
 - o What material characteristics (particle mass, form, grain size distribution, etc.) affect SBS performance at varying throughput rates and input compositions first and foremost?
 - o Under which conditions, e.g. specific material characteristics, is sorting on object- or pixel cluster-basis more advantageous?
 - o What information can the data, captured by the sensor at sorting stage, provide about the performance of this very sorting stage?

12 REFERENCES

This reference list provides references for the framework of the present doctoral thesis. The comprised research papers provide separate references.

- Alaya, M.A., Tóth, Z., Géczy, A., 2019. Applied Color Sensor Based Solution for Sorting in Food Industry Processing. *Period. Polytech. Elec. Eng. Comp. Sci.* 63 (1), 16–22. doi:10.3311/PPee.13058.
- Bauer, M., Lehner, M., Schwabl, D., Flachberger, H., Kranzinger, L., Pomberger, R., Hofer, W., 2017. Bestandsaufnahme und mögliche Perspektiven der nass-mechanischen Aufbereitung von Altkunststoffen für das rohstoffliche Recycling. *Österr Wasser- und Abfallw* 69 (11-12), 446–459. doi:10.1007/s00506-017-0420-1.
- Breitenstein, A., Kieckhäfer, K., Spengler, T. (Eds.), 2016. *TönsLM – Rückgewinnung von Wertstoffen aus Siedlungsabfall- und Schlackendeponien*, 16 pp.
- Crowley, D., Staines A., Collins C., Bracken J, Bruen M., Fry J., Hrymak V., Malone D., Magette B., Ryan M., Thunhurst C., 2003. Health and Environmental Effects of Landfilling and Incineration of Waste - A Literature Review.
- Cubero, S., Aleixos, N., Moltó, E., Gómez-Sanchis, J., Blasco, J., 2011. Advances in Machine Vision Applications for Automatic Inspection and Quality Evaluation of Fruits and Vegetables. *Food Bioprocess Technol* 4 (4), 487–504. doi:10.1007/s11947-010-0411-8.
- Danthurebandara, M., van Passel, S., Vanderreydt, I., van Acker, K., 2015. Assessment of environmental and economic feasibility of Enhanced Landfill Mining. *Waste management (New York, N.Y.)* 45, 434–447. doi:10.1016/j.wasman.2015.01.041.
- Gaustad, G., Olivetti, E., Kirchain, R., 2012. Improving aluminum recycling: A survey of sorting and impurity removal technologies. *Resources, Conservation and Recycling* 58, 79–87. doi:10.1016/j.resconrec.2011.10.010.
- Gundupalli, S.P., Hait, S., Thakur, A., 2017. A review on automated sorting of source-separated municipal solid waste for recycling. *Waste management (New York, N.Y.)* 60, 56–74. doi:10.1016/j.wasman.2016.09.015.
- Jones, P.T., Geysen, D., Tielemans, Y., van Passel, S., Pontikes, Y., Blanpain, B., Quaghebeur, M., Hoekstra, N., 2013. Enhanced Landfill Mining in view of multiple resource recovery: a critical review. *Journal of Cleaner Production* 55, 45–55. doi:10.1016/j.jclepro.2012.05.021.
- Kaartinen, T., Sormunen, K., Rintala, J., 2013. Case study on sampling, processing and characterization of landfilled municipal solid waste in the view of landfill mining. *Journal of Cleaner Production* 55, 56–66. doi:10.1016/j.jclepro.2013.02.036.

- Krook, J., Baas, L., 2013. Getting serious about mining the technosphere: a review of recent landfill mining and urban mining research. *Journal of Cleaner Production* 55, 1–9. doi:10.1016/j.jclepro.2013.04.043.
- Krook, J., Svensson, N., Eklund, M., 2012. Landfill mining: a critical review of two decades of research. *Waste management (New York, N.Y.)* 32 (3), 513–520. doi:10.1016/j.wasman.2011.10.015.
- Lessard, J., Bakker, J. de, McHugh, L., 2014. Development of ore sorting and its impact on mineral processing economics. *Minerals Engineering* 65, 88–97. doi:10.1016/j.mineng.2014.05.019.
- Masi, S., Caniani, D., Grieco, E., Lioi, D.S., Mancini, I.M., 2014. Assessment of the possible reuse of MSW coming from landfill mining of old open dumpsites. *Waste management (New York, N.Y.)* 34 (3), 702–710. doi:10.1016/j.wasman.2013.12.013.
- Parrodi, J.C.H., Höllen, D., Pomberger, R., 2018a. CHARACTERIZATION OF FINE FRACTIONS FROM LANDFILL MINING: A REVIEW OF PREVIOUS INVESTIGATIONS. *Detritus* 2 (1), 46. doi:10.31025/2611-4135/2018.13663.
- Parrodi, J.C.H., Höllen, D., Pomberger, R., 2018b. CHARACTERIZATION OF FINE FRACTIONS FROM LANDFILL MINING: A REVIEW OF PREVIOUS INVESTIGATIONS. *Detritus* 2 (1), 46. doi:10.31025/2611-4135/2018.13663.
- Quaghebeur, M., Laenen, B., Geysen, D., Nielsen, P., Pontikes, Y., van Gerven, T., Spooren, J., 2013a. Characterization of landfilled materials: screening of the enhanced landfill mining potential. *Journal of Cleaner Production* 55, 72–83. doi:10.1016/j.jclepro.2012.06.012.
- Quaghebeur, M., Laenen, B., Geysen, D., Nielsen, P., Pontikes, Y., van Gerven, T., Spooren, J., 2013b. Characterization of landfilled materials: screening of the enhanced landfill mining potential. *Journal of Cleaner Production* 55, 72–83. doi:10.1016/j.jclepro.2012.06.012.
- Rotheut, M., Quicker, P., 2017. Energetic utilisation of refuse derived fuels from landfill mining. *Waste management (New York, N.Y.)* 62, 101–117. doi:10.1016/j.wasman.2017.02.002.
- Serranti, S., Gargiulo, A., Bonifazi, G., 2012. Classification of polyolefins from building and construction waste using NIR hyperspectral imaging system. *Resources, Conservation and Recycling* 61, 52–58. doi:10.1016/j.resconrec.2012.01.007.
- Tsuchikawa, S., Kobori, H., 2015. A review of recent application of near infrared spectroscopy to wood science and technology. *J Wood Sci* 61 (3), 213–220. doi:10.1007/s10086-015-1467-x.
- Wolfsberger, T., Aldrian, A., Sarc, R., Hermann, R., Höllen, D., Budischowsky, A., Zöschner, A., Ragoßnig, A., Pomberger, R., 2015. Landfill mining: Resource potential of Austrian landfills--Evaluation and quality assessment of recovered municipal solid waste by chemical analyses. *Waste management & research : the journal of the International Solid*

- Wastes and Public Cleansing Association, ISWA 33 (11), 962–974. doi:10.1177/0734242X15600051.
- Wotruba, H., Knapp, H., Neubert, K., Schropp, C., 2014. Anwendung der sensorgestützten Sortierung für die Aufbereitung mineralischer Rohstoffe. *Chemie Ingenieur Technik* 86 (6), 773–783. doi:10.1002/cite.201300174.
- Zhou, C., Fang, W., Xu, W., Cao, A., Wang, R., 2014. Characteristics and the recovery potential of plastic wastes obtained from landfill mining. *Journal of Cleaner Production* 80, 80–86. doi:10.1016/j.jclepro.2014.05.083.

13 LIST OF ABBREVIATIONS

2D	Two-dimensional
3D	Three-dimensional
Approx.	Approximately
As	Arsenic
Cd	Cadmium
Cf.	Confer
Cr	Chromium
Cu	Copper
e.g.	Exempli gratia
ELFM	Enhanced landfill mining
etc.	Et cetera
Fe	Ferrous
Gew.-%	Gewichtsprozent
i.e.	It est
L	Litre
LFM	Landfill mining
m ²	Square metre
MBT	Mechanical biological treatment
mm	Millimetre
MSG	Mont-Saint-Guibert
MSWI	Municipal solid waste incineration
NF	Non-ferrous
Ni	Nickel
NIR	Near-infrared
Nm	Nanometre
p%	particle-%
Pb	Lead
PE	Polyethylene
PET	Polyethylene terephthalate
PP	Polypropylene
PS	Polystyrene
PVC	Polyvinylchloride
RDF	Refuse derived fuel
REM	Recoverable energy materials
SBS	Sensor-based sorting
t	tons
wt%	Weight percent
XRF	X-ray fluorescence
Zn	Zinc